NR 2013;47(5)

The Nordic Expert Group for Criteria Documentation
of Health Risks from Chemicals

148. Carbon nanotubes

*Maria Hedmer, Monica Kåredal, Per Gustavsson
and Jenny Rissler*

ARBETE OCH HÄLSA | VETENSKAPLIG SKRIFTSERIE

ISBN 978-91-85971-46-6 ISSN 0346-7821

UNIVERSITY OF GOTHENBURG

ARBETSMILJÖ VERKET

Arbete och Hälsa

Arbete och Hälsa (Work and Health) is a scientific report series published by Occupational and Environmental Medicine at Sahlgrenska Academy, University of Gothenburg. The series publishes scientific original work, review articles, criteria documents and dissertations. All articles are peer-reviewed.

Arbete och Hälsa has a broad target group and welcomes articles in different areas.

Instructions and templates for manuscript editing are available at http://www.amm.se/aoh
Summaries in Swedish and English as well as the complete original texts from 1997 are also available online.

Arbete och Hälsa, University of Gothenburg

Preface

The main task of the Nordic Expert Group for Criteria Documentation of Health Risks from Chemicals (NEG) is to produce criteria documents to be used by the regulatory authorities as the scientific basis for setting occupational exposure limits for chemical substances. For each document, NEG appoints one or several authors. An evaluation is made of all relevant published, peer-reviewed original literature found. The document aims at establishing dose-response/dose-effect relationships and defining a critical effect. No numerical values for occupational exposure limits are proposed. Whereas NEG adopts the document by consensus procedures, thereby granting the quality and conclusions, the authors are responsible for the factual content of the document.

The evaluation of the literature and the drafting of this document on *Carbon nanotubes* were done by Dr Maria Hedmer, Dr Monica Kåredal, Dr Per Gustavsson and Dr Jenny Rissler at Lund University, Sweden.

The draft versions were discussed within NEG and the final version was accepted by the present NEG experts on June 18, 2013. Editorial work and technical editing were performed by the NEG secretariat. The following present and former experts participated in the elaboration of the document:

NEG experts	
Gunnar Johanson	Institute of Environmental Medicine, Karolinska Institutet, Sweden
Merete Drevvatne Bugge	National Institute of Occupational Health, Norway
Anne Thoustrup Saber	National Research Centre for the Working Environment, Denmark
Tiina Santonen	Finnish Institute of Occupational Health, Finland
Vidar Skaug	National Institute of Occupational Health, Norway
Mattias Öberg	Institute of Environmental Medicine, Karolinska Institutet, Sweden
Former NEG expert	
Kristina Kjærheim	Cancer Registry of Norway
NEG secretariat	
Anna-Karin Alexandrie and Jill Järnberg	Swedish Work Environment Authority, Sweden

This work was financially supported by the Swedish Work Environment Authority and the Norwegian Ministry of Labour.

All criteria documents produced by the Nordic Expert Group may be downloaded from *www.nordicexpertgroup.org*.

Gunnar Johanson, Chairman of NEG

Contents

Preface
Abbreviations and acronyms
Terms as used in this document
1. Introduction 1
2. Substance identification 1
3. Physical and chemical properties 4
3.1 Chemical composition 5
3.2 Mechanical properties 5
3.3 Electrical properties 6
3.4 Optical and thermal properties 7
3.5 Specific surface area measurement 7
4. Occurrence, production and use 9
4.1 Occurrence 9
4.2 Production 9
4.3 Use 13
5. Measurements and analysis of workplace exposure 14
5.1 Air exposure 14
5.2 Dermal exposure 19
6. Occupational exposure data 20
6.1 General 20
6.2 Airborne exposure 20
6.3 Dermal exposure 46
6.4 Oral exposure 47
7. Toxicokinetics 47
7.1 Pulmonary deposition 47
7.2 Uptake 49
7.3 Distribution 50
7.4 Biotransformation 53
7.5 Excretion, elimination and biopersistence 54
8. Biological monitoring 67
9. Mechanisms of toxicity 67
9.1 Oxidative stress and inflammation 67
9.2 The fibre paradigm and frustrated phagocytosis 69
9.3 Production of collagen and fibrosis 70
9.4 Genotoxicity 71
9.5 Lung particle overload 72
9.6 Interactions between carbon nanotubes and biomolecules 72
9.7 Alterations in membrane permeability 73
10. Challenges facing toxicological studies 74
11. Effects in animals and *in vitro* studies 77
11.1 Irritation and sensitisation 77

11.2 Effects of single exposure 80
11.3 Effects of short-term exposure (up to 90 days) 127
11.4 Mutagenicity and genotoxicity 133
11.5 Effects of long-term exposure and carcinogenicity 140
11.6 Reproductive and developmental effects 144
12. Observations in man 147
12.1 Irritation and sensitisation 147
12.2 Effects of single and short-term exposure 147
12.3 Effects of long-term exposure 147
12.4 Genotoxic effects 147
12.5 Carcinogenic effects 147
12.6 Reproductive and developmental effects 147
13. Dose-effect and dose-response relationships 148
14. Previous evaluations 205
15. Evaluation of human health risks 206
15.1 Assessment of health risks 206
15.2 Groups at extra risk 208
15.3 Scientific basis for an occupational exposure limit 208
16. Research needs 208
17. Summary 210
18. Summary in Swedish 211
19. References 212
20. Data bases used in search of literature 234
Appendix 1. Previous NEG criteria documents 235

Abbreviations and acronyms

Al_2O_3	aluminium oxide
AP-1	activator protein 1
ApoE	apolipoprotein E
ASAT	aspartate aminotransferase
BAL	bronchoalveolar lavage
BET	Brunauer-Emmett-Teller method
CNT	carbon nanotube
CVD	chemical vapour deposition
DPPC	dipalmitoyl phosphatidylcholine
DTPA	diethylenetriamine pentaacetic acid
DWCNT	double-walled carbon nanotube
EC	elemental carbon
FITC	fluorescein isothiocyanate
HARN	high-aspect ratio nanomaterial
HiPCO	high-pressure carbon monoxide
H_2O_2	hydrogen peroxide
ICP-AES	inductively coupled plasma-atomic emission spectrometry
Ig	immunoglobulin
IL	interleukin
i.p.	intraperitoneal
i.t.	intratracheal
i.v.	intravenous
LD_{50}	lethal dose for 50% of the exposed animals at single administration
LDH	lactate dehydrogenase
LOAEL	lowest observed adverse effect level
LOD	limit of detection
LPS	lipopolysaccharide
MAP	mitogen-activated protein
MCE	mixed cellulose ester
MHC	major histocompatibility complex
MRI	magnetic resonance imaging
MTT	3-(4,5-dimethyl-2-thiazolyl)-2,5-diphenyl-2H-tetrazolium bromide
MWCNT	multi-walled carbon nanotube
NADPH	nicotinamide adenine dinucleotide phosphate
ND	not detectable
NFκB	nuclear factor kappa B
NIOSH	National Institute for Occupational Safety and Health
NMAM	NIOSH manual of analytical methods
NOAEL	no observed adverse effect level
OECD	Organisation for Economic Co-operation and Development
OEL	occupational exposure limit
8-oxodG	8-oxo-7,8-dihydro-2'-deoxyguanosine

PBS	phosphate buffered saline
PEG	polyethylene glycol
PM_x	particulate matter with maximal aerodynamic diameter of x µm
PMN	polymorphonuclear leukocyte
REL	recommended exposure limit
ROS	reactive oxygen species
SDS	sodium dodecyl sulphate
SEM	scanning electron microscopy
STEM	scanning transmission electron microscopy
SWCNT	single-walled carbon nanotube
TEER	transepithelial electrical resistance
TEM	transmission electron microscopy
TGFβ	transforming growth factor beta
TiO_2	titanium dioxide
TNFα	tumour necrosis factor alpha
TWA	time-weighted average
UICC	Union Internationale Contre le Cancer
WHO	World Health Organization

Terms as used in this document

Agglomerate
Nanoparticles or aggregates associated with one another through weak van der Waals forces. Agglomerates of carbon nanotubes (CNTs) are often larger in all dimensions than the nominal cut-off point (100 nm) for nanoparticles. Agglomerates can potentially be dispersed by minor external forces, such binding to proteins in the fluid lining the lungs.

Aggregate
Nanoparticles strongly bonded to one another e.g., by chemical bonding or partial melting together (sintering). The individual particles in aggregates are more difficult to separate.

BAL
Bronchoalveolar lavage (BAL), a medical procedure in which a bronchoscope is passed through the mouth or nose into the lungs to inject fluid into a small portion of the lung and then recollect this fluid for examination. The suspension thus obtained is referred to as BAL fluid and can be examined for its content of cells (e.g., macrophages and other immune cells) or proteins (e.g., cytokines).

Black carbon
Black carbon consists of carbon graphite structures formed in connection with the incomplete combustion of fossil fuels, biofuel, and biomass. Black carbon may be of either natural or anthropogenic origin.

Bulk density
Bulk density is defined as the mass of a sample of particles divided by the total volume they occupy. This property of powders, granules and other "dispersed" solids is most often applied in reference to soil samples. The bulk density is strongly dependent on material properties and particle size and may be altered by handling.

Bundle
A bundle is an aggregate of fibres formed when individual CNTs associate with their nearest neighbours via van der Waals interactions. Bundles characteristically contain many tens of CNTs and can be longer and wider than the original CNTs from which they originated. The typical distance between the CNTs in a bundle is comparable to the inter-planar distance of graphite, i.e., 3.1 Å.

C_{60}
C_{60} is a spherical fullerene, with its 60 carbon atoms structured as a truncated icosahedron, which resembles a football.

Carbon black
In principle, carbon black is the same as black carbon, but often contains smaller amounts of polycyclic aromatic hydrocarbon. This term is often applied for black carbon-based powders used as a pigment and reinforcement in rubber and plastic products. Carbon black is often a powder with low density.

Fibre
According to the World Health Organization (WHO) a particle must have a length >5 μm and a length:width ratio ≥3:1 to be defined as a fibre (354).

Fullerenes
Fullerenes are molecules composed entirely of carbon with the form of a hollow sphere, ellipsoid, or tube.

High-aspect ratio nanoparticles/nanomaterials (HARN)
HARNs are nanomaterials with two external dimensions in the nanoscale with a high length-to-diameter ratio. These include nanorods, nanowires and other nano-fibres, including CNTs. No strict definition of the minimum length-to-diameter ratio for HARNs is described in the literature. Typically this ratio is >100 for CNTs (240), but SWCNTs may have ratios as high as 10^7 (286). On the basis of their structure and dimensions, CNTs are also classified as 2D nanoscale materials (67).

MTT
MTT (3-(4,5-dimethyl-2-thiazolyl)-2,5-diphenyl-2H-tetrazolium bromide) is employed in a colorimetric assay used to test cytotoxicity *in vitro* by determining cellular metabolic activity and, thus, viability.

Nanofibre
A nanofibre is a nanomaterial with two external dimensions in the nanoscale with a nanotube being defined as a hollow nanofibre and a nanorod as a solid nanofibre.

Nanomaterial
Nanomaterial has one or more external dimensions in the nanoscale or material which is nanostructured. Nanomaterials can exhibit properties that differ from those of the same material lacking nanoscale features.

Nanoparticle
A nanoparticle is a nanomaterial with all three external dimensions in the nanoscale.

Nanoscale
The nanoscale ranges between 1 and 100 nm (274).

Nanotube
The nanotube is a hollow nanofibre, i.e., a nanomaterial with two similar external dimensions in the nanoscale and a significantly larger third dimension.

PEGylation
Polyethylene glycol 2000 (PEG2000) and PEG5400 are bound covalently to CNTs in order to render them more hydrophilic. The number denotes the average molecular weight of the PEG polymer. PEGylation (i.e., such covalent binding) causes CNTs to remain in blood circulation for longer periods and this effect is more pronounced with longer and more highly branched PEG chains.

Pluronic
Pluronic is the brand name of a collection of non-ionic surfactants derived from poly(propylene oxide) and poly(ethylene oxide). Different types of Pluronics are added to aqueous solutions to facilitate the dispersion of CNTs. Such reduces the hydrophobicity of the CNTs surface and can thereby be regarded as a non-covalent surface modification.

Pristine CNT
Pristine CNTs are the original products (raw materials) without any surface modifications.

Quantum dot
A quantum dot is a particle of semiconductor crystal with typical dimensions of nanometres to a few microns.

Rope
A nanorope consists of nanofibres in a twisted conformation. Ropes are single-walled carbon nanotubes (SWCNTs) closely packed together through attractive van der Waals interactions. 100-500 SWCNTs can self-organise in this manner, maintaining a constant diameter over the entire length of the rope, which can be longer than 100 μm.

Tensile modulus
Also referred to as Young's modulus, tensile modulus is a material-dependent parameter in solid mechanics that describes the ratio of mechanical stress to strain.

Young's modulus
See tensile modulus.

1. Introduction

Since their initial discovery in 1991 (129), carbon nanotubes (CNTs) have been proposed to be useful for numerous applications, ranging from composite materials to electrical components and drug delivery. CNTs possess truly unique and desirable properties including their mechanical strength, chemical inertness and electrical conductivity that can lead to breakthroughs in many vital industries. Although they are potentially valuable in connection with composite production, energy storage, biomedicine, membrane technologies and electronics (16), even today, 20 years after their discovery, there are very few areas in which CNTs have replaced other materials, due to the problems involved in scaling-up their production.

At present, CNTs are used primarily to make composites (e.g., plastics and rubbers) lighter or stronger (174). Such products are found in cars and aircraft, sports articles and wind power plants. The global production of CNTs is now more than 2.5 tonnes/day and their use is predicted to increase even more rapidly in the future. This rising production, handling, use and machining of CNTs and related products will enhance exposure to CNTs in different occupational environments, with inhalation being the route of exposure that has been identified as potentially most hazardous.

CNTs exhibit two dimensions in the nanoscale (1-100 nm) resulting in fibre-shaped particles with high aspect ratios (i.e., high length-to-diameter ratios). Since they physically resemble asbestos fibres, there are suspicions that exposure to CNTs might be associated with hazards/biological effects similar to those caused by asbestos. The low bulk density of CNTs results in considerable dusting while handling and since they are so small, the number of tubes per unit mass is large. As is the case for all nanoparticles, CNTs also exhibit a very high surface-to-mass ratio. Together, these properties enhance the potential risk of being exposed to a large number (and extensive surface area) of CNTs.

2. Substance identification

CNTs are included in the definition of nanomaterials as adopted by the European Commission 2011: A natural, incidental or manufactured material containing particles, in an unbound state, as an aggregate or as an agglomerate and where, for 50% or more of the particles in the number size distribution, one or more external dimensions is in the size range 1 nm-100 nm. In specific cases and where warranted by concerns for the environment, health, safety or competitiveness the number size distribution threshold of 50% may be replaced by a threshold between 1 and 50%. By derogation from the above, fullerenes, graphene flakes and single wall carbon nanotubes, with one or more external dimensions below 100 nm, should be considered as nanomaterials (80).

CNTs consist of carbon structures resembling graphene sheet rolled into a seamless cylinder. In a graphene sheet, each carbon atom is bonded to three others in a plane, giving rise to fused hexagonal rings, such as those in aromatic hydrocarbons. CNTs can consist of a single cylinder (single-walled carbon nanotubes or SWCNTs) or of many SWCNTs stacked one inside one another in concentric layers held together by van der Waals forces (multi-walled carbon nanotubes or MWCNTs). The larger MWCNTs can contain hundreds of concentric shells, separated typically by a distance of approximately 0.34 nm (261). The C-C bond in the graphene sheet of SWCNTs is 1.42 Å (0.142 nm) in length (356). In the present document, studies using double-walled carbon nanotubes (DWCNTs) (consisting of two graphene cylinders) are combined with investigations involving other MWCNTs. To date, only one CAS number, 308068-56-6, has been assigned to CNTs and therefore the numbers of walls and other intrinsic properties of CNTs are not considered.

Although generally categorised into only two different types, the CNT preparations can vary considerably with respect to diameter, length, atomic structure, surface chemistry, defects, impurities (including catalysts, see Section 3.1), and functionalisation (see Sections 3.1 and 4.2.3).

The diameter of a CNT depends mainly on the number of graphene layers it contains and its chirality (see below). SWCNTs and MWCNTs usually have diameters of approximately 1-3 nm (144) and 10-200 nm (119), respectively. The variation in diameter reflects the synthetic procedure, where the diameter of the catalytic metal particle employed plays a critical role, especially in the case of SWCNTs (see Section 4.2.1).

The length of a typical CNT is a few micrometres, but this length often varies between a few hundred nm and as much as approximately 10 µm. Moreover, tubes as long as 50 µm are common and most CNT preparations contain tubes that vary widely in length. CNTs designed to be used for future biomedical applications (e.g., as drug carriers or contrast agents) are typically shorter (i.e., 100-300 nm) than those used in production processes (373). The longest CNT reported to date was 18 cm (349) and the shortest is the organic compound cycloparaphenylene (139), only one hexagonal ring long.

Scanning electron microscopic (SEM) images depicting typical MWCNTs following synthesis as well as the typical physical characteristics of MWCNTs (Baytubes) in various states of dispersion are shown in Figure 1.

The structure of carbon nanotubes (tube chirality)

The atomic structure of CNTs is described in terms of tube chirality. In principle, the orientation of the graphene sheet when the tube is being formed determines this chirality. Two common conformations are the so-called armchair and zigzag conformations. The chiral angle (defined as the orientation of the axis of the carbon hexagon relative to the axis of the CNT (333) also influences the diameter of the nanotube, since the inter-atomic spacing of the carbon atoms is fixed (as previously mentioned at 1.42 Å) (356). In MWCNTs adjacent layers have different chiralities.

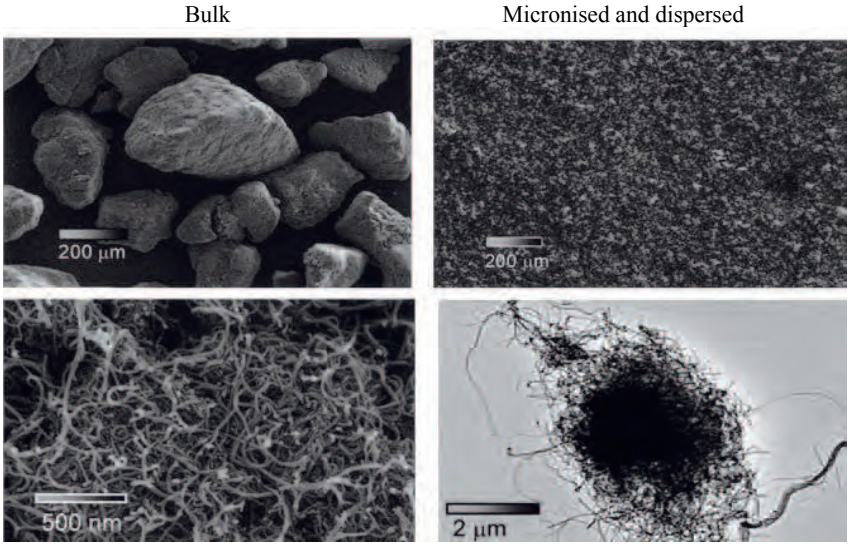

Figure 1. Scanning electron micrographs of MWCNTs (Baytubes) in bulk form and after micronisation and dispersion for inhalation studies. Reprinted from Pauluhn 2010 (255), Toxicological Science 113:226-242 by permission of Oxford University Press.

Moreover, the chirality of a CNT also affects its optical and in particular, the electrical properties. Although graphene in itself is a semi-metal, CNTs can be either metallic or semiconducting, depending on the chiral angle. At the same time, chirality has very little influence on the mechanical properties (333).

To date, the chirality of the CNTs has not been taken into consideration in any toxicological investigation.

Defects in carbon nanotubes

During their synthesis, certain kinds of gross defects could occur in CNTs. One example are collapsed nanotubes such as ‘‘bamboo-like’’ closures, that can easily be identified by transmission electron microscopy (TEM) (286). Such geometrical and topological defects are technologically important, since they can dramatically alter for example the electrical properties of CNTs (136, 286). Defects such as pentagon-heptagon pair (5-7 pair), the simplest and most elegant topological defect (136), can be utilised to connect semi-conducting and metallic tubes, allowing the formation of semiconductor-semiconductor, semiconductor-metal and metal-metal junctions (25).

Consequently, nanoscale devices comprised entirely of carbon can be constructed. CNTs are generally unreactive, although defects in the structure (such as missing carbon atoms and more highly strained curved-end caps) could elevate their reactivity (66, 187). Exogenous impurities are discussed in Section 3.1.

3. Physical and chemical properties

Nanoscale materials possess unique physical and chemical properties, which may differ from materials of similar composition at the macroscale. This section describes the physical and chemical properties of CNTs and CNT preparations – divided into mechanical, electrical, optical and thermal properties. Other important physical properties discussed are the agglomeration/aggregation state, bulk density, impurities, and, finally, the specific surface area, a property thought to be highly relevant with respect to toxicological responses to inhaled nanomaterials such as CNTs.

SWCNTs do not normally exist as individual tubes (174), but rather, due to van der Waals forces, form aggregates or agglomerates of microscopic bundles or ropes (Figure 2) typically 5-50 nm in diameter (204). The bundles subsequently agglomerate loosely into small clumps. The MWCNTs, with several sheets of graphene rolled into a cylinder, also tend to form bundles, but the van der Waals forces involved here are in general weaker than in the case of the SWCNTs. Therefore, MWCNTs more often exist as individual tubes (174, 378).

To determine whether CNTs are present as individual tubes or agglomerates, TEM is performed. Examples of such imaging of CNTs can be seen in Figure 2. From a toxicological point of view, the aggregation/agglomeration state of inhaled tubes is highly relevant since this determines, for example, the site of their deposition in the lungs (discussed further in Section 7.1).

The bulk density of CNTs is quite low and varies with the production procedure employed (see further Section 4.2.1). Comparison of the powder resulting from Laser ablation to that produced by the high-pressure carbon monoxide (HiPCO) process revealed that the latter yielded a bulk density as low as approximately 1 mg/cm^3 (17). Bayer Material Science specifies that the bulk density of their Baytubes (MWCNTs) is 120-170 mg/cm^3, but measurement generally gives a value of approximately 100 mg/cm^3 (254). For comparison the bulk densities of

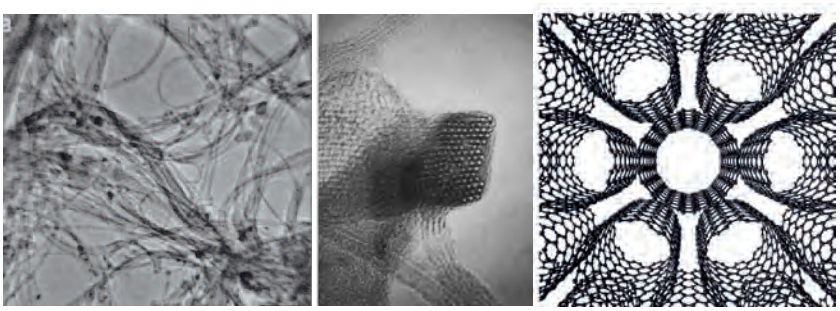

Figure 2. Transmission electron micrographs of ropes and a bundle of SWCNTs (from Thess *et al* 1996 (330), Science 273:483-487. Reprinted with permission from AAAS) and a schematic illustration of ropes of SWCNTs (reprinted by permission from Macmillan Publishers Ltd: Delaney *et al* 1998 (62), Nature 391:466-468, copyright 1998).

pure graphite and graphite powder are 2 200 and 200-600 mg/cm^3, respectively (49, 315).

3.1 Chemical composition

As described in the previous section, pure CNTs consist of only one or several hexagonal graphite sheets of carbon atoms rolled into tubes. CNTs are relatively non-reactive and SWCNTs must be heated to 500 ºC in order to be oxidised and burned in air (383). However, due to manufacturing processes, CNT preparations contain not only SWCNTs and MWCNTs, but also a variety of residual impurities (66).

These impurities can be classified as metals, supporting material or organics (66). In the production of CNTs, metal catalysts are often used, the most common being iron, nickel, cobalt and molybdenum. In producing SWCNTs, the presence of catalytic metals, most commonly molybdenum, is crucial and the finished product demonstrates a higher content of trace metals (160) than in the case of MWCNTs. Supporting material such as fine alumina, magnesium oxide or silica is often included to support the catalyst or region of growth.

Residual organics can be divided into two groups, i.e., organic molecules and various forms (amorphous or micro-structured) of bulk carbon, such as soot particles, fullerenes and/or graphene sheets (174). The levels and types of impurities depend on the procedure used for production (see Section 4.2.1). In general, gas-phase processes tend to produce CNTs with fewer impurities and are also more amenable to large-scale processing. The purity of commercial CNT preparations may vary considerably (60-99.9%, see further Chapter 11). The removal of remaining impurities and unwanted defects in the graphene layers involves harsh conditions (e.g., mechanical handling, treatment with strong acids, etc.) and therefore tends to shorten the CNTs (192).

Other chemicals may be encountered on the surface on the CNTs. The CNTs can be intentionally chemically modified, for example, by coating them with different functional groups to obtain desired chemical and physical properties. Functionalisation is commonly designated to enhance the dispersion of CNTs in aqueous solutions, since unfunctionalised CNTs have a pronounced tendency to interact hydrophobically and form aggregates (166). Functionalisation is described in more detail in Section 4.2.3.

3.2 Mechanical properties

One of the desirable properties of the CNTs is their physical strength. According to Cheung and colleagues, in terms of tensile strength and elastic modulus, CNTs are the strongest and stiffest materials, respectively, yet discovered, with an estimated tensile strength of 200 GPa (44). SWCNTs can be as much 10-fold stronger than steel (44, 341, 378). Closely packed nanotube ropes have a yield strength exceeding 45 GPa, which is more than 20 times that of typical high-strength steels

(2 GPa) (332, 341). With a Young's modulus (also known as tensile modulus) of more than 1 TPa, CNTs can also be 20% stiffer than diamond (44, 332).

This great strength is a result of the covalent bonds (sp^2 hybridisation) formed between the individual carbon atoms. However, high strength is solely an axial property of nanotubes. In the radial direction these tubes are rather soft and can be deformed by van der Waals interactions with adjacent nanotubes (283). They are highly flexible and can be bent repeatedly by as much as 110° without being damaged (130).

CNTs in composite materials

Much effort has been put into exploiting stiffness and strength of CNTs to improve the mechanical characteristics of polymers, mainly as CNT/polymer composite material. Addition of CNTs can alter the mechanical properties of a polymer significantly (105, 333). In addition, the unique properties of CNTs have also been exploited in several other types of composites such as CNT/ceramic composites and CNT/metal composites.

CNTs can also change the thermal properties and enhance the conductivity of the composite material (170). As pointed out by Harris and co-workers, although most interest has been focused on exploiting the mechanical properties of CNTs, interest in their electrical and optical properties is growing (see separate subsections below) (105). Utilisation of the unique properties of the CNTs fully could yield strong, stiff and thermally and electrically conductive composites of low density. However, to date CNTs are used in only a few commercial applications, and for achievement of the full potential of this approach many problems remain to be solved.

3.3 Electrical properties

Depending on their chirality, CNTs can act as either semiconductors or conductors (25). The electrical properties are directly related to the chirality of the tubes and, in case of small-diameter CNTs, the curvature (195). In theory, metallic nanotubes could carry an electric current density of 4×10^9 A/cm^2, which is more than 1 000-fold greater than that of metals such as copper (44, 332).

The potential applications of CNTs as electric components are numerous. For example, SWCNTs with different electrical properties could be joined to form a diode (46). Moreover, since the electrical properties of CNTs can be altered by deformation and stretching of the tubes, they might prove to be valuable in electromechanical devices, especially sensors (200).

As one example, a semiconducting CNT with a diameter of 1 nm has a bandgap of 1 eV, while a semi-metallic CNT of comparable diameter has a bandgap of only 40 meV. For semiconducting CNTs the bandgap is inversely related to the diameter. Their semiconducting properties make them potentially useful as current-carrying elements in nanoscale electronic devices (7).

3.4 Optical and thermal properties

SWCNTs strongly absorb near-infrared light (800-1 600 nm) (44), which spans over wavelengths (800-1 400 nm) that passes through biological tissues without significant scattering, absorption, heating or damaging. Consequently, the optical properties of SWCNTs can be utilised for photothermal therapy (38, 149, 365) and photoacoustic imaging (60).

As expected, CNTs exhibit pronounced thermal conductivity, e.g., SWCNTs should have thermal conductivities as high as 6 000 W/m K (where the corresponding value for diamond is 3 320 W/m K) (332). In addition, SWCNTs are stable at temperatures as high as 2 800 °C in vacuum and 750 °C in air (332). In the future, these thermal properties of CNTs may be utilised in highly conducting components of integrated nanoscale circuits (e.g., in transistors or interconnects) and in thermal management (e.g., in thermal interface materials) (260, 312).

3.5 Specific surface area measurement

Due to their small size and structure, each CNT demonstrates an exceedingly high surface-to-mass ratio, referred to as the specific surface area. The specific surface area depends on the diameter, number of concentric layers, and degree of bundling. Single SWCNTs exhibit a specific surface area of approximately 1 300 m^2/g whereas for single MWCNTs the corresponding value is a few hundred m^2/g (257). Due to bundling, most preparations of SWCNTs have in practise lower specific surface areas than single tubes, often approximately 300 m^2/g (375). Table 1 documents size and surface area-to-mass ratios for some of the CNTs and other nanomaterials used in the toxicological investigations described in Chapters 7-11.

All surface area values presented in this document were obtained with the BET method, the most widely used procedure for determining the specific surface area of powders. It was developed by Brunauer, Emmett, and Teller (33). In the BET method, the surface area of a given amount of powder on a filter is estimated from the adsorption of a gas (at the boiling temperature of the gas and under atmospheric pressure), most often nitrogen, onto its surface. The amount of gas absorbed is converted to the specific surface area by applying the multilayer adsorption theory (33). Several commercial devices utilise this principle. It has been suggested that the BET method underestimates specific surface area in general (162) and that of airborne particles in particular (93). At present, there is no way to estimate the specific surface area of nanomaterial in air directly and indirect methods have so far not been adjusted for high-aspect ratio nanomaterials. Furthermore, the BET method gives a single average for the whole sample, and no information about the surface area size distribution. The BET method requires a large sample, therefore the specific surface area of airborne fibres is often estimated from measurements performed on bulk samples of produced CNTs. It is not certain that the specific surface areas found of the bulk material are representative to what becomes airborne and inhaled.

Table 1. Characteristic size and specific surface areas (surface area per mass) of CNTs, certain other common nanoparticles and reference particles commonly employed in toxicological studies.

Material	Particle size, diameter (nm) × length (μm)	Specific surface area (m^2/g)	Manufacturer	Reference
SWCNT	1-2×0.5-2	343	Cheap Tubes Inc., Brattleborough, VT, USA	(20)
SWCNT	1-2×5-30	510	Same as above	(20)
SWCNT	0.8-1.2×0.1-1	508	Carbon Nanotechnologies, Houston, TX, USA	(305)
SWCNT	0.9-1.7×<1	731	Thomas Swan, Consett, UK	(138)
SWCNT	1-4×0.5-2	1 040	Carbon Nanotechnologies, Houston, TX, USA	(359)
SWCNT	200×0.7 (bundle in air)	1 064	National Institute of Advanced Industrial Science and Technology, Japan	(215)
SWCNT	1.3×3.5	1 700	SES Research, Houston, TX, USA	(102)
MWCNT	110-170×5-9	12.8	Sigma-Aldrich, St. Louis, MO, USA	(249)
MWCNT (Mitsui MWNT-7)	49×3.9	26	Mitsui & Co., Ltd, Tokyo, Japan	(206, 265)
MWCNT	63×1.1 (in air)	69	Nikkiso Co., Ltd, Tokyo, Japan	(216)
MWCNT	10-20×5-15	100	Shenzhen Nanotech, Port, Shenzhen, China	(212, 213)
MWCNT	11×1.1	130	SES Research, Houston, TX, USA	(102)
MWCNT (NC 7000)	5-15×0.1-10	250-300	Nanocyl S.A., Sambreville, Belgium	(198)
MWCNT (Baytubes)	10×0.2-0.3	259	Bayer Material Science, Leverkusen, Germany	(76, 255)
MWCNT	50×10	280	Shenzhen Nanotech, Port, Shenzhen, China	(180, 181)
MWCNT	20-40×0.5-5	300	NanoLab, Inc., USA	(292)
MWCNT	20-40×5-30	380	Nanotech Port, Shenzhen, China	(374)
C_{60} (99% pure)	>20 nm	0.2	M.E.R. Co., Tuscon, AZ, USA	(20)
C_{60} (99.9% pure)	0.7 nm	<20	Sigma-Aldrich, Brøndby, Denmark	(138)
Carbon black, N990	>200 nm	7.7	Engineered Carbons Inc., Borger, TX, USA	(20)
Carbon black, N110	15 nm	111	Cabot Corp., Billerica MA, USA	(20)
Carbon black, Printex 90	14 nm	338	Degussa GmbH, Frankfurt, Germany	(138)
Nano-Al_2O_3	45 nm	28.3	Nanotek Instruments Inc., Dayton, OH, USA	(21)
α-Quartz	Not given	3.6	Quarzwerke GmbH, Frechen, Germany	(76)
Silica crystalline (Min-U-Sil 5)	>0.1-5 μm	5.1	US Silica Company, Berkeley Springs, WV, USA	(20)
Nano TiO_2, rutile	10 nm thick, 40 nm laterally	190	Sigma-Aldrich, St Louis, MO, USA	(20)
Nano TiO_2, anatase	10 nm	274	Nanostructured & Amorphous Materials, Houston, TX, USA	(20)

Al_2O_3: aluminium oxide, C_{60}: spherical fullerene, TiO_2: titanium dioxide.

4. Occurrence, production and use

4.1 Occurrence

CNTs are generated in natural, incidental, and controlled flames (226-230). Naturally occurring MWCNTs have, for example, been detected in 10 000 year-old ice core melt water (227) and in smoke from wood combustion (229), as well as in a mixture of coal and petroleum (353). Anthropogenic MWCNTs are products of the combustion of natural gas (methane and propane) (228) and are present in smoke from paraffin wax candles (183).

MWCNTs generated by combustion of fuel gas occur as aggregates of individual tubes with diameters ranging from approximately 3 to 30 nm (226). The average aggregate diameter range from approximately 1 to 5 µm (aerodynamic) diameter and contain as many as 3 000 primary nanotubes (228). The MWCNTs formed through combustion of paraffin wax candles are 15-20 nm in diameter and approximately 1-3 µm in length (183). Murr and colleagues maintain that aggregates of CNTs are ubiquitous in both indoor and outdoor air, with levels of MWCNT aggregates estimated to be approximately 10^{-1}/cm^3 and 10^{-4}-10^{-5}/cm^3, respectively (228).

SWCNTs can also be generated locally in connection with major disasters e.g., as a result of the combustion of fuel in the presence of carbon and metals during the World Trade Center disaster. Following this attack, tangled, long, hair-like ropes and stacks of SWCNTs were detected both in dust and in the lung tissues of workers involved in rescue, relief and clean-up (364).

4.2 Production

Preparations of CNTs are not homogenous, but contain a diverse mixture of many different types of tubes, with varying numbers of walls, diameters, lengths, chiral angles, chemical functionalisations, purities and bulk densities. The global production in 2005 was estimated to exceed 294 tonnes for MWCNTs and several hundred kilograms in the case of SWCNTs (171). In the following year, the corresponding values were approximately 300 and 7 tonnes, respectively (363). Today, the global capacity for production of CNTs (primarily MWCNTs) is more than 2.5 tonnes/day (78).

For both types of CNTs, Asian production capacity is 2-3-fold greater than the estimated capacity for North America and Europe combined (363), with Japan being the clear leader in the production of MWCNTs.

In the Nordic countries, only a few commercial companies produce MWCNTs (154, 299). In Sweden, at least three companies conduct research concerning applications of CNTs in composites (299). In Finland, one laboratory has developed a CNT-epoxy resin used to manufacture high-tech hockey sticks for professional and amateur players (299). In Norway, one manufacturer is producing MWCNTs by the arc discharge procedure.

4.2.1 Production techniques

A multitude of approaches for synthesis of CNTs have been reported (27). One of the principal techniques involves the use of a transition metal catalyst in the presence of atomic carbon at high temperature and/or pressure (203). Both SWCNTs and MWCNTs are usually produced by one of three different techniques, i.e., chemical vapour deposition (CVD), arc discharge and laser ablation.

Depending on the technique, impurities such as remaining catalyst particles, amorphous carbon, soot, graphite and non-tubular fullerenes are also present in the finished preparation (see also Section 3.1) (78, 171, 174). Removal of impurities requires chemical purification processes such as acid reflux, filtration, centrifugation and repeated washing with solvents and water (78).

Chemical vapour deposition

Thermal CVD (also known as catalyst CVD) is the most widely employed procedure for the production of CNTs, because of its low initial costs, the high yield and purity of the preparation obtained and ease of scale-up (169). This technique provides both simple and economic synthesis of CNTs at low temperature and ambient pressure. According to Karthikeyan and co-workers, low-temperature CVD (600-900 °C) yields MWCNTs, whereas at higher temperatures (900-1 200 °C) SWCNTs are formed (152).

CVD is based on thermal decomposition of a hydrocarbon vapour in the presence of a metal catalyst. The precursor carbon containing gas (e.g., carbon monoxide, methane or acetylene or even ethylene, benzene or xylene) is first heated with a plasma or a coil and then allowed to react with a metal catalyst (such as iron, cobalt or nickel and/or their alloys) which acts as a "seed" for growth (78, 310, 363). In addition to the temperature, the size of the catalyst particle determines whether SWCNTs or MWCNTs are formed (314), with the quality of the latter generally being higher (78). Although MWCNTs can be produced without catalysts, the presence of a small amount of metal catalyst helps to align the CNTs (174).

A procedure for the manufacture of MWCNTs by thermal CVD is illustrated schematically in Figure 3. The raw CNT preparation subsequently undergoes several post-treatments, e.g., dispersion and functionalisation, involving several steps of sonication. A variant of CVD, high-pressure carbon monoxide (HiPCO), is employed for mass production of CNTs.

Arc discharge

Arc discharge, the first technique used to prepare CNTs (129), generally involves an anode and a cathode composed of high-purity graphite. In principle, a voltage is applied across these rods until a stable arc is achieved, with the anode being consumed while CNTs grow on the cathode. The gap between the electrodes is maintained constant by adjusting the position of the anode and the entire process takes place under a helium atmosphere.

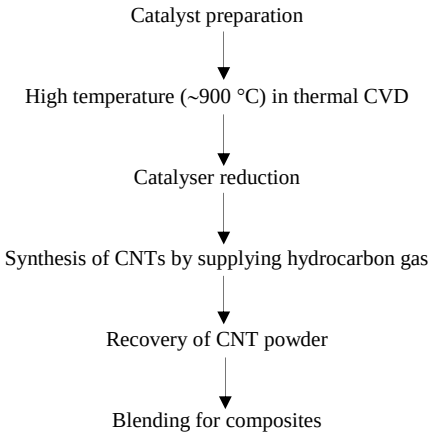

Figure 3. Schematic illustration of a procedure for the manufacture of MWCNTs by thermal CVD. Modified from Han *et al* 2008 (103).

To obtain SWCNTs, the electrodes are doped with a small amount of metallic catalyst particles (146, 302, 333) and the diameter achieved is dependent on the properties of this catalyst (261, 302). Size and shape of the graphite rods, level and nature of doping, etc. can vary. This approach generally produces CNTs in high yield and is a relatively cheap, but results in high levels of impurities (66).

Laser ablation

Laser ablation as a means of generating CNTs was initially discovered by Smalley and co-workers (99). Like arc discharge, this initial method produced MWCNTs. Subsequently, this approach has been refined by introducing catalyst particles (cobalt and nickel mixture), which allows SWCNTs to be synthesised (100, 278, 333). In principle, a graphite target is maintained at close to 1 200 °C while an inert gas (often argon) is bled into the chamber. Thereafter, pulses of a high-intensity laser beam are used to vaporise the graphite target and CNTs develop on the cooler surfaces of the reactor as the vaporised carbon condenses. The use of pure electrodes results in MWCNTs, whereas for formation of SWCNTs, the targets are doped with cobalt and nickel (58, 333). The diameter of these SWCNTs is determined by the reaction temperature and the yield obtained with laser ablation is approximately 70%.

4.2.2 Purification and sorting procedures

A critical issue in connection with the mass production of CNTs for specific applications, as well as for toxicological testing, is the purification and isolation of more homogenous preparations of CNTs. The lack of uniformity in the properties of SWCNT preparations is a major reason why their commercial applications are still quite limited (111).

Although several purification procedures have been suggested, these still need to be refined and scaled up (16, 192). For example, even after the catalyst metals have been removed, significant amounts of residual metals remain in the CNT preparation. Since purification also alters CNTs, removal of impurities must be balanced against the introduction of defects into the tubes. For instance, purified nanotubes are likely to contain additional carboxylic acid (-COOH) residues (66).

The purification methods are of two main types, namely, removal of residual impurities and selective procedures that will result in CNTs with more homogenous properties, such as diameter, length, electrical properties, etc. For removal of amorphous soot, metal catalyst particles and supporting material, washing or ultrasonication in combination with acids or bases is often used. Removal of supporting materials such as silica and alumina requires stronger acids which might destroy the CNTs, so that other types of supporting materials (e.g., magnesium oxide) that dissolve in milder acids are employed more frequently. Other examples of purification procedures include magnetic purification, functionalisation and microfiltration and combinations are often utilised.

CNTs can be separated into fractions that are more homogeneous with respect to length and diameter by chromatography. The most powerful resolution presently available yields preparations that vary in length by <10% (121). CNTs of different diameters can be separated by density-gradient ultracentrifugation (111).

However, to obtain even more homogeneous preparations of CNTs, more specific processes are required. For example, many electronic applications require semiconducting or metallic CNTs (117) and for use in electronic devices conventional synthesis of CNTs of mixed chiralities is inadequate, since specific individual chiralities are required.

Several methods for separating semiconducting and metallic CNTs are available, but not yet for mass production. One promising approach employs density-gradient ultracentrifugation to separate CNTs coated with a surfactant on the basis of their densities (9), since CNTs with different diameters and chirality exhibit slight differences in density. SWCNTs embedded in an agarose gel can be separated by freezing, thawing and compression (325) as well as by column chromatography (326). Purification of CNTs with individual chiralities has been achieved by Tu and colleagues (338).

4.2.3 Functionalisation

Prototype preparations of CNTs in all forms, known as pristine CNTs, are extremely resistant to wetting. They are difficult to disperse and dissolve in aqueous solutions or organic media, because of their strong tendency for hydrophobic aggregation (166). This property also makes it difficult to use CNTs in composites.

Through functionalisation of the CNT, i.e., attachment of functional groups, their chemical, electrical, magnetic, and/or mechanical properties can be altered (117, 166, 313). The water solubility of CNTs can be dramatically improved by coating with different functional groups (166) and the mechanical and electrical properties can be fine-tuned.

The three main types of functionalisation are covalent or non-covalent exohedral functionalisation and endohedral functionalisation. The exohedral functionalisation involves covalent or non-covalent linkage (e.g., through van der Waals forces and π-stacking) while the third type is based on filling the CNTs with atoms or small molecules. With non-covalent linkage of functional entities, the stable and attractive surface structure of the CNT is preserved. This approach can be applied in search of non-destructive methods of purification as well as in transferring CNTs to an aqueous phase.

Since the surface of the CNTs interacts with biological systems, functionalisation may alter their toxicokinetics and toxicity. The large surface area and internal volume of CNTs allows drugs (e.g., antineoplastic drugs) and various small molecules (e.g., contrast agents) to be loaded on- or into the nanotube. The surfaces of CNTs used in medicine are modified to control the degree of aggregation in the intended biological environment (blood, intraperitoneal, interstitial fluids, etc.), which plays an important role in pharmacological performance (44, 166). CNTs coated with amphiphilic macromolecules (e.g., lipid-polyethylene glycol conjugates), copolymers, surfactants and/or single-stranded DNA have found a number of biomedical applications (166), as have covalently functionalised CNTs (e.g., cycloaddition of ammonium groups or acid oxidation to generate carboxylic acid groups).

4.3 Use

CNTs have a wide variety of applications, including incorporation into fabrics, plastics, rubbers, reinforced structures, composite materials and household commodities to render them lighter and/or more wear-resistant (174). Although more extensive applications are expected in the future (Table 2) (2, 27, 77, 166, 171, 299), research and development remains for the most part at the prototype stage. At present, CNTs are found in products made of nanocomposites (polymers containing 1-10% CNTs by mass) such as sports articles (e.g., super-strong tennis rackets, hockey sticks, racing bikes/cycles, cycling shoes, golf clubs, skis, dart arrows and baseball bats), car parts and aircraft and wind power plants (125, 171, 291, 331).

Lithium ion batteries used in e.g., mobile phones and laptops also contain CNTs (171, 381). Moreover, CNTs are utilised in anti-fouling paints designed for marine environments (277). Other promising areas includes textiles made of fibres of CNT/polymer with electrical, antistatic, thermal conductive, flame retardant and tear-proof properties (26, 171, 299) and concrete reinforced with CNTs (171, 299, 361). Table 2 presents a list of different possible applications of CNTs, including medical applications.

Table 2. Future potential applications of CNTs. Taken from Köhler *et al* (171).

Area	Application
Materials and chemistry	Ceramic and metallic CNT composites Polymer CNT composites (heat-conducting polymers) Coatings (e.g., conductive surfaces) Membranes and catalysis Tips of scanning probe microscopes (SPM) Building materials
Medicine and life science	Medical diagnosis (e.g., analyses on a chip, imaging) Medical applications (e.g., drug delivery) Cosmetics (anti-ageing creams) Chemical sensing Filters for treatment of water and food
Electronics and ICT (Information and Communication Technology)	Lighting elements, CNT-based field emission displays Microelectronics (single-electron transistors) Molecular computing and data storage Ultra-sensitive electromechanical sensors Microelectrical-mechanical systems (MEMS)
Energy	Hydrogen storage, energy storage (super capacitors) Solar cells Fuel cells Superconductive materials

5. Measurements and analysis of workplace exposure

5.1 Air exposure

Traditional occupational hygiene measurements of airborne particles are based on whether the particles/dust is fibrous or not. Fibrous particles are usually quantified as number per unit volume (fibre/cm^3), while the non-fibrous particles are measured in terms of mass per unit volume (mg/m^3). Furthermore, most occupational exposure limits (OELs) for particles/dust are based on 8-hour time-weighted average (TWA) levels.

Airborne exposure to CNTs can be measured over time with filter-based methods or monitored by real-time aerosol instruments. Filter-based sampling is suitable both for personal sampling in the breathing zone and for stationary sampling near (or distant from) the source of emission. The period of sampling can range from a specific work task to an entire shift.

Real-time instrumental monitoring reveals levels continuously (e.g., every second) during a specific task or entire shift, as well as information about peak exposure, which is not available from filter-based procedures. However, the real-time instruments presently available are not suitable for personal sampling in the breathing zone of the worker i.e., they are simply too big. Consequently, real-time sampling is stationary, typically in the close vicinity of the source of emission (emission measurement) or in the general work area (background measurement).

Occupational exposure to CNTs has been measured in terms of the mass concentration of total dust, mass concentration of respirable dust, mass concentration of elemental carbon (EC), fibre concentration and numbers of individual tubes or CNT structures (i.e., CNT containing structures) per unit volume of air. Moreover, the size distributions and surface areas of airborne CNTs present in workplaces have been characterised.

Total dust samples

The total dust has been monitored both in the breathing zone of the worker and with stationary sampling, in most cases using open-face sampling cassettes with mixed cellulose ester (MCE) filters (103, 177, 209) or, in case of metals, methylcellulose ester filters (203). The mass concentration of CNTs (together with all other particulate air pollutants) was then determined by gravimetric analysis of the filter samples, but no lower limits of detection (LODs) were indicated in these studies. With gravimetric analysis, no distinction between CNT structures and other types of particles e.g., impurities, background particles etc. is possible.

In one study, the filter samples were analysed by inductively coupled plasma-atomic emission spectrometry (ICP-AES) employing the levels of iron and nickel as surrogates for total CNT mass (the CNT bulk material consisted of 30% catalyst material) (203). The LODs observed for iron and nickel were 0.064 and 0.018 µg, respectively.

Respirable dust samples

In one investigation the MWCNTs in respirable dust were monitored with a personal sampler for particulate matter with maximal aerodynamic diameter of 4 µm (PM_4) (323). No distinction was made between CNT structures and other types of particles e.g., impurities, background particles and the like.

Elemental carbon samples

In one study, respirable EC was collected using cassettes with quartz fibre filters 37 mm in diameter and a cyclone (GK 2.69 BGI) and inhalable EC collected on quartz fibre filters with diameters of 25 mm in open-face plastic cassettes (57). Subsequently, the mass concentration of EC was analysed thermal-optically with a flame ionisation detector (FID) in accordance with the Manual of Analytical Methods (NMAM No. 5040) of the US National Institute for Occupational Safety and Health (NIOSH) (238). No distinction between CNTs and other types of graphite-like impurities was made.

Fibre samples

Sampling of fibres has been performed by sucking air through an MCE filter in asbestos sampling cassettes equipped with an electrically conductive 50-mm extension cowls (19, 21, 22), with subsequent analysis by phase contrast microscopy in accordance with the NMAM No. 7400 (236). The LOD of this procedure with respect to fibre diameter was approximately 250 nm (301).

Samples of individual tubes or CNT structures

The number concentrations of individual tubes or CNT structures have been determined by drawing air through MCE filters in asbestos sampling cassettes equipped with an electrically conductive 50-mm extension cowls, followed by analysis with SEM or TEM in accordance with NMAM No. 7402 for asbestos fibres (57, 103, 177, 237, 321). In two of these cases, the filters were coated with carbon and mounted onto carbon-coated nickel or copper grids (57, 103, 177, 337), and in the other, the filters were coated with nanogold (21) or platinum-palladium (244). The numbers of individual tubes or CNT structures were counted and their morphology and size characterised. Note that the World Health Organization (WHO) rules concerning fibre counting (354) cannot be followed strictly due to tube length shorter than 5 μm and CNTs often not have the typical fibre dimensions (see Section 6.2.3).

Chemical composition

There are several available techniques to determine the chemical composition of a CNT sample e.g., ICP-AES for tracing metals (203), and electron microscopy with energy-dispersive x-ray analyser (EDX) for elemental analysis (19, 21, 22, 103, 177). In one study a photoelectrical aerosol sensor (PAS) was used as indicator for carbonaceous particle composition (376). For additional information on methods employed for determining chemical composition see (51).

Size-related dose metrics

Occupational exposure to airborne CNTs in workplaces has also been characterised by measuring other metrics such as particle number concentration, particle size distribution, particle surface area, particle morphology and size, and chemical composition (19, 21, 22, 56, 143, 177, 203, 209, 244, 321, 337, 376). The various types of real-time aerosol instrumentation and off-line techniques employed are summarised in Table 3, which also includes real-time mass concentration measurements.

As discussed above CNTs can vary, e.g., in wall number, length, shape, particle dimensions and degree of agglomeration (11), the levels and nature of impurities (such as metal (cobalt, iron, nickel and molybdenum) from catalysts, amorphous carbon, soot or graphite from production technique), and surface structure (which may also be intentionally altered through functionalisation or coating with metals, protein or polymers). The physical and chemical properties of CNTs and, thereby, their dosimetry can be influenced by all these factors. Thus, conversions, for example, of number size distributions to other dose metrics such as mass involve assumptions concerning particle shape and effective density and are therefore associated with a great deal of uncertainty. Measurements of exposure to airborne CNTs must be complemented with characterisation of the bulk material, e.g., surface area by the BET method (see Section 3.5).

Table 3. Techniques employed for characterising CNT aerosol exposure in workplaces.

Metric/Technique	Range of measurement (nm)	Detection limit	Reference
Particle number concentration			
Fast mobility particle sizer (FMPS)	5.6-560	Lower: ~100 particles/cm^3 at 10 nm to ~10 particles/cm^3 at 100 nm. Upper: ~1 000 000 particles/cm^3	(19, 21, 22)
Aerodynamic particle sizer (APS)	500-20 000	Upper: ~10 000 particles/cm^3	(21, 22)
Condensation particle counter (CPC)	10-1 000	1-100 000 particles/cm^3	(19, 21, 22, 56, 143, 177, 203, 209, 244, 321)
Ultrafine condensation particle counter (UCPC)	>3	0-100 000 particles/cm^3	(177)
Aerosol photometer (dust monitor)	250-32 000	-	(177)
Optical particle counter (OPC)	300-10 000	Upper: 70 000 particles/cm^3	(143, 203, 209, 244, 321)
Size distribution			
Scanning mobility particle sizer (SMPS) and differential mobility analyzer (DMA)	-		(209)
	4-160		(376)
	4-673		
	14-630		(103)
	14-500		(177)
	14-740	-	(244)
SMPS			(321)
FMPS and APS	5.6-20 000	-	(21, 22, 244, 337)
APS			(103)
UCPC	14-630	-	(103)
Electrical low pressure impactor (ELPI)	-	-	(209)
Aerosol photometer (dust monitor)	250-32 000	-	(177)
Surface area			
Diffusion charger (DC)			(56, 209)
Mass concentration (real-time measurements)			
OPC	300-10 000	-	(203)
Aerosol photometer (Dust Trak)	<2 500		(376)
	100-10 000	-	(21, 22, 56)
ELPI	-	-	(209)
Dust monitor	-	-	(321)
Aethalometer (black carbon particles)	-	-	(103, 177)
Particle morphology, size and number concentration (off-line)			
Thermophoretic precipitator (TP)	1- >100	-	(19, 21, 22)
Electrostatic precipitator (ESP)	1- >100	-	(19, 21, 22, 209)
Transmission electron microscopy (TEM)	-	Lower: 1 nm	(19, 21, 22, 143)
Scanning electron microscopy (SEM)	-	-	(19, 21, 22, 203, 321)
Scanning transmission electron microscopy (STEM)	-	-	(103, 177)
Chemical composition			
Photoionisation potential with photoelectric aerosol sensor (PAS)	-	Upper: 1 000 ng/m^3	(376)
Energy-dispersive x-ray analyser (EDX)	-	-	(19, 21, 22, 103, 177, 209)

Table 4. Comparisons of estimated fibre number and mass concentrations for various sizes of CNT structures [a,b]. Adapted from Schulte *et al* 2012 (300).

Fibre dimension Diameter × length (nm)	Fibre number concentration (fibre/cm^3) that is equivalent to 7 μg/m^3	Fibre mass concentration (μg/m^3) that is equivalent to 0.1 fibre/cm^3
2 × 500	2 200 000	0.0000003
25 × 1 000	7 100	0.00098
5 × 188 000	950	0.00074
100 × 50 000	8.9	0.078
29 × 773 000	6.9	0.10
2 110 × 10 000	0.10	7.0

[a] Based on assumption of individual structure volume and density (~2 mg/cm^3).
[b] Note that airborne CNTs in workplaces rather are agglomerated than individual structures.

Typically in connection with exposure to CNTs, a small mass concentration could contain a large number of CNT structures (both individual structures and agglomerates) due to low density. Schulte and co-workers have made comparisons of the mass and particle number concentrations for CNT structures of various sizes (Table 4) based on the assumption that the fibre number concentrations were equivalent to one given specific mass concentration (7 μg/m^3) and the fibre mass concentration was equivalent to one given fibre number concentration (0.1 fibre/cm^3) (300).

Most measurements of exposure to CNTs in different workplaces have determined mass and particle number concentrations. No direct measurement of the specific surface area of airborne particles is available (see the earlier discussion in Section 3.5).

One problem by measuring mass concentration for CNTs can be that a non-detectable mass does not mean a non-detectable number concentration, and the number concentration can instead be significant (143). Another problem associated with quantification of airborne CNTs is that dust sampling (both total and respirable) also includes all other airborne particles including EC particles from e.g., diesel emissions and seasonal burning of biomass (300). The degree of specificity can be addressed by examining the sample with TEM, SEM or scanning transmission electron microscopy (STEM). By the determination with electron microscopy methods the nature of the particles collected can be identified. In the future, continuous, parallel dust sampling with filter cassettes equipped with MCE filters for TEM analysis or polycarbonate membrane filters for SEM analysis will be necessary to evaluate specificity (210, 244, 321). Some attempts have been made to quantify airborne CNTs at the workplace (39). However, microscopy-based methods have not yet been developed for counting CNT structures and it is not clear how to count CNT fibre-like structures in heterogeneous structures e.g., individual CNT structures within an agglomerate (300). In workplaces the CNT structures are often agglomerated rather than individual structures (196, 300).

Total EC is another metric employed to assess exposure to CNTs and carbon nanofibres, but again parallel characterisation with TEM, SEM or STEM might be necessary to validate EC as a marker for CNT exposure.

The concentration of fibres has also been used to assess the exposure to CNTs (NMAM No. 7400 (236)) but this procedure only analyses fibres in micron size (>0.25 μm) and therefore could no individual or agglomerated CNTs be quantified (21, 22).

The number concentration of individual tubes or CNT structures has also been measured with TEM/SEM/STEM, together with, for example NMAM No. 7402 (237).

Although particle surface area might be a relevant dose metric concerning exposure to CNTs, it is not presently possible to perform personal sampling of surface area due to lack of portable/personal sampling instruments. However, personal monitors for determination of surface areas are under development. Today, the surface area of airborne particle cannot be measured directly, and the indirect methods employed often involve assumptions that are far from being valid for fibres.

Conclusion on air exposure measurements

Although there are a variety of methods and instruments, it is at present not clear which metric for air sampling is most closely correlated with the toxicological effects of CNTs. The different metrics used so far to describe occupational exposure to CNTs are difficult to compare. Until the most relevant metric has been identified (294) exposure to CNTs should be assessed with multiple dose metrics (e.g., EC, number of CNT structures/cm^3, respirable dust). Personal full-shift and time-integrated measurements of above suggested exposure markers can be used to quantify exposures of CNTs.

5.2 Dermal exposure

To date, potential dermal exposure to SWCNTs has been evaluated using cotton gloves placed over the rubber gloves normally worn by the worker, as a surrogate for the skin on the hands. The cotton gloves are removed immediately after handling the SWCNT material; placed in separate, sealed plastic bags; and later analysed for iron and nickel as surrogates for total nanotube mass by ICP-AES. SWCNT mass was estimated assuming that a combination of nickel and iron catalyst particles constituted 30% of the mass of this material. The ratio of iron to nickel was derived from the glove samples. The LODs for iron and nickel were 0.161 and 0.046, respectively (203).

Potential dermal exposure to MWCNTs has been measured using wipe samples collected on different surfaces in the vicinity of a loom in a textile-producing factory weaving with MWCNT-coated yarn (321). Areas of 100 cm^2 were wiped with 1×1.5 cm quartz fibre filters and the EC content of these filters then analysed with a carbon aerosol monitor. The amounts of EC on the shelf plate near the reels and on the top of the loom were 0.05 and 0.03 μg/cm^2, respectively. Thus, large numbers of fragments from the MWCNT-coated yarn were deposited close to where a strong mechanical force was applied to the yarn.

6. Occupational exposure data

6.1 General

Occupational exposure to CNTs can occur during the whole life-cycle of CNTs; from research in laboratories, production (primary manufacturing), research and development for incorporation of CNTs in products (secondary manufacturing), and down-stream applications e.g. manipulating and machining of products containing CNTs as well as via disposal and recycling. Workers are generally exposed to higher levels than the general population (21, 239, 361).

Even though during the research and developmental phases, the material is produced in very small quantities under controlled conditions (11), airborne exposure to CNTs does occur in research laboratories (57, 103, 143, 177). The closed systems generally utilised in the production of CNTs make the likelihood of exposure during this phase small (11). Maynard and co-workers reported that production of SWCNTs by the HiPCO process appears to lead to higher air concentrations and higher levels of glove contamination than other production methods. This may reflect the fact that HiPCO preparations have a lower bulk density and therefore become more easily airborne, than the more compact SWCNTs produced by laser ablation (203).

Emissions and thereby occupational exposure can occur directly in connection with the following sorts of activities in workplaces: primary manufacturing/synthesis, extraction/recovery/determination of yield (collection and manual transfer of product), handling/processing (weighing, mixing, drying, spraying, sonication, deliberate agitation), packaging/bottling, cleaning operations, cutting and sawing, and waste treatment (11, 57, 78, 110, 209). Handling of dry CNT powder is suggested to result in the highest level of exposure (11, 57). Köhler and colleagues found that CNTs are released into the air as agglomerated bulk powder rather than as individual nanotubes (171) (see Figure 1).

Aschberger and colleagues point out that future use of CNTs in drug delivery systems and for imaging may lead to occupational exposure of workers who manufacture and administer these preparations (11).

6.2 Airborne exposure

The limited data on occupational exposure to airborne CNTs currently available are summarised in Table 5. Both stationary measurements and measurements in the breathing zone of workers have been performed. In some cases, air samples were taken during specific procedures (e.g., during CVD growth of CNTs or during removal of the CNT powder produced) and in these cases the sampling time was often short (19, 203). The mass concentrations of airborne CNTs were measured at manufacturing facilities, packing facilities and research laboratories and the number concentrations of individual tubes or CNT structures were determined at primary manufacturers, research laboratories and in connection with down-stream applications. The mass concentrations of airborne EC in primary

manufacturers, secondary manufacturers and associated with one down-stream application have also been reported.

The characteristics of CNTs from workplaces producing and handling different types of CNT material are shown in Table 6. In this case all of the measurements were stationary, with the exception of one conducted in the breathing zone of the operator (21). Phase contrast microscopy cannot reveal whether CNTs are present as agglomerates or not. In eight of these investigations analysis by SEM or TEM revealed particles related to CNTs (103, 143, 177, 203, 209, 244, 321, 337), primarily agglomerated CNT structures or CNT tubes attached to clusters of nanoparticles.

6.2.1 Mass concentration

Primary manufacturers

Only a single study on airborne exposure in workplaces producing SWCNTs has been performed (203). Personal sampling was performed at four different facilities in the US that make SWCNTs either by the HiPCO procedure or laser ablation. The production vessels were placed into enclosures with clean air prior to removal of the powder. Airborne levels of SWCNTs were measured during the period (approximately 30 minutes) the worker spent in this enclosure removing the crude SWCNT material from the production vessel and handling it prior to processing. The mass concentration of unrefined SWCNTs in personal air was estimated to be 0.7-53 $\mu g/m^3$, with the peak value recorded by the real-time instruments of 1 600 $\mu g/m^3$ being associated with the use of a vacuum cleaner inside the enclosure (Tables 5-6).

To date, exposure has been assessed primarily in workplaces where MWCNTs are used or handled and most of the levels of total dust, both in personal and stationary measurements, have been approximately 100 $\mu g/m^3$ or less (Table 5). The first evaluation of occupational exposure to MWCNTs involved a research facility with monitoring both before and after implementation of protective measures. Personal exposure to airborne MWCNTs (total dust) ranged between not detectable (ND) and 332 $\mu g/m^3$ prior to the installation of protective equipment and between ND and 31 $\mu g/m^3$ afterwards. The corresponding ranges for stationary exposure were ND-435 $\mu g/m^3$ and ND-39 $\mu g/m^3$. No LOD was reported. The stationary concentration of black carbon rose to as high as 200 $\mu g/m^3$ when the blending equipment was opened, which may indicate release of MWCNTs (103).

Lee and colleagues assessed exposure in seven workplaces where MWCNTs are handled. The combined mean mass concentrations for all personal and stationary samples were 106 and 81 $\mu g/m^3$, respectively. Some of the personal measurements were performed for 3.1 and 6.0 hours and some of the stationary ones for 3.2 and 6.8 hours, but the range of sampling time was not reported. Nanoparticles and fine particles were most frequently released after opening the CVD cover. Other work processes associated with particle emissions were catalyst pre-

paration, spraying, CNT preparation, ultrasonic dispersion, wafer heating, and opening of the cover to the water bath (177).

When personal measurements of airborne MWCNTs were performed in two packing facilities, one with manual operations and the other automated, the background level was virtually the same (240 μg/m^3) in both cases. However, the workers in the automated packing facility were exposed to almost 10-fold lower concentrations (290 versus 2 390 μg/m^3, respectively) (322).

Down-stream applications

In one investigation, PM_{10} (equivalent to thoracic dust) was measured with an aerosol photometer (Dust Trak) both in the personal breathing zone of the operator and at the source (saw) during both wet cutting (diamond saw) and dry cutting (band saw) of two CNT composite laminate material (CNT-alumina and CNT-carbon) (Table 6). Samples without CNTs were also fabricated for comparison (base-alumina and base-carbon). The mean dust concentrations in the breathing zone of the operator during dry cutting in CNT-alumina and CNT-carbon were 800 and 2 400 μg/m^3 (corrected for background), respectively, with corresponding values at the source of 2 110 and 8 380 μg/m^3. Wet cutting in all, but one test (broken guard) reduced exposures to background levels (21).

The data documented in Table 5 allow the personal exposure associated with a certain work process or situation to be assessed. Manual packing and blending with open equipment result in the highest exposures. The mean and median levels of personal exposure during synthesis of CNT material were estimated to be 365 and 53 μg/m^3, respectively. It is important to note that occupational exposure to CNTs was higher in those facilities lacking process control and with lower industrial hygiene (103, 177).

6.2.2 Mass concentration of elemental carbon

Primary manufacturers

The average EC concentrations from personal and stationary measurements performed at three primary facilities for manufacture of CNTs were 2.42 μg/m^3 (range 0.68-5.25 μg/m^3, n=7) and ND-4.62 μg/m^3 (n=10), respectively. In five outdoor background samples the mass concentration of EC ranged from ND-0.89 μg/m^3 (57).

Secondary manufacturers

The same study as above also included three secondary manufacturers of CNTs and of the nine personal measurements, two showed no amounts of EC, while in the other the EC concentration ranged between 0.8 and 7.86 μg/m^3. The two highest values were observed in connection with extrusion, weighing, and mixing (7.86 μg/m^3) and weighing, mixing and sonication (7.54 μg/m^3). In the stationary samples (n=13) the mass concentration of EC ranged between ND and 2.76 μg/m^3. The one outdoor background sample collected contained no detectable EC (57). This study demonstrated that extensive exposure to CNTs also occurs in secon-

dary manufacturing (i.e. development of composite and polymer material) during handling of dry powder (including mixing and weighing) even when protective measures are in place (e.g., chemical fume hoods and glove boxes).

Down-stream applications
During weaving with MWCNT-coated yarn in a textile factory both personal and stationary air samples were taken and the respirable dust (<6.6 µm) collected with Sioutas cascade impactors. Two personal samples contained 3.5-4.8 µg EC/m^3 and the four stationary values ranged from 1.1-5.3 µg/m^3. The background concentration of EC was lower than 5.3 µg/m^3 (321).

6.2.3 Fibre and number concentration of individual tubes or CNT structures
To date a standardised protocol for counting CNTs is missing and it is not clear how CNT fibre-like structures should be counted when the CNT structures are very heterogeneous and often do not have the typical fibre dimensions. Therefore, fibres of CNT are counted on different criteria's. In some of the studies described below, fibres were counted (based on the definition by WHO (354), which requires a minimum length of 5 µm and a length:width ratio of >3:1), while others quantified CNT-containing structures (57, 196, 300). In studies counting CNTs according to NMAM No. 7400 (236), CNT structures <0.25 µm cannot be observed (21, 22).

Primary manufacturers
During CVD growth and subsequent handling of CNTs in a research laboratory, assessment of the concentration of respirable tubes in a worker's breathing zone revealed no nanoscale fibres or fibrous bundles (19).

In other CNT production and laboratory facilities, personal and stationary measurements of respirable tubes were carried out prior to and after implementation of protective control measures. Personal exposure was up to 194 tubes/cm^3 before and 0.02 tubes/cm^3 after protective measures, with corresponding stationary values up to 173 and 2.0 tubes/cm^3 (103).

Assessment of personal breathing zone samples (n=7) collected at three primary manufacturers of CNTs by TEM revealed 0.003-0.399 CNT structures/cm^3, while the stationary samples (n=9) exhibited ND-0.134 CNT structures/cm^3 (57).

CNT cluster particles were detected in one out of six stationary samples collected during manufacturing and handling of CNTs. The number concentration in the air at the hood opening was 0.002 cluster particles/cm^3 for particles larger than 3 µm (244).

Assessment of personal breathing zone samples from a worker involved in the production MWCNTs (arc discharge) revealed 0.57 CNT structures/cm^3 after nearly 6 hours of work, while stationary air samples collected during cleaving of deposits containing as produced MWCNTs and sieving had concentrations of 3.4 and 11.1 CNT structures/cm^3, respectively. The full day personal exposure measurement also showed clear signs of exposure to free CNT fibres and CNT containing particles with 0.32 CNT fibres/cm^3 as respirable fraction sampled air in the breathing zone (196).

Secondary manufacturers
Assessment of personal breathing zone samples and stationary samples (n=6) collected at three secondary manufacturers of CNTs by TEM revealed ND-1.613 CNT structures/cm^3 and ND-0.295 CNT structures/cm^3, respectively (57).

Down-stream applications
Dry cutting and drilling in CNT-containing composites resulted in extensive exposure to nanoscale and fine particles, as well as to respirable fibres (21, 22). Fibre concentration was assessed according to the WHO definition (354) and NMAM No. 7400 for asbestos (236), see previous page. Dry cutting resulted in an exposure level of 1.6 fibre/cm^3, while the corresponding value during drilling was 0.7-1.0 fibre/cm^3 (22). Although no individual CNT structures or bundles could be identified among the fibres and particle agglomerates that resulted from cutting (21), drilling did produce airborne aggregates of CNTs (22), clearly indicating the occupational exposure to CNTs during machining of composite materials containing CNTs.

Another report has described MWCNTs sticking out of larger particles resulting from mechanical sanding of a composite containing 1% MWCNTs (101).

During textile production involving weaving with MWCNT-coated yarn, with the exception of a single sample, no individual nanosized fibrous MWCNT particles could be observed with SEM (321). However, many particles of micron size, apperently fragments of the yarn were present.

Furthermore, by doping with different levels of CNTs (e.g., 0.2-2 wt%), the mechanical strength of concrete can be enhanced (8, 299, 361). Accordingly, occupational exposure to particles containing CNT or individual CNTs in connection with drilling or cutting and during demolition and recycling of such reinforced concrete may occur (299).

6.2.4 Particle number concentration and size distribution
Primary manufacturers
Opening the CVD cover in one primary manufacturing facility resulted in the release of nanoparticles with a mode diameter of approximately 20 or 50 nm and a geometric mean number concentration that rose to 11 000 particles/cm^3 (177). For more information about the used aerosol instruments see Table 3. In another instance, opening the growth chamber with or without proper ventilation led to 300 and 42 400 particles/cm^3 air, respectively (209). Furthermore, cleaning the inside of the enclosure to remove powder caused very high particle number concentrations (as high as approximately 760 000 particles/cm^3) (203). However, in another research laboratory, no elevation in the total number concentration or size range of airborne particles was observed during CVD growth and handling of CNTs (19).

Tsai and co-workers reported that particle concentrations measured at the source of CVD production of SWCNTs peaked at a dimension of 50 nm and were as high as 10 000 000 particles/cm^3 (337).

During weaving with MWCNT-coated yarn in a textile factory the number concentration of airborne particles <50 nm (mobility diameter) rose to 17 100 particles/cm^3, whereas during weaving with polyester that did not contain MWCNTs this value was approximately 1 500 particles/cm^3. The particle size distribution for particles emitted during weaving with MWCNT-coated yarn had a maxima around 100 nm; and the particle number concentration for the peak of the size distribution was 27 000 particles/cm^3 (321).

Dahm and colleagues reported extensive emission data from three primary manufacturers including particle number concentrations as high as 97 000 particles/cm^3. Measurements of respirable mass and active surface area concentrations were presented as well (see further Table 6) (56).

Secondary manufacturers

Monitoring of airborne particles during blending of MWCNTs in a research laboratory in real time revealed that the number concentration rose to over 12 000 particles/cm^3, with a size range of 14-630 nm (103). Physical handling of and other production activities involving nanomaterials (CNTs and other fullerenes) in a commercial nanotechnology facility resulted in short-term increases the number concentrations of airborne particles (376). Moreover weighing raw and functionalised MWCNTs and sonication of CNT-spiked water resulted in values as high as 2 780 particles/cm^3 (143), while weighing without exhaust and sonication of raw MWCNTs resulted in as many as 1 580 and 2 800 particles/cm^3, respectively (209).

Machining of composite material containing CNTs generated very high numbers of particles (21, 22). The stationary (determined approximately 10 cm from the source) and personal (breathing zone) values during dry cutting were 294 000 and 153 000 particles/cm^3 air, respectively (21). Stationary sampling (again 10 cm from the source) during high- and low- speed drilling of CNT-containing composites resulted maximally in 11 000 000 and 3 900 000 particles/cm^3 air, respectively, with corresponding personal values of 1 300 000 and 2 900 000 particles/cm^3. The size range of the particles produced by dry cutting was of 5.6 nm-20 μm and the size distribution was polydisperse, exhibiting maxima at 12, 20, 230±20 nm and 1±0.1 μm (21).

In another study, extensive emission data from three secondary manufacturers were reported. The highest particle number concentration (156 000 particles/cm^3) were observed in connection with extrusion. In addition, data on mass and surface area concentrations were reported (Table 6) (56).

Table 5. Levels of occupational exposure to different types of CNTs in terms of mass concentration, EC mass concentration and number concentration.

Facility/Worksite Process/activity	Type of CNT	Sampling	No. of samples	Sampling time (h)	Dust fraction examined	Exposure level, median (range)		Sampling procedure	Reference
						Mass concentration ($\mu g/m^3$)	CNT structures ($No./cm^3$)		
Primary manufacturers									
2 laser ablation facilities and 2 HiPCO process facilities									
Removal of CNT material from production vessels inside enclosure	Unpurified SWCNTs, 20-50 nm diameter [a]	Personal	4	0.5	Total	23 (0.7-53) [b]	NA	Open-face conductive filter cassettes with MCE filters (25 mm) [b].	(203)
1 research laboratory									
CVD; production	Unpurified CNTs [c]	Personal	1	1.5		NA	ND	Asbestos sampling cassettes with MCE filters (25 mm).	(19)
1 research facility (3 laboratories)									
Thermal CVD; production, blending, ball milling, weighing, spraying	MWCNTs, 52-56 nm × 1 473-1 760 nm	Personal Stationary	8 10	4-6	Total	ND (ND-332) 37 (ND-435)	0.005 (ND-194) ND (ND-173)	Sampling cassettes with MCE filters (35 mm) [d].	(103)
3 industries, 2 research institutes and 2 laboratories									
Production, handling	MWCNTs	Personal Stationary		3-6.8	Total	106 (7.8-321) 81 (12.6-187) means	ND (ND-0.003)	Open-face sampling cassettes with MCE filters (37 mm).	(177)
2 packing facilities									
Packing	MWCNTs	Personal	4		Total Respirable	1 340 (290-2 390) 235 (80-390) means	NA	Personal sample with $PM_{4.0}$.	(322)

Table 5. Levels of occupational exposure to different types of CNTs in terms of mass concentration, EC mass concentration and number concentration.

Facility/Worksite Process/activity	Type of CNT	Sampling	No. of samples	Sampling time (h)	Dust fraction examined	Exposure level, median (range)		Sampling procedure	Reference
						Mass concentration ($\mu g/m^3$)	CNT structures ($No./cm^3$)		
1 research facility									
CVD production and collection	SWCNTs, 3 nm diameter	Stationary	6	0.88-52	Total >~3 µm >~0.3 µm		 ND (ND-0.002) ND	25-mm stainless steel filter holder with poly-carbonate membrane filters (25-mm diameter; 0.08-µm pore size).	(244)
1 production facility									
Arc discharge production; cleaving of deposits, sieving etc.	MWCNTs, 2-50 nm diameter	Personal Stationary	1 2	5.7 0.4-0.9			0.57 3.4-11.1	37-mm sampling cassette with 0.4 µm polycarbo-nate membrane filters and BGI-4 cyclone.	(196)
1 manufacturing facility									
CVD; production, harvesting	MWCNTs	Personal Stationary	3 4	0.05-0.48 0.13-3.13	Inhalable	2.74 (2.28-5.25) EC 2.17 (ND-4.62) EC		Open-face sampling cassettes with quartz fibre filters (25 mm).	(57)
		Personal Stationary	3 4	0.05-0.48 0.13-3.18			0.123 (0.090-0.399) 0.041 (0.026-0.134)	Open-face sampling cassettes with MCE filters (25 mm; 0.8 µm pore size).	
		Stationary	3	0.13-3.28	Respirable	ND (ND-0.78) EC		37-mm sampling cassettes with quartz fibre filters and BGI cyclone.	

Table 5. Levels of occupational exposure to different types of CNTs in terms of mass concentration, EC mass concentration and number concentration.

Facility/Worksite Process/activity	Type of CNT	Sampling	No. of samples	Sampling time (h)	Dust fraction examined	Exposure level, median (range)		Sampling procedure	Reference
						Mass concentration ($\mu g/m^3$)	CNT structures ($No./cm^3$)		
1 manufacturing facility									
Production, harvesting and weighing	SWCNTs	Personal Stationary	2 3	0.25-4.57 2.73-4.57	Inhalable	1.98 (0.68-3.28) EC 1.02 (0.89-1.13) EC		Open-face sampling cassettes with quartz fibre filters (25 mm).	(57)
		Personal Stationary	2 2	0.25-4.63 2.75-4.52			0.008 (0.003-0.013) 0.010 (0.007-0.012)	Open-face sampling cassettes with MCE filters (25 mm; 0.8 µm pore size).	
		Stationary	2	2.70-4.42	Respirable	- (ND-1.88) EC		37-mm sampling cassettes with quartz fibre filters and BGI cyclone.	
1 manufacturing facility									
Catalytic CVD; production, harvesting, sonication, sieving and spray coating	MWCNTs	Personal Stationary	2 4	2.73-4.45 1.55-6.03	Inhalable	1.37 (1.13-1.6) EC ND (ND-0.47) EC		Open-face sampling cassettes with quartz fibre filters (25 mm).	(57)
		Personal Stationary	2 3	2.63-4.42 1.55-6.10			0.011 (0.010-0.012) 0.002 (ND-0.002)	Open-face sampling cassettes with MCE filters (25 mm; 0.8 µm pore size).	
		Stationary	3	1.77-5.40	Respirable	0.8 (ND-0.96) EC		37-mm sampling cassettes with quartz fibre filters and BGI cyclone.	

Table 5. Levels of occupational exposure to different types of CNTs in terms of mass concentration, EC mass concentration and number concentration.

Facility/Worksite Process/activity	Type of CNT	Sampling	No. of samples	Sampling time (h)	Dust fraction examined	Exposure level, median (range)		Sampling procedure	Reference
						Mass concentration ($\mu g/m^3$)	CNT structures ($No./cm^3$)		
Secondary manufacturers									
1 research facility									
Development of semiconductors; weighing, sonication, waste collection and disposal	MWCNTs	Personal Stationary	4 2	0.35-5.65 0.43-2.57	Inhalable	0.82 (ND-1.06) EC ND EC		Open-face sampling cassettes with quartz fibre filters (25 mm).	(57)
		Personal Stationary	4 2	0.35-5.45 0.43-2.62			ND (ND-0.214) - (ND-0.003)	Open-face sampling cassettes with MCE filters (25 mm; 0.8 µm pore size).	
		Stationary	2	0.43-2.63	Respirable	ND		37-mm sampling cassettes with quartz fibre filters and BGI cyclone.	
1 research facility									
Development of polymer materials; extrusion, weighing, mixing, and milling	MWCNTs	Personal Stationary	3 2	0.33-1.87 0.37-2.30	Inhalable	3.19 (ND-7.86) EC - (ND-1.01) EC		Open-face sampling cassettes with quartz fibre filters (25 mm).	(57)
		Personal Stationary	3 2	0.33-1.87 0.37-2.35			0.067 (ND-0.242) - (ND-0.008)	Open-face sampling cassettes with MCE filters (25 mm; 0.8 µm pore size).	
		Stationary	2	0.37-2.32	Respirable	- (ND-1.89) EC		37-mm sampling cassettes with quartz fibre filters and BGI cyclone.	

Table 5. Levels of occupational exposure to different types of CNTs in terms of mass concentration, EC mass concentration and number concentration.

Facility/Worksite Process/activity	Type of CNT	Sampling	No. of samples	Sampling time (h)	Dust fraction examined	Exposure level, median (range)		Sampling procedure	Reference
						Mass concentration ($\mu g/m^3$)	CNT structures ($No./cm^3$)		
1 research facility									
Development of composites; transferring, weighing, mixing and sonication	MWCNTs/ carbon nanofibres	Personal Stationary	2 2		Inhalable	5.85 (4.15-7.54) EC ND EC		Open-face sampling cassettes with quartz fibre filters (25 mm).	(57)
		Personal Stationary	2 2				0.839 (0.065-1.613) 0.149 (0.003-0.295)	Open-face sampling cassettes with MCE filters (25 mm; 0.8 µm pore size).	
		Stationary	2		Respirable	- (ND-2.76) EC		37-mm sampling cassettes with quartz fibre filters and BGI cyclone.	
Down-stream applications									
1 research laboratory									
Dry cutting in CNT composite	CNT-alumina, CNT-carbon [c]	Personal	1			NA	ND	Asbestos sampling cassette with MCE filters (25 mm) [d].	(21)

Table 5. Levels of occupational exposure to different types of CNTs in terms of mass concentration, EC mass concentration and number concentration.

Facility/Worksite Process/activity	Type of CNT	Sampling	No. of samples	Sampling time (h)	Dust fraction examined	Exposure level, median (range)		Sampling procedure	Reference
						Mass concentration ($\mu g/m^3$)	CNT structures ($No./cm^3$)		
1 textile-producing factory									
Weaving process	MWCNT-coated yarn	Personal	1		Total	159	ND	Personal dust sampler (25-mm diameter) which collected coarse particles and particles <4 µm. Also a Sioutas cascade impactor using 25-mm quartz fibre filters (for EC analysis) or poly-carbonate membrane filters (for SEM analysis) for collection.	(321)
					Respirable	93			
		Personal	2		Respirable	4.2 (3.5-4.8) EC			
		Stationary	1		Total	92			
					Respirable	66			
		Stationary	4		Respirable	4.3 (1.1-5.3) EC			

[a] Manufactured by the National Aeronautics and Space Administration, Rice University and Carbon Nanotechnologies, Inc.
[b] Nanotube concentrations estimated assuming that the combined mass of nickel and iron constitutes 30% of the SWCNT material.
[c] Manufactured by the Massachusetts Institute of Technology.
[d] Equipped with an electrically conductive cowl.
CVD: chemical vapour deposition, EC: elemental carbon, HiPCO: high-pressure carbon monoxide, MCE: mixed cellulose ester, NA: not available; data not collected at this site, ND: not detectable, PMx: particulate matter with maximal aerodynamic diameter of x µm, SEM: scanning electron microscopy.

Table 6. Characterisation of different types of CNT in workplaces employing real-time aerosol instruments and off-line techniques.

Facility Task/process	Nanomaterial	Instrument	Sampling time (min)	Characteristics					Ref.
				Particle size range (nm)	Particle number concentration (particles/cm^3)	Mass concentration[a] (μg/m^3)	Surface area (μm^2/cm^3)	CNT structures on TEM/SEM filter (Yes/No)	
2 laser ablation facilities and 2 HiPCO process facilities									
Removal of CNT material from production vessels inside an enclosure	Unpurified SWCNTs, 20-50 nm diameter	CPC OPC Filter sample	19-50	10-1 000 >300	Up to ~890 000[a]	Up to ~1 600[b]	-	Yes[c] (cluster)	(203)
1 university research laboratory									
CVD growth	Unpurified CNTs	FMPS CPC TP+ESP	90	10-560 10-<1 000	4 000-7 000		-	No	(19)
1 research facility (3 laboratories)									
CVD synthesis and handling	MWCNTs, 52-56 nm × 1.47-1.76 μm	SMPS+DMA+UCPC APS Aethalometer Filter samples	240-360	14-630 500-20 000	Up to ~30 000 b Up to ~12 000[b]	Up to 200 d	-	Yes[e]	(103)
1 production facility									
Fume hood Work zone Background	Raw CNTs and fullerenes	SMPS+DMA+CPC Aerosol photometer	36-52[b]	14-673 4-160	5 300-106 000 4 800-63 000 4 600-63 000	52-150 ($PM_{2.5}$) 36-123 ($PM_{2.5}$) 57-128 ($PM_{2.5}$)	-	-	(376)

Table 6. Characterisation of different types of CNT in workplaces employing real-time aerosol instruments and off-line techniques.

Facility Task/process	Nanomaterial	Instrument	Sampling time (min)	Characteristics					Ref.
				Particle size range (nm)	Particle number concentration (particles/cm^3)	Mass concentration[a] (μg/m^3)	Surface area (μm^2/cm^3)	CNT structures on TEM/SEM filter (Yes/No)	
1 research laboratory									
At the source, wet cutting of:	Composite: Base-carbon (broken guard)	FMPS APS CPC Aerosol photometer TP+ESP	~1-3	5.6-560 500-20 000	94 000 48	54 (PM_{10})	116 000	No	(21)
At the source, dry cutting of:	Composite: Base-alumina	FMPS APS CPC Aerosol photometer TP	~1-3	5.6-560 500-20 000	148 000 140	1 190 (PM_{10})	77 000		
	CNT-alumina	As above		As above	38 000 290	2 110 (PM_{10})	235 000		
	Base-carbon	As above		As above	283 000 1 000	5 610 (PM_{10})	457 000		
	CNT-carbon	As above		As above	294 000 870	8 380 (PM_{10})	393 000		

Table 6. Characterisation of different types of CNT in workplaces employing real-time aerosol instruments and off-line techniques.

Facility Task/process	Nanomaterial	Instrument	Sampling time (min)	Characteristics					Ref.
				Particle size range (nm)	Particle number concentration (particles/cm^3)	Mass concentration[a] (μg/m^3)	Surface area (μm^2/cm^3)	CNT structures on TEM/SEM filter (Yes/No)	
In the personal breathing zone, dry cutting of:	Composite:								
	Base-alumina	FMPS	~1-3	5.6-560	88 000			No	
		APS		500-20 000	72				
		CPC				730	32 000		
		Aerosol photometer							
		TP							
	CNT-alumina	As above		As above	28 000				
					62				
						800	45 000		
	Base-carbon	As above		As above	319 000				
					778				
						5 410	313 000		
	CNT-carbon	As above		As above	153 000				
					216				
						2 400	116 000		
1 research laboratory									
CVD production (small-scale):									(337)
Inside fume hood, next to furnace	SWCNTs	FMPS+APS		5-20 000	10 000 000	-	-		
Out-side fume hood in the breathing zone	SWCNTs	As above		As above	~2 000	-	-		

Table 6. Characterisation of different types of CNT in workplaces employing real-time aerosol instruments and off-line techniques.

Facility Task/process	Nanomaterial	Instrument	Sampling time (min)	Characteristics					Ref.
				Particle size range (nm)	Particle number concentration (particles/cm^3)	Mass concentration[a] (μg/m^3)	Surface area (μm^2/cm^3)	CNT structures on TEM/SEM filter (Yes/No)	
1 research laboratory									
CVD production (industrial scale)	MWCNTs	FMPS Filter sample		5-560	2-3 000 000	-	-	Yes[c] (CNT filaments in clusters)	(337)
Research laboratory									
At the source, high-speed drilling in (max):	Composite: Base-alumina	ESP+TP FMPS APS		 5.6-560 500-20 000	 10 000 000 5 600	 -	 Up to 666	Yes (CNT aggregates during drilling)	(22)
	CNT-alumina			As above	11 000 000 5 800	~120 000	Up to 686		
	Base-carbon			As above	4 600 000 2 500	-	-		
	CNT-carbon			As above	3 900 000 500	-	-		
At the source, low-speed drilling in (max):	Composite: Base-alumina	As above		 5.6-560 500-20 000	 3 600 000 3 900	 -	 Up to 86		
	CNT-alumina			As above	3 900 000 1 700	-	Up to 425		
At the source, high-speed wet drilling in (max):	Composite: Base-alumina	As above		 5.6-560 500-20 000	 150 000 1 400	 -	 -		
	CNT-alumina			As above	200 000 140	-	-		

Table 6. Characterisation of different types of CNT in workplaces employing real-time aerosol instruments and off-line techniques.

Facility Task/process	Nanomaterial	Instrument	Sampling time (min)	Characteristics					Ref.
				Particle size range (nm)	Particle number concentration (particles/cm^3)	Mass concentration[a] (μg/m^3)	Surface area (μm^2/cm^3)	CNT structures on TEM/SEM filter (Yes/No)	
In the breathing zone, high-speed drilling in (max):	Composite: Base-alumina	ESP+TP FMPS APS		 5.6-560 500-20 000	 790 000 300	 -	 -		
	CNT-alumina			As above	1 300 000 5 200	-	-		
	Base-carbon			As above	270 000 800	-	-		
	CNT-carbon			As above	380 000 1 100	-	-		
In the breathing zone, low-speed drilling (max):	Composite: Base-alumina	As above		 5.6-560 500-20 000	 450 000 400	 -	 -		
	CNT-alumina			As above	2 900 000 700	-	-		
3 research and development laboratories									
Opening growth chamber (exhaust)	MWCNTs, 20 nm×0.5 μm	SMPS, ELPI, CPC, OPC, DC Filter sample	1-180	10-1 000 300-500 500-1 000	300[f] 0[f] 0[f]	-	-	-	(209)
Opening growth chamber (no exhaust)	MWCNTs, 20 nm×0.5 μm	As above		As above	42 400[f] 0.35[f] 0.4[f]	-	-	-	

Table 6. Characterisation of different types of CNT in workplaces employing real-time aerosol instruments and off-line techniques.

Facility Task/process	Nanomaterial	Instrument	Sampling time (min)	Characteristics					Ref.
				Particle size range (nm)	Particle number concentration (particles/cm^3)	Mass concentration[a] (μg/m^3)	Surface area (μm^2/cm^3)	CNT structures on TEM/SEM filter (Yes/No)	
Weighing in hood (no exhaust)	Underivatised MWCNTs, 20 nm×10-30 μm, and fullerenes	SMPS, ELPI, CPC, OPC, DC Filter sample		10-1 000 300-500 500-1 000	1 480-1 580[f] 53-120[f,g] 3.9-34.4[f]	-	-	Yes[c]	
Weighing in hood (no exhaust)	Functionalised MWCNTs, 20 nm×10-30 μm, and fullerenes	As above		As above	680[f] 0[f] 3.1[f]	-	-	Yes[c]	
Sonication	Underivatised MWCNTs, 20 nm×10-30 μm, and fullerenes	As above		As above	2 200-2 800[f] 24-43[f] 6.5-24[f]	-	-	Yes[c]	
Sonication	Functionalised MWCNTs, 20 nm×10-30 μm, and fullerenes	As above		As above	730[f] 140[f,g] 65[f]	-	-	Yes[c]	
1 laboratory									
Weighing and transferring to mixing beaker inside a hood (ventilation off)	Underivatised MWCNTs, 10-20 nm× 10-30 μm, purity >95%	CPC OPC Filter sample	25-186	1-1 000 300 500 1 000 3 000 5 000 10 000	1 600[f] 120[f,g] 34[f] 4.3[f] 0.05[f] 0[f] 0[f]	-	-	Yes[c]	(143)

Table 6. Characterisation of different types of CNT in workplaces employing real-time aerosol instruments and off-line techniques.

Facility Task/process	Nanomaterial	Instrument	Sampling time (min)	Characteristics					Ref.
				Particle size range (nm)	Particle number concentration (particles/cm^3)	Mass concentration[a] (μg/m^3)	Surface area (μm^2/cm^3)	CNT structures on TEM/SEM filter (Yes/No)	
Sonication in reconstituted water containing 100 mg/l NOM	Underivatised MWCNTs, 10-20 nm× 10-30 μm, purity >95%	CPC OPC Filter sample		1-1 000 300 500 1 000 3 000 5 000 10 000	2 800 [f] 43 [f] 24 [f] 2.2 [f] 0.09 [f] 0 [f] 0 [f]	-	-	Yes [c]	
Weighing and transferring to mixing beaker inside hood (ventilation off)	Functionalised MWCNTs, 20-30 nm× 10-30 μm, purity >95%	As above		As above	680 [f] 0 [f] 3.1 [f] 1.7 [f] 0.3 [f] 0.004 [f] 0 [f]	-	-	Yes [c]	
Sonication in reconstituted water containing 100 mg/l NOM [c]	Functionalised MWCNTs, 20-30 nm× 10-30 μm, purity >95%	As above		As above	730 [f] 150 [f, g] 65 [f] 6.2 [f] 0 [f] 0 [f] 0 [f]	-	-	Yes [c, e]	

Table 6. Characterisation of different types of CNT in workplaces employing real-time aerosol instruments and off-line techniques.

Facility Task/process	Nanomaterial	Instrument	Sampling time (min)	Characteristics					Ref.
				Particle size range (nm)	Particle number concentration (particles/cm^3)	Mass concentration[a] (μg/m^3)	Surface area (μm^2/cm^3)	CNT structures on TEM/SEM filter (Yes/No)	
3 industries, 2 research institutes and 2 laboratories									
Opening of CVD	MWCNTs	SMPS+DMA+CPC Dust monitor Aethalometer	183-409	14-500 250-3 200	~7 000-16 900 (11 000 GM) ~152-432 (270 GM)	-	-	Yes[e]	(177)
Catalyst preparation	MWCNTs	As above		~3-685 250-3 200	~18 600-75 000 (37 300 GM) (150 GM)	 Up to~30 000[b,d]	-		
CNT preparation	MWCNTs	As above		~3-685 250-3 200	NA (800 GM)	 Up to ~40 000[b,d]			
Opening of CNT spray cover	MWCNTs	As above		~3-685 250-3 200	~6 900-8 100 (7 600 GM) ~540-600 (563 GM)	 Up to ~40 000[b,d]	-		
Wafer heating	MWCNTs	As above		~3-685 250-3 200	(9 000 GM) (600 GM)	 Up to ~30 000[b,d]	-		

Table 6. Characterisation of different types of CNT in workplaces employing real-time aerosol instruments and off-line techniques.

Facility Task/process	Nanomaterial	Instrument	Sampling time (min)	Characteristics					Ref.
				Particle size range (nm)	Particle number concentration (particles/cm^3)	Mass concentration[a] (μg/m^3)	Surface area (μm^2/cm^3)	CNT structures on TEM/SEM filter (Yes/No)	
Opening of water bath	MWCNTs	SMPS+DMA+CPC Dust monitor Aethalometer		~3-685 250-3 200	NA ~590-670 (630 GM)		-		
						-			
Ultrasonic dispersion	MWCNTs	As above		~3-685	~5 300-6 400 (5 800 GM)		-		
				250-3 200	510-1 100 (630 GM)				
						-			
1 research facility									
CVD synthesis including opening	SWCNTs	SMPS+DMA CPC OPC Filter sample		10-1 000 300-10 000	~300-1 000 ~2-11		-		(244)
						-		No	
Cleaning of air filters of the vacuum cleaner inside a fume hood	SWCNTs	As above	10	10-1 000 300-10 000	~1 100-4 300 ~20-500		-		
						-		No	
Collection of CNTs from substrate inside glove box	SWCNTs	As above	4	10-1 000 300-10 000	~300-400 ~2-3		-		
						-		Yes[c] (CNT cluster)	

Table 6. Characterisation of different types of CNT in workplaces employing real-time aerosol instruments and off-line techniques.

Facility Task/process	Nanomaterial	Instrument	Sampling time (min)	Characteristics					Ref.
				Particle size range (nm)	Particle number concentration (particles/cm^3)	Mass concentration[a] (μg/m^3)	Surface area (μm^2/cm^3)	CNT structures on TEM/SEM filter (Yes/No)	
Inside hose used to transfer exhaust air from cyclone vacuum cleaner to fume hood during process of collecting CNTs from substrates	SWCNTs	SMPS+DMA CPC OPC Filter sample	4	10-1 000 300-10 000	~200-1 300 ~1-5	-	-	 No	
Transfer from bin of cleaner to container for storage in-side glove box	SWCNTs	As above	8	As above	~1 100-2 900 ~4-8	-	-	 No	
1 textile-factory									
Weaving with CNT-coated yarn	MWCNTs	SMPS CPC OPC Filter sample	1 440	<50	17 100	2 40	-	 Yes[c]	(321)
3 primary manufacturers									
Production	MWCNTs, 15 nm×100 μm	CPC Aerosol photometer	131-182	10-1000	Up to 26 900 (10 100 GM)	Up to 53[a] (26 GM)	Up to 45 (8.8 GM)	-	(56)
		Diffusion charger	52	As above	Up to 2 800 (2 100 GM)	Up to 22[a] (19 GM)	-	-	
Harvesting	MWCNTs, 15 nm×100 μm	As above	45	As above	Up to 34 400 (31 800 GM)	Up to 37[a] (32 GM)	Up to 42 (24.7 GM)	-	
			17	As above	Up to 8 900 (8 700 GM)	Up to 40[a] (36 GM)	Up to 59 (38.3 GM)	-	

Table 6. Characterisation of different types of CNT in workplaces employing real-time aerosol instruments and off-line techniques.

Facility Task/process	Nanomaterial	Instrument	Sampling time (min)	Characteristics					Ref.
				Particle size range (nm)	Particle number concentration (particles/cm^3)	Mass concentration[a] (μg/m^3)	Surface area (μm^2/cm^3)	CNT structures on TEM/SEM filter (Yes/No)	
Production	SWCNTs, 1.1 nm×2 μm	CPC Aerosol photometer	30-41	10-1000	Up to 43 600 (11 200 GM)	Up to 46[a] (23 GM)	Up to 64 (23 GM)	-	
		Diffusion charger	113-161	As above	Up to 29 200 (9 000 GM)	Up to 67[a] (40 GM)	Up to 43 (13.8 GM)		
			48	As above	Up to 11 700 (6 000 GM)				
Harvesting	SWCNTs, 1.1 nm×2 μm	As above	8	As above	Up to 6 900 (5 900 GM)	Up to 18[a] (17 GM)	Up to 26 (15.6 GM)	-	
			19	As above	Up to 21 700 (10 100 GM)	Up to 46[a] (41 GM)	Up to 28 (14.6 GM)		
Reactor clean-out	SWCNTs, 1.1 nm×2 μm	As above	17-20	As above	Up to 76 900 (14 300 GM)	Up to 26[a] (22 GM)	Up to 69 (21.4 GM)	-	
			25	As above	Up to 12 300 (6 600 GM)	Up to 28[a] (16 GM)	Up to 72 (13.5 GM)	-	
Harvesting	MWCNTs, 15 nm×15 μm	As above	20	As above	Up to 14 000 (12 100 GM)	Up to 47[a] (37 GM)	Up to 86 (55.2 GM)	-	
			23	As above	Up to 4 600 (4 400 GM)	Up to 35[a] (32 GM)	Up to 104 (44.3 GM)	-	

Table 6. Characterisation of different types of CNT in workplaces employing real-time aerosol instruments and off-line techniques.

Facility Task/process	Nanomaterial	Instrument	Sampling time (min)	Characteristics					Ref.
				Particle size range (nm)	Particle number concentration (particles/cm^3)	Mass concentration[a] (μg/m^3)	Surface area (μm^2/cm^3)	CNT structures on TEM/SEM filter (Yes/No)	
Production	MWCNTs, 15 nm×15 μm	CPC Aerosol photometer	204	10-1000	Up to 97 900 (15 300 GM)	Up to 50 [a] (44 GM)	Up to 159 (63.4 GM)	-	
		Diffusion charger	91	As above	Up to 95 100 (11 300 GM)				
Sonication	MWCNTs, 15 nm×15 μm	As above	71	As above	Up to 14 400 (7 400 GM)	Up to 12 [a] (11 GM)	Up to 93 (31.9 GM)	-	
			23	As above	Up to 4 000 (3 500 GM)				
Spray coating and sieving	MWCNTs, 15 nm×15 μm	As above	150-166	As above	Up to 47 500 (32 100 GM)	Up to 17 [a] (12 GM)	Up to 66 (30.4 GM)	-	
			16	As above	Up to 47 300 (42 600 GM)				
3 secondary manufacturers									
Weighing	MWCNTs, 2.5 nm×1 μm	As above	25-28	As above	Up to 14 500 (510 GM)	-	Up to 741 (16.1 GM)	-	(56)
Sonication	MWCNTs, 2.5 nm×1 μm	As above	157-158	As above	Up to 9 600 (10 GM)	-	Up to 120 (30.8 GM)	-	

Table 6. Characterisation of different types of CNT in workplaces employing real-time aerosol instruments and off-line techniques.

Facility Task/process	Nanomaterial	Instrument	Sampling time (min)	Characteristics					Ref.
				Particle size range (nm)	Particle number concentration (particles/cm^3)	Mass concentration[a] (μg/m^3)	Surface area (μm^2/cm^3)	CNT structures on TEM/SEM filter (Yes/No)	
Extrusion	MWCNTs, 12 nm×5 μm	CPC Aerosol photometer Diffusion charger	108-115	10-1000	Up to 156 000 (16 000 GM)	Up to 3 468[a] (107 GM)	Up to 2 501 (148.3)	-	
Batch mixing	MWCNTs, 12 nm×5 μm	As above	21	As above	Up to 20 000 (9 400 GM)	Up to 284[a] (33 GM)	-	-	
Milling MWCNT composite	MWCNTs, 12 nm×5 μm	As above	22	As above	Up to 20 200 (6 800 GM)	Up to 18[a] (16 GM)	-	-	
Weighing and mixing	MWCNTs, 140 nm×100 μm	As above	122	As above	Up to 530 (35 GM)	Up to 10[a] (6 GM)	Up to 247 (9.3 GM)	-	
Mixing and sonication	MWCNTs, 140 nm×100 μm	As above	140	As above	Up to 100 (12 GM)	Up to 12[a] (6 GM)	Up to 90 (27.4 GM)	-	

[a] The mass concentrations measured as $PM_{2.5}$ or PM_{10} also include other particles than CNTs. The PM_{10} values have been background corrected.
[b] Values are extracted from figures and thereby approximates.
[c] Agglomerates.
[d] Measured as black carbon.
[e] Individual particles.
[f] Measured number concentrations have been background adjusted by subtraction.
[g] Value exceeding the upper limit of quantitation for the OPC and HHPC (70 particle/cm^3) and should be interpreted with caution.

APS: aerodynamic particle sizer, CPC: condensation particle counter, CVD: chemical vapour deposition, DC: diffusion charger, DMA: differential mobility analyser, ELPI: electrical low-pressure impactor, ESP: electrostatic precipitator, FMPS: fast-mobility particle sizer, GM: geometric mean, HHPC: hand-held particle counter, HiPCO: high-pressure carbon monoxide, NA: not available or data not collected at this site, NOM: natural organic matter (a naturally acting surfactant), OPC: optical particle counter, PMx: particulate matter with maximal aerodynamic diameter of x μm, SEM: scanning electron microscopy, SMPS: scanning mobility particle sizer, TEM: transmission electron microscopy, TP: thermophoretic precipitator, UCPC: ultrafine condensation particle counter.

6.2.5 Particle morphology

Examination of stationary filter samples collected at SWCNT production facilities by SEM indicated that the particles were agglomerated (203).

STEM analysis of filter samples from a research laboratory where both production and subsequent handling occurred revealed exposure to airborne MWCNTs with an average tube diameter and length of approximately 54 nm and 1.5 µm, respectively, and various shapes, including individual tubes, multiple tubes and clumped tube structures (agglomerates) (103). These MWCNTs demonstrated a strong tendency to form ropes due to van der Waals forces.

In another study, a multitude of CNT filaments a few nm in diameter and a few nm to several µm in length were seen to be attached to clusters of nanoparticles upon analysis by TEM (337). In contrast, filter samples from another CNT production facility evaluated in the same manner did not reveal the presence of CNTs, but larger carbonaceous particles, up to 1 µm, were seen, especially during the opening of the furnace (19). In addition, TEM evaluation of samples collected during processing (such as weighing and sonication) of raw MWCNTs in a laboratory detected no typical tubular structures (143). In connection with dry cutting of CNT-containing composites, no clearly distinguishable contours of individual CNTs, bundles of CNTs or CNTs attached to larger particles could be observed (21). On the other hand, drilling of CNT composites generated airborne clusters of CNT aggregates of respirable size (a few µm) (22). In the study by Dahm and colleagues, the CNT structures ranged from single CNTs to large agglomerates (57).

6.2.6 Chemical composition

Depending on the method used for producing CNTs, impurities in the form of catalyst particles, amorphous carbon and non-tubular fullerenes are also produced (78). In one study, analysis of personal air samples revealed that SWCNTs produced by the HiPCO method contained 30% catalyst metals (iron and nickel) (203). Aerosol particles collected during production of MWCNTs by the CVD method contained iron catalyst (337). In contrast, no iron or nickel were detected in another study analysing chemical composition of airborne MWCNTs produced by the CVD method, even though these metals were employed as catalysts during the synthesis (103). Airborne particles and fibres produced during machining of different CNT containing composites typically contained the elements carbon, oxygen, iron, cobalt, nickel, aluminium and silicon. Aluminium and silicon were found only on TEM grids from cutting CNT-alumina composites. Silicon was found in the alumina fibre itself (21).

The MWCNTs used for generation of MWCNT-aerosol in animal inhalations studies showed presence of metal oxide impurities e.g., 9.6 wt% aluminium and traces of iron and cobalt (total 0.4 wt%) (198), 0.38 wt% cobalt (255), and 0.53 wt% nickel, 0.08 wt% sulphur, 0.02 wt% magnesium, <0.01 wt% sodium and vanadium and <0.005 wt% for all other tested metals (75). For more details of metal impurities in individual studies, see Chapter 11.

Conclusion on airborne exposure

The number of exposure and emission measurements performed at workplaces is few and the occupational exposure data is limited. Both stationary and personal measurements have been performed, but often under a specific exposure situation and during a short sampling period. Most studies used real-time aerosol instruments for monitoring exposure, but also filter-based methods have been used. When filter-based samples collected during manufacturing/handling of MWCNTs were analysed, the mass concentrations of total dust and inhalable/respirable EC were typically up to 100 $\mu g/m^3$ (range ND-2 390 $\mu g/m^3$) and 5 $\mu g/m^3$ (range ND-7.86 $\mu g/m^3$), respectively, and the number concentrations reported were commonly up to 0.01 CNT structures/cm^3 (range ND-194 CNT structures/cm^3). The corresponding ranges extracted from the few studies concerning SWCNTs were 0.7-53 $\mu g/m^3$, 0.68-3.28 $\mu g/m^3$ and ND-0.013 CNT structures/cm^3 (Table 5). Real-time aerosol monitoring during production/handling of MWCNTs revealed mass concentrations up to 3 468 $\mu g/m^3$, particle number concentrations as high as 3×10^6 particles/cm^3 and surface areas up to 2 501 $\mu m^2/cm^3$. For SWCNTs these values were 1 600 $\mu g/m^3$, 10^7 particles/cm^3 and 72 $\mu m^2/cm^3$ (Table 6). Extensive exposure were reported in connection with transfer, weighing, mixing, milling, blending, spraying and packing, but also when preparing CNT-composites.

The exposure concentrations reported so far vary widely. The level of exposure is dependent primarily on 1) the properties of CNTs, 2) the specific work task, and 3) the exposure control. It is difficult to assess representative exposure levels at different work conditions. With the available sampling techniques it is possible to evaluate the effectiveness of engineering controls to airborne exposure to CNTs. Based on the knowledge so far real-time aerosol instruments are non-specific and erroneous conclusions regarding workplace exposures can potentially be drawn according to Dahm and co-workers (56). To be able to confirm and quantify exposures of CNTs selective, time-integrated, laboratory-based methods must be used.

6.3 Dermal exposure

In connection with the manufacturing and handling of CNTs, particulate matter might be deposited on the unprotected skin of workers (174). The one report on potential dermal exposure to unpurified SWCNTs published to date documents deposition of an estimated 0.2-6 mg on the glove on each hand (203). In most cases, glove contamination was clearly visible at the end of the sampling period, chiefly on the inner surfaces of the fingers and on the palms. The maximal daily dermal exposure was calculated to be 14.3 $\mu g/cm^2$/day (78) or 1.2 mg/person (11), and could be reduced by 90% by wearing gloves (78).

The HiPCO process for production of SWCNTs appeared to lead to a higher level of glove contamination than production by laser ablation (203). Moreover, with HiPCO synthesis there is a propensity for large clumps (agglomerates) of SWCNTs to become airborne during handling of the material (203).

Another investigation designed to assess potential dermal exposure to MWCNTs, involved wipe sampling of surfaces during weaving with MWCNT-coated yarn (321). It was demonstrated that dust containing fragments from the MWCNT-coated yarn was deposited on surfaces near the loom.

6.4 Oral exposure

No reports concerning oral exposure to CNTs could be found.

7. Toxicokinetics

Of the three major potential routes by which CNTs could be taken up by humans -- namely, inhalation, dermal absorption and ingestion -- in the workplace the first two routes, and in particular inhalation, are most important. However, in experimental situations, CNTs can also be administered by intraperitoneal (i.p.), intrapleural, intravenous (i.v.) and intrascrotal injection, as well as by intratracheal (i.t.) instillation and pharyngeal aspiration.

Our current knowledge on the toxicokinetics of CNTs is based on a small number of animal studies involving various kinds of CNTs and routes of administration and designed to elucidate the potential hazardous effects of commercial CNTs or the influence of functionalisation on drug delivery. The physical dimensions, chemical modifications, number of animals employed, and other aspects of the investigations described in this chapter are summarised in Table 8.

The mechanism of cellular uptake of CNTs is not fully understood. Published data suggest that CNTs can be taken up by cells via phagocytosis, pinocytosis, caveolae- and clathrin-mediated endocytosis, diffusion or by piercing the cell membrane. Phagocytosis and pinocytosis are the main pathways for macrophages whereas clathrin- and caveolae-mediated endocytosis are used by most cells including endothelial cells. The different mechanisms of cell uptake may be due to the different surface characteristics of CNTs, but may also be size dependent (15, 96, 106, 218).

7.1 Pulmonary deposition

In general, the site of deposition of particles in the respiratory tract is determined by several physical processes, i.e., impaction, diffusion, sedimentation, interception and electrostatic precipitation. Spherical particles larger than approximately 500 nm and smaller than approximately 10 nm in diameter will be deposited in the head airways and bronchial region by impaction and diffusion, respectively. Particles of intermediate sizes can penetrate deep into the lung, where some of them will be deposited, mainly by diffusion (114). In the size range of 200-500 nm deposition is minimal, with only approximately 20% of the particles being deposited (based on the International Commission on Radiological Protection (ICRP) model) (127) and the rest exhaled.

In the case of non-spherical nanomaterials, such as nanofibres, the pulmonary deposition is more complex and not as well understood. The "apparent diameter" that determines the deposited fraction and site of deposition requires further definition and, moreover, is dependent on the mechanism of deposition under consideration. For example, in the size range where diffusion is the dominant mechanism, the particle mobility diameter has proven to be directly proportional to the particle diffusion, and thereby the major determinant of deposition (114, 279).

The critical determinant of how deep in the lungs long fibres will travel before being deposited is the aerodynamic diameter (127, 324). This parameter is defined as the diameter of a spherical particle of unit density that has the corresponding gravitational settling velocity and provides a measure of the extent to which the particle/fibre follows the flow of air (114). A large aerodynamic diameter favours impaction in the upper airways, where the air velocity is high. Typically, the aerodynamic diameter of a fibre is three times the diameter of the fibre (68, 189). The aerodynamic diameter is not strongly dependent on fibre length as fibres tend to align parallel to the flow axis in the airways (327).Thus, fibres of several tens of µm may reach into the deep lung.

Due to their large size, ceramic fibres are not deposited to any great extent by diffusion, although diffusion does affect the alignment of such fibres in the airflow and, thereby, the probability of interception. CNTs are generally shorter and thinner than ceramic fibres and thus the Brownian motion affect the alignment in the air flow considerably. Furthermore, due to the Brownian motion, for fibres shorter than a few hundreds of nanometers, deposition by diffusion increases considerable (126) and thus the mobility diameter might be more important than the aerodynamic diameter determining the fibre lung deposition.

Dealing with the much larger, micron sized mineral fibres, Morgan and colleagues demonstrated that for glass fibres 5-60 µm in length (1.5 µm in diameter) deposition in the lower respiratory tract decreases with increasing length, a phenomenon they explained as reflecting elevated deposition in the upper respiratory tract instead. Fibres longer than 30 µm exhibited virtually no alveolar deposition, whereas fibres approximately 10 µm in length were recovered to a significant extent at this location (214). In general, CNTs have smaller diameters and lower densities and may therefore penetrate deeper into the lungs compared to glass fibres (214). In a semi-empirical model study by Högberg and colleagues, deposition in the pulmonary region was most extensive for fibres 10-100 nm in diameter and with lengths of several micrometres, two properties shared by many MWCNTs (126).

Fibres deposited in upper the airways, where mucociliar movement acts as a clearing mechanism, will be moved up to the larynx and swallowed, resulting in secondary oral exposure. For the fibre paradigm (see Section 9.2) to become significant, fibres must follow the airstream down to and be deposited in pulmonary regions where the major defence and clearing mechanism involves macrophages.

Critical determinants of the fate of inhaled CNTs are their shape and state of aggregation/agglomeration. Bundles or larger aggregates have much larger aero-

dynamic diameters than individual CNTs and are consequently deposited higher up in the respiratory tract. As discussed further in Chapter 10, the state of aggregation is relevant not only to deposition, but also to the translocation, uptake and toxicological response.

7.2 Uptake

7.2.1 Uptake via lungs

Several studies have shown that substantial amounts of CNTs remain in the lungs up to several months after pulmonary exposure (1, 63, 75, 222, 255, 265), indicating that these CNTs are biopersistent in the lungs (see further Sections 7.5 and 9.2).

In one recent study, uptake of CNTs from the lungs to the systemic circulation has been demonstrated following administration of SWCNTs (diameter 0.8-2.4 nm) to mice by inhalation. The SWCNTs were detected by Raman spectroscopy in the alveolar region of the lungs and in the blood 24 hours after a single exposure, but no quantitation of the uptake was performed (132). Furthermore, inhaled MWCNTs (length 0.3-50 μm) appear to reach the subpleural tissue, being recovered in the subpleural wall and within macrophages (284), and MWCNTs (median length 3.9 μm, dose 20-80 μg) administered by pharyngeal aspiration rapidly reach the visceral pleura (207, 265). Microscopic examination of mice exposed to a single dose of MWCNTs at concentrations of 80 μg by pharyngeal aspiration showed that MWCNTs had migrated to the pleura 56 days after exposure (265).

Macrophage phagocytosis of dispersed SWCNTs was rarely observed when administered by pharyngeal aspiration to mice (208), but SWCNTs were detected in alveolar macrophages in rats following inhalation as well as i.t. instillation (164, 215) and in macrophages of the interstitial tissues following i.t. instillation (164).

I.t. instillation of MWCNTs to mice resulted in deposition in the lung, but no detectable levels in the blood (63). Similar observations were made when MWCNTs were instilled i.t. into rats. The MWCNTs were detected in alveolar macrophages, alveolar wall and bronchus-associated lymphoid tissue for up to 91 days post-exposure (1). MWCNTs were detected in lungs by nickel impurity tracing and the majority of CNTs were recovered in parenchyma and alveolar cells. After 1 month the CNTs could be detected in lymph nodes. The CNTs were observed within macrophages in the lung and lymph nodes. The CNTs were not found to cross the alveolar barrier into the vascular system as no CNTs were detected in organs other than the lung. However, it cannot be ruled out that a very limited translocation of CNTs occurs that correspond to levels of CNTs below the detection limit of the Ni dosage method (75). Following instillation of either raw or highly purified SWCNTs into the lungs of rats, the nanotubes could be detected by magnetic resonance imaging (MRI) in the lungs themselves, but not in any other organ (4). One month after i.t. delivery of MWCNTs histopathological examinations using light microscopy of internal organs such as the liver and kidney revealed tissue damage, which was supported by increased levels of biomarkers indicative of organ toxicity (275). The authors suggested that the effects were a consequence

of translocation of the CNTs into these organs. However, this conclusion was based solely on assessment of toxic effects and a description or discussion of attempts to detect any presence of CNTs in the damaged tissue was omitted. There is thus a possibility that the effects were induced by inflammatory mediators released into the systemic circulation and not a consequence of translocated CNTs.

An alternative route by which exposure and uptake could take place is via the olfactory nerve. Uptake and transport of ultrafine manganese oxide particles (72) and nanosized titanium dioxide (TiO_2) particles (344) via the olfactory nerve of experimental animals have been observed, but no information concerning possible uptake of CNTs by this route is yet available.

There is no information about uptake in the conducting airways.

7.2.2 Uptake via gastrointestinal tract

Gastrointestinal exposure may be relevant not only in connection with direct ingestion, but also when CNTs are cleared from the lungs by mucociliary movement (see further Section 7.1).

Non-functionalised SWCNTs (diameter 0.8-1.2 nm, length 0.05-0.3 μm) were detected both in the intestinal tissues and in several other organs including the liver, brain and heart with TEM following administration via gastrogavage to mice (373). Wang and co-workers delivered ^{125}I-labelled hydroxylated SWCNTs (diameter 1.4 nm, mean length 0.34 μm) to mice by gavage and found distribution to the internal organs, with the highest ^{125}I-activity in the stomach, kidney, lungs and bone, within 3 hours after exposure (342). Finally, no ^{14}C-activity was detected in blood or organs other than the stomach and intestines following administration of MWCNTs functionalised with ^{14}C-taurine via oral gavage to mice (63).

7.2.3 Dermal and subcutaneous uptake

Literature searches revealed no reports concerning dermal absorption of CNTs. However, subcutaneous injection of hydroxylated SWCNTs into mice has been reported to lead to uptake and prominent distribution to stomach, kidney and bone within 3 hours (342).

7.3 Distribution

Few studies have addressed tissue distribution of CNTs following inhalation exposure and the studies described below concern distribution following i.v., i.p., subcutaneous and oral gavage administration. Chemically modified CNTs were employed in the majority of these studies.

SWCNTs

Twenty-four hours after dispersion of pristine SWCNTs in the detergent Pluronic F108 and i.v. administration to rabbits, the SWCNTs were found almost entirely in the liver, with none of the other organs examined exhibiting significant amounts of nanotubes (43). These SWCNTs were detected on the basis of their intrinsic near-infrared fluorescence, but no quantification was performed.

In contrast, Yang and collaborators reported that when pristine ^{13}C-enriched SWCNTs were dispersed in Tween-80, administered i.v. to mice and analysed by isotope ratio mass spectroscopy uptake from the circulation was rapid and the nanotubes were localised primarily in the liver, spleen and lungs after 1 day, with detectable levels in these same organs even 7 and 28 days after exposure. A low, but detectable level of nanotubes was also present in the brain, indicating that SWCNTs may cross the blood-brain barrier (370). A similar study involving doses ranging from 40-1 000 µg per animal revealed large amounts of nanotubes in the lungs, but much lower levels in the liver and spleen 90 days post-exposure (372).

When SWCNTs functionalised with hydroxyl groups and labelled with ^{131}I were administered i.v. and i.p. to mice, radioactivity was detected in all major organs, with the exception of the brain, within as little as 2 minutes. These nanotubes did not accumulate in the heart, lungs, muscle or skin, but were retained in the liver, spleen, stomach, kidneys and intestine (343).

In another investigation involving i.p. injection of 1.5 µg hydroxylated and ^{125}I-labelled SWCNTs to mice, the biodistribution was monitored for up to 18 days. The SWCNTs were taken up and distributed preferentially to the stomach, kidneys, bone, blood and skin within 3 hours and after 18 days they were still detectable in bone. Administration by oral gavage, i.v., i.p. or subcutaneous injection resulted in similar patterns of distribution with the stomach, kidney and bone exhibiting highest levels 3 hours after exposure (342).

SWCNTs covalently modified with polyethylene glycol (PEGylated SWCNTs) and administered i.v. to mice were detected within 1 hour in all major organs, except the brain, intestines and muscles. After 7 days, significant levels of SWCNTs were only detected in the liver and spleen, with these levels being higher than at 1 hour following exposure (369).

In another report PEGylated SWCNTs were found to localise to the liver and spleen 24 hours after i.v. administration and to still be present in these same organs 30, 60 and 90 days after exposure. In principle, the shorter the PEG molecule, the higher the level of persistent retention in these organs. Lower, although detectable levels of SWCNTs were present in the kidneys, intestines and bladder after 24 hours (194).

SWCNTs functionalised in two different ways with the chelating agent diethylenetriamine pentaacetic (DTPA) dianhydride and also labelled radioactively with ^{111}In have been injected i.v. into mice and monitored by scintillation counting. After 30 minutes, both types were detected both in the major organs (with highest levels in the kidneys) and in the circulation, but were cleared from all organs within 3 hours (311).

Positron emission tomography (PET) has been employed to follow SWCNTs rendered water-soluble by covalent functionalisation with the chelator 1,4,7,10-tetraazacyclododecane-1,4,7,10-tetraacetic acid (DOTA), mixed with ^{86}Y and administered i.v. or i.p. to mice. The control group received a mixture of free nanotubes, free chelating agent and ^{86}Y. Three hours after exposure, nanotubes

had accumulated in the kidney (primarily in the cortex), spleen, liver and bone. I.v. injection led to higher levels in the spleen and liver in comparison to i.p. injection. After 24 hours, these levels were similar to those after 3 hours, but the levels in the kidneys had declined, suggesting clearance of the nanotubes. The control group demonstrated no organ-specific uptake of radioactivity and rapid clearance of the mixture from the blood (205).

SWCNTs non-covalently linked to chitosan (a biocompatible polymer composed of glucosamine units) were delivered i.v. to mice and subsequently detected by Raman spectroscopy. After 24 hours, most of the nanotubes (50% of the injected dose/g bw (50% ID/g)), were localised in the liver, which was also the case for nanotubes further functionalised with a fluorescent probe (40% ID/g). Significant uptake into the spleen and kidneys also occurred (150).

In another investigation involving detection by Raman spectroscopy, mice were injected i.v. with SWCNTs (the vehicle, dispersant and/or functionalisation not indicated) and selective monitoring of the liver revealed accumulation starting 10 minutes after exposure and increasing for the next 90 minutes. Moreover, nanotubes remained present in the liver until the end of the experiment 12 days after administration (155).

Two forms of SWCNTs -- functionalised with PEG molecules (diameter 1-5 nm, length 0.1-0.3 µm, molecular weight of either 2 000 or 5 400 Da) and SWCNTs further functionalised with arginine-glycine-aspartic acid (RGD)-peptides -- were labelled radioactively with ^{64}Cu and injected i.v. into mice. Both SWCNT-PEG2000 and -PEG5400 were taken up by organs within 24 hours, mostly by the liver and spleen, with less uptake of SWCNT-PEG5400 than of SWCNTs functionalised with the shorter PEG2000 molecule. Further functionalisation with the RGD peptide resulted in a similar pattern of uptake, but with somewhat higher levels in the lungs and kidney. When the mice were pre-injected with U87MG tumour cells, RGD-bearing SWCNTs were taken up to a larger extent by these tumour cells than were SWCNTs bearing only PEG molecules. These observations based on radioactive detection were confirmed by Raman spectra (193). It should be noted that these SWCNTs were much shorter (0.1-0.3 µm) than the CNTs employed in most other studies.

MWCNTs

Translocation of MWCNTs to lung associated lymph nodes was detected in mice, but only at the end of a 13-week inhalation exposure (255). The biodistribution of MWCNTs functionalised with ^{14}C-labelled-taurine (which results in good solubility in aqueous solutions) and delivered to mice by i.v. or i.t. injection or by gavage (10 µg/animal) was examined. Shortly after i.v. administration, MWCNTs were detected in the heart, liver, lung and spleen, but not in the brain, stomach, muscle, bone or intestines. After 28 and 90 days, 80% and 20% of the MWCNTs injected, respectively, remained in the liver. After being delivered i.t., 78% of the dose was detected in the lungs 1 day later and 20% remained in this organ after 28 days.

Following oral gavage MWCNTs were present in the stomach, small and large intestine, but not in the systemic circulation (63).

Following i.p. injection of MWCNTs functionalised with ^{99m}Tc and glucosamine into mice, the nanotubes were distributed within 1 hour to major organs, including the blood, heart, lungs, liver, spleen, kidneys, stomach, intestines, fur, muscles and enterogastric region. Twenty-four hours later, radioactivity was still present in these animals, especially in the stomach (97).

The distribution of oxidised MWCNTs labelled for detection with the fluorescent molecule porphyrin was characterised 1, 7 and 130 days following subcutaneous injection into mice. Fluorescence was observed in the heart, liver, spleen, lungs, kidneys and submucosa. The intensity of the fluorescence seen in the liver, spleen and kidneys increased initially, but was lower after 130 days than after 7 days in the case of the spleen and kidneys. Fluorescence was still present at the site of injection after 130 days (141).

Following labelling with ^{14}C in another investigation, MWCNTs were sonicated with serum, and given i.v. to rats, after which their distribution was monitored by radioimaging. The nanotubes were rapidly cleared from the blood and taken up into organ, in particular the liver, but also the lungs, spleen and kidneys. No other organs exhibited any detectable uptake. The levels of nanotubes in all organs examined decreased from 1-14 days after exposure. Nanotubes were also detected in the urine and faeces (91).

7.4 Biotransformation

Available information concerning the biotransformation of CNTs is highly limited. These structures are generally considered to be metabolically inert, but some conflicting evidence does exist.

SWCNTs

SWCNTs injected i.v. and subsequently recovered from the liver and lungs exhibited no biotransformation and had retained their shape and size (372).

After injection of SWCNTs dispersed in Pluronic F108, their Pluronic coating was displaced by blood proteins, apparently within seconds after administration (43).

Functionalised SWCNTs administered i.v. have been found to have their functional moieties removed in the liver. For instance, with SWCNTs functionalised with PEG, Raman spectrometry revealed that the covalently attached PEG molecules were removed in the liver and spleen over a period of 8 weeks (371). Such modification could well have consequences for the biological behaviour of CNTs.

Moreover, Kagan and collaborators reported that short antibodies bound to SWCNTs can be degraded by myeloperoxidase in neutrophils and macrophages *in vitro* and that these digested SWCNTs caused less pulmonary inflammation after instillation by aspiration into mice (147). Eventhough this was an *in vitro* study, it does indicate that under the right circumstances protein bound to SWCNTs can be degraded.

MWCNTs

Observation of MWCNTs of unaltered length and diameter in the lungs, liver and faeces of mice 1, 7 and 14 days after administration suggests a lack of any physical transformation (63).

On the other hand, 15 days after instillation of MWCNTs into the airways of male Sprague Dawley rats (n=3) these nanotubes were found to contain alcohol, carbonyl and nitrogen groups not originally present, suggesting that biotransformation had occurred. In addition, the nanotubes in the lungs had been shortened (75).

7.5 Excretion, elimination and biopersistence

Following airway exposure, CNTs are slowly eliminated via airway clearance mechanisms. Most studies of biopersistence and elimination have been carried out using non-inhalation exposure routes, these are less relevant for occupational exposure. The half-times and circulation times for pristine and functionalised CNTs in blood following i.v. administration are summarised in Table 7.

SWCNTs

Pristine SWCNTs injected i.v. into mice were found to be excreted only to a very limited extent and appeared to be retained in the body, even after 28 days (370).

In contrast, the half-time of DTPA-functionalised SWCNTs in the blood of mice following i.v. delivery was 3-3.5 hours, with observation of intact CNTs in the urine indicating that renal clearance was the major route of excretion (311). At the same time in another report, pristine SWCNTs dispersed in Pluronic F108 and delivered i.v. to rabbits demonstrated a half-time of 1 hour in blood and these investigators' argued that Singh and collaborators (311) had measured at too few time-points to allow accurate calculation of the half-time (43).

SWCNTs functionalised with chitosan and/or a fluorescent probe have been reported to exhibit a half-time of 3-4 hours in the blood of mice after i.v. injection. In the case of the liver disappearance of the nanotubes was much slower; the levels were highest after 3 hours and remained virtually the same 24 hours after exposure. Fifty per cent of the nanotubes were recovered in the urine within the 24-hour period following injection (150).

The half-time of PEGylated SWCNTs in the blood of mice following i.v. injection was as long as 15.3 hours. The PEG prevents protein adhesion to the nanotubes, which may explain this long retention time. These nanotubes were also found to be slowly excreted in the urine (369).

Hydroxyl-functionalised SWCNTs were injected (i.v. and i.p.) into mice and the pharmacokinetic data obtained fitted to a two-compartment model. The half-time of the first-phase was approximately 4 minutes and the elimination half-time was approximately 50 minutes (343), suggesting rapid clearance.

In yet another investigation, 80% hydroxyl-functionalised SWCNTs injected i.p. into mice had been excreted into the urine (94% of the total) or faeces (6%) 11 days post-injection (342).

Table 7. Examples of half-times and circulation times of various CNTs in the blood of rodents following intravenous administration.

Nanotube preparation/ Functionalisation	Species	Methods of detection	Half-time (h)	Ref.
SWCNT				
Pristine, dispersed in Pluronic F108	Rabbit	Near-IR fluorescence spectroscopy	1	(43)
Hydroxyl groups, ^{131}I-labelled	Mouse	γ-detection	0.83	(343)
Chitosan, fluorescent probe	Mouse	Raman spectroscopy, fluorescence	3-4	(150)
DTPA, ^{111}In-labelled	Mouse	γ-detection	3-3.5	(311)
PEG7000 (branched)	Mouse	Raman spectroscopy	15 [a,b]	(194)
PEG1500	Mouse	Mass spectrometry (^{13}C/^{12}C-isotopic ratio)	15.3	(369)
MWCNT				
Glucosamine, ^{99m}Tc-labelled	Mouse	NaI(Tl)scintillation	5.5 [a]	(97)

[a] blood circulation time.
[b] intraperitoneal injection.
DTPA: diethylenetriamine pentaacetic acid, IR: infrared, PEG: polyethylene glycol.

Following an i.p. dose of 300 or 500 mg/kg bw, non-functionalised SWCNTs have been detected in the urine and faeces of Swiss mice, but no concentrations were reported in this case (165).

Modification of SWCNTs with PEG molecules enhances the blood circulation time, in a manner dependent on the length and branching of these PEG molecules. The longest circulation time (15 hours) was exhibited by CNTs modified with one of the longest and most highly branched PEG molecules (PEG7000). These CNTs appeared to be excreted via the biliary pathway into the faeces, as well as to some extent in the urine. The investigators proposed that smaller particles are excreted via the urine (194).

When mice (n=4/group) were injected i.p. with amine-functionalised SWCNTs (diameter 0.8-1.2 nm, length 0.3 µm, molecular weight 350-500 kDa), these CNTs were rapidly cleared by glomerular filtration in the kidneys. Mathematical modelling suggested that the nanotubes could align perpendicular to the filtration slits and thus pass readily through the glomerulus (282).

In the blood of mice, the half-times of SWCNTs (ultrashort, with length of about 0.1-0.3 µm) bearing PEG2000 or PEG5400 molecules were approximately 0.5 and 2 hours, respectively (193).

Following both i.v. and i.p. injection, ^{86}Y-labelled SWCNTs were found to be excreted by the kidneys in mice. Clearance from the liver, spleen and bone was not significant during the 24-hour period of study, but, only 20% and 11% of the radioactivity administered by i.v. and i.p. injection, respectively, remained in the body 24 hours later. The lack of any radioactivity in the blood 3 hours after exposure suggested rapid clearance. The same investigators also reported that ^{111}In-labelled CNTs are cleared within hours, with no radioactivity remaining 15 days after exposure. This labelled form of CNTs was also cleared more rapidly from the kidneys than from the liver or spleen (205).

MWCNTs

Several investigations have revealed that MWCNTs may be retained in the lungs, suggesting biopersistence. Pauluhn calculated based on kinetics analysis of the lung burden of cobalt, an elimination half-time of MWCNTs (Baytubes with 0.5% residual cobalt) of 350 days at 0.4 mg/m^3, the highest concentration studied without overload effects (255). Most CNTs are probably eliminated from the lungs by macrophages (207).

MWCNTs instilled into rat trachea were eliminated to the extent of 63% and 84% 3 and 6 months after exposure, respectively. The lack of any MWCNTs in systemic organs suggested that these CNTs were, indeed, eliminated, rather than translocated (75). In another case 80% of the MWCNTs instilled i.t. into rats remained in the lungs 60 days later (222). Taurine-functionalised MWCNTs instilled i.t. into mice were gradually eliminated from the lungs, with 20% of the dose still being detected in this organ 28 days after exposure (63). If MWCNTs are administered via the gastrointestinal route, they are eliminated in the faeces, as illustrated by the recovery of 74% of ^{14}C-taurine MWCNTs in the faeces of mice within 12 hours after delivery by gavage (63).

In another report, 300 µg MWCNTs functionalised with the chelating agent DTPA and reacted with $^{111}InCl_3$ to obtain a radioactive tracer were injected into the tail vein of 6-week-old male nude rats and the animals subsequently subjected to micro single photon emission tomography/computed tomography (micro SPECT/CT) scanning up to 24 hours (or placed in metabolic cages when not scanned). During the period 60 seconds-30 minutes after exposure, radioactivity rapidly accumulated in the kidneys, followed by relocalisation to the bladder, as later confirmed by post-mortem analysis of organs and urine (n=3). After 24 hours, little radioactivity was present in the kidneys. In this same study for purposes of comparison, Wistar rats received a single tail vein injection of 600 µg MWCNTs either conjugated with DTPA (n=4) or pre-incubated with serum (n=4), followed by sacrifice 24 hours later. Whereas histological analysis revealed no accumulation of the DTPA-MWCNTs in any of the examined organ, pristine MWCNTs were detected in the lungs and liver. Neither type of MWCNTs could be seen in the kidneys, nor were any morphological changes observed. These findings suggest that functionalised MWCNTs are excreted primarily in the urine (173).

Another investigation indicates that the conformation and diameter of CNTs are important determinants of renal excretion. In this case, 6-week-old female mice were injected through the tail vein with 400 µg pure or functionalised MWCNTs (outer diameter 20-30 nm, length 0.5-2 µm), sacrificed 5 and 30 minutes later, and kidney biopsies examined with TEM. MWCNTs were seen in the glomeruli at both time-points and well dispersed MWCNTs could be seen crossing the capillary lumen, with their length aligned vertically to the fenestrations in the endothelium (172).

When MWCNTs functionalised with glucosamine and labelled with ^{99m}Tc were administered i.p. to mice, more than 70% of the radioactivity was detected in the

urine and faeces within 24 hours and the half-time in blood of 5.5 hours, is among the longest reported to date (97).

Finally, following i.v. injection of ^{14}C-radioactively labelled MWCNTs into rats, the nanotubes were cleared from the blood and detected in both the urine and faeces. However, only two animals were monitored at each time-point in this case (91).

Conclusions

Following pulmonary exposure MWCNTs have been shown to translocate into the subpleura and to the visceral pleura. MWCNTs have also been detected in the interstitial tissue and inside macrophages in the alveolar space as well as in lymph nodes. In one recent study, translocation of CNTs from the lungs to the circulatory system was reported subsequent to inhalation exposure of mice. The SWCNTs were detected in blood by Raman spectroscopy. In another study, effects on the internal organ were reported following i.t. instillation of MWCNTs into rats. However, these effects were not necessarily indications of translocation, but may instead be evoked by mediators released from the lungs into the systemic circulation. No data confirming presence of CNTs in these organs was presented. Although the majority of published studies reported no detection of CNTs in blood or internal organs, minor degree of systemic translocation, i.e., below the employed methods' detection limits cannot be excluded.

In contrast, there are two reports of absorption of both non- and functionalised SWCNTs (fibre length 0.050-0.450 μm) in the gastrointestinal tract. Following i.v. or i.p. administration, CNTs are detected in all major organs (including the brain, indicating passage across the blood-brain barrier), in most cases primarily in the liver, but also in the spleen and lungs. The presence of CNTs in the liver for a long time suggests that excretion from the liver is very slow as compared to the kidneys and is likely related to the population of macrophages. There are no data to support a common pathway and mechanisms involved in degradation, transformation and excretion. CNTs functionalised with water-soluble moieties have been reported to be excreted mainly via the kidneys, but also in the faeces. The excretion of non-functionalised CNTs has been little examined and no conclusions can be drawn. In general, chemical modification exerts a substantial influence on the toxicokinetics of CNTs. Most studies concerning biodistribution have focused on CNTs functionalised for drug delivery or bioimaging and only a few have examined the distribution of pristine CNTs.

Reported differences in rates and extents of excretion could, of course, also be due to methodological differences. Raman spectrometry detects intrinsic properties of the CNTs, whereas fluorescence or radioactive detection require the coupling of appropriate probes to the CNTs. There is always a risk that such tracer molecules may detach from the CNTs and result in false-positive detection of nanotubes. In addition, tracer molecules might themselves alter the pharmacokinetics of CNTs, in a manner analogous to modification with PEG.

Table 8. Summary of the dimensions, modifications and toxicokinetics observations for various CNTs.

Absolute dose (µg)	Dose (mg/kg bw)	Species/ Strain	No. and sex of animals	Type of CNT	Diameter (nm)	Length (µm)	Attributes	Observation period	Toxicokinetic observations	Reference
Inhalation										
22 ppm for 15 min	-	Mouse CD1	-	SWCNT	0.8-2.4	-	Purity >96%	24 h	SWCNTs reached the alveolar regions of the lung and were detected in the blood.	(132)
30 mg/m^3 for 6 h	4	Mouse C57BL/6	10 males	MWCNT	10-50	0.5-50	Mass median aerodynamic diameter of 183 nm	6 weeks	MWCNTs reached the subpleural tissue and were found within macrophages.	(284)
Intratracheal instillation										
1	0.01	Rat Sprague Dawley	6 males	MWCNT	20-50	0.5-2	0.53% Ni. Dispersed in BSA, 80% of agglomerates smaller than 10 µm	180 days	Not detected in lung or other organs.	(75)
10	0.05	Rat Sprague Dawley	6 males	MWCNT	20-50	0.5-2	0.53% Ni. Dispersed in BSA, 80% of agglomerates smaller than 10 µm	180 days	Detected in the lungs up to 90 days post-exposure. Not detected in organs other than the lung.	(75)
	0.2	Rat Wistar	6 males	MWCNT	90-150	-	Agglomerated ropes, produced by arc discharge	3 months	Liver damage detected by histopathological examination. Suggested translocation, but no detection of CNTs by histopathology.	(275)
	0.2	Rat Wistar	6 males	MWCNT	60-80	-	Agglomerated ropes, produced by CVD	3 months	Same as above.	(275)
10	0.4	Mouse Kunming	5 males	MWCNT	10-20	0.01-0.6	Taurine functionalised, (highly soluble), ^{14}C-labelled	90 days	Radioactivity detected in the lungs, but 80% eliminated by 28 days post-exposure. No radioactivity detected in other internal organs or the blood.	(63)

Table 8. Summary of the dimensions, modifications and toxicokinetics observations for various CNTs.

Absolute dose (μg)	Dose (mg/kg bw)	Species/ Strain	No. and sex of animals	Type of CNT	Diameter (nm)	Length (μm)	Attributes	Observation period	Toxicokinetic observations	Reference
100	0.5	Rat Sprague Dawley	6 males	MWCNT	20-50	0.5-2	0.53% Ni. Dispersed in BSA, 80% of agglomerates smaller than 10 μm	180 days	Detected in the lungs up to 180 days post-exposure and in lymph nodes after 30 days. Detected in alveolar cells up to 90 days post-exposure. 30 days after exposure, 69% of the present dose was detected in the lungs and 28% in the lymph nodes.	(75)
	1	Rat Wistar	6 males	MWCNT	90-150	-	Agglomerated ropes, produced by arc discharge	3 months	Suggested translocation, but no detection of MWCNTs by histopathology. Liver damage detected by histopathological examination (periportal lymphocytic infiltration, haemorrhage, ballooning foamy hepatocytes, focal inflammation and necrosis). Increased serum levels of biomarkers indicative of liver damage.	(275)
	1	Rat Wistar	6 males	MWCNT	60-80	-	Agglomerated ropes, produced by CVD	3 months	Same as above.	(275)
500	2	Rat	6	SWCNT	0.8-1.2	0.1-1	35% impurities	14 days	Increased iron content in lung. SWCNTs detected only in lung.	(4)
500	2	Rat	6	SWCNT	0.8-1.2	0.1-1	Purified (5% impurities)	14 days	SWCNTs detected only in lung.	(4)

Table 8. Summary of the dimensions, modifications and toxicokinetics observations for various CNTs.

Absolute dose (µg)	Dose (mg/kg bw)	Species/ Strain	No. and sex of animals	Type of CNT	Diameter (nm)	Length (µm)	Attributes	Observation period	Toxicokinetic observations	Reference
	5	Rat Wistar	6 males	MWCNT	90-150	-	Agglomerated ropes, produced by arc discharge	3 months	Suggested translocation, but no detection of MWCNTs by histopathology. Liver damage detected by histopathological examination (periportal lymphocytic infiltration, haemorrhage, ballooning foamy hepatocytes, focal inflammation and necrosis). Kidney damage detected (tubular necrosis and interstitial nephritis). Increased serum levels of biomarkers indicative of liver and kidney damage.	(275)
	5	Rat Wistar	6 males	MWCNT	60-80	-	Agglomerated ropes, produced by CVD	3 months	Same as above.	(275)
Pharyngeal aspiration										
80	3.6	Mouse C57BL/6J	4 males	MWCNT	49	3.86	Unmodified	56 days	Distributed throughout the lungs. CNTs engulfed by alveolar epithelial cells and macrophages within 1 h. At later time-points the MWCNTs were no longer present at the surface of epithelium, but located within alveolar interstitium and alveolar macrophages. MWCNTs recovered in the pleura 56 days post-exposure.	(265)

Table 8. Summary of the dimensions, modifications and toxicokinetics observations for various CNTs.

Absolute dose (μg)	Dose (mg/kg bw)	Species/ Strain	No. and sex of animals	Type of CNT	Diameter (nm)	Length (μm)	Attributes	Observation period	Toxicokinetic observations	Reference
Gastrogavage										
1.5	0.06	Mouse Kunming	5 males	SWCNT	1.4	0.28-0.45	Hydroxyl functionalised, ^{125}I-labelled	3 h and 11 days post-exposure	Distributed to stomach, kidneys, lungs and bone, but also to intestine, spleen, liver, heart and blood within 3 h.	(342)
10	0.4	Mouse Kunming	5 males	MWCNT	10-20	0.01-0.6	Taurine functionalised, (highly soluble), ^{14}C-labelled	90 days	Radioactivity only detected in the stomach, intestines and faeces. 74% excreted within 12 h.	(63)
	400 (once daily for 10 days)	Mouse Kunming	20 males	SWCNT	0.8-1.2	0.05-0.3	Ultrashort	10 days	Uptake in intestinal wall, liver, brain and heart, detected by TEM. Damage to lysosomes and mitochondria.	(373)
Subcutaneous injection										
1.5	0.06	Mouse Kunming	5 males	SWCNT	1.4	0.28-0.45	Hydroxyl functionalised, ^{125}I-labelled	3 h and 11 days post-exposure	Distributed to stomach, kidneys and bone, but also to lungs, liver, spleen, intestine, blood, muscle and skin within 3 h.	(342)
500	15.6	Mouse CD-ICR	12 males	MWCNT	20-30	0.15	Oxidised, conjugated with porphyrin	1-130 days	Detected in heart, liver, spleen, lung and kidney by fluorescent spectro-scopy. Retention in liver, spleen and kidney.	(141)
Intraperitoneal injection										
	0.03	Mouse Kunming	5 males	SWCNT	-	-	Hydroxyl functionalised, ^{131}I-labelled	1 h	Rapid distribution to organs, except for the brain, within 2 min. Half-time in blood of 50 min. No toxicity reported.	(343)

Table 8. Summary of the dimensions, modifications and toxicokinetics observations for various CNTs.

Absolute dose (µg)	Dose (mg/kg bw)	Species/ Strain	No. and sex of animals	Type of CNT	Diameter (nm)	Length (µm)	Attributes	Observation period	Toxicokinetic observations	Reference
1.5	0.06	Mouse Kunming	5 males	SWCNT	1.4	0.28-0.45	Hydroxyl functionalised, ^{125}I-labelled	3 h and 18 days post-exposure	Distributed to stomach, kidneys, and bone, but also to lungs, liver, spleen, intestine, blood, muscle and skin within 3 h. After 18 days mainly found in bone.	(342)
12	0.4	Mouse athymic nude	3 males	SWCNT	-	0.042	DOTA functionalised, ^{86}Y-labelled	24 h	Uptake into kidneys, liver, spleen and bone 3 and 24 h post-exposure (detected with PET).	(205)
0.5 mCi	-	Mouse Kunming	5 females	MWCNT	20-40	Tens of µm	Glucosamine functionalised, ^{99m}Tc-labelled	24 h	Half-time in blood of 5.5 h.	(97)
Intravenous injection										
75	0.02	Rabbit	4	SWCNT	1	0.3	Pristine, suspended in Pluronic F108	24 h	Half-time in blood of 1 h, significant levels of SWCNTs in the liver only after 24 h. No toxic or adverse effects observed. Pluronic molecules on the SWCNTs rapidly replaced with serum proteins.	(43)
	0.02	Mouse Kunming	5 males	SWCNT	-	-	Hydroxyl functionalised, ^{131}I-labelled	1 h	Rapid distribution to organs, except for the brain, within 2 min. Half-time in blood of 50 min. No toxicity reported.	(343)

Table 8. Summary of the dimensions, modifications and toxicokinetics observations for various CNTs.

Absolute dose (μg)	Dose (mg/kg bw)	Species/ Strain	No. and sex of animals	Type of CNT	Diameter (nm)	Length (μm)	Attributes	Observation period	Toxicokinetic observations	Reference
1	0.04	Mouse nude bearing tumours	3-4	SWCNT	1-5	0.1-0.3	Phospholipid-PEG2000 functionalised. DOTA/^{64}Cu labelled. With or without RGD peptides.	24 h	Half-time in blood of 0.5 h. Uptake in liver and spleen. SWCNTs bearing RGD peptides specifically localised in implanted tumours.	(193)
1	0.04	Mouse nude bearing tumours	3-4	SWCNT	1-5	0.1-0.3	Phospholipid-PEG5400 functionalised. DOTA/^{64}Cu labelled. With or without RGD peptides.	24 h	Half-time in blood of 2 h. Uptake in liver and spleen. SWCNTs bearing RGD peptides specifically localised in implanted tumours.	(193)
1.5	0.06	Mouse Kunming	5 males	SWCNT	1.4	0.28-0.45	Hydroxyl functionalised, ^{125}I-labelled	3 h and 11 days post-exposure	Distributed to stomach, kidneys and bone, but also to lungs, liver, spleen, intestine, blood, muscle and skin within 3 h.	(342)
5	0.18	Mouse nude	-	SWCNT	1-3	0.05-0.2	Chitosan functionalised, fluorescent labelling	24 h	Rapid clearance from blood, half-time of 3-4 h.	(150)
7	0.35	Mouse athymic nude	3 males	SWCNT	-	0.042	DOTA functionalised, ^{111}In-labelled	Up to 15 days	Rapid clearance from blood (within 20 h). No radioactivity in blood 15 days after exposure.	(205)
10	0.4	Mouse Kunming	5 males	MWCNT	10-20	0.01-0.6	Taurine functionalised (highly soluble), ^{14}C-labelled	90 days	Rapid uptake into organs, 80% of the dose administered retained in the liver. 5% taken up into the spleen and lungs, but rapidly eliminated.	(63)
12	0.4	Mouse athymic nude	3 males	SWCNT	-	0.042	DOTA functionalised, ^{86}Y-labelled	24 h	Uptake into kidneys, liver, spleen and bone 3 and 24 h post-exposure.	(205)

Table 8. Summary of the dimensions, modifications and toxicokinetics observations for various CNTs.

Absolute dose (μg)	Dose (mg/kg bw)	Species/ Strain	No. and sex of animals	Type of CNT	Diameter (nm)	Length (μm)	Attributes	Observation period	Toxicokinetic observations	Reference
20	0.73	Mouse nude	-	SWCNT	1-3	0.05-0.2	Chitosan functionalised	24 h	Rapid clearance from the blood, with a half-time of 3-4 h. The CNTs were retained in the liver.	(150)
20	0.82	Mouse BALB/c	3-4	SWCNT	-	0.1	PEG functionalised (PEG of different lengths and patterns of branching)	Up to 90 days	Time required for reduction in the blood level to 5% of the injected dose/g as long as 15 h. Uptake into liver and spleen, less in kidneys and intestine. The larger the PEG molecule, the less the uptake. Analysis using Raman spectroscopy.	(194)
350	1.25	Rat	6	MWCNT	40	Majority <5	^{14}C-labelled	1-14 days	Uptake into liver, lungs, spleen and kidneys. Detected in urine and blood. Levels of radioactivity decreased in all organs with time, but still detectable in liver and urine after 14 days.	(91)
500	2	Rat	3	SWCNT	0.8-1.2	0.1-1	35% impurities	14 days	SWCNTs detected in spleen and kidneys by MRI.	(4)
500	2	Rat	3	SWCNT	0.8-1.2	0.1-1	Purified (5% impurities)	14 days	SWCNTs not detectable by MRI.	(4)
	2.4	Mouse Kunming, BALB/c or C57BL	3	SWCNT	10-20	1-1.5	PEG1500 functionalised (highly soluble)	Up to 7 days	Uptake into liver, spleen, kidneys and skin. 30% of the injected dose still present after 24 h. Half-time in blood of 15.3 h.	(369)

Table 8. Summary of the dimensions, modifications and toxicokinetics observations for various CNTs.

Absolute dose (μg)	Dose (mg/kg bw)	Species/ Strain	No. and sex of animals	Type of CNT	Diameter (nm)	Length (μm)	Attributes	Observation period	Toxicokinetic observations	Reference
60	3.2	Mouse BALB/c	3 females	SWCNT	1	0.3-1	DTPA functionalised, ^{111}In-labelled. Saturated with DTPA	24 h	Half-time in blood of 3 h. Distributed to femur, kidney, lung, muscle and skin within 30 min. Little retention after 3 h.	(311)
60	3.2	Mouse BALB/c	3 females	SWCNT	1	0.3-1	DTPA functionalised, ^{111}In-labelled. 60% DTPA, 40% free amine groups	24 h	Half-time in blood of 3.5 h. Distributed to femur, kidney, muscle and skin after 30 min. Little retention after 3 and 24 h.	(311)
100	4.10	Mouse BALB/c	3-4	SWCNT	-	0.1	PEG functionalised (PEG of different lengths and patterns of branching)	Up to 90 days	The circulation time in blood was up to 15 h. Uptake into liver and spleen, less into kidney and intestine. The larger the PEG molecule, the less the uptake.	(194)
200	8	Mouse Kunming	3 males	SWCNT	Bundles of 10-30	Bundles of 2-3	Bundles dispersed in 1% Tween-80	28 days	Intact SWCNTs distributed throughout entire body. Most uptake in liver, lungs and spleen.	(370)
400	21	Mouse BALB/c	4 females	MWCNT	20-30	0.5-2	DTPA functionalised	24 h	Excretion of intact MWCNTs in the urine within 18 h.	(311)
400	21	Mouse BALB/c	4 females	SWCNT	1	0.3-1	DTPA functionalised	24 h	Excretion of intact SWCNTs in the urine within 18 h.	(311)
400	22.3	Mouse BALB/c	females	MWCNT	20-30	0.5-2	Purified, bundled and not functionalised or DTPA functionalised and unbundled	30 min	Individual, but not bundled CNTs were able to translocate through the kidney filtration system.	(172)

Table 8. Summary of the dimensions, modifications and toxicokinetics observations for various CNTs.

Absolute dose (µg)	Dose (mg/kg bw)	Species/ Strain	No. and sex of animals	Type of CNT	Diameter (nm)	Length (µm)	Attributes	Observation period	Toxicokinetic observations	Reference
600	24	Mouse CD-ICR	3 males	SWCNT	-	0.3-1	PEGylated following oxidation, present as single tubes or thin bundles	8 weeks	SWCNTs detected in liver 7 days post-injection and in spleen. SWCNTs defunctionalised in the liver, but not in the spleen.	(371)
1 000	40	Mouse CD-ICR	5 males	SWCNT	10-30 bundles	2-3	Bundles dispersed in 1% Tween-80. 0.4% Fe, 3% Ni, 1.3% Y	3 months	SWCNTs retained in the lung after 90 days and to a lesser extent in the liver and spleen. Detected by Raman spectroscopy and TEM.	(372)
60 pmol	-	Mouse nude	Females	SWCNT	3	0.2	PEGylated and conjugated with RGD peptides	24 h	Uptake into liver detected by Raman spectroscopy.	(155)
600	-	Rat Wistar	4	MWCNT	20-30	A few hundred nm	DTPA functionalised	24 h	Most of the radioactivity excreted in the urine by 6 h after exposure.	(173)
8 or 10	-	Mouse NCr/nu/nu	8 males	SWCNT	0.8-1.2	0.2-0.3 on the average	DOTA functionalised, ^{86}Y and/or AlexaFluor 488/680 labelled	7 days	SWCNTs localised to kidneys (some in nuclei) and excreted.	(282)

-: not reported, BSA: bovine serum albumin, CVD: chemical vapour deposition, DOTA: 1,4,7,10-tetraazacyclododecane-1,4,7,10-tetraacetic acid, DTPA: diethylenetriamine pentaacetic acid, Fe: iron, MRI: magnetic resonance imaging, Ni: nickel, PEG: polyethylene glycol, PET: positron emission tomography, RGD: arginine-glycine-aspartic acid, TEM: transmission electron microscopy, Y: yttrium.

8. Biological monitoring

At present, no techniques for biological monitoring of CNTs are in practical use. Nor have we been able to locate any literature reports that explicitly address the question of biological monitoring of or biomarkers for CNT exposure. However, some possibilities have been explored in experimental animals, e.g., determination of gene and protein expression in the blood (79).

9. Mechanisms of toxicity

Even though recent findings have deepened our understanding of the mechanisms underlying the toxicity of CNTs, much still remains unclear. In summary, in connection with inhalation CNTs are deposited in the lungs, where they may cause not only local toxic effects, but also lead to effects on other organs.

Furthermore, CNTs may migrate to the pleura and the local lymph nodes and there is also a potential risk of their being translocated across the alveolar barrier into the systemic circulation, as indicated in the study by Ingle and co-workers (132). As mentioned in Section 7.2.2, CNTs deposited in regions of the lungs where the mucociliary escalator is active will end up in the gastrointestinal tract.

CNTs administered to the lungs have been shown to induce oxidative stress, inflammatory responses (including an acute increase in the number pulmonary polymorphonuclear leukocytes (PMNs) and formation of granulomas) and fibrosis. Certain investigations also indicate direct genotoxic effects and mesothelioma.

An important parameter in this context is the fibrous structure of CNTs, which has led to parallels being drawn to the observed health effects of asbestos fibres. Several decades of research have given rise to the "fibre paradigm", or "the classical fibre pathogenicity structure/activity paradigm", explaining the basis for the harmful effects of resistant fibres on the lungs (68, 316). This paradigm also addresses the issues of biopersistence and bioaccumulation of inhaled fibres.

Some evidence indicate that the mechanism triggering pulmonary inflammation is dependent on the volumetric overload of alveolar macrophages and that the health effects of CNTs are linked to the accumulated lung burden rather than the recent dose (254, 255).

Likely, several different mechanisms of toxicity work in parallel depending on fibre dimensions and morphology but also depending on parameters such as content of metal and other impurities (113, 267), degree of agglomeration (208) and surface chemistry (35, 295). A general description of potentially important mechanisms underlying the toxic effects of CNTs is given below.

9.1 Oxidative stress and inflammation

One mechanism contributing to the toxicity of CNTs is oxidative stress caused by the generation of free radicals including reactive oxygen species (ROS) that may activate signalling pathways controlling inflammatory responses. ROS may

be generated by the particles themselves and/or by endogenous processes. Oxidative damage of cellular components such as proteins, DNA and lipids as well as activation of transcription factors that ultimately enhance the synthesis of pro-inflammatory proteins may occur. Oxidative stress has been observed in a variety of cell types exposed to CNTs, including pulmonary epithelial, mononuclear, mesothelial and keratinocyte cells (30, 202, 246, 268, 273), as well as in mice that have inhaled SWCNTs (305).

This generation of ROS could be due to metal impurities present in the CNTs (267). Bello and co-workers demonstrated that as much as 93% of the biological oxidative damage caused by various nanomaterials (including several different CNTs) could be explained on the basis of their specific surface area and content of transition metals, including iron, cobalt and molybdenum, which are common contaminants of CNTs produced on an industrial scale (20).

Contradictory findings were reported by Fenoglio and colleagues who observed that not only did CNTs not generate oxygen free radicals in an aqueous solution containing e.g., hydrogen peroxide (H_2O_2), but that MWCNTs actually acted as scavengers of free radicals (82). Such conflicting results may well be due to differences in assay conditions and in the CNTs examined.

Endogenous ROS (i.e., superoxide anion) can be formed by nicotinamide adenine dinucleotide phosphate (NADPH) oxidase present on the surface of phagocyting cells. A potential role of this endogenous ROS in the fibrotic response to CNTs was proposed by Shvedova and co-workers. These investigators reported that SWCNTs administered by pharyngeal aspiration led to more extensive accumulation of PMNs, more pronounced cytotoxicity, lower expression of the cytokine transforming growth factor beta (TGFβ) and less deposition of collagen in the lungs of NADPH-oxidase-deficient than of control mice (308).

When mononuclear cells are exposed to long and straight CNTs *in vitro*, they produce elevated levels of pro-inflammatory tumour necrosis factor alpha (TNFα) (30). Furthermore, both SWCNTs and MWCNTs can activate the transcription factor NFκB (nuclear factor kappa B) in cell cultures (107, 202, 374) and elevated NFκB activated production of pro-inflammatory cytokines have also been detected in response to *in vitro* exposure to CNTs (115). In addition, when epidermal cells were exposed to SWCNTs containing 30% or 0.23% iron, the former but not the latter activated the activator protein 1 (AP-1), a transcription factor involved in oxidative stress (246). Both of these preparations activated NFκB (231).

Inflammation following exposure to CNTs has been observed in several *in vivo* studies as well. A link between oxidative stress and inflammation is indicated by the report that SWCNTs induce more pronounced inflammation in mice with reduced levels of the anti-oxidant vitamin E (307). Acute pulmonary inflammation declined with time, but was still present 90 days after rats were exposed to MWCNTs via inhalation (76).

Furthermore, the levels of pro-inflammatory cytokines in bronchoalveolar lavage (BAL) fluid collected from mice rose rapidly 1 day after inhalation of SWCNTs (305). Inflammatory changes in the lungs of rats were also observed

following long-term exposure to MWCNTs (255), as well as in the peritoneum of mice after i.p. injection of MWCNTs (259). Systemic inflammation in mice following pulmonary exposure is also indicated by the elevated serum levels of cytokines detected following i.t. instillation of MWCNTs (249) and the enhanced levels of inflammatory cells in the blood after administration of SWCNTs via pharyngeal aspiration (79).

9.2 The fibre paradigm and frustrated phagocytosis

The fibre paradigm, originally proposed based on effects of asbestos and other inorganic fibres, describes three fibre characteristics as major toxicological determinants (67, 68):

- thin enough to penetrate deep into the lungs.
- long enough to cause frustrated phagocytosis and not be cleared effectively.
- biopersistent so that the fibrous shape is retained and accumulation occurs.

When inhaled, long fibres will align parallel to the airflow and may be transported deep into the lungs, where due to their length or Brownian motion, they eventually hit the wet surface of the lung and are deposited (see also Section 7.1). Deep in the lungs, the primary mechanism for the removal of non-soluble particulate matter involves phagocytosis by the macrophages, which are usually 10-20 µm in diameter. If the fibres are longer than this and are also stiff and cannot be bent (i.e., straight and not entangled), the phagocytic capacity of the macrophages, as well as mucociliary clearance of fibres in incapacitated macrophages may be impaired, leading to prolonged biopersistency and resulting dose accumulation (Figure 4) (68).

This reasoning has given rise to the high-aspect ratio nanoparticle (HARN) hypothesis of toxicity, which predicts that pathogenic events similar to those caused

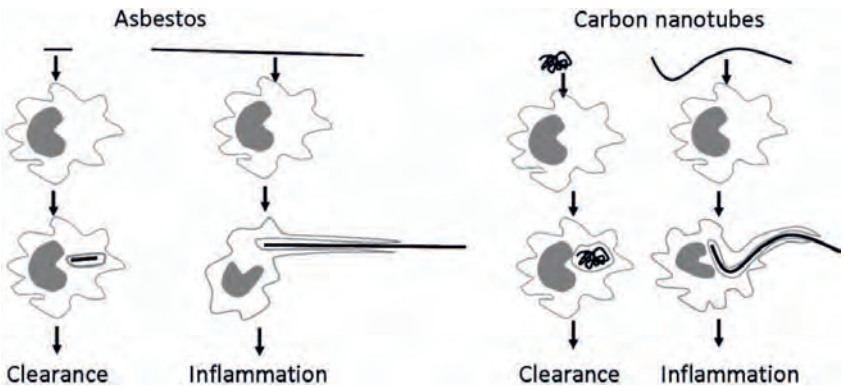

Figure 4. Illustration of the frustrated phagocytosis of long stiff fibres. Reprinted from Donaldson *et al* 2010, Particle and Fibre Toxicology 7:5 (68).

by asbestos will occur if the HARNs fulfill the criteria of the fibre paradigm (68). Accordingly, the thickness, length and biopersistence of CNTs would be important determinants of their toxicity.

Such frustrated phagocytosis (i.e., uncompleted uptake) has been reported to occur when monocytes are exposed *in vitro* to CNTs (30). In addition, frustrated phagocytosis has been detected in macrophages obtained from the peritoneal cavity by lavage following i.p. injection of long CNTs (259). These observations support the HARN hypothesis, as do the reports that long, straight and well-dispersed CNTs lead to higher levels of ROS and TNFα than do tangled CNTs, indicating higher inflammatory potential.

Palomäki and collaborators also concluded that the toxic response to CNTs involves ROS and inflammation and is dependent on their morphology and length. These investigators demonstrated that, long needle-like MWCNTs, but not short or tangled MWCNTs activate the NLRP3 (nucleotide-binding domain and leucine-rich repeat pyrin 3 domain) inflammasome in lipopolysaccharide (LPS)-primed macrophages via cathepsin B, the $P2X_7$ receptor, Src and Syk tyrosine kinases and ROS to produce interleukin (IL)-1β (248). Furthermore, MWCNTs with a high-aspect ratio induced more toxicity in lung cells *in vitro* than those with a low ratio (157).

The role of release of mediators during frustrated phagocytosis was investigated by Murphy and collaborators. They showed that mesothelial cells exposed *in vitro* to short and long MWCNTs induced no significant release of pro-inflammatory cytokines. On the contrary, when the mesothelial cells were treated with conditioned media from long MWCNT-exposed macrophages the release of cytokines was strongly amplified. The result indicates that mediators released during phagocytosis stimulated the pro-inflammatory response in the mesothelial cells (225).

9.3 Production of collagen and fibrosis

Fibrous material that cannot be cleared from the lungs by phagocyting cells may provoke excessive formation of connective tissue. Subpleural fibrosis (284), as well as lung fibrosis (characterised by elevated deposition of collagen or thickening of alveolar walls) (208, 255) and focal lung fibrosis (76) have all been observed after administration of CNTs to rodents via inhalation, i.t. instillation or pharyngeal aspiration. Progressive lung fibrosis was present 28 days post-inhalation of SWCNTs (305). Intrapleural injection of long MWCNTs (84% >15 μm) into mice promoted acute inflammation and progressive fibrosis of the parietal pleura (223).

Several *in vitro* studies support the findings that CNTs initiate fibrogenic events either via direct contact or through pro-fibrogenic signals. Enhanced collagen production by human lung fibroblasts *in vitro* following exposure to CNTs (dispersed in a natural lung surfactant) has also been seen (346). Furthermore, profibrinogenic growth factors TGFβ1 and platelet-derived growth factor (PDGF) were shown to be released from macrophages exposed to MWCNTs *in vitro*. When fibroblasts were cultured in conditioned medium from MWCNT-treated macrophages an

increased production of α-smooth muscle actin was measured, and it was indicated that the fibroblasts transformed into myofibroblasts, the cell type producing collagen I (107). *In vitro* SWCNT exposure of murine macrophages also resulted in stimulation of TGFβ1 production (306).

Foreign matter may evoke the formation of granulomas, i.e., collections of macrophages (which may fuse to become giant cells), as well as other types of cells including neutrophils and fibroblasts. Formation of such granulomas has been observed following administration of CNTs to animals via inhalation (198, 255, 305), i.t. instillation (1, 3) and pharyngeal aspiration (206-208, 265). These lesions only occurred after exposure to non- or poorly dispersed SWCNTs (208). I.p. injection of MWCNTs into mice also gave rise to granulomatous lesions comprised of giant cells, aggregates of cells containing fibres and collagen deposits, with longer and thicker CNTs evoking larger numbers of granuloma and more thickening of the mesothelial lining (259).

9.4 Genotoxicity

MWCNTs injected i.p. into p53 heterozygous mice have caused mesotheliomas (319, 320). Mesothelioma, mesothelial cell hyperplasia and hypertrophy have been caused also by MWCNTs injected intrascrotally into rats (288). Genotoxicity is generally considered to be one important mechanism involved in the pathogenesis of cancer. MWCNTs have caused increased number of micronuclei in type II pneumocytes after i.t. instillation in rats (219) and DNA strand breaks and elevated numbers of chromosomal aberrations after i.p. injection in mice (252). SWCNTs have caused mutations in the K-*ras* gene in lungs of mice following inhalation exposure (305) and DNA strand breaks in BAL cells of apolipoprotein E (ApoE) -/- mice following i.t. instillation (137). Genotoxic effects have been observed also in several *in vitro* studies (see Section 11.4).

Primary as well as secondary genotoxicity pathways may be induced. Primary genotoxicity includes direct interactions of CNTs with DNA. Secondary genotoxicity is driven by reactive species generated from inflammatory cells (297). In the studies by Takagi and colleagues, mononuclear cells of which some contained MWCNTs were accumulated right next to mesothelial hyperplastic lesions suggesting that the inflammatory response is linked to the pathogenesis of cancer (319, 320).

Several investigations focused on the generation of ROS in response to CNTs in relationship to genotoxic effects. For example, Jacobsen and colleagues found that exposure of mouse lung epithelial cells to SWCNTs led to ROS production and effects on DNA, including oxidation of purines (138). Similarly, Folkmann and co-workers observed increased production of ROS and elevated levels of oxidised nucleotides (8-oxo-7,8-dihydro-2'-deoxyguanosine (8-oxodG)) in the liver and lungs following oral exposure of rats to SWCNTs (85).

Direct genotoxicity events have also been suggested. SWCNTs have been suggested to interfere with the division of epithelial cells *in vitro* through disruption of

the mitotic spindle, leading to an aneuploidy of a number of chromosomes after 24 hours (290). Signs of interference with the mitotic spindle during the anaphase of macrophage cell division were also observed in mice following inhalation of SWCNTs (5 mg/m^3, 5 hours/day for 4 days) (305). Yi and co-workers reported that SWCNTs (diameter <2 nm) and MWCNTs (diameter 10-20 nm) can interact with DNA polymerase and restriction endonucleases in a cell-free system. In this respect carboxylated SWCNTs were more effective than pristine SWCNTs, which were in turn more effective than MWCNTs (377).

Genotoxic activity may be due to the fibrous nature of CNTs with a possible contribution by catalyst metals of unpurified CNTs (188). Longer and thicker MWCNTs caused more DNA strand breaks in cultured cells and more extensive inflammation in mice than did shorter and thinner SWCNTs (368).

9.5 Lung particle overload

Chronic inhalation of poorly soluble particles including talc, carbon black, coal dust and titanium dioxide have been shown to result in pulmonary inflammation, fibrosis, epithelial hyperplasia and, eventually, adenomas and carcinomas in the peripheral lungs of rats. These effects are considered to be caused by the so-called lung overload phenomenon, which is caused by exposures that result in a retained lung burden of particles that is greater than the steady-state burden predicted from the deposition rates and clearance kinetics of particles inhaled during exposure (131). The hallmark of particle overload is impaired alveolar clearance, which has been suggested to occur at a volumetric loading of 60 μm^3 per alveolar macrophage (representing approximately 6% of the alveolar macrophage's displacement volume) with a total macrophage stasis occurring at a loading of 600 μm^3 (31, 217). Pauluhn exposed Wistar rats to MWCNTs (Baytubes) at the dose levels of 0, 0.1, 0.4, 1.5 and 6 mg/m^3 for 13 consecutive weeks (6 hours/day, 5 days/week) and observed a marked inhibition of lung clearance of MWCNTs at 1.5 and 6 mg/m^3 (255). The retention half-time of MWCNTs at 6 mg/m^3 matched well with the retention half-time of carbon black at 7 mg/m^3, which has been calculated to correspond to about six times the overload threshold (253). Because of the lower density of MWCNTs, MWCNTs may trigger pulmonary overload at lower mass-based exposure levels than the above mentioned poorly soluble particles. Concentration-dependent pulmonary toxicity was in this study observed beginning from 0.4 mg/m^3 with granulomatous inflammation and bronchoalveolar hyperplasia seen at 6 mg/m^3. The appearance of pulmonary changes matched well with the inhibition of lung clearance, which supported the role of lung overload-related phenomenon in lung effects (255).

9.6 Interactions between carbon nanotubes and biomolecules

An important determinant of the biological effects of nanoparticles such as CNTs is the adsorbance of biomolecules to their surface, which occurs upon entry into any organism, fresh water or soil. CNTs that enter an organism are covered pre-

dominantly by proteins to form what is referred to as protein corona, the constituents of which depend on binding constants and the shape of the CNT (see Lynch and Dawson for a review) (197).

Dutta and colleagues found that the main protein in foetal bovine plasma or human plasma that binds to SWCNTs is albumin. When plasma from rats lacking serum albumin was employed instead, a different profile of adsorbed proteins was observed. Moreover, coating the SWCNTs with Pluronic F127 led to less absorption of albumin. The ability of these SWCNTs to inhibit LPS-induced activation of cyclooxygenase-2 was dependent on the binding of albumin molecules (71) (see Section 11.2.2.4 for experimental details).

Another example of an interaction with proteins that might modulate the biological effects of CNTs is the binding of complement factors described by Salvador-Morales and collaborators (289). In a cell-free system, the protein Cq1, which is involved in inflammatory responses, bound directly to CNTs, as did fibrinogen and various apolipoproteins. Likewise, Sund and collaborators found that when MWCNTs where incubated with plasma, fibrinogen binding occurred and that pulmonary surfactants could reduce this binding. No binding of plasma proteins to SWCNTs was detected (317). SWCNTs (diameter 2 nm, bundle length 5-30 µm) were, however, shown to bind to serum proteins (i.e., bovine fibrinogen, gamma globulin, transferrin, ferritin and bovine serum albumin) resulting in a change of the secondary structure of bovine fibrinogen and gamma globulin (90).

CNTs have also been shown to interact with nutrients in cell medium leading to medium depletion and thereby indirect cytotoxicity (37).

Another study suggested that the observed cytotoxicity of MWCNTs towards phagocytosing cells (murine macrophages) involves disruption of the cell membrane as a result of association between these CNTs and the scavenger receptor referred to as the macrophage receptor with collagenous structure (MARCO) (116).

Direct interactions between CNTs and enzymes, followed by enzyme inhibition have been described (350, 351, 377). For example, both SWCNTs (diameter 2 nm, length 5-15 µm) and MWCNTs (diameter 10-20 nm, length 5-15 µm) can adsorb to acetylcholinesterase (AChE) and in inhibit its enzymatic activity 50% at concentrations (IC_{50}) of 96 mg/l and 156 mg/l, respectively (351). Moreover, both SWCNTs and MWCNTs also adsorb to and inhibit butyrylcholinesterase (BChE) with IC_{50} values of 49 and 97 mg/ml (350). It should be noted that the levels of CNTs employed in both of these studies were very high compared to the levels used *in vitro* by others, so that such adsorption or inhibition does not necessarily occur *in vivo*.

9.7 Alterations in membrane permeability

CNTs can alter the permeability of lung cells *in vitro*, but this effect has not yet been confirmed *in vivo.* This is an important question, since damage to cellular walls might facilitate translocation of CNTs.

When rat alveolar cells were exposed to SWCNTs *in vitro*, the transmonolayer resistance (which reflects passive ion transport) was transiently reduced, whereas the active ion-transport was not affected (367). Similarly, MWCNTs can alter the paracellular permeability of lung epithelial cells *in vitro* (281) and long SWCNTs (0.5-100 μm) and MWCNTs (5-9 μm), but not short CNTs can diminish the trans-epithelial electrical resistance (TEER) of these same cells, with no alteration in the expression of junction proteins (280).

10. Challenges facing toxicological studies

As pointed out in a European report (78), production of CNTs by many different processes yields nominally the same material, but these CNTs can nonetheless vary widely with respect to crystal structure, aspect ratio and residual impurities and, consequently, might exert quite different toxic effects (388). Therefore, to properly interpret and assess their observed toxic effects, the CNTs used in each individual study should be characterised in detail with respect to all of the physical and chemical properties that might have biological relevance, including the possible presence of impurities such as metals.

Dose metrics

At present, there is no consensus among researchers in the field of nanotoxicology concerning how to express dose metrics of CNTs. Weight/volume and weight/body weight are employed most commonly, but area/weight is also occasionally reported. The number of particles present is seldom stated, due to difficulties in assessing this number.

Reporting only the weight/volume of the CNTs administered may lead to difficulties in comparing studies, since the number of particles present may differ depending on their size. No preparations of particles with such exact sizes actually exist, since there is always a size distribution (generally with Gaussian distribution) and the pristine particles are usually agglomerated (242) (see also Section 5.1).

Aerosolisation and deposition

A critical question in connection with the effects of CNTs on the airways is whether they are inhaled as individual tubes or in bundles or clues, which has relevance both for human exposure and toxicological testing by inhalation. For example, aggregates often have a larger aerodynamic diameter than singlet CNTs and may therefore be deposited higher up in the respiratory tract, where removal mechanisms other than the macrophages are active. Clearly, aerosolisation of CNTs in a controlled and reproducible manner is a problem for toxicological inhalation studies. As a consequence, i.t. instillation and aspiration have been the methods most commonly used for pulmonary studies. Among the few attempts to develop appropriate procedures for inhalation studies, atomisation from liquid (176) and agitation of powder appear promising (203).

Functionalisation and dispersion

To evaluate the responses of cells to CNTs, which are inherently hydrophobic, it is often necessary to first increase their solubility in aqueous solutions. This is relevant for *in vitro* studies, but also when doing *in vivo* studies using aqueous solutions of CNTs, such as instillation or aspiration studies. One way to do this is by functionalising the surface of the CNTs, e.g., by introducing hydroxyl (–OH) or carboxyl (–COOH) groups by acid treatment, or by the addition of amino ($–NH_2$) moieties.

In vitro, CNTs that have not been rendered more water-soluble by functionalisation are often dispersed in aqueous media utilising sonication or some type of detergent. Addition of detergents is problematic, since some are in themselves toxic. At the same time, sonication may shorten the carbon skeleton of the CNTs, so that proper characterisation following sonication is required.

The dispersing ability of detergents and surfactants, as well as their potential to mask or exacerbate the toxic effects of CNTs have been addressed in several investigations. The biocompatible detergents, Tween-80 and different forms of Pluronics have been used extensively in connection with exposures of cell cultures or for instillation *in vivo*. Alternatively, serum or components thereof, such as albumin, may be employed (discussed further in Section 9.6) (73).

Vippola and collaborators examined the capacity of bovine serum albumin and dipalmitoyl phosphatidylcholine (DPPC) at physiologically relevant doses to disperse SWCNTs and MWCNTs in two cell culture media, i.e., bronchial epithelial growth medium (BEGM) and RPMI-1640 with 10% foetal calf serum. When foetal calf serum was present, no additional dispersing agent was required and bovine serum albumin alone improved dispersion (357).

Herzog and colleagues found that the degree of dispersion influences the level of oxidative stress evoked by SWCNTs in human carcinoma epithelial and normal bronchial epithelial cells. After sonication in culture medium alone (leading to polydispersed agglomerates) or in medium containing DPPC (resulting in smaller agglomerates), SWCNTs (HiPCO or produced by arc discharge) caused different levels of cellular oxidative stress, with higher ROS formation in presence of DPPC. This formation was lower when foetal calf serum was present in medium, suggesting a protective role (112).

SWCNTs successfully dispersed in Survanta, a natural lung surfactant without cytotoxic effect of its own, promoted collagen production by human lung fibroblasts *in vitro* as well as lung fibrosis in mice exposed via pharyngeal aspiration (346).

When Dong and colleagues exposed human astrocytoma (1321N1) cells to SWCNTs dispersed with sodium dodecyl sulphate (SDS) or sodium dodecyl benzene sulphonate (SDBS), the SDS and SDBS molecules on the surface of the SWCNTs were found to be toxic. No effect on cell proliferation or cytotoxicity was exhibited by SWCNTs alone (69).

SWCNTs dispersed in Triton X-100 were toxic towards rat liver epithelial (WB-F344) cells and *E. coli* whereas these SWCNTs had no effect when dispersed in gum arabic, polyvinyl pyrrolidone, amylose or natural organic matter (6).

To emphasize the need for standardising assay conditions to allow comparison of different toxicity assays, Geys and collaborators compared the influence of serum and Tween-80 on the effects of CNTs and Min-U-Sil silica particles on lung epithelial (A549) cells and macrophages (stimulated THP-1 cells). The presence of serum rendered Min-U-Sil particles much less toxic towards A549 cells, but had considerably less effect on CNT toxicity (92).

It has been discussed to what extent traditional cell cultures submerged in media reflect the exposure in real life. For these cells, the degree to which the particles/fibres reach the cell surface, where they can interact, is determined by properties such as sedimentation and diffusion in the liquid environment (328). Since such parameters are strongly dependent on particle size, dispersion efficiency becomes a critical issue and, consequently, the concentration of the nanoparticles in the cell culture media (mg/ml) might not provide the most relevant measure of exposure (256).

In order to resemble the genuine conditions of exposure more closely, deposition of airborne particles directly onto cells has been tested (28, 89, 256, 293, 335). To date, there are no reports concerning the application of this approach to CNTs.

Cytotoxicity testing

A number of reports have described how CNTs, as well as other nanomaterials can interact with *in vitro* tests for cytotoxicity, for instance the colorimetric MTT (3-(4,5-dimethyl-2-thiazolyl)-2,5-diphenyl-2H-tetrazolium bromide) assay, to give false results. In brief, MTT is taken up by cells and converted to a purple formazan precipitate in the mitochondria of cells and the intensity of the colour considered being proportional to the overall metabolic activity of viable cells, which is in turn thought to reflect their number. Unfortunately, CNTs interfere with this assay, presumably by adhering to the MTT-formazan crystals to form complexes that cannot be solubilised by using the protocol, thereby producing a falsely low value for viability. Accordingly, the results obtained with this assay need to be interpreted with care and validated by other procedures (23, 36, 362).

The clonogenic (colony formation) assay simply involves culturing cells in presence of CNTs and assessing numbers and size of the colonies formed, with colony size being a much more sensitive end-point (113). However, CNTs may induce cytotoxicity in this assay indirectly by depletion of the cell medium (37). Casey and colleagues first incubated SWCNTs (HiPCO or produced by arc discharge) with medium alone and then removed these CNTs by filtration. Lung epithelial (A549) cells cultured in such pre-treated medium exhibited reduced proliferation. At the same time, the HiPCO SWCNTs exerted direct cytotoxicity that was both time- and dose-dependent (37).

Adsorption of micronutrients from the cell culture medium by both purified SWCNTs and SWCNTs functionalised with aryl sulphonate groups has been de-

scribed by Guo and co-workers. Riboflavin, biotin, folic acid and thiamine adsorbed to a lesser extent to functionalised, than to pristine SWCNTs, and this phenomenon influenced the survival of human hepatoma (HepG2) cells negatively (98). Although adsorption of micronutrients may or may not be relevant *in vivo*, this possibility should be considered when employing *in vitro* system.

11. Effects in animals and *in vitro* studies

The animal studies described in this chapter are summarised in Tables 9-15 in Chapter 13.

11.1 Irritation and sensitisation

11.1.1 Irritation

In an attempt to evaluate different systems for assaying dermal irritation, the eyes and skin of rabbits (n=3), hen eggs and cultured skin were exposed to two types of MWCNTs. One was 110-170 nm in diameter and 5-9 μm in length with a surface area of 10-15 m^2/g and a dimension of 901 nm in solution while the other was 10-15 nm in diameter and 0.1-10 μm in length with a surface area of 30-45 m^2/g and a dimension of 554 nm in solution. When 0.5 mg of each MWCNT preparation was applied to the skin for 4 hours and the effect examined after 60 minutes and 24 hours later, no irritation was observed in either case. When 18 mg of nanotubes was applied to the eyes and the results evaluated by the Draize procedure conjunctival redness occurred, but had disappeared totally after 96 hours. Injection of 0.3 mg of nanotubes into hen eggs gave rise to no irritation 5 minutes later. Exposure of skin *in vitro* to 3.3 mg nanotubes/ml for 42 hours did not alter cell viability. These results indicate that MWCNTs are not particularly irritating (158).

When fullerene soot with a high content of CNTs was applied to one eye of each of four rabbits (the other eye being used as reference) for 72 hours in a modified Draize test, no effects were observed after 24, 48 and 72 hours (122). The experimental evidence presented in this report is, however, somewhat weak and no information concerning the concentration of CNTs in the soot was provided, making it impossible to compare with others studies.

There was no evidence of skin irritation and only a very mild eye irritation in rabbits when MWCNTs (Baytubes) were tested according to OECD guidelines 404 and 405 (254). No other details reported.

11.1.2 Sensitisation

Several observations of aggravated allergic inflammation of the airways in response to CNTs have been published. When mice (n=12-13) were each repeatedly exposed by i.t. instillation to 50 μg (corresponding to 1.61 mg/kg bw) SWCNTs (diameter 0.8-1.2 nm, length 0.1-1 μm, <35% Fe) once a week for 6 weeks and allergen response was induced by repeated instillation of ovalbumin, the SWCNTs aggravated the mucus hyperplasia and the production of cytokines

and chemokines involved in the T-helper cell allergic response to ovalbumin. The SWCNTs acted as adjuvants in connection with the production of immunoglobulin (Ig)G and IgE directed against the allergen. Formation of markers against oxidative stress and the maturation of dendritic cells *in vitro* were also strengthened by exposure to the SWCNTs. Thus, at this dose the SWCNTs exacerbated allergic airway inflammation. The authors stated that a similar response was observed with 25 µg per animal, but no supporting data were presented. In addition, the effects of different preparations of SWCNTs (diameter 1.2-2 nm, length 1-15 µm, 75% CNTs, the rest being amorphous carbon) were found to be similar. These investigators concluded that SWCNTs cause such effects regardless of their characteristics (135).

When mice (n=12-13) were administered 50 µg MWCNTs (diameter 67 nm, length not provided, surface area 26 m^2/g, 99.79% pure) once a week for 6 weeks by i.t. instillation with or without co-exposure to ovalbumin every second week to induce allergic airway inflammation, the animals receiving both MWCNTs and allergen developed more severe inflammation than those receiving allergen alone. Infiltration of eosinophils, neutrophils and mononuclear cells into the lungs was observed, together with a larger number of goblet cells in the epithelium of the bronchi. Increases in the levels of IgG, IgE, T-helper cell cytokines and chemokines, as well as T-cell proliferation were detected. Administration of MWCNTs alone (i.e., to healthy mice) resulted in much less pronounce changes. These findings also indicate that CNTs can worsen allergic airway inflammation. Exposure to a different type of MWCNT (diameter 2-20 nm, several µm in length, 40-50% pure) led to similar results, which the authors suggest might be due to similarities in fibrous structures of the two preparations examined (133).

When mice (n=8/group) were administered 4 mg/kg bw of either SWCNTs (diameter 1.2-1.4 nm, length 2-5 µm) or MWCNTs (diameter 2-20 nm, length 0.1 µm to several microns) (both 75% pure with the remainder being amorphous carbon and other carbon nanoparticles) by i.t. instillation, both preparations elevated the number of neutrophils recovered in the BAL fluid, but only SWCNTs enhanced the total number of cells and level of protein. When combined with an LPS-induced disturbance in coagulation, both SWCNTs and MWCNTs increased these parameters even more. The levels of proinflammatory cytokines in the lungs were higher after CNT exposure and even more so when combined with LPS. The SWCNTs caused a rise in plasma levels of fibrinogen, both alone and more so in combination with LPS, whereas the MWCNTs only had a similar effect in combination with LPS. Moreover, MWCNTs alone, but not together with LPS, increased the circulatory levels of macrophage chemoattractant protein (MCP-1) and keratinocyte-derived chemoattractant (KC). Interestingly, the pattern with SWCNTs was the opposite, i.e., no effects on cytokines except in combination with LPS. In conclusion, exposure to CNTs aggravated the disturbance in coagulation caused by LPS, with SWCNTs being more potent, and enhanced systemic inflammation (134).

In another investigation, mice with experimentally induced allergy to ovalbumin were exposed to SWCNTs (diameter 4 nm, length 0.5-100 μm, 50% graphitic material, 25% SWCNTs and 25% MWCNTs) and MWCNTs (diameter 15 nm, length 0.5-200 μm, 90% pure, many defects) either by subcutaneous injection or intranasal instillation. The CNTs were applied in low, medium and high doses, but only the highest dose was actually stated (200 μg for subcutaneous injection and 400 μg for intranasal instillation). The combination of either CNT and ovalbumin elevated the level of ovalbumin-specific IgE in the blood, as well as the number of eosinophils in the BAL fluid and secretion of Th2-associated cytokines in mediastinal lymph node cells. MWCNTs together with ovalbumin led to higher levels of IgG2a, numbers of neutrophils and levels of inflammatory cytokines in the BAL fluid, whereas the SWCNTs did not. These authors also concluded that CNTs aggravated allergic inflammation in mice (241).

Mice (n=10-12) were exposed to MWCNTs (diameter 110-170 nm, length 5-9 μm, 90% pure, surface area 12.83 m^2/g, doses of 5, 20 or 50 mg/kg bw) via i.t. instillation and examined during a 14-day period. The exposure induced an allergic response, as indicated by elevated levels of cytokines and IgE antibodies in the blood and BAL fluid, a larger number of cells in the BAL fluid as well as a larger proportion of B-cells in the spleen and blood. In the BAL fluid the number of macrophages fell, the number of lymphocytes and neutrophils rose, and the levels of cytokines exhibited a dose-dependent increase. Pulmonary injury was detected 1 day after administration of all three doses and was still present after 14 days. The number of B-lymphocytes in the blood and spleen were elevated at 50 mg/kg. Levels of IgE were highly elevated in the blood after 7 and 14 days, with a less extensive increase in the BAL fluid as well. The results indicate that MWCNTs are toxic to murine pulmonary tissue, causing inflammation and enhancing the number of B-cells in the lungs and blood levels of IgE, which may cause allergic responses (249).

MWCNTs (Baytubes) did not produce skin sensitisation in a modified maximisation test in guinea pigs performed in accordance with OECD guideline 406 (254). No other details reported.

Conclusions concerning irritation and sensitisation

Present data suggest that CNTs are slightly irritating to the eyes, but not irritating to the skin (158, 254) and do not produce skin sensitisation (254). Moreover, these particles may act as adjuvants to allergens such as ovalbumin and thereby exacerbate pre-existing allergic airway inflammation (133, 135, 241) and may also augment LPS-induced lung inflammation (134). One study showed that MWCNTs elevated the levels of IgE in the BAL fluid and serum in mice, suggesting respiratory sensitisation (249), but additional investigations are required in order to draw firm conclusions.

11.2 Effects of single exposure

11.2.1 In vivo studies
11.2.1.1 Lethality
SWCNTs
I.t. instillation of a high dose of SWCNTs (0.5 mg/animal, CarboLex brand containing large amounts of nickel) led to the death of 5 out of 9 mice within 4-7 days after exposure. The animals showed signs of lethargy, inactivity and loss of body weight prior to death. The investigators speculated that during the preparation of these SWCNTs, which included sonication, nickel became bioavailable on the surface of the SWCNTs and could have been responsible for the observed effects (175).

When Swiss mice (n=10/group) were administered 1 000 mg/kg bw raw (diameter 1 nm, length >1-2 µm, 25% Fe), purified (diameter 1 nm, length 1-2 µm, <4% Fe) or ultra-short (diameter 1 nm, length 0.02-0.08 µm, <1.5% Fe) SWCNTs orally, no death and no pathological effects were observed. The authors concluded that the lowest lethal dose for Swiss mice is greater than the one employed (165).

MWCNTs
Acute oral (LD_{50} > 5 000 mg/kg bw) and dermal (LD_{50} > 2 000 mg/kg bw) toxicity studies of MWCNTs (Baytubes) in rats according to OECD guidelines 423 and 402, respectively, did not reveal any specific toxicity (254). No other details presented.

Conclusion
Limited data suggest that CNTs are of low acute oral and dermal toxicity (165, 254).

11.2.1.2 Pulmonary toxicity
SWCNTs
Mice were subjected to pharyngeal aspiration of SWCNTs (diameter 0.8-1.2 nm, length 0.1-1 µm, containing 17.7% Fe, a single dose of 5-20 µg SWCNTs for dose-response studies or 10 µg for time-course studies) and the effects were assessed 1, 7, or 28 days after the final exposure. The dose of 5, 10 and 20 µg led to significant and dose-dependent elevations in the levels of PMNs, lactate dehydrogenase (LDH), total protein, TNFα and IL-6 in BAL fluid after 1 day. Pharyngeal aspiration of 10 µg of instilled SWCNTs evoked less extensive production of inflammatory markers and, in particular, less fibrosis than did 5 µg of inhaled SWCNTs (5 mg/m^3, 5 hours/day for 4 days, see Section 11.3 for details). In short, exposure via inhalation produced more severe inflammatory responses and fibrosis than aspiration (305).

When female mice (n=12/group) received a single exposure to 0, 10, 20 or 40 µg SWCNTs (99.7% pure, 0.23% Fe) via pharyngeal aspiration and examined 1, 3, 7, 28 and 60 days later, their lungs exhibited granulomatous inflammation associated

with aggregates of SWCNTs and thickening of the alveolar walls and diffuse interstitial fibrosis. Depositions of collagen were found in all cases (306).

Mice (n=4-6/group) were exposed to 10 µg of dispersed or non-dispersed HiPCO SWCNTs (labelled with gold nanoparticles or quantum dots to allow visualisation) by pharyngeal aspiration and examined 1 hour, 1 and 7 days and 1 month later. Eighty per cent of the non-dispersed SWCNTs were detected as large agglomerates within granulomatous lesions that could be identified by light microscopy in the vicinity of the proximal alveolar region, while the remaining 20% entered the alveolar walls. In the case of dispersed SWCNTs electron microscopy revealed a broad distribution localised to the interstitial region of the lungs. Little or no phagocytosis by macrophages was detected. The BAL fluid contained elevated numbers of PMNs after 1 day that returned to normal after 7 days, as well as significant increases in the numbers of macrophages after both 1 and 7 days, with a return to normal levels after 30 days. Examination of these macrophages by TEM revealed a normal morphology and no indication of activation. In contrast to the non-dispersed SWCNTs, the dispersed particles did not evoke granulomatous lesions. However, the average thickness of connective tissue in alveolar regions increased after exposure from 1 hour (0.1 µm) up to 1 month (0.88 µm) post-exposure indicating a gradual build-up of collagen (208).

When both vitamin E-adequate and -deficient C57BL/6 mice were exposed to SWCNTs (HiPCO, diameter 1-4 nm, surface area 1 040 m^2/g, 40 µg/animal) via pharyngeal aspiration and then monitored for 28 days, their body weight was reduced after this period, regardless of their vitamin E status. The vitamin E-deficient mice had only 10% of the normal vitamin E level in their lungs. The general oxidative stress caused by vitamin E depletion was further aggravated by the SWCNTs. Extracellular superoxide dismutase, which is part of the anti-oxidant system in the lungs, was cleaved at a higher rate in animals administered SWCNTs, but vitamin E deficiency had no effect on this parameter. After 24 hours, the total numbers of inflammatory cells, and of PMNs, level of LDH and total level of protein in the BAL fluid were elevated by the exposure to SWCNTs, even more so in the vitamin E-deficient mice. Granulomatous bronchointerstitial pneumonia was also detected and after 28 days, fewer PMNs were seen and histiocytic granulomatous lesions were formed. The SWCNTs also evoked more collagen deposition and thickening of the alveolar septa and this fibrosis was worse in the vitamin E-deficient animals. In conclusion, dietary vitamin E can influence the inflammatory response following pulmonary exposure to SWCNTs and might provide protection against this response (307).

In another study by the same research group, SWCNTs (HiPCO, diameter 1-4 nm, surface area 1 040 m^2/g, >99% pure, 0.23% Fe, 40 µg/animal) were administered to male NADPH-oxidase-deficient and C57BL/6 mice by pharyngeal aspiration and the animals were examined 1, 7 and 28 days later. NADPH-oxidase null mice responded with a marked accumulation of PMNs and neutrophils, elevated levels of apoptotic cells, production of pro-inflammatory cytokines, decreased production of the anti-inflammatory and pro-fibrotic cytokine, TGFβ, and signifi-

cantly lower levels of collagen deposition in the lungs as compared to C57BL/6 mice (308).

In yet another investigation, pristine or acid-functionalised SWCNTs (40 µg of either) were administered to female mice by oropharyngeal aspiration. The pristine SWCNTs formed tight agglomerates, making characterisation impossible, while the acid-functionalised SWCNTs were well dispersed, forming particles less than 150 nm in size and with zeta-potentials of -40 to -60 mV. Mice exposed to acid-functionalised CNTs exhibited many more cells in their alveolar fluid than did control mice or mice exposed to pristine CNTs as well as higher levels of total protein and cytokines. The more pronounced toxicity of the functionalised CNTs was probably due to better dispersion and their negative surface charge (295).

When male C57BL/6J mice (n=3/group) were exposed to 10 µg non-dispersed or dispersed SWCNTs (diameter 0.8-1.2 nm, length 0.1-1 µm, 99% pure, 0.23% Fe, dispersant Survanta) via pharyngeal aspiration and examined 2 weeks later, increased collagen production in the lungs was observed. According to the authors, the similarity of the fibrogenic effect of non-dispersed and dispersed SWCNTs indicates that Survanta did not mask the bioactivity of SWCNTs (346).

Lam and colleagues instilled 0.1 or 0.5 mg SWCNTs dispersed using inactivated mouse serum (dimensions not stated) i.t. into mice (n=4-5) and examined them 7 or 90 days later, employing three different kinds of SWCNTs (raw, purified and CarboLex) and comparing these to carbon black (Printex-90) and quartz (Min-U-Sil-5) at the same doses. SWCNTs containing high levels of nickel and yttrium (manufactured by CarboLex) caused extensive mortality, whereas the others did not. At the 0.5-mg dose, the raw CNTs evoked mild signs of inactivity and hypothermia which disappeared after 8-12 hours, while purified CNTs did not cause such effects. At this same dose, CarboLex CNTs produced weight loss in the surviving animals. The lungs of animals which died following exposure to 0.5 mg of CarboLex CNTs demonstrated signs of congestion and after 90 days, the surviving animals exhibited aggregated particles inside macrophages in the alveolar space, as well as some aggregates in the interstitium, giving rise to granulomas. Interstitial inflammation was also detected. The 0.1-mg dose did not cause granulomas. Exposure to 0.5 mg raw or purified CNTs also produced granulomas, mainly located beneath the bronchial epithelium and containing macrophages. These cells were activated and had engulfed black particles that were rarely seen outside the granulomas. The lesions observed 90 days after exposure to 0.5 mg of either kind of CNTs were more severe than those after 7 days. Some of the mice showed necrosis, interstitial inflammation in the alveolar septa and peribronchial inflammation. In contrast, carbon black did not cause any pathological effects, while quartz at a dose of 0.5 mg increased the number of macrophages in BAL fluid and led to mild-to-moderate interstitial inflammation (175).

When SWCNTs (bundles with a diameter of 12 nm, length 0.32 µm, metal content 0.05%, suspended in phosphate buffered saline (PBS) and 10 mg/ml Tween-80, and doses of 0.04, 0.2, 1 and 2 mg/kg bw) were administered to rats (n=6/group) by i.t. instillation and pulmonary and systemic responses assessed for as long as 6

months, the exposure was found to produce a dose-dependent pulmonary inflammatory response. At the lowest dose a minimal increase in inflammatory cells, including alveolus macrophages, was observed after 3 days and persisted minimally for as long as 6 months, but the lung weights were unchanged. At 0.2 mg/kg bw the weight of the lungs was significantly elevated after 1 week and more neutrophils were detected in the BAL fluid at all time-points. Also, at this dose and the two higher increased levels of alveolar and interstitial macrophages were seen throughout the observation period and at 2 mg/kg bw alveolar and interstitial macrophage uptake of CNTs was seen by TEM at all time-points. No individual CNTs were detected in the cells of the interstitium. At 1.0 and 2.0 mg/kg bw lung weights were significantly increased throughout the observation period. At 1 mg/kg bw histopathological examination showed formation of granulomas and hypertrophy of the alveolar epithelium and foamy macrophages appeared at 3 and 6 months. Levels of inflammatory cells in BAL fluid were consistently elevated up to 3 months at this dose. Histopathological examination did not reveal fibrosis at doses up to 2.0 mg/kg bw although at 2.0 mg/kg bw the lung tissue thickened progressively. No effects were seen in organs other than the lung (164).

Following i.t. installation of 0.5 mg SWCNTs into mice and subsequent monitoring after 3 and 14 days, the alveoli was found to be injured. Macrophages in the alveoli were activated and pulmonary granulomas were present. Genomic analysis suggested that this injury resulted from activation of transcription factors in the macrophages following uptake of CNTs, leading to enhanced oxidative stress and activation of other immune functions. Such activation of immune cells would, according to the authors, explain the chronic inflammation and formation of granuloma observed (48). The dose was, however, very high and no information on CNTs dimensions was provided.

Al Faraj and colleagues characterised the distribution and histopathology of SWCNTs in rats for 1-90 days post-exposure. These SWCNTs were suspended by sonication and incubated with albumin and administered by i.t. instillation at doses of 0.4, 2 and 4 mg/kg bw (n=9 or 13/group). The animals receiving 2 mg/kg bw were followed for 90 days and the others for 30 days. MRI revealed SWCNTs in the lung at 1 day post-exposure, but level had decreased after 7 and 30 days. No effects on ventilation were observed at any time-point or with any dose, and no SWCNTs were detected in organs such as the liver, spleen and kidneys. After 30 days, small intense pixels thought to represent to inflammatory nodules could be detected by MRI in the rats exposed to 2 and 4 mg/kg bw. At the same time, MRI revealed no acute inflammation. Histopathology revealed aggregates of SWCNTs in the bronchioles and alveoli after 1 day, without any apparent epithelial damage with any of the doses. After 7 days, the alveolar septa had increased in thickness, and SWCNTs were seen to adhere to the bronchiolar wall. After 30 days, multifocal granulomas, accompanied by invading inflammatory cells and collagen deposition with alveolar collapse, were observed. These effects were enhanced and the fibrosis became more severe with increasing dose. Pneumonitis also occurred as indicated by the presence of PMNs. The lowest dose of 0.4 mg/kg bw evoked

an inflammatory response at the site of deposition in the airways, but no inflammatory events in the pleura could be detected by histopathology or MRI. In conclusion, i.t. instillation of SWCNTs led to progressive inflammation and fibrosis in a dose-dependent manner (3). The SWCNTs employed were reported to contain 10% iron, but no information concerning dimensions or dispersion state was provided.

When SWCNTs (diameter 1.3 nm, length 3.5 µm, specific surface area 1 700 m^2/g, 150 µg/animal) suspended in foetal bovine serum were administered to mice (n=8) by intranasal instillation, airway hyper-responsiveness induced by methacholine was elevated 24 hours later. Moreover, a significant increase in number of macrophages in airways was detected (102).

Jacobsen and colleagues examined the genotoxic and pulmonary effects of 5 different types of nanoparticles on female ApoE -/- mice. SWCNTs (diameter 0.9-1.7 nm, length <1 µm, 2% Fe), carbon black, C_{60}, gold and quantum dots were compared. When mice (n=7) received 54 µg SWCNTs by i.t. instillation and were examined 3 and 24 hours later increased levels of mRNA encoding macrophage inflammatory protein (MIP-2), macrophages/monocyte chemoattractant protein-1 (MCP-1) and IL-6, all associated with inflammation, were detected in the pulmonary tissue at both time-points, being somewhat higher after 3 hours. After 3 hours the BAL fluid contained more protein and the cells in this fluid exhibited elevated levels of DNA damage (see further Section 11.4). After 24 hours the level of total protein remained elevated, and moreover the proportion of neutrophils and macrophages in the BAL fluid was increased. Overall the toxicity of the SWCNTs and carbon black was less than that of quantum dots, but greater than that of gold and C_{60} (137).

C57BL/6 mice (n=4-8/group) were administered 40 µg (corresponding to 1.6 mg/kg bw) SWCNTs (diameter 1-2 nm, length 0.1-2 nm, either aggregated in PBS or nanoscale dispersed in Pluronic) by i.t. instillation and monitored 30 days later. Granuloma-like structures with mild fibrosis were observed after exposure to aggregated, but not nanoscale dispersed, SWCNTs. The authors concluded that the toxicity of SWCNTs is attributable to aggregation rather than the large aspect ratio of the individual tubes (232).

MWCNTs

Wistar rats (n=6) were exposed to 11 or 241 mg/m^3 MWCNTs (diameter 10-16 nm, specific surface area 253 m^2/g, containing 0.53% Co, Baytubes), 11 mg/m^3 acid-treated MWCNTs (containing 0.12% Co, Baytubes) or 248 mg/m^3 α-quartz (DQ12, specific surface area 3.2 m^2/g) in a single nose-only aerosol exposure for 6 hours and monitored for 3 months thereafter. The MWCNTs were dispersed with a Wright Dust-Feeder. Overall, the effects of both the pristine MWCNTs and those containing a reduced level of cobalt on the BAL fluid were similar, increasing for 7 days and thereafter, persisting, but to a diminishing degree. These findings suggest that the pulmonary response was not associated with the metal impurities alone. The BAL fluid contained significantly higher numbers of inflammatory cells after exposure to pristine MWCNTs at either concentration, as well as more

LDH and collagen. Most of these effects declined with time, but still remained after 90 days. In contrast, the more pronounced response to the quartz particles increased with time. The levels of inflammatory markers γ-glutamyl transferase, β-N-acetyl glucosaminidase and alkaline phosphatase in the BAL fluid were also elevated by doses of MWCNTs, again, declining with time. The weight of the lungs was elevated as well. Thus, the nanotubes induced dose-dependent toxicity that diminished with time. Histopathological examination revealed significant hypercellularity of the bronchoalveolar tissue and focal septal thickening in the animals exposed to 241 mg/m^3 MWCNTs. Dark spots were present in macrophages following both concentrations, whereas focal increases in the septal level of collagen occurred only with the higher concentration. Similar results were obtained following exposure to quartz. Genomic analysis of the pulmonary tissue revealed up-regulation of genes encoding chemo- and cytokines, complement factors and surface markers of inflammatory cells. Moreover, stress-response genes and genes whose products are involved in preserving vascular integrity were also induced. In summary, when inhaled, MWCNTs induce an inflammatory response (76).

Mice (n=10) were exposed 1 or 30 mg/m^3 MWCNTs (diameter 10-30 nm, length 0.5-40 μm) for 6 hours and controls exposed to 30 mg/m^3 carbon black or saline vehicle. Assuming that 10% of the inhaled MWCNTs were deposited, these dosages corresponded to 0.2 and 4 mg/kg bw, respectively. MWCNTs were ingested by macrophages and these migrated to the subpleura. The nanotubes were recovered in the subpleural wall and within macrophages. Macrophages containing nanotubes were observed in aggregates on the pleural surface. CNTs were still detected in the subpleural wall at the end of the observation period. However, no quantification was made to measure the clearance of the MWCNTs. Subpleural fibrosis, as assessed by image analysis, was increased in the high-dose group 2 and 6 weeks, but not 14 weeks, after exposure. Most of the subpleura appeared normal, the fibrotic lesions being focal and regional. No increase in subpleural fibrosis was seen in the low-dose group (284).

In another study, healthy mice and ovalbumin sensitised mice inhaled an aerosol containing 100 mg/m^3 MWCNTs for 6 hours. According to the manufacturer, these MWCNTs were 10-30 nm in diameter and 0.5-40 μm in length, had a surface area of 40-300 m^2/g and were 95% pure with 0.12% nickel. However, independent measurements revealed a diameter of 30-50 nm, a length of 0.3-50 μm, a surface area of 109.29 m^2/g and a purity of 94% with a 5.53% nickel content. The authors estimated that 4 and 12 mg/kg bw were deposited in the alveoli and the tracheobronchial tract, respectively. Examination after 1 and 14 days revealed nanotubes in the lungs (with no obstruction of the airways), in macrophages and epithelial cells. Sensitised mice had developed airway fibrosis after 14 days, whereas the healthy mice had not. In addition, the sensitised mice exhibited elevated levels of mRNA coding for IL-5, a pro-inflammatory cytokine, which might had potentiated the fibrosis. On the basis of their findings, these authors suggested that for MWCNTs to induce fibrosis, inflammation must be present prior exposure and that individuals

with pre-existing allergic airway inflammation such as asthma might therefore be particularly sensitive to airway fibrosis evoked by nanotubes (285).

When mice were exposed to a single dose (10-80 μg) of MWCNTs (mean diameter 49 nm, median length 3.9 μm containing 0.41% Na and 0.32% Fe, Mitsui MWNT-7) by pharyngeal aspiration, the levels of inflammatory markers in the BAL fluid were elevated in a dose-dependent manner. These levels were highest after 7 days post-exposure and had returned to normal after 56 days, except with the 40-μg dose, where they remained elevated. SEM revealed deposition of MWCNTs on the alveolar epithelium, with rapid uptake by alveolar macrophages and alveolar epithelial cells. The occurrence of pulmonary fibrosis after 7 days was confirmed by histopathological examination and granulomatous inflammation was still present after 56 days. Some of the MWCNTs migrated to the pleura (265).

To examine effects of MWCNTs (mean diameter 49 nm, median length 3.9 μm, 0.41% Na, 0.32% Fe, Mitsui MWNT-7) on the alveolar epithelium, subpleural tissue and intrapleural space, mice (n=7-8, 7 weeks old) were exposed to 10, 20, 40 or 80 μg MWCNTs by pharyngeal aspiration and monitored for up to 56 days. After 1 day 18% of the particles were in the airways (the majority in the airspace), 81% in the alveolar region (60% within macrophages) and only 0.6% in the subpleural tissue. These MWCNTs were found to penetrate the pleura and reach both the intra- and subpleural tissues in a dose- and time-dependent manner (although no statistical analysis was indicated). At 80 μg, the frequency of these penetrations was initially increased, but declined until day 7, rising again on day 28 and then persisting until 56 days post-exposure. Penetration of the alveolar epithelial was also dose-dependent (effective dose for 50% response (ED_{50}) 15.3 μg) and the CNTs were engulfed by macrophages. Granulomatous lesions were reported at a dose of 20 μg, but there was no statistical analysis or information on the frequency of such lesions, nor were they reported with the higher doses (207).

Fibrotic response to MWCNTs (mean diameter 49 nm, median length 3.9 μm, 0.41% Na, 0.32% Fe, surface area 26 m^2/g, Mitsui MWNT-7) administered to male C57BL/6J mice (n=8/group) via pharyngeal aspiration at doses of 10-80 μg was monitored for 1-56 days by field emission SEM. MWCNTs were deposited on the epithelial surface and then rapidly taken up into the mucus layer and alveolar epithelium. MWCNTs were observed in the mucous lining layer at the early time-points of 1 hour and 1 day post-aspiration, but were rapidly cleared as demonstrated by their absence in the airways 7, 28 and 56 days after exposure. The majority of the MWCNTs were within the alveolar macrophages at these later time-points. With the 80-μg dose, penetration of MWCNTs through the endothelial walls into a pulmonary venule occurred. Fifty-six days after exposure to this same dose, 68% of the MWCNTs were located inside alveolar macrophages, 8% in the alveolar tissue, 1.6% in the subpleural tissue and visceral pleura, and 20% in granulomas in the alveoli. At the same time-point, a dose-dependent increase (73% with 80 μg) in the thickness of the alveolar wall (assessed by Sirius red staining of collagen fibres) had occurred, although this increase was much less than that evoked by SWCNTs (see reference (208) in previous Section on SWCNTs) (206).

MWCNTs (total dose 25 µg/mouse) of different dimensions and morphology (NT_{short}: diameter 26 nm, length 1-2 µm; $NT_{tangled}$: diameter 15 nm, length 1-5 µm; NT_{long}: diameter 165 nm, mean length 36 µm, 84% >15 µm) were administered to mice by pharyngeal aspiration and pulmonary and pleural effects were assessed 1 and 6 weeks post-aspiration. A length-dependent inflammatory response was indicated by increased levels of granulocytes in BAL fluid after 1 week in mice exposed to long CNTs. Long CNTs also induced extensive interstitial thickening after 6 weeks, whereas tangled CNTs caused small localised granulomas. Furthermore, the long, but not tangled or short CNTs induced increased levels of granulocytes in lavage from the pleura after 1 week and after 6 weeks these levels were highly increased. SEM examination of the parietal pleura facing the diaphragm, 6 weeks post-aspiration, revealed cellular aggregates on the mesothelial surface that contained leukocytes and collagen deposition after exposure to long CNTs. The short and tangled CNTs did not produce any significant change in the pleura (224).

After male C57BL/6 mice (n=6-8/group) were administered MWCNTs (diameters 12.5 and 25 nm, length several µm, 5 wt% Fe) by oropharyngeal aspiration at doses of 1, 2 and 4 mg/kg bw, histological examination revealed formation of granulomas with collagen deposition, aggregates of MWCNTs and MWCNT laden macrophages throughout the lung parenchyma and surrounding the bronchi. With all three doses, the number of neutrophils and epithelial cells in the BAL fluid were elevated, but only the highest dose increased macrophage number as well (348).

When mice were injected directly into the pleura with MWCNTs (total dose 5 µg/mouse) of different dimensions (NT_{short}: diameter 20-30 nm, length 0.5-2 µm; $NT_{tangled}$: diameter 15 nm, length 1-5 µm; NT_{long1}: diameter 40-50 nm, mean length 13 µm; NT_{long2}: diameter 20-100 nm, maximal length 56 µm, 77% >20 µm) or amosite asbestos (50% >15 µm) and subsequently monitored for 1 and 7 days and 4, 12 and 24 weeks, the long, but not tangled or short CNTs caused acute inflammation and progressive parietal pleura fibrosis. After 1 day, the total number of cells, as well as of granulocytes in lavage fluid from the pleura was elevated only by exposure to $NT_{long1\ or\ 2}$ or asbestos. Not until 4 weeks after the injection with NT_{long2} did the number of granulocytes begin to decline, but still remained higher than in control animals 24 weeks post-exposure. Histological examination following exposure to $NT_{tangled}$ and NT_{long2} revealed aggregates of inflammatory cells in the pleural wall in both $NT_{tang1ed}$ and NT_{long2} samples 1 day after exposure, but only in NT_{long2} samples after 7 days. At every time-point the pleura of NT_{long2}-exposed mice exhibited a fibrotic layer, in contrast to the mesothelial monolayer of unexposed mice, and this fibrosis was progressive. Furthermore short fibres were cleared through the stomata, whereas long fibres were retained within the pleura (223).

When Wistar rats (n=10/group) were exposed to MWCNTs (diameter 48 nm, length 0.94 µm (range 0.22-8.9 µm), specific surface area 69 m^2/g, doses of 0.2 and 1 mg/animal corresponding to 0.66 and 3.3 mg/kg bw) by i.t. instillation and pulmonary toxicity assessed 3 days, 1 week and 1, 3 and 6 months later, the level

of cytokine-induced neutrophil chemoattractant-1 (CINC-1) in lung tissue was elevated at all time-points up to 3 months in the high-dose group. Both doses increased the total number of cells and of neutrophils in the BAL fluid after 3 days. Although no granulomatous lesions were observed with the low dose, the high-dose exposure led to transient deposition of collagen as well as small granulomas. Histopathological examination revealed infiltration of neutrophils, eosinophils and alveolar macrophages throughout the entire period of observation. Uptake of MWCNTs into the phagolysomes of macrophages was detected by TEM (216).

The pulmonary toxicity of MWCNTs (diameter 40-60 nm, length 0.5-500 µm, 95% pure, dispersed in saline containing 1% Tween-80 by sonication for 1 hour, single dose of 0, 1, 3, 5 and 7 mg/kg bw) administered to male rats by i.t. instillation has been monitored 1 day, 1 week, and 1 and 3 months post-exposure. A time- and dose-dependent toxicity was observed, with inflammatory cells (including macrophages, lymphocytes, neutrophils and eosinophils) present in the alveolus interstitium after the doses of 3, 5 and 7 mg/kg bw. Thickening of the alveolar septa and cracked alveolus were also seen at these doses. After 3 months, CNTs were still present in the lungs, and localised to capillary vessels and intracellular cytoplasmic vacuoles (190). The number of animal studied was not stated and this investigation was qualitative rather than quantitative.

In another report, structural defects were found to be a major determinant of toxicity. The following four different preparations of MWCNTs were compared: ground (MWCNT-g), in which structural defects in the carbon backbone has been introduced mechanically; ground and then heated to 600 °C (MWCNT-g600), which, in addition to structural defects, reduced the number of oxygenated carbons and content of metal oxide; ground and then heated to 2 400 °C (MWCNT-g2400) to remove all metals, while at the same time, annealing and reducing carbon defects; or, finally, heated to 2 400 °C and then ground (MWCNT-2400g), which also removed metals, but introduced structural defects. These preparations were administered i.t. to rats at a dose of 2 mg/animal and the effects monitored for 3 or 60 days. The structural defects turned out to be the cause of the acute pulmonary toxicity observed. MWCNT-g and MWCNT-g600 were more toxic than MWCNT-g2400. After 60 days, exposure to MWCNT-g led to the formation of granulomas containing collagen throughout the parenchyma, while exposure to MWCNT-g600 or -g2400 led to formation of smaller granulomas. In addition, MWCNT-g and -g600 were genotoxic *in vitro*, whereas CNT-g2400 was not (for details see Section 11.4). The further observation that the animals exposed to MWCNT-2400g (with structural defects, but containing no metal) demonstrated signs of acute pulmonary and genotoxicity similar to those receiving MWCNT-g indicated that structural defects in the carbon skeleton were the major cause of toxicity both *in vivo* and *in vitro* in this investigation (221). A more thorough analysis of the physiochemical properties of these structural defects was carried out in a companion paper (81). The CNTs with the largest number of structural defects and most pronounced hydrophilicity exhibited the highest toxicity, whereas those with the fewest defects and no contamination of transition metals were almost inert in this respect (81).

Following administration of MWCNTs (diameter 50 nm, length 10 μm, surface area 280 m^2/g, 95% pure, dose 0.05 mg) to mice (n=5/group) by i.t. instillation, agglomerates of CNTs were present in the bronchi 8 and 16 days later, but visible inflammation appeared only after 24 days. The injury and destruction to alveoli became more severe between 8 and 24 days post-instillation. In comparison to repeated inhalation (see further Section 11.3) performed by these same researchers, more pronounced effects were detected after instillation (181). The CNTs were not well dispersed in the solution instilled, which may have affected the outcome of this study.

In another case, guinea pigs were instilled i.t. with 12.5 mg/animal of four types of MWCNTs and examined 3 months later. The dimensions of these nanotubes were not provided, but they were reported to be free of iron, except for one preparation which contained <0.01 ppm iron. The MWCNTs fabricated by Showa Denko enhanced the level of IL-8 in the BAL fluid. After exposure to 95% pure NanoLab MWCNTs, the numbers of macrophages, lymphocytes and neutrophils in this fluid were elevated. The less pure (80%) NanoLab MWCNTs enhanced macrophage numbers to a similar extent and also increased the number in eosinophils, but with no effect on lymphocytes and neutrophils. Histopathological examination revealed most severe pulmonary lesions following instillation of Showa Denko nanotubes, while all of the preparations evoked infiltrating of inflammatory cells into the perivascular, peribronchial and interstitial regions (95). Although these findings show that with exposure by i.t. instillation, different types of MWCNTs can produce different responses, the preparations employed were not characterised sufficiently to explain why.

When guinea pigs were exposed to 15 mg of 6 different kinds of MWCNTs by i.t. instillation and examined 90 days later, all of these animals exhibited signs of pneumonitis with or without mild fibrosis. Exposure to MWCNTs produced by Carbon arc discharge increased pulmonary resistance, and in all animals except those exposed to Pyrograf CNTs, inflammatory cells had infiltrated the lungs. Histopathological examination revealed, however, infiltration by inflammatory cells as well as atelectasis, emphysema and alveolar exudation in all cases. In some cases, CNTs were observed inside macrophages and other phagocytic cells (123). The experimental evidence presented here is somewhat weak, with too few figures and very little statistical analysis.

Sprague Dawley rats (n=4-6) have also been instilled i.t. with either MWCNTs (diameter 9.7±2.1 nm, length 5.9 μm, specific surface area 378 m^2/g) or ground MWCNTs (diameter 11.3±3.9 nm, length 0.7 μm, specific surface area 307 m^2/g) at concentrations of 0.5, 2 and 5 mg/animal and monitored thereafter for 1 hour-60 days. Asbestos of Rhodesian Chrysolite "A" (length 2.4±2.3 μm, width 0.17±1.8 μm) and carbon black (specific surface area 66.8 m^2/g, density 174 kg/m^3, but no physical dimensions given) were used for comparison. After 28 days, similar levels of both types of CNTs (78.4%) remained in the lungs. Thereafter, intact CNTs were eliminated more slowly (81.2% remaining after 60 days) than ground CNTs (36% still present after 60 days). At the doses of 0.5 and 2 mg, ground CNTs enhanced

the level of LDH activity in the BAL fluid, while only the higher dose of intact CNTs gave such an effect. Moreover, 2 mg of ground CNTs resulted in elevated protein levels in the BAL fluid that were comparable to or higher than those produced by the asbestos control. After 60 days pulmonary fibrosis at levels comparable to the asbestos control was produced by both types of CNTs in a dose-dependent manner. 2 and 5 mg of intact CNTs raised the pulmonary level of hydroxyproline, whereas only the higher dose of ground CNTs had this effect. The level of collagen was enhanced by 2 and 5 mg intact CNTs and 0.5-5 mg ground CNTs. The intact CNTs evoked granuloma formation in the bronchi, while the more well-dispersed ground CNTs caused granulomas in the alveolar spaces or interstitium. Asbestos led to parenchymal thickening with fibrosis, whereas carbon black exerted very little effect compared to the other particles. After 3 days the pulmonary levels of TNFα was elevated by 0.5 or 2 mg ground CNTs, but only by 2 mg intact CNTs (222).

Other investigators have exposed rats (170-200 g) with two different kinds of MWCNTs (one intact and one ground in a mortar, both suspended in an artificial lung surfactant, dose of 5 mg/animal) by i.t. instillation followed by observation for 91 days. The intact CNTs were 100 nm in diameter and 27.5% were longer than 5 μm, but the dimensions of the ground particles were not stated, although these were observed to be shorter and less agglomerated than the intact nanotubes. The ground MWCNTs increased the total number of cells in the BAL fluid after 8 days and the neutrophil ratio after 29 days. The levels of LDH and total protein were elevated 8, 29 and 91 days after both exposures. Ground MWCNTs could be observed in the alveolar region after 2 days, whereas intact MWCNTs were localised in the bronchial region. After day 8, macrophages containing intact MWCNTs were detected in the interstitium, while those containing ground MWCNTs were located predominantly in the alveolus. Black macrophages were present in the bronchiolar lymph nodes of rats exposed to either type of MWCNT. These authors suggest that the degree of agglomerates influences the toxicity of MWCNTs (339).

When male Fischer rats (n=8/group) were instilled i.t. with 40 or 160 μg corresponding to 0.16 or 0.64 mg/kg bw MWCNTs (mean diameter 88 nm, mean length 5 μm (38.9% being longer), aspect ratio 57, Mitsui MWNT-7) or 160 μg α-quartz as control and then monitored for 1, 7, 28 and 91 days, MWCNTs were observed in the bronchiolar and alveolar spaces. Deposition in the alveolar wall was not detected after 1 day, but was present after 28 days and had decreased again by day 91. Free MWCNTs disappeared more rapidly from the bronchiolar and alveolar spaces than did those that had been phagocytised. The bronchiolar associated lymph tissue exhibited uptake of MWCNTs, generally to a lesser extent with the lower than the higher dose. Multifocal microgranulomas consisting of alveolar macrophages engulfing MWCNTs were observed with the high dose and rose in number with time. In some cases, these microgranulomas were associated with fibrosis. In the low-dose group, slight fibrosis without associated microgranulomas was observed after 91 days. α-Quartz exerted effects similar to those of the lower dose of CNTs. The bronchi and bronchioles demonstrated no histological alterations, nor were

any lesions detected in the pleura. The number of multinucleated macrophages, the levels of total protein and albumin, and activities of LDH and alkaline phosphatase in the BAL fluid were elevated in a dose- and time-dependent manner. The highest levels were reached after 1 day, declining thereafter, but were still remaining elevated after 91 days. No pathological changes were observed in the visceral pleura. These investigators argued that the presence of fibrosis and microgranulomas in the alveoli might be due to the presence of MWCNTs in the alveolar wall and interstitium, which could cause long-term release of proinflammatory and profibrogenic cytokines by macrophages (1). Signs of frustrated phagocytosis were reported by Takaya and co-workers who assessed dispersion of MWCNTs (length 5 μm) in the lungs 1 day after the i.t. administration described by Aiso and co-workers (1, 323).

In another report mice (n=10/group) were exposed by i.t. instillation to undoped MWCNTs (diameter 50 nm, length up to 450 μm, 2-2.5% Fe) or MWCNTs doped with nitrogen (N) (diameter 20-40 nm, length 100-300 μm, 2-4% N, 2-2.5% Fe). Both CNT preparations were subjected to acid treatment to achieve effective dispersion and doses of 1, 2.5 or 5 mg/kg bw were employed. With 2.5 mg/kg N-doped CNTs, a mononuclear cell granuloma was observed after 30 days in one mouse only, with no other effects. At 5 mg/kg, aggregates of nanotubes were present in the lumen of bronchioles, the bronchiolar wall was damaged and granulomas containing immune cells and aggregates of CNTs were present in the interstitium after 48-72 hours. Although free of CNTs, draining lymph nodes were hyperplasic. After 7 and 30 days, fibrosis was observed in the peribronchiolar interstitium. In addition, mononuclear infiltration, disruption of the bronchial epithelium and papillomatous hyperplasia were seen after 7 days. In the case of undoped CNTs, death due to asphyxiation occurred at all doses, e.g., at 5 mg/kg, 90% of the mice died. Fifteen days after exposure to 1 mg/kg, multiple granulomas were detected in the interstitium, goblet cell hyperplasia had occurred in small bronchioles, CNTs were detected in the interstitium and granulomatous inflammation was seen in the bronchial lumen. Higher doses produced similar effects after 24 and 48 hours. Some of these differences were suggested to be due to the rougher surface of and lower van der Waals forces between the N-doped MWCNTs, resulting in less agglomeration. More highly agglomerated tubes would then lead to asphyxiation (35). In these same study CNTs administered to mice by nasal instillation caused no mortality or pulmonary toxicity.

When rats were exposed by i.t. instillation to 0.04, 0.2 or 1 mg/kg bw MWCNTs (diameter 60 nm, median length 1.5 μm) or to 5 mg/kg silica particles and then followed for 6 months, only animals in the high-dose group exhibited transient pulmonary inflammation. After 3 days, the total numbers of cells and of eosinophils in the BAL fluid were elevated at 1 mg/kg, while the number of neutrophils increased after exposure to 0.2 and 1 mg/kg. No significant alterations in BAL cells were seen at other time-points. The levels of LDH and total protein were enhanced at 1 mg/kg, but only transiently, returning to control levels after 1 month and 1 week, respectively. In contrast, in animals exposed to silica particles almost all of

the parameters examined in the BAL fluid were elevated for the entire 6-months period of observation. Histopathological examination showed dose-dependent responses, with no significant effects at 0.04 mg/kg. Slight accumulation of macrophages in the alveoli occurred at 0.2 mg/kg and 3 days to 1 month after exposure to the highest dose, a partially granulomatous accumulation of macrophages was observed in the alveoli and interstitium. Hypertrophy of the bronchial epithelium and infiltration by inflammatory cells were also seen. Three to six months post-exposure, similar, but less extensive changes persisted. Assessment by TEM revealed MWCNTs inside macrophages in the alveoli and interstitium, but not in other tissues. Little deposition of MWCNTs was seen in the peribronchial lymph nodes, even with the highest dose and 6 months after exposure. It was proposed that macrophages can clear MWCNTs from the lungs under the experimental conditions employed (163).

Reddy and collaborators instilled two different types of MWCNTs i.t. into Wistar rats (n=6). One of these preparations was produced by arc discharge (diameter 90-150 nm, surface area 197 m^2/g) and the other by CVD (diameter 60-80 nm, surface area 252 m^2/g) and both were dispersed in PBS containing Tween-80 and administered at doses of 0.2, 1 or 5 mg/kg bw. The control rats were exposed to the same doses of quartz and all groups were monitored from 24 hours to 3 months post-exposure. The level of LDH in the BAL fluid exhibited a transient dose-dependent increase with both variants of MWCNTs, although those produced by CVD evoked a stronger response. This level was elevated as early as 24 hours after exposure and gradually decreased during the ensuing 3 months. A transient dose-dependent rise in the alkaline phosphatase activity in the BAL fluid also occurred. Moreover, the level of malondialdehyde, a product of lipid peroxidation, was higher in the BAL fluid of all groups and the level of protein in this fluid was increased by exposure to 1 or 5 mg/kg MWCNTs. Dose-dependent development of multifocal granulomas and focal peribronchiolar lymphoid aggregates occurred 24 hours to 1 week after exposure. After 1 month, multifocal granulomas containing macrophages were also seen in the alveoli and after 3 months the number of such lesions was reduced. Quartz particles produced effects similar to those caused by the MWCNTs (276).

When the pulmonary effects of instilling MWCNTs (diameter 20-50 nm, length 0.5-2 μm, dose 1, 10 or 100 μg) dispersed in a solution of albumin into the trachea of rats (n=6/group) and assessed 1, 7, 30, 90 and 180 days later, no signs of fibrosis or granuloma were observed. Pulmonary macrophages underwent apoptosis 30 and 90 days after exposure to 10 μg and 30, 90 and 180 days after administration of 100 μg. Caspase activity was induced by 10 μg after 90 days and by 100 μg after 30, 90 and 180 days. The lowest dose of 1 μg exerted no effects. The reason why no inflammation or pulmonary injuries occurred could, according to the authors, be the low doses of nanotubes used, their dimensions and/or the use of bovine serum albumin as a dispersant. The apoptosis of macrophages was not necessarily pathological, but could be a defensive step in the elimination of nanotubes from the lungs (74).

When DWCNTs (diameter 1.2-3.2 nm, length 1-10 μm, dose 1.5 mg/kg bw) were instilled intranasally into mice and followed by monitoring for 6-48 hours, bundles of DWCNTs as long as 100 μm were observed. The reduction of free radicals detected 24 and 48 hours after instillation were attributed to the scavenging capacity of the DWCNTs. Plasma levels of inflammatory cytokines were elevated. Clusters of DWCNTs were present in the lobar bronchus, the bronchioles and alveoli and pulmonary macrophages were more numerous in the exposed animals. Thickening of the alveolar wall was also observed (52). This attenuated production of ROS is in disagreement with several reports on the production of ROS as a major toxic mechanism, illustrating the many difficulties involved in directly comparing different investigations on CNTs.

Intranasal instillation of MWCNTs (diameter 11 nm, length 1.05 μm, specific surface area 130 m^2/g, dose 150 μg) into mice (n=8) did not enhance methacholine-induced airway hyper-responsiveness 24 hours later, nor was the number of airway macrophages elevated (102).

When agglomerated MWCNTs functionalised with -COOH (diameter 40 nm diameter, length 0.5-5 μm, dose 100 μg) dissolved in either PBS (MWCNTs-1) or in PBS containing 1% Tween-80 (MWCNTs-2) were injected i.v. into mice (n=10/group) with follow-up for 7-28 days, the less dispersed MWCNTs-1 were taken up from the circulation by the lungs and phagocytised by pulmonary macrophages. These CNTs caused inflammation and were only partially cleared from the lungs after 28 days. On the other hand, the more well-dispersed and less agglomerated MWCNTs-2 were not taken up by the lungs under any circumstance. It was proposed that agglomeration influence the toxicity of MWCNTs (269). It should be noted here that the effect on the lungs was observed after i.v. injection of MWCNTs, and not after administration via the airways.

To examine whether CNTs exert effects similar to those of asbestos, Huczko and collaborators instilled CNTs synthesised by arc discharge (25 mg of a soot sample) into the lungs of 250-g guinea pigs and examined these animals 4 weeks later. The tidal volume, frequency of breathing and pulmonary resistance were not altered by exposure, nor were the number of cells in or the protein content of the BAL fluid. These investigators concluded that exposure to CNTs in soot is not likely to be associated with adverse health effects (124). However, the most relevant end-points were not studied. CNTs employed were not characterised, statistical analysis are not described, and the results are poorly presented and evaluated.

In another study, MWCNTs (diameter 50 nm, length 10 μm, 95% pure with <3% amorphous carbon and <0.2% La and Ni, surface area 280 m^2/g, doses of 0.1 and 2 mg per animal) were instilled into the trachea of 250-g rats (n=5-8/group) and the pulmonary response evaluated using X-ray phase contrast imaging 5 days later. Three other rats received 0.1 mg MWCNTs and were examined 140 days post-exposure. The MWCNTs were sonicated in saline solution containing 1% Tween-80, so that most of them were individually dispersed, while a smaller proportion formed aggregates. Imaging of the airways of the animals exposed to

MWCNTs revealed that the structure of the lungs was more disordered than in control rats and those treated only with 1% Tween-80 in saline. This finding was confirmed by microscopic examination. In the animals followed for 140 days, granulomas were observed, both by microscopic examination and X-ray phase contrast imaging. In the latter imaging procedure, the granulomas appeared as black speckles, probably due to a change in the refractive index of the lung tissue. The lesions detected after the long-term follow-up were focal, while the low-dose short-term lesions were more diffuse in appearance. It was suggested that X-ray imaging might prove useful in detecting pulmonary lesions in workers exposed to CNTs, although considerable additional research in this context is required. The resolution of this procedure is not sufficiently good yet to allow observation of single alveoli, for instance (179). Little detail was provided concerning the pathological characterisation of exposed animals after 5 days.

Implantation of MWCNTs (5 or 20 mg) into the muscular fascia on the back of rats (n=2) led to acute pulmonary oedema, and a pleural response, including inflammatory liquid in the pleura of one animal, that died 180 minutes after exposure. The other rat survived for 7 days and exhibited inflammation and fibrosis only at the site of implantation. In addition, mice injected i.p. with 10 mg/kg bw MWCNTs exhibited no antigenic reaction (45). This report did not provide sufficient information concerning the dimensions of the CNTs and animal responses to allow the findings to be evaluated properly.

Combined exposure

To examine for possible synergistic effects, female C57BL mice were pre-exposed to 20 µg MWCNTs (diameter 20-30 nm, length 50 µm, purified by acid treatment) by pharyngeal aspiration 12 hours prior to a 3-hour exposure to ozone. When the BAL fluid and lung tissue examined 5 and 24 hours after ozone exposure, generally, ozone exposure alone generated only mild effects, whereas the CNTs caused alterations in cell numbers and protein levels. TNFα was increased 5 hours after ozone exposure, but not 24 hours after. On the other hand, exposure to the CNTs resulted in elevated levels of both TNFα and IL-1β both 5 and 24 hours later. Exposure to both CNTs and ozone gave rise to higher levels of TNFα and IL-1β after 5 hours, but after 24 hours only the level of IL-1β remained elevated. The level of mucin in all exposed groups was elevated after 24 hours. Although this combined exposure did not result in additive or synergistic effects, the exposure to CNTs may have produced cross-tolerance to other pollutants and thereby compromised the defences of the lung (104).

MWCNTs (diameter 40-60 nm, length 5-15 µm, surface area 40-300 m^2/g, 95% pure, 1.25% Ni, dispersed by sonication, bended and agglomerated, dose 6.67 mg/kg bw), benzene (dose 2.67 mg/kg bw) or MWCNTs-benzene combination (9.34 mg/kg bw (containing 6.67 mg/kg bw MWCNTs and 2.67 mg/kg bw benzene) were instilled into trachea of mice (n=9) and the result monitored for 3 and 7 days. As benzene like many other organic molecules is adsorbed on CNTs most of it is retained in the lung together with the CNTs. As a result, the benzene is concentrated

in lung by MWCNTs. More extensive pathological alterations were seen following co-exposure than after exposure to the MWCNTs alone. Benzene alone had little or no effects. After 3 days, the total level of protein and LDH activity in the BAL fluid were increased after exposure to MWCNTs with or without benzene, whereas the levels of the markers alkaline phosphatase and acid phosphatase were only elevated by co-exposure. After 7 days, all of these markers remained abnormally high only in the animals co-exposed. Histopathological examination after 3 days revealed aggregated MWCNTs in the inner wall of the bronchi and in the alveoli, with inflammatory cells in the vicinity of the latter. No lesions were evident in the benzene-exposed mice. Co-exposed animals demonstrated blockage of bronchi by MWCNT aggregates and greater destruction of the alveolar structure than in mice receiving MWCNTs alone. After 7 days the MWCNT-exposed animals exhibited fewer aggregates in the bronchi and the alveoli appeared intact. Again benzene-exposed animals exhibited no lesions. Co-exposure was associated with aggregates adsorbed to the inner wall of bronchi, but no blockage. The netted structure of the alveoli had recovered from the injury caused by aggregates of MWCNTs, but not entirely. In conclusion, the combined exposure to MWCNTs and benzene aggravates the pathological effects of the former on the airways of mice. The enhanced pulmonary toxicity may be due to the change of MWCNTs aggregation ability after benzene is adsorbed on them (182).

11.2.1.3 Dermal toxicity

MWCNTs

When 0.1 mg of MWCNT clusters (MWCNTs-1: diameter 20-50 nm, length 0.22 µm, specific surface area 300 m^2/g or MWCNTs-2: diameter 20-50 nm, length 0.825 µm, specific surface area 320 m^2/g) were implanted in the thoracic skin of mice and left there for 1 or 4 weeks, the MWCNTs-1 had produced a less pronounced inflammatory response in the subcutaneous tissue 1 week after implantation, than the MWCNTs-2. This difference might reflect the fact that macrophages can ingest 0.220-µm CNTs more easily than the longer 0.825-µm CNTs. Nevertheless, no necrosis, degeneration or neutrophil invasion was detected with either type of CNT (292).

11.2.1.4 Cardiovascular toxicity

SWCNTs

When mice (n=4-10) were subjected to a single exposure to SWCNTs (diameter 0.7-1.5 nm, length 1 µm, 10 or 40 µg/animal=0.4 or 1.4 mg/kg bw) via pharyngeal aspiration and monitored for as long as 60 days, haeme oxygenase-1, an indicator of oxidative insult, was activated in the lungs, aorta and cardiac tissue. Damage to aortic mitochondrial DNA, along with alterations in the levels of glutathione and protein carbonyl in the aorta also occurred. These findings suggest that pulmonary exposure to SWCNTs affects the cardiovascular system. In addition, experiments involving repeated exposure of ApoE -/- mice to SWCNTs were performed (see Section 11.3) (184).

Evaluation of the cardiovascular effects of pristine (undetermined size due to aggregation) and acid-functionalised SWCNTs (diameter 22-138 nm in solution) 24 hours after oropharyngeal aspiration of 10 or 40 μg (corresponding to 0.3 and 1.3 mg/kg bw) into mice (n=5-10) revealed no SWCNTs in heart tissue, with myofibre degeneration only in the mice exposed to 40 μg acid-functionalised SWCNTs. The myocytes in the papillary muscle and interventricular septum were shrunken, rounded and had pyknotic nuclei. Both pristine and acid-functionalised SWCNTs led to systemic effects, including increased plasma levels of creatine kinase and aspartate aminotransferase (ASAT) with the 40 μg dose. In addition, the acid-functionalised SWCNTs reduced the red blood cell count and enhanced coronary flow rate at this higher dose. When experimental ischaemia was induced, in these latter mice, they exhibited less functional recovery and larger areas of infarct. Thus, acid-functionalised, but not pristine SWCNTs can damage cardiovascular parameters. The authors point out, that acid-functionalisation increases the solubility and disperses the nanotubes more effectively in aqueous solution, which can potentially affect their translocation (336).

MWCNTs and SWCNTs

Mice (n=5) were exposed to 1.5 mg/kg bw MWCNTs (diameter 80 nm, length 10-20 μm, 0.27% Fe) or SWCNTs (diameter 0.8-1.2 nm, length 0.1-1 μm, 8.8% Fe) by pharyngeal aspiration and analysis of BAL fluid, gene and protein profiling of pulmonary tissue and blood, and enzyme-linked immunosorbant assay (ELISA) in lung and plasma performed 4 hours later. The BAL fluid demonstrated significant neutrophil influx and enhanced activity of LDH, the latter only significantly after exposure to MWCNTs. Furthermore, CNT exposure resulted in expression of genes in the lungs encoding mediators of inflammation, oxidative stress, remodelling and thrombosis. The lung response resulted in alterations in the systemic circulation, including elevated expression of several biomarkers of neutrophil response, increased number of neutrophils and induction of cytokines (e.g., IL-6) and chemokines. Interestingly, the level of plasminogen activator inhibitor 1 (PAI-1), a protein involved in inhibition of the fibrinolytic cascade, were elevated in both the blood and lungs. However, no up-regulation of this gene was observed in blood, indicating that the PAI-1 protein most likely had been released from the lungs into the systemic circulation. In most cases, the effects reported were more pronounced following MWCNT exposure, which may according to the authors be related to more rigid and better dispersed MWCNTs. This report identified some possible biomarkers for exposure to CNTs and, more importantly, revealed communication between the lungs and circulation following such exposure (79).

When rats (n=5) with experimentally induced vascular thrombosis were injected i.v. with 25 μg of either SWCNTs or MWCNTs, the rate of vascular thrombosis accelerated. The effects were found to be more potent than those of standard urban particulate matter (SRM1648), with SWCNTs being more potent than MWCNTs (270). No physical or chemical characterisation of the CNTs employed was presented.

11.2.1.5 Immunotoxicity

SWCNTs

When mice were exposed to a single dose of SWCNTs (diameter 1-4 nm, length 1-3 µm, dose 10 or 40 µg) by pharyngeal aspiration and/or *Listeria monocytogenes* (10^3 bacteria) 3 days later and then monitored for 3-7 days, the animals exposed to both SWCNTs and bacteria demonstrated slower bacterial clearance, reduced production of nitric oxide and an enhanced inflammatory response. The lowering of bacterial clearance was partially due to less extensive phagocytic activity by macrophages. The conclusion drawn was that SWCNTs may increase susceptibility to pulmonary bacterial infections (304).

MWCNTs

The effects of contaminated and clean MWCNTs on peripheral T-cells in mice have been examined utilising three types of MWCNTs (diameter 100-150 nm, length 10-20 µm) - one raw preparation containing 1.2% Fe, one purified by heating to 1 800 °C containing 0.008% Fe and one purified by heating to 2 800 °C containing less than 0.002% Fe. These CNTs were implanted subcutaneously (n=5) at a dose of 1 mg/mouse and 4 weeks later the animals were killed and their immune response characterised. The percentage of CD4+ cells was equal in all groups, while the percentage of CD8+ cells was lower in the animals exposed to the raw preparation and the ratio of CD4+/CD8+ cells higher in these same mice as well as in animals exposed to the MWCNTs containing 0.008% Fe. The plasma levels of IL-4, IL-6, IL-10 and interferon gamma (IFNγ) were elevated following exposure to the raw preparation, but not to the purified nanotubes. It was suggested that purified MWCNTs are less immunotoxic, i.e., more biocompatible with the immune system (167).

To examine the effects of CNTs on metabolism, immunological modification and toxicity, Chiaretti and co-workers injected a single dose of 10, 20 or 40 mg/kg bw MWCNTs i.p. into CD1 Swiss mice (n=3-5/group) and sacrificed them 7 days later. During this post-exposure period the death of one animal, both at 20 and 40 mg/kg was registered. Autopsy revealed adhesive peritonitis following exposure to 20 or 40 mg/kg bw, but nothing else except aggregates of CNTs. Ten mg/kg bw caused mild peritoneal irritation, but no CNT aggregation was observed (45). These responses have also been examined following repeated exposure (see Section 11.3).

SWCNTs and MWCNTs

Koyama and co-workers investigated the immunological response of mice to sub-cutaneous implantation of four different types of CNTs. These CNTs included SWCNTs (diameter 0.8-2.2 nm, no data on length, surface area 641 m^2/g, 1-1.5 wt% Fe), two kinds of MWCNTs (MWCNTs-I: diameter 10-50 nm, length 10-20 µm, surface area 56 m^2/g, 3-5% Fe; MWCNTs-II: diameter 50-150 nm, length 10-20 µm, surface area 18 m^2/g, <0.03% Fe) and cup-stacked CNTs (diameter 50-150 nm, length up to 100 µm, surface area 50 m^2/g, 1 wt% Fe). Each animal (n=30/group) received 2 mg nanotubes and was monitored for up to 12 weeks.

No differences in body weight were observed between the groups and no animals died during the experiment. SWCNTs activated the major histocompatibility complex (MHC) class I pathway of the antigen-antibody response system (higher CD4+/ CD8+ value) along with oedema formation in the vicinity of the implant after 1 week. After 2 weeks, increased values in CD4+ and CD4+/CD8+ without change in CD8+ signified an activated MHC class II for all four CNTs. At 3 weeks, SWCNTs activated the MHC class I pathway, MWCNTs-I and cup-stacked MWCNTs inhibited the MHC class II pathway and MWCNTs-II inhibited both these pathways. Histopathological examination revealed cell infiltration and granulomatous tissue for all samples (168). It was proposed that characterisation of T-cell levels in the peripheral blood of workers might be useful for assessing exposure to CNT.

In addition, immunosuppression following repeated exposure to MWCNTs has been documented (see Section 11.3).

11.2.1.6 Hepatotoxicity

SWCNTs

When chitosan-functionalised SWCNTs (diameter 1-3 nm, length 0.05-0.2 μm, 20 μg) were administered to mice by i.v. injection, they were rapidly taken up and accumulated in the liver, which exhibited pathological changes, including macrophage injury. Alterations in blood coagulation parameters also occurred (150).

MWCNTs

When rats were instilled i.t. with 0.2, 1 or 5 mg/kg bw of two kinds of well-dispersed MWCNTs (diameter either 60-80 or 90-150 nm) and monitored for up to a month, histopathological examination of the liver revealed dose-dependent foamy degeneration of hepatocytes, fatty accumulation, focal inflammation and necrosis. In addition, serum levels of glutamate pyruvate transaminase (also called alanine aminotransferase) and creatinine (markers for liver and kidney toxicity, respectively) were elevated after exposure to 1 or 5 mg/kg bw of either kind of nanotube (275). Although no MWCNTs were seen in the liver, these authors suggested that MWCNTs are able to translocate from the lungs into the liver and other organs.

When acid-oxidised (O-MWCNTs: diameter 10-20 nm, length 0.1-1 μm, 98% pure, 0.86% Ni, 0.06% Fe) and Tween-80-dispersed MWCNTs (T-MWCNTs: diameter 10-20 nm, length 0.1-1 μm, 98% pure, 0.86% Ni, 0.06% Fe) were given as one i.v. injection (10 or 60 mg/kg bw) to mice (n=20), with subsequent examination after 15 or 60 days, the T-MWCNTs proved to be more toxic to the liver. The higher dose of T-MWCNTs resulted in less body weight gain than seen in the other groups; a lower relative liver weight; infiltration of inflammatory cells into the portal region; and cellular and focal necrosis both 15 and 60 days post-injection. This same dose of O-MWCNTs evoked only a little infiltration. Administration of 60 mg/kg T-MWCNTs also evoked mitochondrial swelling both 15 and 60 days later, as well as reductions in reduced glutathione and superoxide

dismutase activity after 15 days. The blood level of ASAT was elevated by both types of CNTs at both time-points, while level of total bilirubin was only increased after 60 days. The levels of mRNA encoding proteins involved in drug metabolism and liver injury were also altered by both types of CNTs. These changes with respect to certain cytochrome P450s (CYP450s) were confirmed by quantitative-PCR. In summary, these findings reveal that at high dosage MWCNTs dispersed in Tween-80 induced liver damage, while oxidised MWCNTs exhibited less toxicity. No analyses designed to determine whether CNTs were still present in the liver were carried out. Visual inspection revealed that the liver was darker in colour after exposure to the higher than the lower dose of CNTs, which led the authors to conclude that CNTs were still present after 60 days (140).

Zhang and co-workers examined the effect of PEGylation on the hepatotoxicity of MWCNTs (diameter 10-20 nm, length <1 μm) by i.v. injection of 10 and 60 mg/kg bw non-functionalised or PEGylated MWCNTs into mice (n=10/group), with sacrifice 15 or 60 days later. In no case was the relative liver weight altered. The colour of the liver became darker as the dosage of CNTs was increased, indicating accumulation of CNTs in this organ. Both types of CNTs caused hepatic inflammatory response, spot necrosis and mitochondrial destruction at the high dose, with the non-PEGylated ones being slightly more potent. Both types of CNTs also altered gene expression in the liver, especially in the TNFα and NFκB signalling pathway. No significant alterations in the hepatic levels of glutathione or superoxide dismutase activity were observed. In summary, both types of CNTs induce some degree of liver inflammation and functionalisation with PEG ameliorates this negative biological effect (380).

When mice (20-22 g, n=10/group) received 100 μg of MWCNTs functionalised with –COOH moieties (diameter 40 nm, length 0.5-5 μm, MWCNT-1 dissolved in PBS; MWCNT-2 dissolved in PBS containing 1% Tween-80) by i.v. injection and were followed for 7-28 days, increasing amounts of MWCNTs-1 were taken up by the liver, with some remaining even after 28 days. The less agglomerated and more well-dispersed MWCNTs-2 were also taken up, but cleared after 28 days (269).

11.2.1.7 Splenic toxicity

SWCNTs

In a preliminary investigation, mice (n=3-4/group) received 1 μM SWCNTs modified non-covalently with PEG (diameter 1-5 nm, length 0.1-0.3 μm, dose 151 mg/animal) or oxidised and covalently modified with PEG (diameter 1-5 nm, length 0.05-0.2 μm, dose 47 mg/animal) by i.v. injection and the spleen examined by haematoxylin and eosin staining, immunohistochemical analysis of macrophages and micro-Raman mapping 4 months later. Weak Raman signalling was seen, brownish pigment believed to be nanotubes was present in macrophages, but no histological abnormalities were observed (298).

MWCNTs

When mice (20-22 g, n=10/group) received 100 µg of MWCNTs functionalised with –COOH moieties (diameter 40 nm, length 0.5-5 µm, MWCNT-1 dissolved in PBS; MWCNT-2 dissolved in PBS containing 1% Tween-80) by i.v. injection and were monitored thereafter for 7-28 days, more megakaryocytes and multinucleated giant cells were present in the spleen 1 and 7 days following injection of either type of CNTs, but these cells had disappeared after 28 days (269).

When MWCNTs rendered water-soluble by functionalisation with taurine (diameter 12.6 nm, length 0.269 µm) were injected i.v. into mice (n=6/group) at doses of 60 and 100 mg/kg bw and the animal studied for 1-60 days thereafter, the relative spleen weight was initially elevated after receiving 60 mg/kg, but returned to normal during the period of observation. The spleen phagocytic index, (i.e., the level of phagocytosis) and removal of particles in this organ were unaltered. Moreover, the splenic levels of glutathione, superoxide dismutase and malondialdehyde, another marker of oxidative stress, were unchanged. Histological and ultrastructural examination revealed accumulation of MWCNTs in the spleen during the 60-day period, phagocytised by macrophages or endothelial cells. No damage to tissue integrity was detected (64). It should be noted that the MWCNTs used in this case were very short.

11.2.1.8 Neurotoxicity

MWCNTs

After MWCNTs (diameter 10-30 nm, length 2 µm, purity 97%, 2.94% metal contaminants and <1% carbon soot) coated with the surfactant Pluronic F127 were injected into the cerebral cortex of mice (n=3) at a dose of 35 ng/animal, the volume of the injury was the same as in control animals administered Pluronic F127 alone 3 days later, indicating that injection of such dispersed nanotubes in such a low concentration poses no short-term threat to the nervous system. The number of animals used in the experiment was, however, small. Interestingly, the reduction in cellular respiration by Pluronic F127 *in vitro* was counteracted by the MWCNTs coated with Pluronic F127 (experimental details described in Section 11.2.2.6). These findings suggest that Pluronic F127-coated MWCNTs are not harmful to cells of the nervous system (14).

11.2.1.9 Peritoneal toxicity

MWCNTs

In order to assess the response of MWCNTs having different morphologies with, regard to fibre pathogenicity, 50 µg of four different types of MWCNTs (dimensions according to the manufacturer: $NT_{tangled1}$ (NanoLab): diameter 15 nm, length 1-5 µm; $NT_{tangled2}$ (NanoLab): diameter 15 nm, length 5-20 µm; NT_{long1} (Mitsui): diameter 40-50 nm, mean length 13 µm; NT_{long2}: diameter 20-100 nm, max length 56 µm) were i.p. injected into C57BL/6 mice. The peritoneal cavities of the mice were lavaged and histopathological examinations were made after 24 hours and 7 days. The long CNTs, but not the tangled ones caused an inflammatory response

indicated by increased number of PMNs and levels of total protein in the lavage 24 hours post-exposure and granuloma formation with significantly increased numbers of foreign body giant cells 7 days post-exposure. The long MWCNTs caused frustrated phagocytosis (259).

Conclusions concerning effects of single exposure

Single exposure studies in animals are summarised in Tables 9, 10 and 12. In general, single pulmonary exposure to CNTs evokes acute inflammation, with more neutrophils and macrophages and higher levels of pro-inflammatory cytokines in the lungs, as well as formation of multifocal granulomas (often containing CNTs-engulfed macrophages) and fibrotic lesions.

It has been demonstrated that CNTs may migrate to the pleura. Following inhalation of a high concentration (30 mg/m^3) of MWCNTs as long as 50 μm by mice, CNTs were detected in the subpleura and subpleural fibrosis developed after 2 weeks (284).

Intrapleural migration of MWCNTs (length approximately 4 μm) was seen after pharyngeal aspiration (207, 265) as well as progressive fibrosis of the pleura following injection of MWCNTs directly into the pleural space (223). In this study, only long (84% >15 μm) and not short (0.5-2 μm) fibres induced an inflammatory response and fibrosis, suggesting that fibre dimensions such as length have an important influence on the pathogenesis of fibrosis once MWCNTs have reached the pleural space (223). Similarly long, but not short MWCNTs produced pulmonary and pleural inflammation and fibrosis following pharyngeal aspiration (224). In summary, some evidence from single exposure studies supports the HARN hypothesis, but further studies are required in order to draw a firm conclusion.

Some systemic effects have been reported following exposure to CNTs via the lungs including cardiovascular pathologies in mice exposed to SWCNTs via the airways (79, 184, 336). Furthermore, CNTs stimulated platelet aggregation and accelerated the rate of vascular thrombosis in rat carotid arteries (270). Thus, there are certain indications that exposure to CNTs via the airways can have adverse effect on the cardiovascular system. Likewise, liver and kidney damage have been reported after i.t. instillation of MWCNTs, although no identification of CNTs in the organs was demonstrated (275). Such effects could either result from the release of inflammatory mediators from the lungs into the systemic circulation and/or translocation of CNTs.

Immunotoxicity related to the impurities present in the preparations of CNTs has been reported after subcutaneous administration, as has activation of peripheral T-cells (167, 168).

One investigation revealed a low degree of toxicity following intracerebral administration of MWCNTs, but no purely neurotoxicological study *in vivo* has been found in the literature (14).

Liver and kidney toxicity is less likely considering occupational exposure via inhalation and most studies showing effects on liver have assessed effects following

i.v. injection (140, 269, 384). Effects of the liver were however also observed in a study following single i.t. instillation of MWCNTs in rats (275). The few investigations on hepatotoxicity reported to date indicate that exposure to MWCNTs via the circulation can cause molecular pathological changes in the liver. Some effects have been observed after high i.v. doses.

11.2.2 In vitro studies

Methodological shortcomings in *in vitro* studies of CNTs are described in Chapter 10.

11.2.2.1 Effects on cells from the pulmonary system

SWCNTs

Low acute toxicity (50% effective concentration (EC_{50}) >800 µg/ml) was observed when lung epithelial A549 cells were exposed to SWCNTs (HiPCO, diameter 0.8-1.2 nm, approximately 10% Fe) at concentrations of 1.56-800 µg/ml in the presence or absence of serum. The same concentrations of quartz particles were used as positive controls. After 24 hours, a battery of assays and examination by TEM revealed significant cytotoxicity in the concentration range of 200-800 µg/ml. The calculated concentration that produced 50% of the maximal effect (EC_{50}) was in general greater than the highest concentration employed, except in one instance where this value was 744 µg/ml. No intracellular localisation of CNTs was detected (59).

The toxic effect of SWCNTs (diameter 1.2-1.5 nm, length 2.5 µm, purified by acid, dose 0.5-500 µg/ml) on human lung epithelial A549 cells and three other cancer cell lines after exposure for 72 hours was proposed to involve production of ROS. This production was induced in a concentration-dependent manner, and the effect was more potent than with particles of iron oxide or silica. Cytotoxicity (as determined by the MTT-assay) was observed at all time-points and concentrations examined. At levels of 250 and 500 µg/ml in the medium, the SWCNTs also induced more apoptosis (60%) than did the other particles (47). Some drawbacks associated with this study include lack of information concerning the number of experiments performed, the failure to examine all particles in all of the assay procedure employed, which makes comparisons difficult. Moreover, as discussed in Chapter 10, the reliability of the MTT assay in this context has frequently been questioned.

The relationship between contamination of CNTs by metals and amorphous carbon and the formation of ROS has been evaluated in a number of *in vitro* studies. Pulskamp and colleagues concluded that CNTs do not induce oxidative stress in lung epithelial A549 cells if amorphous carbon and metals have been removed. These investigators cultured A549 cells in presence of three different types of SWCNTs: commercial SWCNTs containing cobalt and molybdenum, SWCNTs treated in-house with the solvent dimethylformamide and SWCNTs acid-treated in-house. No effect on expression of the anti-oxidative protein haeme oxygenase 1 (after 24 hours incubation, 0-100 µg/ml, 0-62 µg/cm^2) was observed with any of these SWCNTs. The extent of the biphasic burst in oxidative stress

that occurred 10 minutes and 24 hours after exposure to 5-100 μg/ml of any of these preparations was found to depend on their contents of amorphous carbon and metal (268).

The findings by Herzog and collaborators that SWCNTs with a higher metal content are more toxic than those with little metal contamination were based on the clonogenic assay. When human carcinoma alveolar epithelial (A549), normal bronchial epithelial (BEAS-2B) and normal keratinocyte (HaCaT) cell lines were incubated with two different types of SWCNTs (HiPCO: diameter 0.8-1.2 nm, average length 0.8 μm, 10 wt% Fe; arc discharge produced: diameter 1.2-1.5 nm, length 2-5 μm, 20-μm long bundles, <1 wt% Ni and Y) the 50 % effective concentration (EC_{50}) values for colony size and colony number differed, with the former being much lower (between 15 μg/ml (HiPCO) and 28 μg/ml (arc discharge)). With both preparations, the normal cell lines exhibited a dose-dependent decrease in number of colonies formed and the response of the keratinocyte cell line regarding colony size was also dose-dependent. The HiPCO SWCNTs were more toxic than those produced by arc discharge or than carbon black towards all of the cell lines with all end-points (113).

The pronounced influence of the dispersion agent employed was demonstrated by comparing the oxidative stress produced in lung epithelial (A549) cells and normal human primary bronchial epithelial (NHBE) cells by two different kinds of SWCNTs (50 μg/ml). One variant was synthesised by the HiPCO procedure (diameter 0.8-1.2 nm, length 0.8 μm (bundles), 10% Fe, surface area 487 m^2/g) and the other by arc discharge (diameter 1.2-1.5 nm, length 20 μm (bundles), 50-70% SWCNTs with contaminants of amorphous carbon, turbostratic graphite and <1% Ni and Y, surface area 239 m^2/g). The effects were compared to those evoked by carbon black (Printex 90) and crocidolite asbestos (diameter 0.5 μm, length 5 μm). The low-to-moderate oxidative stress produced in NHBE cells by CNTs or carbon black was higher when these particles were dispersed in DPPC (smaller agglomerates) than in culture medium (non-dispersed). Asbestos (observed to be single individual fibres, regardless of the method of dispersion) did not induce ROS formation. This formation by A549 cells was lower when foetal calf serum was present in medium, suggesting a protective role (112).

When murine lung epithelial cells were exposed to (10-50 μg/ml for 2-4 days) pristine (tight agglomerates which could not be characterised) or acid-functionalised SWCNTs (well dispersed, size <150 nm, zeta-potentials -40 to -60 mV), the survival rate was higher in presence of the pristine SWCNTs at all concentrations. Only the acid-functionalised SWCNTs altered DNA synthesis, whereas both induced apoptosis in epithelial cells at a concentrations of 40 μg/ml. Neutralisation of the negative charges on the functionalised SWCNTs attenuated their toxic effects (295).

Yacobi and collaborators exposed monolayers of rat alveolar epithelial cells to SWCNTs (diameter 0.8-1.2 nm, length 0.1-1 μm) for as long as 30 hours and monitored barrier function in terms of the transmonolayer resistance (Rt) and the potential difference, which were also utilised to calculate the equivalent short cir-

cuit current (Ieq). In addition, LDH was measured as an indicator of cytotoxicity. At concentrations of 22-88 µg/ml, the SWCNTs lowered the Rt during the first hour of exposure, but this value had returned to normal after 5 hours were it remained until the end of the experiment after 25 hours. Ieq was not significantly altered and cytotoxicity was not detected. The conclusion was that apical exposure to SWCNTs can alter barrier function, an effect believed to reflect changes in cellular transport and dependent the on composition, shape and/or surface charge of the particles (367).

When SWCNTs (diameter 1.3 nm, length 3.5 µm, specific surface area 1 700 m^2/g) were added to cultures of mouse alveolar macrophages, morphological changes (e.g., an irregular plasma membrane) along with activation of macrophages occurred. SWCNTs also disrupted lipid rafts in the cell membrane, which could potentially alter cell function. After 48 hours, 200 µg/ml SWCNTs induced apoptosis slightly (102).

Although the duration of exposure to CNTs exerts important impact on the cytotoxic response, this factor is not always taken into account. Bruinink and colleagues demonstrated that the accumulation of raw and purified SWCNTs in target compartments of cells in culture rose with time and the cytotoxic response was thus influenced by the duration of exposure (32).

MWCNTs

MWCNTs (diameter 11 nm, length 1.05 µm, specific surface area 130 m^2/g) have been reported not to alter the morphology of mouse alveolar macrophages *in vitro*. After 48 hours, only the highest dose (200 µg/ml) was cytotoxic (20% reduction in viability) (102).

When lung epithelial A549 cells were exposed to MWCNTs (0.1-0.2 µm in size, but forming micrometre-sized agglomerates in solution), DNA damage was already detected at a concentration of 1 $\mu g/cm^2$ and was even more pronounced at 20 or 40 $\mu g/cm^2$. The number of viable cells was reduced at 40 $\mu g/cm^2$, although no oxidative damage to DNA or increase in intracellular levels of ROS was observed. Moreover, metal impurities were shown not to be the cause of the toxicity (151).

Upon exposure to concentrations of 0.5-10 µg/ml for as long as 24 hours, MWCNTs (no physical dimensions or chemical impurities provided) caused dose-dependent production of ROS that resulted in lipid peroxidation in rat lung epithelial cells. Cell viability was also lowered in a dose-dependent manner (from 2.5-10 µg/ml) and the activities of apoptotic caspase-3 and -8 enhanced. These results suggest that MWCNTs cause cytotoxicity by inducing oxidative stress (273).

When lung epithelial A549 cells were exposed to two kinds of MWCNTs (MWCNT-R produced by arc evaporation and MWCNT-N formed by nickel catalysis) at a concentration of 5 µg/ml, the MWCNTs-N evoked a much higher production of ROS. Asbestos and various carbon soots led to similar changes. These authors suggested that ROS production could cause cell toxicity (88), but

statistical evaluation of their data and physical and quantitative description of the MWCNTs they employed were lacking.

The degree of functionalisation was shown to exert an impact on toxicity by exposing astrocytes and lung epithelial A549 cells to various doses (1-100 µg/ml and 400-800 µg/ml, respectively) of MWCNTs functionalised with NH_2 or COOH groups (diameter 20-30 nm, length 0.1-0.3 µm), pristine MWCNTs (diameter 20-30 nm, length 0.5-2 µm) or MWCNTs highly functionalised with NH_2 groups (diameter 20-30 nm, length 0.05-0.1 µm). All of these MWCNT preparations were contaminated by low levels of metal (0.3-1.5 wt% Ni, 0.0002-0.0009 wt% Co and 0.003-0.25 wt% Fe). The highly functionalised MWCNTs reduced cell viability in a manner similar to silicon dioxide (SiO_2) particles (50% cell loss at 800 µg/ml, significant effect already at 100 µg/ml), while the other particles exerted no such effect. Their findings with the MTT assay were deemed to be somewhat unreliable by these authors themselves. The enhancement of toxicity by addition of NH_2 groups could be due to the better solubility in aqueous solution (50).

When cultures of epithelial (A549) cells were incubated with 0.1-100 µg/ml MWCNTs (diameter 12 nm, length 0.1-13 µm, 2.4% Al, 2% Fe, surface area 219.2 m^2/g) for as long as 72 hours (using asbestos fibres for comparison) the CNTs, which were not internalised, reduced cellular metabolism, but did not alter cell permeability or the levels of oxidative stress or apoptosis. However, 100 µg/ml did decrease the DNA content of the cell cultures (318).

The viability of A549 epithelial cells exposed to MWCNTs (diameter 20-40 nm, length 5-30 µm, specific surface area 380 m^2/g, 0.18% Fe) was reduced at concentrations of 150 and 200 µg/ml after 24 hours. Concentrations of 25-150 µg/ml resulted in a dose-dependent rise in the level of IL-8, which involved NFκB and the production of ROS (374).

The intracellular accumulation and toxicity of two variants of MWCNTs (short: diameter 10-160 nm, length 0.1-3.5 µm; long: diameter 10-160 nm, length 0.1-12 µm) (specific surface area 42 m^2/g and 4.2% Fe in both cases), as well as purified long MWCNTs, in cultures of A549 cells has been compared to aluminium oxide (Al_2O_3) and TiO_2. Suspensions of these MWCNTs were prepared by sonication in water containing 0.25 wt% Arabic gum, which prevented the formation of agglomerates and concentrations of 1-100 µg/ml and an exposure period of 1-24 hours were utilised. A dose- and time-dependent cytotoxic response was observed, with no difference between longer or shorter MWCNTs or with different levels of contamination by iron. The short MWCNTs were internalised by the cells, as individual tubes, with no agglomeration, leading to morphological changes such as the formation of multi-lamellar bodies. Al_2O_3 and TiO_2 nanoparticles were also internalised and had similar effects, but were less toxic (309). In contrast to many other reports, these findings indicate that the length of MWCNTs or the level of contamination by iron has no influence on the cytotoxic response. However, no statistical evaluation of the cytotoxicity was presented.

Furthermore, MWCNTs with a high-aspect ratio have been found to cause more pronounced cytotoxicity than those with a low ratio, regardless of the procedure utilised to assess cytotoxicity. In this case, human embryonic lung WI-38 cells were exposed to either MWCNTs with a high-aspect (diameter of 10-15 nm, two peak length distributions at 0.545 and 10.45 μm, containing 5% non-specified contaminants, surface area 177.6 m^2/g) or low-aspect ratio (diameter of 10-15 nm, peak length distribution at 0.192 μm, containing 1.2% unspecified contaminants, surface area 195 m^2/g) both dispersed in medium containing DPPC for 24, 48 or 72 hours at concentrations of 12.5-200 μg/ml. The low-aspect ratio MWCNTs were found to be more efficiently dispersed. Cytotoxicity was evaluated on the basis of trypan blue exclusion, the WST-1 assay and release of LDH. The trypan blue procedure revealed reduced cell survival at all concentrations and time-points for both types of MWCNTs, with the high-aspect ratio nanotubes exerting a more pronounced effect. The WST-1 assay demonstrated cytotoxic effects with 50-200 μg/ml of either type of MWCNTs after 24 hours, while all concentrations (12.5-200 μg/ml) were cytotoxicity after 48 and 72 hours in both cases. With the low-aspect ratio MWCNTs, release of LDH activity after 24 hours was enhanced by all concentrations, and after 48 and 72 hours at 50 μg/ml and higher; while corresponding values for the high-aspect ratio particles were 25 μg/ml and higher, 50 μg/ml and higher and all concentration except 25 μg/ml. Iron oxide was found not to be cytotoxic. The investigators concluded that high-aspect ratio MWCNTs are more cytotoxic (157).

Hirano and collaborators examined the cellular uptake and cytotoxicity of MWCNTs (mean diameter 67 nm, length not specified, purity 99.79%, 0.2% Fe, surface area 26 m^2/g) when added to cultures of human bronchial epithelial (BEAS-2B) cells in comparison to crocidolite. Both were suspended in 10% Pluronic F68, which resulted in well-dispersed MWCNTs present as individual fibres or small bundles. At a concentration of 10 μg/ml, the BEAS-2B cells took up MWCNTs in a time-dependent manner (up to 12 hours). In connection with cytotoxicity during a 24-hour period the half maximal inhibitory concentration (IC_{50}) for the MWCNTs was 12 μg/ml, while the corresponding value for crocidolite was 678 μ/ml. High-density cultures of BEAS-2B cells were not as sensitive to MWCNTs as low-density cultures, e.g., 10 μg/ml eliminated cell viability totally in the latter, but caused only 10% reduction in high-density cultures. The Chinese hamster ovary (CHO-K1) cells, which were more sensitive than BEAS-2B cells at both high density and low density, exhibited lowered viability in the presence of 1 μg/ml MWCNTs. MWCNT exposure also up-regulated the expression of cytokines, including IL-6 and IL-8, in a dose-dependent manner (2-10 μg/ml). Moreover, the levels of the phosphorylated (and thus activated) forms of signal transduction elements such as extracellular-signal regulated kinase (ERK) 1/2, p38 mitogen-activated protein (MAP) kinase and heat shock protein (HSP) 27 and expression of NFκB were higher. In conclusion, MWCNTs were found to activate stress-related signal transduction in BEAS-2B cells and cause production of pro-inflammatory cytokines (115). This is one of the few studies that have

resulted in an IC_{50} for any CNT and compared this value to that of a reference material, thus making it an important contribution.

When MWCNTs (diameter 20 nm, aspect ratio 80-90), carbon nanofibres (mean diameter 150 nm, aspect ratio 30-40) or carbon black (aspect ratio 1) were added to cultures of lung cancer cells, including the H596, H446 and Calu-1 cell lines, MWCNTs reduced the cell survival of all three of these cell lines in a dose-dependent manner (0.02 and 0.2 µg/ml) over a period of 5 days, with H596 cells being most sensitive. At a concentration of 0.2 µg/ml, MWCNTs were less potent in reducing the proliferation of H596 cells than carbon nanofibres and carbon black, with the latter being slightly more potent than the former. Light revealed that H596 cells, which normally associate with each other in clusters, lost their connections to each other and had smaller nuclei when exposed to 0.02 µg/ml MWCNTs for 1 day. MWCNTs and carbon nanofibres with carbonyl- (-C=O), COOH- and OH-groups on their surfaces reduced cell viability somewhat more than their unmodified counterparts. The conclusion drawn was that carbon nanoparticles reduce the proliferation of lung cancer cells, with MWCNTs being less toxic in this respect than carbon nanofibres and carbon black (199). The length of these MWCNTs was not specified; nor was the size of the carbon black stated.

SWCNTs and MWCNTs

Pulskamp and collaborators concluded that metal contaminants play an important role in connection with the biological effects of CNTs on cells *in vitro*. These investigator exposed rat alveolar (NR8383) macrophages and human alveolar epithelial (A549) cells for 24-96 hours to three different CNT preparations (NT-1: >50% SWCNTs, diameter 1-2 nm, length not described, 3% O, 2.8% Co, 4.2% Mo; NT-2: 95% MWCNTs, diameter 10-20 nm, length not described; and NT-3: 95% pure MWCNTs, diameter 30-50 nm, 1.86% Ni, 0.55% Fe) together with an additional SWCNT preparation (65.7% C, 25.3% O, around 1.2-1.5% Ni, Co and N, diameter and length was not described) that was acid-treated to remove metal impurities. All CNT preparations were used at concentrations of 5-100 µg/ml (3.1-62.5 µg/cm^2) with carbon black (diameter 14 nm) and crystalline quartz (<5 µm) serving as controls. Along with individual CNTs, large bundles or ropes were formed in solution and these agglomerates were tightly packed, both in water and culture medium, despite sonication. Light and electron microscopy demonstrated that CNT agglomerates were taken up by rat alveolar macrophages. No acute toxicity was detected employing the WST assay, the MTT assay revealed a dose-dependent reduction in cell viability upon exposure to all these CNTs. Carbon black also reduced viability in a dose-dependent fashion, a finding which was supported by measurements of LDH released. The results of the WST test were confirmed by propidium iodide staining, which showed no damage to cell membrane integrity. After 24 hours of incubation, dose-dependent production of ROS occurred with all of these CNTs except for the acid-treated preparation (267).

The negative impact of CNTs on airway epithelial barrier was exhibited by exposing human lung epithelial Calu-3 cells to two kinds of SWCNTs and

MWCNTs. The SWCNTs were either long (L-SWCNTs: diameter 1.1 nm, length 0.5-100 μm, surface area 1 700 m^2/g) or short (S-SWCNTs: diameter 1-2 nm, length 0.5-2 μm, surface area 480 m^2/g), as were the MWCNTs (L-MWCNTs: diameter 110-170 nm, length 5-9 μm long, surface area 130 m^2/g; S-MWCNTs: diameter 40-70 nm, length 0.5-2 μm, surface area not stated). Exposure at a concentration of 100 μg/ml for 7 days resulted in cytotoxicity only in the case of S-SWCNTs. Exposure to 100 μg/ml carbon black had no such effect. The TEER, an indicator of barrier function, was progressively reduced by L-SWCNTs and L-MWCNTs, while the shorter CNTs and carbon black did not alter this parameter. The levels of mRNA encoding occludin and zonula occludens-1, which are involved in forming junctions between epithelial cells, were not changed under any conditions. The conclusion was that the epithelial barrier is functionally comprised by the longer CNTs, without changes in the expression of junctional proteins (280).

The paracellular permeability of airway epithelial cells has been monitored by exposing human lung epithelial Calu-3 cells to SWCNTs (diameter 0.7-1.2 nm, length 2-20 μm, surface area 1 700 m^2/g, 40% SWCNTs and the rest various other types of CNTs), MWCNTs (diameter 110-170 nm, length 5-9 μm, surface area 130 m^2/g, at least 90% pure with less than 0.1% metal contaminants) or a mixture designated AD-CNTs of 30% SWCNTs, 50% MWCNTs (diameter 10-40 nm, length 1-5 μm) and 20% amorphous carbon/fullerenes (no other characteristics of this preparation described). Carbon black served as control. The TEER was lowered in a time-dependent fashion (1-6 days) following exposure to MWCNTs or SWCNTs at concentrations of 100 μg/ml, the MWCNTs being more potent in this respect. More detailed experiments with the MWCNTs revealed time- and dose-dependent reductions in the TEER upon exposure to 5-100 μg/ml for 4 days. Furthermore, the MWCNTs elevated the permeability of epithelial cell barrier to mannitol during a period of 30-180 minutes. In addition, exposure of Calu-3 cells with MWCNTs or, to a lesser extent, SWCNTs or AD-CNTs at the time of seeding prevented the formation of a functional TEER. Co-exposure to cytokine IL-4, which lowers the TEER of Calu-3 cells, caused the TEER to continue to decrease in the presence of MWCNTs even after the IL-4 had been removed, whereas with the other CNTs the TEER returned to normal following the removal of IL-4. None of these CNT preparations altered the viability of Calu-3 cells. The investigators concluded that MWCNTs interfere with the formation and integrity of the airway epithelial barrier, i.e., with tight junctional complexes between epithelial cells (281).

Moreover, the effect of incubating SWCNTs (diameter 1-2 nm, length 5-30 μm) and MWCNTs (diameter 20-30 nm, length 10-30 μm) dispersed in 0.04% Tween-80 at concentrations of 2, 5 and 10 ppm with lung MSTO-211H cells for 60 minutes has been evaluated on the basis of the uptake of fluorescein diacetate. Only 10 ppm SWCNTs and all concentrations of the MWCNTs promoted such uptake. Lung cells were less sensitive in this respect than lymphocytes, but slightly more sensitive than keratinocytes. These authors conclude that toxicity is dependent on the nature of the CNTs and on type of cell being examined (120).

11.2.2.2 Effects on cells from dermal tissue

SWCNTs

SWCNTs containing 30% iron or purified SWCNTs containing 0.23% iron were applied to engineered human skin, cultured epidermal cells or immune-competent hairless SKH-1 mice (see also Section 11.3). A dose of 75 µg unpurified SWCNTs in 150 µl of the medium of cultures of the engineered skin evoked parakeratosis, hyperkeratosis and accumulation of fibroblasts and basal squamous cells in the epidermis after 18 hours. Increased production of collagen, a 1.5-fold thickening of the skin and production of proinflammatory cytokines was also observed. Culturing epidermal cells with unpurified and purified SWCNTs at concentrations of 0.06, 0.12 and 0.24 mg/ml promoted production of free radicals at the 0.12 mg/ml concentration. The purified CNTs lowered cell viability by 6.6%, 11.9% and 27.7% at 0.06, 0.12 and 0.24 mg/ml, respectively, with corresponding values for the unpurified CNTs being 10.2%, 22.1% and 53%. The transcription factors AP-1 and NFκB were induced in a dose-dependent manner by unpurified SWCNTs, whereas the purified SWCNTs only activated NFκB (231). The physical characteristics of the SWCNTs were not determined in this investigation.

When keratinocytes and epithelial cells, along with two lung carcinoma cell lines were exposed to SWCNTs at concentrations ranging from 0.1-10 µg/ml for 12-72 hours, survival of all these types of cells was reduced in a dose-dependent fashion, the lowest dose exerting an effect being 0.5 µg/ml. Moreover, NFκB was induced dose-dependently in keratinocytes as a result of the activation of stress-related MAP kinases. Oxidative stress was higher and cell proliferation slower in these same cells as well. These findings suggest that the toxic mechanism with all four cell types is similar, as well as that SWCNTs are toxic to keratinocytes, and, thus maybe to exposed skin (202). The MTT assay, with its serious limitations (see Chapter 10), was employed to evaluate cell survival. However, the authors did complement this assay with microscopic examination of the cells. The dimensions of the SWCNTs were not reported.

When SWCNTs functionalised with 6-aminohexanoic acid (AHA-SWCNTs) were administered to cultured human epidermal keratinocytes (HEK) at concentrations of 0.05 ng/ml-0.05 mg/ml for 24 and 48 hours, cell viability assessed with the MTT assay was reduced at the 0.05 µg/ml concentration. The levels of the pro-inflammatory cytokines IL-6 (from 1-48 hours) and IL-8 (from 24-48 hours) were elevated. The CNTs were located in cytoplasmatic vacuoles in the HEK cells. Dispersion with the surfactant Pluronic F127 attenuated the cytotoxicity. Thus, low concentrations of AHA-SWCNTs are mildly toxic, while high concentrations may irritate skin (382). The physical characteristics of the CNTs were not described.

Addition of unrefined SWCNTs containing 30% iron to the medium of cultures of human epidermal keratinocytes (HaCaT) at concentrations of 0.06, 0.12 and 0.24 mg/ml for a maximum of 18 hours (n=3 per concentration) led to formation of free radicals. The cellular morphology was altered, with the nucleus, mitochondria and tonofilaments being affected. The cells separated from the monolayers and the level of F-actin was modified in a dose-dependent manner. In addition,

there were indications of oxidative stress including reductions in the levels of vitamin E and protein thiol-groups. Cell viability was also lowered and all of these effects were dependent on concentration. The authors suggest that the effects observed were due to the high content of iron in the SWCNT preparation (303), but, no experiments with iron alone or purified SWCNTs were carried out. The physical characteristics of the SWCNTs were not determined.

Sayes and collaborators investigated the influence of functionalisation of the CNT surface on cytotoxicity towards human dermal fibroblasts, employing pristine SWCNTs dispersed in 1% Pluronic F108 or more water-soluble SWCNTs functionalised with phenyl-dicarboxyl or phenyl-SO_3H groups at various ratios (18, 41 or 80), both containing <1% contamination of metals. With 0.2-2 000 µg/ml, cell death increased with the concentration of pristine SWCNTs (lowest toxic dose=0.2 µg/ml) and SWCNTs-phenyl-dicarboxyl (lowest toxic dose=10 µg/ml) whereas SWCNTs-phenyl-SO_3H did not induce such cytotoxicity at any concentration tested. For the different SWCNTs-phenyl-SO_3H, the least functionalised (ratio 80) were most toxic, and the most functionalised (ratio 18) least toxic. When SWCNTs-phenyl-SO_3H and their precursors SWCNT-phenyl-SO_3Na were compared the precursor form with a ratio of 80 was slightly more toxic; with a ratio of 41 the effects were more similar; and neither was toxic when the ratio was 18. In addition, the SWCNTs precipitated from the cell growth medium and were deposited on the plasma membrane of the cells. It was concluded that the toxicity of water-soluble SWCNTs is dependent on the density of functional groups on their surface (296).

SWCNTs and MWCNTs

Tian and collaborators tried to correlate various physicochemical properties of CNTs to their cytotoxic effects on human dermal fibroblasts. Their test material were SWCNTs (diameter 2 nm, length 0.5 µm, surface area 3.15 μm^2), MWCNTs (diameter 50 nm, length 5 µm, surface area 789 μm^2), active carbon (radius 25 nm, surface area 7.85 μm^2), carbon black (radius 200 nm, surface area 502 μm^2) and carbon graphite (radius 500 nm, surface area 3.14 mm^2), all refluxed in HCl for 19 hours to remove metals and other contaminants. After 5-day exposure to 25 µg/ml of any of these nanomaterials cell survival was reduced, mostly with the SWCNTs and least upon exposure to carbon graphite. More detailed examination with the SWCNTs revealed that in this case cytotoxicity was dose- and time-dependent at concentrations of 0.8-100 µg/ml for a period of 5 days. Cell adhesion was reduced and more cell death was observed. Moreover, alteration in cell morphology (e.g., ruffled cell membranes), and rearrangement of cell adhesion proteins occurred. Western blotting revealed attenuated expression of fibronectin, laminin and collagen IV, proteins that promote cell adhesion. These investigators concluded that surface area is the best predictor of cytotoxicity; refined SWCNTs are more toxic than unrefined SWCNTs; and that dispersed nanomaterials can give rise to morphological changes and cell detachment (334). These results stands in disagreement with other reports showing that unrefined materials are more toxic than

refined materials (with less contamination by metals). In addition, dispersed CNTs, usually rendered water-soluble by acid treatment, are generally found to be less toxic. The evidence concerning correlation between surface area and other physical parameters with toxic effects as well as the statistical analysis of cell survival were not clearly presented.

In another report, the effects of agglomerated MWCNTs (diameters ~10 nm, length not characterised), bundles of SWCNTs (diameters 1 nm, length not characterised), carbon fibres (diameter 10 µm) and carbon nanofibres (diameter 100 nm diameter) all at concentrations of 5-50 µg/ml on cultures of mouse keratinocytes were characterised for 72 hours. Analysis of iron in the particles that was available to the cells revealed significant levels in both MWCNTs and SWCNTs, but not in the other particles. Only MWCNTs and SWCNTs reduced cell survival at all concentrations between 12 and 48 hours of exposure, but after 72 hours the cells had recovered. Moreover, only the CNTs promoted the production of ROS, indeed even more than the positive control (H_2O_2). These authors concluded that the size and chemistry of the particles alone cannot explain their effects and that their morphology and impurities must also be taken into consideration (94).

11.2.2.3 Effects on cells from the cardiovascular system

SWCNTs

When SWCNTs dispersed in Tween-80 at concentrations of 0.25, 2.5, 25 and 50 µg/ml were added to cultures of ventricular cardiomyocytes from neonatal rats, the conduction velocity was slightly higher, but only at 2.5 µg/ml, the upstroke velocity was slightly elevated with 0.25 and 2.5 µg/ml, and myofibrillary structure and level of ROS were unchanged. In contrast, TiO_2-particles altered all of these parameters and diesel exhaust particles enhanced the production of ROS, but did not affect the functioning of the heart. Thus, nanotubes dispersed in Tween-80 do not appear to damage cardiomyocyte function (109).

In addition, when cardiac muscle cells from H9c2 (2-1) rat were exposed to highly purified SWCNTs at a concentration of 0.2 mg/ml for 3 days, the integrity and survival of the cells were not altered. However, SWCNTs attached to the surface of the cells and it was impossible to remove them by washing. Furthermore, when cells cultured with CNTs were harvested and reseeded, they exhibited poorer survival (87). These results should be treated with some caution, since only one concentration of CNTs was examined, the number of experiments performed is not indicated, and no characterisation of the particles is presented.

SWCNTs and MWCNTs

Radomski and colleagues exposed isolated human platelets to 0.2-300 µg/ml SWCNTs or MWCNTs dispersed by sonication in Tyrode's solution. The CNTs stimulated platelet aggregation *in vitro* (n=6-10) via the glycoprotein IIb/IIIa pathway, as indicated by inhibition of this aggregation by prostacyclin as well as by *S*-nitroso-glutathione (270).

When human aortic endothelial cells were exposed for 3 and 24 hours to purified SWCNTs (8.8% Fe) or MWCNTs (0.27% Fe) at concentrations of 0.04-4.5 µg/ml (equivalent to 1-150 µg/10^6 cells) (n=3), no effects were observed at concentrations below 1.5 µg/ml or after 3 hours. At higher concentrations, especially at 1.5 and 4.5 µg/ml, cytotoxicity, enhanced production of IL-8, disruption of VE-cadherin and a reduced ability to form tubules were apparent. Taken together, these findings suggest that when endothelial cells come into contact with CNTs, they may lose their ability to form new blood vessels and their survival might be compromised (340). The physical and chemical characteristics for the CNTs were not clearly stated.

11.2.2.4 Effects on cells from the immune system

SWCNTs

When primary cultures of immune cells (B-cells, T-cells and macrophages) isolated from the spleen, lymph nodes and peritoneal cavity of mice were exposed to SWCNTs functionalised by 1,3-dipolar cycloaddition to render them water-soluble or by oxidation/amidation and derivatisation with PEG to obtain aqueous suspensions, as well as further modified with fluorescein isothiocyanate (FITC) to allow fluorescent detection, all of these cell types engulfed these SWCNTs with no damage to their viability. Nor was the proliferation of B- and T-cells affected by either of these SWCNT preparations and the water-soluble SWCNTs did not activate macrophages. In contrast, the PEG-derivatised SWCNTs induced production of pro-inflammatory cytokines by macrophages (70). Thus, functionalisation can affect both solubiltity of and biological responses to SWCNTs.

Kiura and collaborators examined the effect of SWCNTs (diameter 1.3-1.5 nm, forming bundles micrometres long, surface area 405 m^2/g) on human monocytes and mouse splenocytes *in vitro* employing SWCNTs purified by acid treatment and made more water-soluble with H_2O_2. Hat-stacked carbon nanofibres (H-CNFs) were used for comparison. In addition, human acute monocytic leukaemia (THP-1) cells were exposed to 50 or 500 ng/ml of these same particles and the resulting effects compared to a positive control (10 ng/ml of a mycoplasmal diacylated lipopeptide (referred to as FSL-1) that activates monocytes). SWCNTs caused much more potent activation of the THP-1 cells (as indicated by TNFα production) than did H-CNFs at both concentrations, although FSL-1 was even more potent. Similarly, activation of splenocytes (by 0.1 or 10 µg/ml particles or 100 ng/ml LPS as a positive control and analysed on the basis of the level of TNFα mRNA) was more pronounced after exposure to SWCNTs than H-CNFs at all doses, while LPS was even more potent. Interestingly, although significantly elevated at all concentrations, the level of TNFα mRNA was lower at higher concentrations of SWCNTs and H-CNFs than at the lowest concentrations of these particles tested. Neither SWCNTs nor H-CNFs had any effect on splenocyte survival. These investigators speculated that the surface area and more flexible structure of the SWCNTs explain the differences observed and that hydrophobic region on the nanoparticles may interact with hydrophobic domains on the cell surface (161).

When macrophages derived from human monocyte (HMDM) were exposed to 0.1 mg/ml SWCNTs (diameter 1-4 nm, length 0.5-2 µm, surface area 1 040 m^2/g, 99.7 wt% carbon, 0.23 wt% Fe) for 6-24 hours, no alteration in cell viability (as assessed by trypan blue exclusion) was apparent at either time-point (n=3). Chemotaxis and the phagocytosis of apoptotic cells were suppressed (n=3). These findings suggest that SWCNTs may disrupt normal macrophage behaviour, but the underlying mechanism(s) remains unknown (359).

The viability and morphology of human macrophages were unaffected up on exposure to pristine or acid-treated, water-soluble SWCNTs at concentrations from 0.31-10 µg/ml for 4 days. The diameter of most of the CNTs was within the range of 0.9-12 nm and the acid-treated SWCNTs contained more functional groups and were less aggregated inside the cells. Ultrastructural examination revealed bundles and free SWCNTs in lysosomes (262).

When murine and human macrophages were exposed to SWCNTs (diameter 1 nm, length 1-3 µm) at concentrations of 15, 30 and 60 µg/ml, with and without co-stimulation by LPS, these SWCNTs did not influence the production of nitric oxide, in contrast to the positive graphite control. In addition, the SWCNTs as well as fullerenes were engulfed to a lesser extent than graphite. Very little toxicity was evoked by SWCNTs (4% apoptotic, 2% necrotic cells), in contrast to the 25% dead cells resulting from exposure to graphite. The authors suggested that the higher potency of graphite could be attributed to its surface structure and that the absence of a toxic response to SWCNTs was due to their high degree of purity (84).

When CVD synthesised SWCNTs (diameter 0.9-1.2 nm) at doses from 0.31-10 µg/ml were incubated with macrophages derived from human monocytes for 2-4 days dose-dependent cytotoxicity occurred. The MTT and Neutral red assays gave conflicting results, with the former indicating cell death with 0.62 µg/ml and the latter at 2.5 µg/ml and above. TEM and confocal microscopy revealed that after 4 days, the nanotubes were localised in the nucleus of the cells and had also fused with their long axes parallel to the plasma membrane. Some were also present in structures identified as early endosomes (263).

When Kagan and colleagues exposed RAW 264.7 macrophages with two kinds of SWCNTs (unpurified with diameter 1-4 nm, surface area 950 m^2/g, 26% Fe; purified with diameter 1-4 nm, surface area 1 040 m^2/g, 0.23% Fe), both dispersed by sonication and added at concentrations of 0.12-0.5 mg/ml, they obtained no effect on the production of intracellular superoxide radicals or nitric oxide after 1-2 hours. However, when the macrophages were co-stimulated with zymosan, the non-purified SWCNTs induced production of hydroxyl radicals, whereas the purified did not. The non-purified SWCNTs also influenced biomarkers of oxidative stress, reducing the level of glutathione and enhancing lipid peroxidation. Thus, iron might contribute to the toxic effects of SWCNTs on macrophages (148).

To evaluate how adsorbed proteins might influence the activity of nanomaterials, including cellular targeting, Dutta and co-workers exposed mouse macrophages RAW 264.7 with SWCNTs (diameter and length not determined,

ropes with lengths >150 nm, surface area 274.1 m^2/g, 2.9% Y, 17.3% Ni) that were resuspended in normal growth medium containing 10% foetal bovine serum by sonication or resuspended by sonication in Pluronic F127 followed by incubation with 10% foetal bovine serum. Silica particles (10-nm sized) were employed as the control. Less protein was adsorbed in the presence of Pluronic F127. In the case of normal medium, SDS-PAGE (polyacrylamide gel electrophoresis) revealed major bands of absorbed protein with molecular weights between 49 and 62 kDa, whereas with Pluronic F127 the major band seen was 18-28 kDa in size. The smaller proteins were caseins, haemoglobins and lactoglobulins, glycoproteins, apoplipoprotein and keratins, while the major 49-62-kDa protein adsorbed to SWCNTs was albumin. The SWCNTs resuspended in absence of Pluronic F127 reduced macrophage proliferation at concentrations of 12.5-30 μg/ml and also evoked anti-inflammatory changes, while those treated with Pluronic F127 lacked the latter property because they lacked adsorbed albumin. In addition, the SWCNTs were taken up by macrophages via scavenger receptors. Similar findings concerning the influence of protein adsorption on cytotoxicity were made with amorphous silica. In conclusion, adsorbed proteins influence the biological response of cells in culture to SWCNTs (71).

MWCNTs

Alterations in the functioning of dendritic cells of the immune system upon exposure *in vitro* to carboxylated MWCNTs with four different ranges of diameter (M_{10}: diameter 10-20 nm, mean length 0.54 μm; M_{20}: diameter 20-40 nm, mean length 0.38 μm; M_{40}: diameter 40-60 nm, mean length 0.66 μm; M_{60}: diameter 60-100 nm, mean length 0.69 μm, all 95% pure) have also been explored. Dendritic cells were obtained by isolating monocytes from human peripheral blood and subsequent differentiation and maturation in the presence of granulocyte macrophage-colony stimulating factor (GM-CSF), IL-4 and LPS for 48 hours. No cytotoxicity was observed regardless of the type of MWCNTs or concentration (10, 50 or 100 μg/ml) employed. The dendritic cells phagocytosed M_{10} and M_{20} to the same extent, M_{60} slightly more and M_{40} in highest amount in a concentration-dependent manner. None of the exposures altered the expression of cell surface markers associated with immunological functions. The conclusion drawn was that the dendritic cells did not recognise the MWCNTs, possibly due to chemical modification of the particle surface (345). It should be noted that the MWCNTs used here were much shorter than those used in most other investigations, with mean lengths of less than 0.7 μm.

When T-cells isolated from rat thymus were exposed to MWCNTs (length 1-5 μm, some surface carboxyl groups, 12.5 and 25 μg/ml) or C_{60} (99.5% pure, 7.2 and 14.4 μg/ml) for as long as 24 hours, only the higher level of C_{60} reduced the activity of Ca^{2+}-stimulated ecto-ATPase which hydrolyses extracellular ATP and participates in purinergic cell signalling. When the cells were co-exposed to H_2O_2, the MWCNTs raised their viability after 2 and 24 hours, while C_{60} had the same effect only after 24 hours. When, instead, the cells were first treated with H_2O_2

and then incubated with the carbon particles viability was enhanced after 2 or 24 hours in the presence of C_{60}, but only after 24 hours with the MWCNTs. In summary, both MWCNTs and C_{60} protected thymocytes from H_2O_2-induced injury, but only C_{60} influenced the activity of Ca^{2+}-stimulated ecto-ATPase (266). The physical and chemical properties of the CNTs were not described in detail.

The effect of two kinds of MWCNTs (diameter 20-40 nm, length 1-5 µm, 95% pure) -- one pristine and the other oxidised with nitric acid and thereby more water-soluble, shorter (length not determined) and straighter -- on T-lymphocytes were examining by treating cultures of Jurkat T-cells for 24-120 hours with 1 or 10 ng/cell (corresponding to 40 or 400 µg/ml). With the pristine MWCNTs, toxicity appeared after 96 and 120 hours at 10 ng/cell, and after 48-120 hours with the same amount of oxidised MWCNTs, with the pristine MWCNTs having a much smaller effect. Both types of MWCNTs also induced dose-dependent apoptosis in Jurkat T-cells and isolated human T-lymphocytes. In addition, 40 µg/ml oxidised MWCNTs stimulated T-cell receptor activation and phosphorylation weakly. These results indicate that 40 µg/ml (or 1 ng/cell) MWCNTs is not cytotoxicity towards T-lymphocytes *in vitro* (29).

When mouse macrophages were exposed to MWCNTs (average diameter 67 nm, fibres mostly curled, but following filtration length 3-30 µm, surface area 26 m^2/g, 99.79 wt% pure) or fibres of crocidolite asbestos (50% >1 µm and 99% <20 µm) at concentrations of 10-1 000 µg/ml for 16-32 hours, the crocidolite resulted in typical dose-dependent cytotoxicity (lethal concentration to 50% of the cells (LC_{50}) 637 µg/ml), whereas with the MWCNTs a concave dose-response curve was obtained, with doses >100 µg/ml being less toxic. The LC_{50} value for the MWCNTs was 26 µg/ml after 24 hours and 22 µg/ml after 32 hours. Neither oxidative stress, glutathione levels, MAP kinases nor caspase-3 (normally involved in apoptosis) appeared to play a role in these cytotoxic effects. Ultrastructural examination showed that the MWCNTs disrupted and infiltrated the plasma membrane of the macrophages and these nanotubes were associated with a scavenger receptor known as macrophage receptor with collagenous structure (MARCO). The authors proposed that injury of the plasma membrane during membrane extension, led to cell death (116).

In another investigation, human mononuclear cells and human acute monocytic leukaemia (THP-1) cells were exposed to 15.6-125 µg/ml of three different types of MWCNTs: NT-1: diameter 20-100 nm, 5% Fe, surface area 180 m^2/g, containing both individual fibres and mats; NT-2: diameter 150 nm, 1.3% Fe, surface area 25 m^2/g, and nanofibres, mainly micron-sized aggregates; and NT-3: diameter 20 nm, 2.7% Fe, surface area 183 m^2/g, mainly micron-sized aggregates. No enhanced release of LDH from the cells was seen at any concentration (n=3). NT-2 and, in particular, NT-1 were not entirely phagocytised and the cells showed signs of frustrated phagocytosis, whereas the cells could phagocytise NT-3. NT-1 and NT-2 also led to elevated release of TNFα by the mononuclear cells at 31.25 and 62.5 µg/ml, and the THP-1 cells exhibited a similar trend. Unstimulated human mononuclear cells increased the production of superoxide with 31.25 µg/ml NT-2,

but not with NT-1 or NT-3; while stimulated cells produced more after exposure to NT-1 and NT-2 at both 15.62 and 31.25 µg/ml, while NT-3 did not enhance this production at all. Following 4-hour exposure to 15.62-62.5 µg/ml, NT-1 attenuated the phagocytosis of *E. coli* by THP-1 cells and a similar effect was obtained with 62.5 µg/ml NT-2. In summary, these MWCNT preparations prevented phagocytic cells from performing their main task, i.e., phagocytosis (30).

Exposure of peripheral blood mononuclear leukocytes to 25 or 250 µg/ml MWCNTs produced by arc discharge (diameter 10-50 nm, length up to 10 µm, free of metal contaminants, well-dispersed in the culture media by sonication) led to cell death after 24 hours. The frequencies of both apoptosis and necrosis rose from 3-18 hours of exposure in a concentration-dependent fashion. In addition, induction of apoptosis by chemoterapeutic agents was potentiated by increasing concentrations of MWCNTs (61). It was not indicated at which concentration these effects became statistically significant.

Fiorito and collaborators incubated macrophages derived from human monocytes with catalyst-assisted CVD synthesised MWCNTs (diameter 10-20 nm, no data on length) either used as-prepared (pristine) or after annealing at 2 400 °C (a-MWCNTs) to obtain greater electroconductivity. Both preparations were free of most metals, but pristine nanotubes contained 0.5% cobalt. Cells were exposed to 30 µg/ml of either type for 45 minutes-24 hours and the resulting effects compared to those of graphite fibres. Both a-MWCNTs and graphite fibres led to more cell death, but much less so than the pristine MWCNTs. Moreover the former two preparations promoted more efficient phagocytosis of fluorescent beads than did the pristine MWCNTs. At the same time, the a-MWCNTs evoked a stronger inflammatory response (as assessed on the basis of cytokine levels) than did pristine MWCNTs. The membrane potential of mitochondria was increased in cells exposed to pristine MWCNTs, less in graphite-exposed cells and actually slightly decreased by a-MWCNTs. Furthermore, the intracellular pH was elevated in cells exposed to pristine MWCNTs or graphite, but reduced by the a-MWCNTs. The a-MWCNTs also enhanced membrane currents, in contrast to the other two particles examined. To conclusion, there is an electro-chemical interaction between cells and conductive MWCNTs (83).

When human macrophages were exposed to unpurified (diameter 68 nm, length 2-164 µm, surface area 50 m^2/g, 6.2% Fe) or purified MWCNTs (diameter 68 nm, length 4-65 µm, surface area 50 m^2/g, 0.0005% Fe, shown by Raman spectroscopy to be more crystalline than the unpurified MWCNTs) at concentrations ranging from 0.31-20 µg/ml, 2.5-2 µg/ml unpurified MWCNTs exhibited cytotoxicity in the MTT-assay, while with Neutral red and Live dead staining toxicity was only present with a concentration of 20 µg/ ml. Interaction between these stains and the MWCNTs was found to be minimal. TEM analysis revealed that the majority of dead cells had undergone necrosis. The purified MWCNTs induced cytotoxicity at concentrations of 1.125-20 µg/ml i.e., lower levels than that for the unpurified MWCNTs. Iron oxide (Fe_2O_3) at concentrations of 0.016-1 µg/ml (similar to the expected levels in unpurified MWCNTs) did not resulted in any cytotoxicity.

Microscopy revealed penetration of cells, including their nucleus by the unpurified MWCNTs, which were taken up both actively and passively. The authors concluded that MWCNTs can prevent completion of phagocytosis and/or simply pierce the plasma membrane, thus causing injury (40).

Wang and co-workers focused on how the diameter influences the effects of 95% pure MWCNTs on alveolar macrophages isolated from guinea pigs, using nanotubes with diameters of 10-20 nm (MWCNT-10, surface area 133.7 m^2/g, 0.85% Ni), 40-60 nm (MWCNT-40, surface area 45.75 m^2/g, 1.89% Ni) or 60-100 nm (MWCNT-60, surface area 40.57 m^2/g, 2.3% Ni). All three kinds of MWCNTs were 1-5 μm in length following sonication, contained approximately 0.05% iron or 0.02-0.08% cobalt, exhibited not bundling and were added in concentrations of 2.5-20 μg/ml and compared to quartz particles (diameter 5 μm, surface area 21.6 m^2/g, 99% pure). After 3 hours of exposure, the MTT assay indicated concentration-dependent cytotoxicity, with the MWCNT-60 being more toxic than MWCNT-40 and MWCNT-10. Fever phagocytosing cells were present following exposure to the large-diameter MWCNT-60 than with other preparations and this effect on phagocytosis was concentration-dependent for MWCNT-60 and MWCNT-40, but not for the thinner MWCNT-10. The frequency of apoptosis was enhanced by all three preparations, to the greatest extent with MWCNT-40. The authors concluded that the diameter influences the cytotoxic effects of CNTs on macrophages, while and the metal content does not contribute as much to the responses observed (347).

SWCNTs and MWCNTs

When SWCNTs (diameter 1.3 nm, length 3.5 μm, specific surface area 1 700 m^2/g) and MWCNTs (diameter 11 nm, length 1.05 μm, specific surface area 130 m^2/g) were added to cultures of mouse alveolar macrophages and their antigen presentation assessed, both CNTs enhanced production of interferon gamma (IFNγ) and attenuated IL-13 levels. In addition, pattern of cytokine expression upon exposure to antigen was altered, with reduction in the level of TNFα, an increase in the level of IL-1β and, with the SWCNTs only an elevated level of IL-12 (102).

In another series of experiments, the effects of SWCNTs (diameter <2 nm, length 1-5 μm, surface area 436 m^2/g, traces of Co) and MWCNTs (diameter 10-30 nm, length 1-2 μm, surface area undetermined, traces of Ni) on antigen-presenting cells were compared to those of other nanomaterials, i.e., TiO_2 (30-40 nm in size, 90% rutile-10% anatase, surface area 23 m^2/g), TiO_2-silica (10×40 nm in size, all rutile, surface area 132 m^2/g) and zinc oxide (ZnO, 20 nm in size, surface area 50 m^2/g). The particles were dispersed by sonication and were added at concentrations of 3-300 μg/ml for 24 hours to cultures of RAW 264.7 mouse macrophages and dendritic cells derived from murine bone marrow cells. All of these particles demonstrated dose-dependent cytotoxicity towards both types of cells, with TiO_2 (30-300 μg/ml) being more potent in this respect than SWCNTs and MWCNTs in the case of macrophages. In contrast, with the dendritic cells, the CNTs and ZnO were more potent than TiO_2 particles. Neither type of CNT in-

duced cytokine production by macrophages, whereas TiO_2 and TiO_2-silica both enhanced the production of IL-6 and macrophage inflammatory protein 1α (MIP-1α). The CNTs did not alter cytokine production by the dendritic cells either nor did they influence expression of cell surface markers such as CD11c, CD40 and MHCII. The authors concluded that antigen-presenting cells may not be targeted by CNTs (247).

Hu and co-workers evaluated the effects of SWCNTs (diameter 1-2 nm, length 5-30 μm) and MWCNTs (diameter 20-30 nm, length 10-30 μm) both dispersed in 0.04% Tween-80 and present at concentrations of 2, 5 and 10 ppm for 60 minutes on T4 lymphocyte A3 cells on the basis of their uptake of fluorescein diacetate. All doses of CNTs promoted such uptake for 60 minutes, with the lymphocytes being more sensitive in this respect than the lung cells and keratinocytes. TEM analysis revealed penetration of the cell membrane of lymphocytes by unmodified SWCNTs, which was proposed to be the cause of cell damage (120).

Another comparison involved SWCNTs (diameter 1.4 nm, mean length 1 μm, 90% pure, concentrations 1.41-226 μg/cm^2), MWCNTs (diameter 10-20 nm, length 0.5-40 μm, 95% pure, 1.41-22.6 μg/cm^2) and C_{60} (99.9% pure, 8.36×10^{14} molecules/μg), all dispersed by sonication in the cell culture medium containing 10% foetal bovine serum. Tight aggregates consisting of 10-100 SWCNTs and thin bundles of 4-6 MWCNTs were found upon exposure of macrophages isolated from guinea pigs to these CNTs and C_{60} for 6 hours, dose-dependent cytotoxicity was obtained with the former, starting at the lowest concentration employed. The SWCNTs were generally more potent than the MWCNTs in eliciting a cytotoxic response in the MTT assay, whereas C_{60} caused no detectable toxicity at similar concentrations (1.41-11.3 μg/cm^2). In addition, the SWCNTs inhibited phagocytosis of latex beads already at a concentration of 0.38 μg/cm^2, while for the other nanoparticles 3.06 μg/cm^2 was required. Ultrastructural examination showed that the SWCNTs gave rise to morphological alterations, such as plywood body formations, in macrophages at concentrations of 0.76 μg/cm^2, with the higher dose of 3.06 μg/cm^2 leading to swelling of the endoplasmic reticulum and changes in vacuoles and phagosomes. At 0.76 μg/cm^2 MWCNTs led to the formation of large phagosomes and at 3.06 μg/cm^2 nuclear degeneration occurred. Both CNTs caused condensation of chromatin and organelles and surface protrusions at 3.06 μg/cm^2 (142). This early publication on toxicity of CNTs provides ultra-structural studies and particle characterisation that are unmatched in much more recent reports.

11.2.2.5 Effects on cells from the kidneys

SWCNTs

When SWCNTs were present in concentrations of 0.78-200 μg/ml in culture medium of human embryonal kidney (HEK293) cells, which also contained 10% foetal calf serum, for 5 days, cell survival was lowered in a dose-dependent fashion. At concentrations of 25-200 μg/ml during 6 days, a dose- and time-dependent reduction in cell adhesion was detected, even at the lowest level. Apoptosis (detected by flow cytometry) was present with 25 μg/ml for 24 hours.

Expression of cell adhesion proteins (including laminin, fibronectin, focal adhesion kinase and cadherins) was lowered by 5-day exposure to 25 μg/ml, as were the levels of mRNA encoding proteins related to apoptosis (e.g., p53, TGFβ receptor), and proteins involved in the regulation and progression of the cell cycle. The profile of gene expression confirmed that the HEK293 cells were arrested at the G1/S phase transition, and thereby unable to proliferate (54). The SWCNTs employed were not characterised either physically or chemically.

MWCNTs

In an investigation on the effects of various nanoparticles on cells from the lungs, kidneys and liver, both two forms of long MWCNTs (diameter 8-177 nm, length 0.1-20 μm, surface area 42 m^2/g, containing 4.2 or 0.08% Fe) and short MWCNTs (diameter 7-180 nm, length 0.1-5 μm, surface area 42 m^2/g) were suspended by sonication in the culture medium containing 10% foetal bovine serum. At 10-50 μg/ml, all three preparations reduced viability of kidney cells by 20-30%, with longer MWCNTs being more potent (although still less potent than TiO_2 particles (12-140 nm) at similar concentrations (50 μg/ml), and unpurified long MWCNTs more potent than purified long or short MWCNTs. In general, kidney cells were less sensitive in this respect than liver and lung cells, which was suggested to have something to do with the secretion of surfactants by lung cells and plasma proteins by hepatocytes. However, with TiO_2 particles, the kidney cells were more sensitive and the proposed explanation was that since kidney cells are specialised for uptake and recycling of molecules, they might take up CNTs and TiO_2 by different mechanisms. The isolated tubes seen in cytoplasmic vesicles in kidney and lung cells were suggested to have been taken up by micropinocytosis or caveolae-mediated endocytosis. The MWCNTs promoted ROS formation by the kidney cells, with the long MWCNTs with less iron doing so at all concentrations (10, 20, 50 and 100 μg/ml), the long-Fe containing ones at 50 and 100 μg/ml, and the shorter nanotubes only at 100 μg/ml. DNA damage was induced in kidney cells by 100 μg/ml of both kinds of long MWCNTs, but no formation of micronuclei was evoked under any conditions (20-200 μg/ml) (15).

Single CNTs penetrate plasma membranes, while bundles of CNTs are taken up by endocytosis. With this in mind, Mu and colleagues explored the penetration of MWCNTs (diameter 20-30 nm, average length following functionalisation with COOH or NH_2 groups and sonication 1 μm, coated with FITC-bovine serum albumin to allow fluorescent detection) through plasma membrane and into the nucleus of human embryonal kidney HEK293 cells. Flow cytometric analysis revealed temperature-dependent uptake both of MWCNTs with COOH or NH_2 functionalisation and TEM analysis showed that individual MWCNTs functionalised with COOH entered the cell by penetrating the plasma membrane, while bundles of these same MWCNTs entered through endocytosis. Individual MWCNTs either escaped the endosomal system and were free in the cytoplasm or were released from the bundles within the endosomes and then escaped to the cytoplasm. Similar observations were made with the MWCNTs-NH_2. No MWCNTs were found in

the endoplasmic reticulum or the Golgi apparatus, which was unexpected, since endosomal trafficking between these compartments normally occurs. TEM analysis also verified the presence of MWCNTs-NH_2 in the cell nucleus. Surface charge (negative or positive) did not affect these processes, perhaps because the charge was masked by adsorption of proteins to the surface of the CNTs. TEM analysis revealed that the individual tubes inside cells were approximately 250 nm in length in the case of MWCNTs-COOH and 175 nm for MWCNTs-NH_2, indicating that shorter tubes were more prone to directly penetrate the plasma membrane. No cell death was observed. A model which of how CNTs are taken up by cells and either located to endosomes/lysosomes or to the nucleus was presented (218).

11.2.2.6 Effects on cells from the nervous system

SWCNTs

Belyanskaya and co-workers exposed primary cultures of neuronal cells derived from chicken embryonic spinal cord and dorsal root ganglia to two particular types of SWCNTs, both dispersed with the detergent PS80 and at concentrations of 7.5, 15 and 30 µg/ml. The SWCNTs-a formed rope-like aggregates 100 nm in diameter and contained 2.4% Ni, 0.5% Y and 48% SWCNTs. The SWCNT-b consisted of bundles 20 nm in diameter and contained 5.5% Ni, 0.7% Y and 50% SWCNTs. Both aggregates and bundles reduced the total DNA content (which reflects cell number) of the mixed neuronal-glia and glia-enriched cultures, with aggregates being more potent in this respect, even at the lowest concentrations. The SWCNTs were cytotoxic towards glial cells in both types of cultures, but towards neurons only in dorsal root ganglia derived cultures. Neurite outgrowth was unaffected by nanotubes at a concentration of 30 µg/ml. With neurons from dorsal root ganglias, the inward conductivity was lowered and resting membrane potential made more positive by exposure. The agglomeration status of the SWCNTs appeared to influence their toxicity, i.e., the more well-dispersed bundles were less cytotoxic than the aggregates (24).

Zhang and collaborators incubated pheochromocytoma PC12 cells, a model neuronal cell line, with SWCNTs (diameter 0.8-1.2 nm, purity >98.5%) or graphene layers (80% with 3-5 layers resulting in 3-5 nm thick sheets, 8% with 1-3 layers, 12% with 6-10 layers, >98.5% pure) either in medium with (SWCNTs; 5% foetal bovine serum and 10% horse serum) or without serum (graphene) at concentrations of 0.01-100 µg/ml. The MTT assay revealed attenuated metabolic activity with 0.1-100 µg/ml concentrations of either preparation, with the SWCNTs being slightly more potent. Release of LDH was enhanced by 1-100 µg/ml SWCNTs, but only with 100 µg/ml and to a much lower extent with graphene. The SWCNTs were more potent than graphene, possibly due to the ability of these needle-like structures to pierce the cell membrane (381).

The influence of 0.1, 0.5, 1 and 5 µg/ml PEGylated SWCNTs on endocytosis and exocytosis in cultures of rat hippocampal neurons has also been probed. In this case, the SWCNTs were also labelled with the fluorescent FM1-43 which is

taken up by cells preferentially via endocytosis rather than passive diffusion, and the period of exposure was 3 days. The exposure increased the length of neurites. In addition, endocytosis was reduced at all concentrations in a dose-dependent manner and this reduction was proposed to explain the longer neurites (201). No physical or chemical properties of the SWCNTs were described.

MWCNTs

When cultured neurons and glial cells were exposed either to Pluronic F127 alone or to MWCNTs dispersed in Pluronic F127 a higher proportion of these cells were present in cultures that contained the MWCNTs and there was also a higher proportion of apoptotic cells in cultures that contained only Pluronic F127. When pristine MWCNTs, MWCNTs coated with Pluronic F127, and Pluronic F127 were compared, only Pluronic F127 reduced cellular respiration (MTT assay) and this effect could be counteracted by addition of 3.5 µg/ml MWCNTs. Thus, Pluronic F127-coated MWCNTs appear not to be harmful to cells of the nervous system (14).

Primary cultures of cortical neurons have been exposed for 24 and 48 hours to 1 µg/ml MWCNTs (diameter 20-30 nm, length 0.5-2 µm, 95% pure) with and without functionalisation by conjugation with either GRGDSPC or IKVAVC, peptide sequences present in fibronectin and laminin which are known to promote cell adhesion. The oxidative treatment prior to peptide conjugation also made the MWCNTs shorter 0.050-0.5 µm. Neither peptide functionalisations gave rise to cytotoxic activity towards Jurkat cells and splenocytes. Nor did the GRGDSPC-MWCNTs, the NH_2-functionalised nanotube precursors or the peptide itself influence the synaptic activity of the cortical neurons. Apparently, NH_2-functionalisation or peptide functionalisation renders MWCNTs tolerable by neuronal cells (86).

When pheochromocytoma PC12 cells were incubated together with 5 µg/ml carboxyl-terminated MWCNTs (diameter 40-50 nm, length 0.3-0.8 µm, dispersed by sonication in cell medium containing 15% horse serum and 5% foetal bovine serum) for 6, 12 and 24 hours, potassium channels were inhibited, with suppression of the transient outward current (I_{to}), delayed rectifier current (I_K) and the inward rectifier current (I_{K1}) (n=4-5 for each incubation). This time-dependent and irreversible suppression was most pronounced after 24 hours and was not due to elevated production of ROS or alterations in the mitochondrial membrane potential, as assessed by flow cytometry (n=3). There was no effect on calcium channels, which were suspected of influencing the potassium channels (n=3). In summary, CNTs may interfere with electrical signalling by neurons, thus compromising neuronal function (366). The authors did not examine possible contamination of the CNT preparation by catalytic metal.

Zhang and collaborators exposed pheochromocytoma PC12 cells to MWCNTs before (original diameter 10-30 nm, length 5-15 µm, 95% pure) and after functionalisation with phosphorylcholine (to improve water solubility) at concentrations of 40, 200 and 1 000 µg/ml in medium containing 15% serum for 48 hours. The MTT and the WST-1 assays revealed little cytotoxicity, although the pristine

MWCNTs were more toxic than the phosphorylcholine-MWCNTs in the MTT assay (385).

A battery of assays was employed to elucidate the effects of three types of MWCNTs: one with diameter 20-40 nm, length 2 μm, 97% pure and consisting of 20-42 layers of graphene; the second with diameter 35-40 nm, length 0.5 μm, 99% pure and consisting of at least 30 graphene layers; and the last with diameter 20-40 nm, length 0.5 μm, 97% pure and consisting of 20-40 graphene layers, and acid-treated to oxidase 8% of its surface. All of these preparations were dispersed with Pluronic F127 prior application to human neuroblastoma (SH-SY5Y) cells for 72 hours to 2 weeks. The WST-1 assay did not indicate any cytotoxicity, whereas the MTT assay indicated moderate cytotoxicity with all three types after 72-hour exposure to 5 μg/ml. Exposure to this same concentration for a week attenuated viability, except with the MWCNTs that were 99% pure. After 2 weeks all three preparations reduced cell viability, with the 99% pure MWCNTs being less potent. A dose-response study (5-500 μg/ml) and showed that the oxidised 97% pure MWCNTs had this effect at a concentration as low as 50 μg/ml, while for the other two 500 μg/ml was required to achieve the same extent of reduction. The level of ROS was not elevated under any condition. It was concluded that a concentration of 5-10 μg/ml would be useful when conducting cellular testing for drug development based on MWCNT technology (360).

11.2.2.7 Effects on other types of cells

SWCNTs

Albini and co-workers incubated cultures of human umbilical vein endothelial cells with SWCNTs (diameter 1.33 nm, length 1-5 μm) that were either pristine or functionalised by oxidation and dispersed the culture in medium containing 10% foetal bovine serum by sonication and found that with 5-10 μg/ml of either type of SWCNTs for 24-72 hours, the number of cells was unaltered (n=3). Nor did pristine or oxidised SWCNTs at concentrations of 10, 25 or 50 μg/ml influence cell migration (n=3) or morphogenesis (except for a slight alteration following incubation with 50 μg/ml) (n=3). The MTT assay indicated reduced viability after exposure to 50 μg/ml pristine or oxidised SWCNTs for 24-72 hours. Release of LDH progressed with time and concentration in the case of the pristine preparation, while oxidised SWCNTs caused more release after 24 hours with return to control levels thereafter. Staining with Neutral red indicated maximal toxicity with the pristine nanotubes after 48 hours, with slightly less staining after 72 hours, while oxidised SWCNTs led to uptake after 24 hours with return to the control situation after 72 hours. Application of lysosomal tracking dyes revealed that the endothelial cells took up the SWCNTs in a transient manner and examination with TEM showed intracellular vesicles containing these structures. These authors concluded that SWCNTs exert limited toxicity and may therefore be useful for drug delivery (5).

When sonicated carboxylated SWCNTs (average diameter 1.4 nm, bundles 4-5 nm in diameter and 0.5-1.5 μm in length, 5-10% Ni) were added to cultures of

differentiated and non-differentiated human colon carcinoma Caco-2 cells that contained 10% foetal calf serum in the medium except during the 24-hour period of exposure at concentrations of 5-1 000 µg/ml, cytotoxicity towards the non-differentiated cells was observed with 100-1 000 µg/ml or 400-1 000 µg/ml as determined with the Neutral red assay or MTS (metabolism of tetrazolium salt) procedure, respectively. The level of total protein was lowered by 1 000 µg/ml, while significant release of LDH occurred with 200-1 000 µg/ml. In the case of differentiated cells, staining with Neutral red indicated cytotoxicity with 100-1 000 µg/ml with the corresponding value for the MTS procedure being 200-1 000 µg/ml. The level of total protein was lowered with 400-1 000 µg/ml and LDH was released with 200-1 000 µg/ml. Trypan blue exclusion showed reduced viability after incubation of non-differentiated cells with 500 or 1 000 µg/ml oxidised SWCNTs. Light microscopy revealed only slight concentration-dependent morphological changes, with i.e., hydropic degeneration and vacuoles. At the higher concentrations, agglomerates of undispersed SWCNTs were seen. In summary, theses SWCNTs were toxic towards Caco-2 cells at concentration of 100 µg/ml and greater (145).

Raja and colleagues studied how exposure, dosage and aggregation influenced the response of smooth muscle cells to SWCNTs and activated carbon particles (1-35 µm in size) *in vitro*. The size of the individual SWCNTs was not determined, but acid-treated bundled SWCNTs were 10-15 nm in size. The SWCNTs were suspended in medium containing 9% foetal bovine serum by sonication and added at concentrations of 0.01-0.1 mg/ml either as prepared or after filtration to remove agglomerates. The activated carbon particles were only used at 0.1 mg/ml. The exposure continued for up to 3.5 days (n=3). The unfiltered SWCNTs, reduced the number of cells dose-dependently during the 3.5-day period, although by the end of this period the number of cells was almost normal even with the highest dose of 0.1 mg/ml. Activated carbon at the level of 0.1 mg/ml exerted similar effects in this respect. Filtered SWCNTs did not reduce cell numbers as much, with 0.01 mg/ml having no effect and 0.05 mg/ml attenuating growth only slightly. The cells were not allowed to become confluent in these experiments, and exposure to 0.1 mg/ml of either filtered or unfiltered SWCNTs reduced cell growth. Characterisation of the filtrates revealed smaller spherical particles (20-60 nm) as well as bundles of SWCNTs smaller than 5 nm. Amorphous carbon was still present in these SWCNTs, despite the acid treatment. It was concluded that the aggregates are responsible for inhibiting growth (271).

Crouzier and collaborators focused on how the surface chemistry of SWCNTs influenced their interactions with various types of cells. The SWCNTs were used as purchased (contained 3.15% O, 0.73% Ni, 0.38% Y) or refined by sonication in water and subsequent treatment with HCl (resulting in 17.7% O, 0.07% Ni, 0.04% Y). The refined SWCNTs were also treated either with plasma or with bovine serum albumin and, in addition all 4 of these different SWCNTs were coated with collagen. Unrefined and refined SWCNTs sedimented in solution within hours, whereas albumin- and in particular plasma-coated SWCNTs did not. The order of

relative conductivity was unrefined SWCNTs > refined SWCNTs > albumin-coated = plasma coated SWCNTs. Moreover, refined SWCNTs caused less red blood cell lysis than the unrefined preparations and the albumin- and plasma-coated particles caused no such lysis at all. Collagen-coated refined SWCNTs resulted in slower cell proliferation than exposure to collagen alone, while covering albumin- and plasma-SWCNTs with collagen as well stimulated the proliferation of pheochromocytoma PC12 cells and 3T3 fibroblasts, respectively. In conclusion, composition and hydrophobicity exert significant impact on interactions between SWCNTs and cells in culture (53). The physical dimensions of the SWCNTs employed in this study were not clearly stated.

Holt and co-workers examined the effects of SWCNTs on the cytoskeleton of HeLa cells and NIH-3T3 fibroblasts, with a main focus on actin. Purified and fractionated SWCNTs with a diameter of 0.7-1.3 nm and average length of 0.145 μm were suspended in Pluronic F127 and then centrifuged to remove any bundles, leaving well-dispersed, individual nanotubes. When HeLa cells were exposed to 50 or 200 μg/ml of these SWCNTs both doses reduced cell proliferation, but only the higher dose induced cell death. Pluronic F127 alone had no effect on either of these parameters. Furthermore, exposure to these SWCNTs led to defects in the cell proliferation, e.g., the formation of giant and multinucleated cells. Following exposure, actin, which is normally located at periphery of the cell, was spread throughout the interior of the cells. In addition, force generation by the cytoskeleton of fibroblasts attenuated. *Ex vivo* experiments revealed that these SWCNTs both induced actin bundling and interacted with actin filaments, but not with individual actin monomers. These investigators concluded that the SWCNTs were not acutely toxic, but could cause reorganisation of the cell interior, which might have long-term functional consequences (118).

Since the physical characteristics of CNTs in solution are considered to influence the toxicological response, Wick and colleagues asked how agglomeration of SWCNTs affected their toxicity towards the human mesothelioma MSTO-211H cell line. Four preparations produced by different procedures were employed: raw SWCNTs (SWCNT-raw, containing 13.8% Ni, and 1.6% Y); SWCNTs agglomerated by heating, acid treatment and sonication (SWCNT-agglomerates, 2.4% Ni, 0.5% Y); bundles of SWCNTs produced by sonication in Tween-80 (SWCNT-bundles, 5.5% Ni, 0.7% Y); and a pellet produced by centrifugation of the solution of SWCNT-bundles (SWCNT-pellet, 8.5% Ni, 1.1% Y). Physical characterisation by TEM showed that the SWCNT-agglomerates consisted of rope-like aggregates with a diameter of microns, while the SWCNT-bundles were well-dispersed with a diameter of approximately 20 nm, and the SWCNT-pellet contained particulate matter that was not in the shape of tubes. Cytotoxicity was compared to that produced by crocidolite asbestos. All of the SWCNT preparations reduced cell proliferation and induced cytotoxicity in a dose-dependent fashion, as did asbestos, with the SWCNT-agglomerates being most cytotoxic. In addition, all the preparation except the SWCNT-bundles formed aggregates in the cell culture and evoked morphological changes of the cells. The authors conclude that the degree of agglo-

meration and dispersion are important factors in connection with cytotoxicity and that aggregates may be stiffer than more well-dispersed SWCNTs (355).

MWCNTs

When pristine MWCNTs (diameter 10-30 nm, length 5-15 μm, 95% pure) or MWCNTs functionalised with phosphorylcholine (which made them highly water-soluble) were added to cultures of human colon carcinoma Caco-2 cells at concentrations of 40, 200 or 1 000 μg/ml in medium containing 15% serum for 48 hours, both the MTT and WST-1 assays indicated little cytotoxicity, although the pristine MWCNTs appeared to be somewhat more toxic with the MTT assay (385).

Zhu and colleagues tested how adsorption of serum proteins influenced the biological effects of purified, cut and functionalised MWCNTs (diameter 40-100 nm, length 600-800 nm, 95% pure) and three kinds of carbon black (CB PG: 51 nm; CB S160: 20 nm; CB P90: 14 nm) on HeLa cells. The levels of adsorption of serum proteins to these particles during 2-hour incubation were 0.47, 0.28, 0.68 and 0.96 mg/mg, respectively. Binding to the MWCNTs reached equilibrium after 5 minutes, as did binding to CB P90. Atomic force microscope analysis revealed proteins wrapped around the entire nanotubes and the authors speculated that these protein-MWCNTs would behave very differently in biological system than pristine MWCNTs. Indeed, cellular uptake of all of these particles in media without serum was almost 5-fold higher than in media containing serum, probably because aggregation of the carbon nanoparticles in serum-free media promoted uptake. Moreover, in serum-free media, the carbon nanoparticles (concentrations of 0.1-100 μg/ml) induced higher levels of cytotoxicity. For instance the MWCNTs and CB P90 induced more lipid peroxidation and higher levels of superoxide dismutase than in the presence of serum suggesting that serum proteins attenuated the production of ROS. In summary, in the presence of serum MWCNTs exerted less cytotoxicity on cells in culture (387).

SWCNTs and MWCNTs

When mesenchymal stem cells were incubated with carboxylated SWCNTs (diameter <2 nm, length 5-15 μm) or carboxylated MWCNTs (diameter <5 nm, length 5-15 μm) suspended in culture medium containing 10% foetal calf serum, both preparations were cytotoxic after incubation for 48 or 72 hours with concentrations of 3, 6 or 30 μg/ml. The activity of alkaline phosphatase (an ectoenzyme that serves as marker for osteogenic differentiation) was attenuated by both CNTs in a concentration-dependent manner, this reduction being, in general, more pronounced after 14 than after 7 days. However, 30 μg/ml SWCNTs led to equal decreases of this activity after 7 and 14 days, decreases that were less than those obtained following exposure for 14 days to 3 or 6 μg/ml. Mineralisation of the cells was reduced in a dose-dependent manner by both types of CNTs and adipogenic differentiation attenuated both in a time- and dose-dependent fashion, more so by the SWCNTs. Gene expression profiling by quantitative PCR revealed lower expression of genes whose products are involved in the osteogenic and adipogenic differentiation of

mesenchymal cells. Neither preparation led to any elevation in production of ROS, which is normally associated with CNT toxicity. In conclusion, carboxylated CNTs impair adipogenic and osteogenic differentiation of mesenchymal stem cells without evoking generation of ROS (191).

Heister and co-workers examined the influence of a wide variety of parameters on the stability of dispersions of CNTs and the biological responses of cultured colon cancer cells. The 5 types of CNTs employed included two oxidised SWCNTs (designated oxSWCNT(Nanolab) and oxSWCNT(CoMoCAT)), one oxidised DWCNT (oxDWCNT) and two oxidised MWCNTs (oxMWCNTs(long and thin) and oxMWCNT(short and thick)). In addition, oxidised SWCNTs were also functionalised with RNA or PEG. Following oxidation by acid treatment, the physical appearance of oxSWCNTs(Nanolab) and oxMWCNTs(long and thin) as well as of the oxDWCNTs remained largely unchanged, while oxSWCNTs(CoMoCAT) and oxMWCNTs(short and thick) were altered slightly. The differences between the oxSWCNTs(CoMoCAT) and oxSWCNTs(Nanolab) was thought to be due to the thinner diameter of the former (0.8 nm versus 1.5 nm). The oxMWCNTs(short and thick) were completely solubilised by acid treatment and sonication, probably because of their large diameter (110-170 nm). Washing the oxidised preparation with an aqueous solution of NaOH effectively removed debris, that can influence the bundling and debundling of nanotubes and changing particle size and thus experiment results. For example, the unwashed oxSWCNTs were covered with a layer of oxidative debris, as determined by atomic force microscopy. In addition, the zeta potential (a measure of surface charge difference that indicates the extent of electrostatic repulsion between particles in solution) was much lower for washed than unwashed oxMWCNTs. In addition, the pH and buffer strength in the solution and type and shape of CNTs present was also found to influence the stability of suspensions. For all of the CNTs examined, this stability rose as the concentration of foetal calf serum increased, with pristine RNA-wrapped SWCNTs being least stable. Although more extensive PEGylation also increased stability in the presence of foetal calf serum this property was higher and the level of PEGylation made little difference. The size of oxSWCNTs was larger than that of these same nanotubes functionalised with PEG (600 nm versus 500 nm). Cell viability was little affected by the 5 different preparations, although there was a slight reduction with increasing concentration (0.5-20 μg/ml) and oxidised PEGylated SWCNTs were less toxic in this respect than oxSWCNTs or RNA-wrapped SWCNTs. In summary, the dimensions and functionalisation of CNTs play important roles in their dispersion and effects *in vitro*. The aspect ratio, presence or absence of oxidative debris and serum proteins, salt levels and pH all influence the stability of dispersions (108). This article describes physical characterisation of the CNTs employed very well, but its main objective was optimisation for purposes of drug delivery. Comparison of a physiological setting to one where the stability of CNTs has been radically improved may give a false impression of the toxicological impact of exposure.

11.3 Effects of short-term exposure (up to 90 days)

SWCNTs

The effects of SWCNTs (diameter 0.8-1.2 nm, length 0.1-1 μm, surface area 508 m^2/g, 17.7% Fe) following whole-body inhalation (5 mg/m^3, 5 hours/day for 4 days, estimated deposition in the pulmonary region=5 μg) was examined in mice (n=5/group) 1, 7 and 28 days after the final exposure. Analysis of BAL fluid revealed more total cells and macrophages after 7 and 28 days, as well as more PMNs already after 1 day. The levels of LDH, total protein, TNFα, IL-6 and TGFβ were all also elevated at all time-points examined. The amount of collagen and the thickness of alveolar connective tissue increased progressively from 1-28 days. Breathing patterns were also changed with the respiratory times being shortened. SWCNTs caused oxidative stress and mutations in the K-*ras* gene in the lungs. After 1 day, all 5 animals exhibited inflammation and epithelial changes in the bronchi and after 7 days, 4 of 5 animals had macrophages without nuclei. The situation was similar after 28 days, when 4 of 5 animals showed changes in the bronchiolar epithelium and all 5 animals had macrophages without nuclei. In comparison to an exposure to 10 μg SWCNTs by pharyngeal aspiration, the inhaled SWCNTs (accumulated dose 5 μg) resulted in higher production of inflammatory markers and much more fibrosis. In short, inhalation evoked more severe inflammation and fibrosis than exposure via aspiration (see also Section 11.2.1.2) (305).

When mice (n=6/group) were exposed to SWCNTs (diameter 1-2 nm, length 0.5-2 μm, purity >90%) via nose-only inhalation for 20 minutes daily for 7 days (daily dose 100 μg/mouse), histopathology revealed homogenous distribution of these nanotubes in the lungs, including distal portions of this organ. Pulmonary inflammation occurred, as reflected by more total cells and PMNs and elevated levels of total protein in the BAL fluid. Furthermore, fibrosis was indicated by elevated levels of soluble collagen. Both SWCNTs and MWCNTs (see further next section on MWCNTs), induced oxidative stress, as shown by enhanced myeloperoxidase activity and higher levels of ROS and lipid peroxidation, with the responses to the SWCNTs being consistently more pronounced (272).

In another report, Wistar rats (n=10/group) were exposed to SWCNTs (bundles in air: diameter 200 nm and length 0.7 μm (bundles in suspension: diameter 12 nm and length 0.32 μm), surface area 1 064 m^2/g, 0.05% metals) by whole-body inhalation of 0.03 and 0.13 mg/m^3, 6 hours/day, 5 days/week for 4 weeks and the pulmonary status was assessed 3 days, and 1 and 3 months later. There were no signs of histopathological alterations, i.e., no infiltration of neutrophils into the alveolar space or formation of granulomas and no consistent changes in the levels of cytokine-induced neutrophil chemoattractant-1 and -2 in lung tissue. Decreased levels of haeme oxygenase-1 and alkaline phosphatase in BAL fluid were observed 3 days and 1 month post-exposure in both dose groups (215). These changes were transient with no clear dose-effect relation and, although statistically significant, are not considered as being indicative of pulmonary inflammation, as inflammatory processes would be expected to cause increased rather than lowered levels of these enzymes.

Teeguarden and co-workers administered SWCNTs (diameter 0.4-1.2 nm, length 0.5-2 μm, purity 99.7%, 0.23 wt% Fe) to female C57BL/6 mice by pharyngeal aspiration (40 μg/mouse, twice a week for 3 weeks) and compared the responses detected 24 hours after the final exposure to those evoked by ultrafine carbon black particles and crocidolite asbestos. The SWCNTs generated a strong inflammatory response, as reflected in the higher total numbers of cells, alveolar macrophages and PMNs in BAL fluid. Carbon black caused the same changes, but to a much lesser extent, while asbestos increased the total numbers of cells and of PMNs. The SWCNTs led to formation of fibrotic granulomas, with aggregates of these tubes being detected in the vicinity of the bronchioles and alveoli. The asbestos did not result in granulomas, but did enhance the presence of fibrous tissue and thicken the septal wall. In addition, the SWCNTs evoked strongest cytokine response, followed by asbestos and carbon black, in that order. Proteomic analysis revealed that the SWCNTs, asbestos and carbon black altered the expression of 376, 231 and 184 proteins, respectively. Of the proteins whose expressions were altered by asbestos and carbon black, 96% and 93%, respectively, were also affected by exposure to the SWCNTs. The proteins affected fell into 13 functional categories associated with inflammatory and immune responses, fibrosis and tissue remodelling. In conclusion, the pathways by which asbestos and CNTs affect pulmonary tissue may be similar (329).

Repeated exposure (once every second week for 8 weeks) of ApoE -/- mice to 20 μg SWCNTs (corresponding to 2.8 mg/kg bw) by pharyngeal aspiration led to more rapid development of atherosclerotic plaques than did vehicle exposure. Moreover, the plaques in SWCNTs exposed mice were larger than in those exposed to vehicle alone. The SWCNTs did not alter systemic levels of markers of inflammation, but did result in damage to aortic mitochondrial DNA. These findings indicate that pulmonary exposure to SWCNTs might accelerate the development of atherosclerosis and thereby influence the cardiovascular system negatively (184).

In another study, 8 rats were exposed to 1 mg/kg bw SWCNTs (diameter 1.2-1.6 nm, length 2-5 μm) by i.t. instillation once and then again 2 weeks later and the baroreflex function (which stabilises arterial pressure by modulating heart rate), atrial pressure and heart rate subsequently monitored during a 4-week observation period. SWCNTs reduced the number of baroreflex sequences, progressively, with the lowest value being observed after 4 weeks, indicating that these nanotubes altered the autonomic regulation of arterial pressure and heart rate. The authors noted that the CNTs employed contained metal contaminants such as nickel that might have contributed to the reduction in baroreflex response (178).

When Swiss Webster mice were injected i.p. 5 times at 24-hour intervals with carboxyl-functionalised SWCNTs (diameter 15-30 nm, length 15-20 μm) at doses of 0.25, 0.5 or 0.75 mg/kg bw and sacrificed 24 hours later, all of the doses were found to induce oxidative stress in the liver in the form of ROS. The two higher doses elevated the hepatic level of lipid hydroperoxides, while only the highest led to enhanced alanine aminotransferase and alkaline phosphatase activity in the blood. The histopathological findings included disruption and vacuolation of

hepatocytes at doses of 0.25 mg/kg bw and higher. Condensed nuclei and partial disruption of the central vein were observed with 0.5 mg/kg bw. At 0.75 mg/kg bw degeneration of the liver occurred and the central vein was injured. However, all of these changes were statistically significant only at 0.75 mg/kg bw. The authors concluded that the effects observed were due to oxidative stress unrelated to metal contaminants in the SWCNTs, which were thoroughly purified prior application (250).

Hairless SKH-1 mice treated topically with 40, 80 or 160 µg of unpurified SWCNTs (30 wt% Fe) once daily for 5 days exhibited thickening of the skin with the highest dose, as well as more epidermal cells at the two higher doses. SWCNT exposure to 160 µg also enhanced infiltration by mast cells, myeloperoxidase activity, accumulation of collagen and cytokine production. Moreover, oxidative damage was observed with 80 and 160 µg. Thus, unpurified SWCNTs containing iron can cause dermal toxicity, including inflammation (231).

After mice received SWCNTs (diameter 0.8-1.2 nm, length 0.05-0.3 µm) by gastrogavage as a bolus dose of 5-500 mg/kg bw once daily for 10 days, SWCNTs were detected by TEM in the ileum, liver, brain and heart. In the case of the brain, CNTs were present only in neurons and neuritis, not in glial cells. Ultrastructural examination revealed that the major target organelles were lysosomes and mitochondria, with uptake into lysosomes at doses of 50-500 mg/kg bw and accumulation in mitochondria above 400 mg/kg bw. In addition, doses of 400 and 500 mg/kg bw damaged the lysosomes and mitochondria. The lysosomes were dilated, had disrupted membranes, had lost their contents and/or exhibited cavity formation, while mitochondria containing SWCNTs were swollen and had few or no cristae. The level of ROS in mitochondria, but not in lysosomes was elevated (373). The main purpose of this investigation was to evaluate ultra-short SWCNTs as potential therapeutic agents for treatment of Alzheimer's. Thus, the CNTs utilised were very short (50-300 nm) compared to those used in other applications. Moreover, the doses resulting in adverse effects were relatively high, i.e., 400 and 500 mg/kg bw. The lowest dose associated with SWCNT uptake into any organ is impossible to determine from the information provided and no statistical analysis of the uptake was performed.

MWCNTs

The effects of MWCNTs (mass median aerodynamic diameter 1.5 µm, no data on length, 1.06% Fe) following whole-body inhalation (10 mg/m^3, 5 hours/day for 2, 4, 8 or 12 days, estimated lung burden 7, 13, 23 and 31 µg, respectively) was examined in male C57BL/6J mice. The MWCNTs induced dose-dependent pulmonary inflammation and cytotoxicity as reflected by more PMNs, elevated levels of LDH, albumin and chemokine KC (neutrophil chemoattractant) in whole lung lavages. Minimal to mild lung fibrosis present at the site of inflammation was observed after 8 and 12 days exposure. Fibrosis was also associated with an expanded interstitium and the presence of interstitial MWCNTs. Furthermore, MWCNTs translocated from the lung to the tracheobronchial lymph nodes where they were

detected inside cells resembling macrophages and dendritic cells. In conclusion, inhalation exposure evoked a dose-dependent pulmonary inflammation and rapid development of fibrosis (264).

Repeated inhalation of MWCNTs (diameter 50 nm, length 10 μm, surface area 280 m^2/g, 95% pure, <0.2% La and Ni, <3% amorphous carbon) by mice (n=9/group) has been carried out at a weighted average air concentration of 32.6 mg/m^3 (range 13-80 mg/m^3). The animals were exposed 6 hours/day (90 minutes 4 times) every second day for 30 or 60 days. The aerosol administered was shown to contain well-dispersed MWCNTs of respirable size. The levels of total protein and activities of alkaline phosphatase, acid phosphatase and LDH in the BAL fluid were slightly elevated in the 30-day group and significantly higher in the 60-day group. Histopathology of the former animals revealed aggregates of MWCNTs on the bronchial wall, as well as inside the alveolar wall, which occasionally led to thickening. In the 60-day group, the aggregates in the bronchi were larger, while those in the alveolar region were smaller, but caused more wall thickening. The authors concluded that MWCNTs exert severe pulmonary toxicity after a 60-day exposure, but not after 30 days (180). The calculated total doses per unit body mass (7 and 14 mg/kg bw for the 30- and 60-days group, respectively) were rather high compared to other inhalation studies and no examination of the cells in the BAL fluid was carried out.

Repeated exposure (6 hours/day for 5, 10 or 15 days) of mice (n=6/group) to MWCNTs (diameter 50 nm, length 10 μm, surface area 280 m^2/g, 95% pure) by inhalation of an aerosol (average 32.61 mg/m^3) and monitoring of the responses after 8, 16 and 24 days revealed aggregates of CNTs in the bronchi along with smaller aggregates in the alveoli. No inflammation was present in the bronchi. The only lesions observed in the alveoli were cell proliferation and thickening of the alveolar wall, but the pulmonary structure remained intact. Comparison to exposure by i.t. instillation, which resulted in injury to and destruction of the alveoli, suggested that these two different routes of exposure, instillation and inhalation, evoke highly different responses and pathologies (see also Section 11.2.1.2) (181). However, no quantification of the severity of lesions or inflammation was performed. Moreover, the choice of dosing regimens was not explained, i.e., why was exposure by inhalation performed repeatedly and instillation only once.

Ravichandran and collaborators exposed mice (n=6/group) to 100 μg MWCNTs (diameter 20-50 nm, length 0.006-0.013 μm, purity >99%) via nose-only inhalation for 20 minutes daily for 7 days and found a homogenous distribution of MWCNTs in the lungs, including distal regions. Pulmonary inflammatory was indicated by the larger total numbers of cells and of PMNs and elevated total level of protein in the BAL fluid. Furthermore, the increased level of soluble collagen was indicative of fibrosis. These MWCNTs also induced oxidative stress, i.e., an elevation in myeloperoxidase activity and enhanced formation of ROS and lipid peroxidation (272).

When Wistar rats (n=10/group) were exposed to MWCNTs (in air: diameter 63 nm, length 1.1 μm (in solution: diameter 48 nm, length 0.94 μm), surface area

69 m^2/g) by whole-body inhalation of 0.37 mg/m^3 6 hours/day, 5 days/week for 4 weeks and pulmonary responses assessed after 3 days, 1 and 3 months, transient increases in chemokines (cytokine-induced neutrophil chemoattractant-1, -2 and -3) in the lung tissue and myeloperoxidase in BAL fluid occurred 3 days post-exposure. There were no signs of histopathological alterations in the lungs such as neutrophil infiltration, granulomatous lesions, or fibrosis during the observation period (216).

Systemic immunosuppression following repeated exposure to MWCNTs has been documented in two sets of experiments performed Mitchell and co-workers. In the first of these, mice were exposed to MWCNTs (diameter 10-20 nm, length 5-15 µm, surface area 100 m^2/g) by whole-body inhalation of 0.3, 1, or 5 mg/m^3, 6 hours/day for 7 or 14 days following which the number of increase of leukocytes in the BAL fluid was unchanged at any dose. MWCNTs had been engulfed by macrophage, some of which were enlarged, but there were no signs of fibrosis or granuloma. Upon evaluating formation of T-cell dependent antibodies in spleen cells, no alteration occurred after 7 days, whereas after 14 days, suppression was noted at all doses. The levels of IL-6, IL-10 and NA(D)PH quinone oxidoreductase 1 (NQO1) mRNA in the lung tissue were normal, in contrast to the elevated levels of mRNA encoding IL-10 and NQO1 (a marker of oxidative stress) in spleen homogenate (the latter increase demonstrating dose-dependency) (212).

In a later study by the same group, whole-body inhalation of 0.3 or 1 mg/m^3 of MWCNTs (diameter 10-20 nm, length 5-15 µm, surface area 100 m^2/g, 97% pure, 0.5% Fe, 0.5% Ni, aerosolised by a jet mill coupled to a dry chemical screw feeder) by mice (n=7) was carried out for 6 hours/day for 14 days. The deposited doses were calculated to be 0.15 and 0.5 mg/kg bw, respectively. Ibuprofen was administered to some of the animals to modulate the immune response. MWCNT exposure reduced the T-cell dependent production of antibodies to sheep red blood cells and T-cell proliferation was also attenuated. Gene expression of prostaglandin synthase enzymes (PTGS2 and PTGES2, the latter also called cyclooxygenase 2 (COX-2)) was upregulated in the spleen, a response that could be partially ameliorated with ibuprofen. No suppressed immune function was observed at the lower concentration. In mice lacking the COX-2 gene, exposure to the MWCNTs did not alter T-cell proliferation. When exposed *in vitro* to the proteins in the BAL fluid, the splenocytes from wild-type mice exhibited less antibody production, whereas with the corresponding cells from the COX-2 knockout mice, there was no immunosuppressant effect. The authors concluded that signals from the lung activate signalling in the spleen, which in turn suppresses the immune response of animals exposed to MWCNTs (213).

When mice (n=8 males and 8 females/group) were injected i.p. once daily for 28 days with 10, 50 or 250 mg/kg bw MWCNTs (diameter 10-40 nm, length 0.2-2 µm) functionalised with phosphorylcholine, the animals receiving the highest doses appeared sluggish and lethargic and the body weight of male mice was lowered. Many organs, including the liver, spleen and lungs (and in female mice the kidney as well) exhibited elevated tissue-to-body weight ratios at the highest dose. In case of the spleen, such elevations also occurred in both sexes with 50

mg/kg bw and for the liver in males with 10 mg/kg bw. The blood level of urea nitrogen was reduced in mice exposed to 50 or 250 mg/kg bw. Histopathology revealed CNTs in the liver, lungs and spleen after administration of 250 mg/kg bw, as well as some presence even with 50 mg/kg bw. The liver was infiltrated with inflammatory cells after exposure to the highest dose. In the lungs, CNTs were trapped in the interstitial space of the alveolar wall and in some cases, thickening of the alveolar wall, expansion of capillary vessels and infiltration of inflammatory cells were observed. The responses to 50 mg/kg bw, included mild inflammation of the liver, spleen and lungs. The authors state that their data suggest that MWCNTs are "relatively safe for human consumption" (185). No quantification of changes in weight or serum levels of biochemical parameters was presented.

To evaluate toxic effects of MWCNTs on metabolism and immune system in greater detail, 4 mice were injected i.p. with 5 mg/kg bw MWCNTs once daily for 7 days. The body weight of the animals did not change. Autopsy revealed deposition of MWCNTs in the intraperitoneal cavity and connections between the surface of the liver and adjacent organs. The structure of the liver was found to be heterogeneous (45).

Conclusions concerning effects of short-term exposure

Short-term exposure studies in animals are summarised in Tables 9, 11 and 13. Only a few studies have addressed the effects of subacute repeated pulmonary exposure to CNTs via inhalation. One of these showed that pulmonary toxicity, as indicated by elevated levels of markers in the BAL fluid and thickening of the alveolar wall, was aggravated at increasing accumulated doses of MWCNTs and was more pronounced after 60 than 30 days of exposure of mice to 32.6 mg/m^3 (180). Moreover, repeated inhalation exposure to 10 mg/m^3 MWCNTs (264) and 5 mg/m^3 SWCNTs (305) induced pulmonary inflammation with rapid development of fibrosis in mice. Similarly, pharyngeal aspiration of SWCNTs evoked pulmonary inflammation and granulomas with associated fibrosis in mice (329). At lower concentration, MWCNTs (0.37 mg/m^3) caused transient inflammatory responses, but no histopathological alterations in the lungs of rats (216). At 0.03 and 0.13 mg/m^3 SWCNTs no pulmonary effects were observed (215).

In two investigations, inhalation exposure to 0.3 and 1 mg/m^3 MWCNTs did not cause damage to the lungs of mice, but caused a systemic effect on the immune system, i.e., reduced formation of T-cell-dependent antibodies in the spleen (212, 213).

Some findings suggest that repeated exposure to SWCNTs can lead to cardiovascular effects. Thus, repeated exposure to SWCNTs by pharyngeal aspiration promoted the formation of atherosclerotic plaques in ApoE -/- transgenic mice and altered signals involved in the regulation arterial pressure and heart rate (184). Effects on the arterial baroreflex function occurred following repeated i.t. instillation of SWCNTs to rats (178).

SWCNTs caused inflammation and oxidative stress when administered topically to mice. Infiltration of immune cells, accumulation of collagen and elevated levels of cytokines were detected in the skin (231).

Furthermore, uptake of very short SWCNTs (0.05-0.3 μm) via the gastro-intestinal tract and subsequent translocation to the liver, brain and heart has been reported (373). Detection of CNTs in the brain implies that these nanotubes could cross the blood-brain barrier.

11.4 Mutagenicity and genotoxicity

SWCNTs

An elevated frequency of mutations in the K-*ras* gene in lung tissue of mice exposed to 5 mg/m^3 SWCNTs (diameter 0.8-1.2 nm, length 0.1-1 μm, 17.7% Fe) via inhalation was observed by Shvedova and collaborators. No such changes were observed following pharyngeal aspiration of a single dose (5-20 μg) of the same SWCNTs (305).

When 0.4 mg/kg bw SWCNTs (diameter 0.7-1.5 nm, length 1 μm) were administered to mice via pharyngeal aspiration aortic mitochondrial DNA was damaged (184).

Jacobsen and colleagues examined the genotoxic and pulmonary effects (see Section 11.2.1.2) of 5 different types of nanoparticles on female ApoE -/- mice. SWCNTs (diameter 0.9-1.7 nm, length <1 μm, 2% Fe), carbon black, C_{60}, gold and quantum dots were compared. When mice (n=7) received 54 μg SWCNTs by i.t. instillation and were examined 3 and 24 hours later the cells in the BAL fluid exhibited elevated levels of DNA damage (as determined by the comet assay). The DNA damage of the SWCNTs and carbon black was less than that of quantum dots, but greater than that of gold and C_{60} (137).

In another investigation, pristine SWCNTs (diameter 0.9-1.7 nm, length <1 μm) were delivered to rats (n=8) as a single dose by gavage at concentrations of 0.064 and 0.64 mg/kg bw using physiological saline or corn oil as vehicle. In physiological saline the peak sizes of these particles at the lower dose were determined to be 195, 797 and 5 457 nm; while in corn oil these peak sizes were 34 and 178 nm at the lower dose and 1 015 nm with the higher dose. After 24 hours, both concentrations of nanotubes in either of vehicle resulted in elevated levels of 8-oxodG in the liver and lungs, but not in the mucosa of the colon. The SWCNTs were also found to increase the production of ROS, but had no effects on DNA repair (85).

Pacurari and collaborators found that SWCNTs (diameter 0.8-2.0 nm, 21% Ni, 6.2% Y) activate signalling pathways associated with oxidative stress in cultures of normal and malignant human mesothelial cells. The SWCNTs were dispersed by sonication in 1% foetal bovine serum, which resulted in homogenous dispersions of small agglomerates of nanoropes and mats. The concentrations used were generally 12.5-125 μg/cm^2 and exposure was for as long as 24 hours. Doses of 150 and 500 μg/ml of the SWCNTs resulted in production of ROS by both kinds of cells,

while crocidolite asbestos was even more potent in this respect. Exposure to 25 or 50 μg/cm^2 SWCNTs for 24 hours revealed dose-dependent DNA damage (determined by comet assay) in both cell types. Enhanced phosphorylation of the histone protein γ-H2AX, a marker of DNA damage, in both cell types after exposure to crocidolite, but not with SWCNTs suggested that these two different particles may induce different types of DNA damage (246).

When two airway epithelial (BEAS-2B and SAEC) cell lines were subjected to SWCNTs (diameter 1-4 nm, length 0.5-1 μm, surface area 1 040 m^2/g, 99% purity, 0.23% Fe) at concentrations of 24, 48 and 96 μg/cm^2 with vanadium pentoxide as a positive control, viability was reduced and interference with cell division through formation of anaphase bridges resulted in an aneuploid number of chromosomes, abnormal mitotic spindles (monopolar, tripolar and quadrapolar spindles) and fragmented centrosomes after 24 hours. These effects were dose-dependent, and statistically significant at all concentrations of SWCNTs employed (with the exception of the reduction of viability, which was only significant with 48 and 96 μg/cm^2). Both cell lines exhibited similar responses. One possible explanation for these observations is that the nanotubes are similar in size and shape to the cytoskeleton, which might allow detrimental interactions between CNTs and the mitotic apparatus (290).

Lindberg and co-workers exposed human bronchial epithelial (BEAS-2B) cells to SWCNTs (diameter 1.1 nm, length 0.5-100 μm, containing 50% SWCNTs and 40% other CNTs) and monitored effects after 24, 48 and 72 hours by trypan blue exclusion and the comet and micronucleus assays. The concentrations in the cell culture medium was 1-100 μg/cm^2, corresponding to 3.8-380 μg/ml. Cell viability was reduced by 50% with 10-40 μg/cm^2 after 24 hours and with 40-60 μg/cm^2 after 48-72 hours. DNA damage was observed with all concentrations after 48 and 72 hours (as well as after 24 hours with 1 μg/cm^2 and 60-100 μg/cm^2) in a dose-dependent manner. After 48 hours, 10, 60 and 100 μg/cm^2 CNTs induced micronuclei, but this effect was not seen after 24 or 72 hours. These observations indicate that SWCNTs can cause DNA damage. This could be due to the fibrous nature of this material and/or, possibly, the presence of metal catalysts such as cobalt and molybdenum (188).

No DNA strand-breaks were detected using the comet assay, but oxidation of purines was increased when mouse lung epithelial (FE1-MML) cells were incubated with SWCNTs (diameter 0.9-1.7 nm, length <1 μm, surface area 731 m^2/g, 95% pure, 2% Fe). The accompanying reduction in the number of cells was probably due to attenuated proliferation, rather than reduced survival. With 100 μg/ml SWCNTs for 0, 24, 48 and 72 hours, a larger proportion of the cells were in the G1 phase of the cell cycle. Thus, SWCNTs can apparently affect the DNA of epithelial cells (138).

Incubation of human peripheral blood lymphocytes with pristine SWCNTs (diameter 1.1 nm, average length 50 μm, 90% pure, 2.9% Co) dispersed in the culture medium by sonication and added at concentrations of 1, 5 and 10 μg/ml was without effect on the integrity of cellular DNA (evaluated with an alkaline comet assay)

after 6 hours. On the other hand, cell growth was slower with 25 and 50 µg/ml, which was attributed to reduced metabolic activity. According to the authors, their dispersion of the SWCNTs in cell culture medium by sonication might explain the discrepancies between their findings and those of others (379).

Upon exposure of lung fibroblast (V79) cells to 24, 48 and 96 µg/cm^2 SWCNTs purified by acid treatment (diameter 0.4-1.2 nm, length 1-3 µm, surface area 1 040 m^2/g, 0.23% Fe) for 3 or 24 hours, cell survival was compromised at both time-points with the two higher concentrations. The comet assay revealed significant DNA damage with 96 µg/cm^2 after 3 hours as well as with both 48 and 96 µg/cm^2 after 24 hours. However, 12-96 µg/cm^2 did not alter the frequency of micronuclei and the results of the *Salmonella* gene mutation assay with 60-240 µg/plate were negative (159).

To assess the genotoxic potential of modified CNTs with the cytokinesis-block micronucleus assay rat lung epithelial cells were exposed to 25 µg of different CNT preparations per ml. The following preparations were compared: ground (MWCNT-g), in which structural defects in the carbon backbone has been introduced mechanically; ground and then heated to 600 °C (MWCNT-g600), which, in addition to structural defects, reduced the number of oxygenated carbons and content of metal oxide; ground and then heated to 2 400 °C (MWCNT-g2400) to remove all metals, while at the same time, annealing and reducing carbon defects; or, finally, heated to 2 400 °C and then ground (MWCNT-2400g), which also removed metals, but introduced of structural defects. MWCNT-g or MWCNT-g600 induced significant increases in the frequency of micronucleated binucleated cells whereas MWCNT-g2400 did not. The investigators concluded that the reduction in genotoxicity went better paired with the decrease of structural defects induced by the thermal treatments than with the metal content. Pulmonary toxicity of these MWCNTs is described in Section 11.2.1.2) (221).

MWCNTs

When Kato and co-workers instilled 0.05 or 0.2 mg MWCNTs (diameter 90 nm and length 2 µm, Mitsui-MWNT-7) i.t. into male ICR mice (n=5/group) dose-dependent damage to the DNA in lung cells from ICR mice was detected with the comet assay 3 hours later. Furthermore, the levels of 8-oxodG and heptanone ethenodeoxyribonucleosides in DNA extracted from the lungs of mice exposed to 0.2 mg MWCNTs were elevated for as long as 72 hours after exposure, indicating oxidative damage. I.t. instillation of 0.2 mg of the same MWCNTs into guanine phosphoribosyltransferase (gpt) delta transgenic mice (n=6-7/group) did not alter the frequency of mutations in the *gpt* gene in the lungs. However, this frequency was enhanced 2-fold 8-12 weeks after repeated administration of 0.2 mg once each week for 4 weeks (153).

To examine the effect of aspect ratio on genotoxicity, two types of MWCNTs -- one with a high-aspect ratio (diameter 10-15 nm, length 10 µm) and the other a low-aspect ratio (diameter 10-15 nm, length 0.15 µm) -- were tested in the Ames test (12-1 000 µg/plate), an *in vitro* chromosomal aberration test (3.12-200 µg/ml)

and for the formation of micronuclei in mice (12.5, 25 and 50 mg/kg bw), all in accordance with OECD guidelines. The mice (n=6) were injected i.p. with the MWCNTs in DPPC solution, the femur later dissected out, the bone marrow prepared and the resulting cells examined with fluorescence microscopy. In none of these tests were any genotoxic effects observed. However, these MWCNTs were cytotoxic towards cultures of Chinese hamster ovary cells (CHO), with the high-aspect particles being more harmful in this respect. The authors concluded that there were no direct genotoxic effects, but possibly indirect effects due to oxidative stress or inflammation (156).

In contrast, MWCNTs were found to be genotoxic in several other studies. Swiss Webster mice were injected i.p. once daily for 5 days with 0.25, 0.5 and 0.75 mg/kg bw non-functionalised (diameters 15-30 nm, length 15-20 μm) or carboxylic-functionalised MWCNTs (2-7% w/w COOH-groups) and the bone marrow subsequently dissected out to look for genotoxic and clastogenic effects. Both types of MWCNTs elevated the number of chromosomal aberrations and the level of ROS at all doses, with the non-functionalised being less potent in the latter respect. Both also reduced the mitotic index, the functionalised particles causing a more potent effect in this case. The number of micronuclei also increased in a dose-dependent manner, more so with the functionalised nanotubes. The comet assay revealed concentration-dependent DNA fragmentation at all concentrations with both preparations, more pronounced with the functionalised CNTs. It was suggested that MWCNTs can give rise to genotoxic effects that are influenced by the nature of their functionalisation (252).

In another case, the clastogenic and aneugenic effects of MWCNTs (diameter 11.3 nm, length 0.7 μm, 98% pure, traces of Co and Fe, mostly aggregated with a hydrodynamic diameter of 1 μm) were tested *in vivo*, *ex vivo* and *in vitro*. Three days after i.t. administration of 0.5, 2 or 5 mg/rat (n=6), the LDH activity and total protein content in BAL fluid were elevated in a dose-dependent fashion. Only the highest dose resulted in more macrophages and neutrophils in this fluid. In the *ex vivo* experiments, type II pneumocytes (AT-II cells) isolated from rat lung after i.t. administration of 0.5 or 2 mg of MWCNTs contained more micronuclei at the higher dose. The *in vitro* experiments involved incubation of rat lung epithelial (RLE) and human epithelial (MCF-7) cells with MWCNTs (10, 25, 50, 100 or 150 μg/ml) for 6-24 hours (n=2). In the case of the RLE cells cytotoxicity was observed after exposure to 100 and 150 μg/ml, while mitochondrial activity (and thus apparent viability) was reduced at 50 μg/ml and higher. Apoptosis occurred with concentrations ≥25 μg/ml and 10-50 μg/ml produced more micronuclei. In the case of MCF-7 cells, one of the two experiments demonstrated micronuclei at 10-50 μg/ml, while the other yielded no micronuclei at all. In addition, these MWCNTs induced centromere-positive and -negative micronuclei in MCF-7 cells (219). Although this study is presented well, the number of *in vitro* experiments performed was small.

When cultures of mouse embryonic stem cells were incubated with 5 or 100 μg/ml purified, catalyst-free MWCNTs for 24 hours, the nanotubes accumulated

inside the cells in a time-dependent manner, beginning already after 2 hours. The tumour suppressor protein p53, was activated dose-dependently after 2 hours (remaining activated after 4 hours), thereby leading to apoptosis. The expression of the base-excision repair protein 8-oxoguanine-DNA glycosylase 1 (OGG1) and double-strand break repair protein Rad 51 were enhanced by exposure, indicating the occurrence of mutations and DNA damage. Another repair protein XRCC4 was also activated, as was H2AX (a marker for double-strand breaks in DNA). When the mutation frequency was determined directly, the incidence with 5 µg/ml nanotubes was twice as high as that in non-exposed cells. These observations indicate that MWCNTs can be genotoxic and mutagenic (386). However, with exception for the mutagenesis study (n=10), the number of experiments was not stated. The Western blots were not quantified, with only estimates based on ocular inspection being presented, although the figures shown appear convincing. Moreover, no physical characterisation of the CNTs employed was performed.

Ochoa-Olmos and collaborators exposed cultures of human lymphocytes to 10, 20, 40 and 60 µg/ml pristine MWCNTs (diameter 10-20 nm, length 10-50 mm (sic!)) and MWCNTs functionalised with nylon-6 (which according to a previous report by the same authors renders the nanotubes more biocompatible). The pristine nanotubes led to the formation of a larger number of micronuclei (although this effect was only statistically significant at the highest concentration), whereas the nylon-6 MWCNTs evoked no such response. The pristine CNTs did not increase the frequency of chromatin buds significantly, although linear regression analysis did reveal a significant correlation between dose and response. With the second highest dose of pristine MWCNTs, more nucleoplasmic bridges were also observed. Except for enhanced apoptosis at 20 µg/ml, the nylon-6 MWCNTs produced no negative responses. This report suggests that pristine MWCNTs can cause genotoxic events in lymphocytes, while the toxicity of the corresponding functionalised nanotubes was probably due to contaminants remaining from the procedure employed to achieve functionalisation (243).

When the Ames test was carried out with MWCNTs (diameter 110-170 nm, length 5-9 µm, surface area 130 m^2/g) at doses of 0.01-9 µg/plate, no mutagenicity or cytotoxicity was observed. These investigators speculated that limited uptake of these relatively large MWCNTs into the *Salmonella typhimurium* bacterial cells was responsible for this lack of mutagenicity (65).

Macro-sized agglomerates of MWCNTs (Baytubes) were found to be spherical with diameters of 10-150 µm, but to unbundle into individual nanotubes (diameter not stated, length 0.2-1 µm) upon sonication. When Chinese hamster lung fibroblast V79 cells were incubated with such tubes at concentrations of 2.5, 5 and 10 µg/ml in the presence or absence of S9 liver homogenates (according to OECD guidelines) for 4 hours and then harvested 18 hours later, no cytotoxic or clastogenic effects were seen. Moreover, Ames test with as much as 5 000 µg nanotubes per plate was also negative, both in the absence and presence of S9. It was concluded that Baytubes are neither mutagenic nor clastogenic under these conditions (358).

Patlolla and colleagues subjected cultures of human dermal fibroblasts to 40, 200 and 400 μg/ml purified, carboxylic-functionalised MWCNTs (diameter 15 nm, length up to 12 μm, surface area 41-42 m^2/g after sonication) and observed dose-dependent cytotoxicity. The comet assay revealed DNA damage at all concentrations, with a maximum after 48 hours with 400 μg/ml MWCNTs. This was confirmed by agarose gel electrophoresis which also showed dose-dependent DNA fragmentation at all concentrations. Furthermore, these MWCNTs induced dose-dependent apoptosis in the fibroblasts. Together, these results indicate that these functionalised MWCNTs were genotoxic in this system (251).

At levels of 0-400 μg/ml in the culture medium, MWCNTs (diameter 80 nm, length 5±4.5 μm, with 38.9% of the fibres >5 μm) or chrysotile asbestos (15% fibres, length 2-5 μm), the former were cytotoxic towards Chinese hamster lung (CHL/IU) cells in a dose-dependent manner and influenced by the solvent in which they were dispersed and the duration of sonication. Under conditions where less agglomeration occurred and thus hydrodynamic diameters were smaller, cytotoxicity was enhanced. On a weight basis, chrysotile was more cytotoxic than these MWCNTs. MWCNTs increased the number of cells showing polyploidy in a dose-dependent manner at and above 5 μg/ml after 24 hours and at and above 1.3 μg/ml after 48 hours. Also the numbers of bi- and multi-nucleated cells increased dose-dependently at and above 0.31 and 3.1 μg/ml CNTs, respectively. The MWCNTs were taken up into the cells. It was proposed that the effects observed reflect interactions between the MWCNTs and the mitotic spindle (10).

Pacurari and co-workers showed that exposure to MWCNTs (diameter 81 nm, length 8 μm, surface area 26 m^2/g, 99.5% pure) which formed long and loosely associated particulates or agglomerated mat-like structures in solution led to moderate increases in ROS production in both normal and malignant mesothelial cells. In addition, release of LDH revealed cytotoxicity in these cells after exposure to 50 or 100 μg/ cm^2. In comparison, crocidolite asbestos induced cytotoxicity in the normal cells at a concentration of 5 μg/cm^2 and in the malignant cells at 25 μg/ cm^2. The cell viability of both kinds of cells was reduced by exposure to either the MWCNTs or crocidolite at 12.5-125 μg/cm^2 and apoptosis occurred with 25 and 50 μg/cm^2 MWCNTs. The MWCNTs also caused DNA damage at these same concentrations, with the malignant cells being more susceptible. The level of γ-H2AX, another marker of DNA damage, was elevated to similar extents in both the normal and malignant cells by 12.5-50 μg/cm^2 of either MWCNTs or crocidolite (245).

SWCNTs and MWCNTs

The role of the shape of CNTs on the DNA damage and inflammation they evoke has also been examined by exposing human alveolar carcinoma epithelial A549 cells and mice to three different types of MWCNTs designated M1 (diameter 20-60 nm, length 5-15 μm), M2 (diameter 60-100 nm, length 1-2 μm) and M3 (diameter <10 nm, length 1-2 μm) and one type of SWCNTs (S4, diameter <2 nm, length 5-15 μm). These CNTs were sonicated in 0.001% Triton X-100 and applied

in vitro at concentrations of 1-1 000 µg/ml. After exposure for 24 hours, none of the four types of CNTs had altered viability of the A549 cells, as determined by the methylene blue assay. DNA damage, as determined by the comet assay, was most pronounced in the presence of M1, the longest CNTs employed. I.p. injection of mice with 50 µg M1 or M2 resulted in more inflammatory cells in the abdominal lavage fluid, this response being twice as strong with M1. The authors proposed that longer and thicker CNTs cause more pronounced DNA damage and inflammation (368).

When purified or amide-functionalised SWCNTs (no data on dimensions) or MWCNTs (diameter 20-40 nm, length 1-5 µm, 99% pure) were applied to lymphocytes (at concentrations of 25-100 µl/ml or 150 µl/ml), the purified SWCNTs induced micronuclei and attenuated proliferation at the concentrations of 25 and 50 µl/ml, while the functionalised SWCNTs evoked these same responses at all concentrations. The MWCNTs led to the appearance of micronuclei at 25 µl/ml and also reduced cell growth. Similar exposure of fibroblasts produced similar results. There was an inverse relationship between the incidence of micronuclei and proliferative potential in all cases. The induction of γ-H2AX revealed that the nanotubes caused double-strand breaks in DNA. The negative electric potential of the nanotubes was put forth as one possible explanation for the phenomena observed (55). The concentrations employed (given in µl/ml) are difficult to interpret, since the concentration of nanotubes in the stock solution was not provided.

When an alveolar macrophage cell line, RAW 264.7, was exposed to SWCNTs (diameter 0.7-1.2 nm, length 0.5-100 µm, surface area 400 m^2/g) or MWCNTs (diameter 110-170 nm, length 5-9 µm, surface area 22 m^2/g) at concentrations of 0.01-100 µg/ml for 2-48 hours, the frequency of micronuclei was elevated at doses above 0.1 µg/ml and 1 µg/ml, respectively. In addition, the comet assay revealed DNA damage with 1-100 µg/ml SWCNTs or 1-10 µg/ml MWCNTs and cytotoxic effects were seen with both types of CNTs at concentrations of 10 and 100 µg/ml (211).

Conclusions concerning mutagenicity and genotoxicity

Mutagenicity and genotoxicity studies in animals are summarised in Table 14. Although some contradictory findings have been reported and the result of Ames test in generally been negative, a number of studies indicates that SWCNTs and MWCNTs are potentially mutagenic and genotoxic both *in vivo* and *in vitro*. The Ames test may give false-negative results because the bacteria involved cannot perform endocytosis (310) and are thereby apparently unable to take up CNTs. Genotoxic effects observed with CNTs include chromosomal aberrations, micronuclei, DNA strand-breaks and modification of bases in DNA. The genotoxicity induced by CNTs may be mediated either by direct or indirect pathways (see Section 9.4).

In one study longer and thicker CNTs caused more genotoxic damage than thinner and shorter ones and in another study functionalised MWCNTs were more potent in this respect than pristine nanotubes. In a third study pure SWCNTs re-

vealed no genotoxic effects, suggesting that such responses might be evoked by impurities such as metals. However, based on available studies it is not possible to make any conclusions how variables such as dimensions, functionalisation and metal impurities modify the genotoxicity of CNTs.

11.5 Effects of long-term exposure and carcinogenicity

11.5.1 Pulmonary toxicity

The effects of long-term exposure to CNTs have been evaluated in two studies performed according to OECD guidelines.

In the study by Ma-Hock and co-workers, male and female Wistar rats head-nose inhaled MWCNTs (diameter 5-15 nm, length 0.1-10 µm, surface area 250-300 m^2/g, 9.6% Al_2O_3 and traces of Fe and Co, Nanocyl NC 7000) at air levels of 0.1, 0.5 and 2.5 mg/m^3 for 6 hours/day, 5 days/week for a total of 13 weeks. In the respirable dust aerosol employed, which was generated in-house, the median aerodynamic diameter of the MWCNTs was 0.7-2 µm, with 66-90% of the particle mass being smaller than 3 µm. Accordingly, a high proportion of these MWCNTs should have been deposited in the alveolar region. Free MWCNTs were also present in the alveoli, but not quantified. Analysis by TEM revealed clumps of MWCNTs micrometres in size, with individual MWCNTs as well. The dustiness of these MWCNTs was considered low. Dose-dependent formation of multifocal granulomatous inflammation, diffuse histiocytosis and intra-alveolar lipoproteinosis was observed in the lungs and goblet cell hyperplasia in the nasal cavity. Granulomatous inflammation was also present in the mediastinal lymph nodes, suggesting long retention of the MWCNTs. These effects were most pronounced after exposures to 0.5 and 2.5 mg/m^3, but minimal granulomatous inflammation and minimal diffuse histiocytosis were also observed at 0.1 mg/m^3. Although intraseptal granulomas containing macrophages, fibroblasts and connective tissue were seen, no thickening of the alveolar walls indicative of fibrosis was observed. With the medium and high doses diffuse neutrophilic inflammation of the lungs also occurred, as well as an increase in the number of circulating white blood cells at the highest dose. Moreover, the weights of the lungs elevated dose-dependently, but no pathological changes were observed in other organs. Based on the incidence of minimal granulomatous inflammation 0.1 mg/m^3 was considered as the lowest observed adverse effect level (LOAEL) (198).

Pauluhn examined the effects of MWCNTs (diameter 10 nm, length 0.2-0.3 µm, surface area 259 m^2/g, Baytubes) administered to male and female Wistar rats by nose-only inhalation at air levels of 0.1, 0.4, 1.5 and 6 mg/m^3 for 5 hours/day, 5 days/week for 13 weeks with follow-up for additional 26 weeks. The MWCNTs employed were inherently inclined to "form coiled, intertwined and tangled structures". Since harsh conditions were required to prepare individual CNTs for analysis, the physical parameters reported may not reflect those of the CNTs as actually administered. The material was reported to exhibit low dustiness and

chemical analysis showed 98.6% purity in bulk form and 99.1% after micronisation. The major contaminant was cobalt, which was present at a level of 0.46% or 0.53% (depending on the method of determination). Upon aerosolisation, these MWCNTs were present as micron-sized agglomerates, rather than free nanotubes. Most effects observed were dose-dependent. The total number of cells in the BAL fluid was higher during study week 13 (post-exposure day 1) with the dose of 0.4 mg/m^3 and during study weeks 8-39 with 1.5 and 6 mg/m^3. The number of lymphocytes in this fluid was elevated by 1.5 and 6 mg/m^3, while the number of PMNs increased at all levels of exposure except the lowest (0.1 mg/m^3). The number of alveolar macrophages was enhanced by the two highest concentrations, while foamy macrophages were observed only after exposure to 6 mg/m^3. Biochemical markers of cytotoxicity and fibrosis (the activities of AP-1 and LDH, the levels of collagen and total protein, etc.) in the BAL fluid were also increased by all concentrations except 0.1 mg/m^3. The level of soluble collagen and the number of PMNs were closely correlated. All of these responses were maximal at the end of the 13-week exposure to CNTs. The weight of the lungs increased continuously during the entire 39-week period, but significantly only at the two highest concentrations. The lung-associated lymph nodes also weighted more between study weeks 8 and 17, after which they decreased in size again. Histopathology revealed macrophages containing particles, dose-dependent thickening of the septal alveolus indicative of interstitial fibrosis, infiltration by inflammatory cells, goblet cell hyper-/metaplasia in the upper respiratory tract, again at all concentrations except the lowest. Following exposure to 6 mg/m^3 MWCNTs, pleural thickening was observed from week 13 and thereafter. Moreover, more intense staining for collagen was observed following exposure to 0.4-6 mg/m^3 MWCNTs. The concentration 0.1 mg/m^3 was considered to be the no observed adverse effect level (NOAEL). No systemic effects were observed under any condition. The retention half-time of MWCNTs in the lungs following 13 weeks of exposure to 6 mg/m^3 was determined to be 375 days, which was longer than the post-exposure follow-up. No dissolution of MWCNT agglomerates into free nanoparticles was seen in the alveoli (255). The investigators interpreted the responses seen at concentrations of 1.5 and 6 mg/m^3 as due to particle overload by agglomerates with a high volume of displacement, similar to the phenomena observed with carbon black.

11.5.2 Carcinogenicity

The abdominal cavity and the internal organs inside is lined with a membrane called peritoneum which is composed of mesothelial cells, the same cell type that forms the pleura. The use of i.p. injections, i.e., into the peritoneal cavity, is considered appropriate to screen for fibres that have the potential to induce formation of mesotheliomas.

The effects of a single i.p. injection of 10^9 (3 mg) MWCNTs (mean diameter 100 nm, length 27.5% >5 µm, 3.55×10^{11} particles/g, Mitsui MWNT-7) into p53 heterozygous mice (n=19, which are particular sensitive to the toxic effects of asbestos) during the subsequent 180 days have been compared to similar exposure

to crocidolite (10^{10} particles, 3 mg/animal, obtained from the Union Internationale Contre le Cancer (UICC)) or another type of fullerenes (3 mg/animal), with the control animals receiving the vehicle alone. After 10 days, particles were present on the surface of organs and the intestinal loops were oedematous. The MWCNTs caused highest mortality, followed by the crocidolite, whereas fullerenes and vehicle alone resulted in no deaths. The formation of fibrous scars and a foreign body reaction led to peritoneal adhesion and fibrous thickening in the animals receiving MWCNTs. Mesothelial lesions of various grades, including large tumours were observed. The mortality from mesothelioma was 87.5% (14/16 animals) for the MWCNT-group and 77.8% (14/18 animals) with crocidolite (320).

In another study by the same research group, MWCNTs (median diameter 90 nm (range 70-170 nm), median length 2 μm (range 1-20 μm), 0.35% Fe, Mitsui MWNT-7) were administered by single i.p. injections into p53 heterozygous mice (n=20/group) at doses of 3 μg (10^6 fibres), 30 μg (10^7 fibres) or 300 μg (10^8 fibres) per mouse and the animal were followed-up for a year. A dose-dependent induction of mesothelioma was observed with an incidence of 5/20, 17/20 and 19/20 in the low-, middle- and high-dose group, respectively. The time of tumour onset was, however, independent of the dose. Histopathological examination revealed that the mesotheliomas ranged from a differentiated epithelioid type to an undifferentiated sarcomatous type. The mesotheliomas of the low-dose group were devoid of foreign body granulomas or fibrotic tissue, as were the focal mesothelial atypical hyperplasia present in all mice in this group that survived until terminal kill. Instead, these latter lesions were backed up by an accumulation of mononuclear inflammatory cells. As this atypical hyperplasia is considered as precursor lesion of mesothelioma, these investigators suggested that mesothelioma originates from these inflammatory lesions without granulomas and fibrous scars formed against MWCNT agglomerates and that the mesothelial atypical hyperplasia can be regarded as a lesion driven by the frustrated phagocytosis against MWCNTs. Moreover, individual MWCNTs were detected in several organs including the liver, brain and lungs, likely delivered via the systemic circulation (319).

In another investigation, two kinds of MWCNTs (diameter 11.3 nm, length 0.7 μm, with and without structural defects in the carbon skeleton) were implanted in the peritoneal cavity of rats (n=50) at doses of 2 or 20 mg/animal (with defects) or 20 mg/animal (without defects) and the animal monitored for 2 years thereafter. The effects were compared to those evoked by crocidolite (diameter 330 nm, length 2.5 μm, UICC-grade, 2 mg/animal). Histopathological examination showed no significant incidence of abdominal tumours in the animals exposed to either kind of MWCNTs, whereas crocidolite asbestos induced mesotheliomas in 34.6% of the rats. Body weight and survival were not affected by any of the exposures. The absence of a carcinogenic response to MWCNT implantation could, according to the authors, be explained by the absence of a sustained inflammatory response in the peritoneal cavity. The discrepancy between these findings and those reported by Takagi and co-workers (319, 320) might be due to their use of different animals. In addition, it was proposed that rats were not sensitive enough to the short

CNTs used by Muller and collaborators (220), since this model for producing carcinogenesis by i.p. injection has been reported to be most sensitive to fibres longer than 5 µm. Moreover, the MWCNTs employed here do not generate ROS, but act rather as scavengers of free radicals, in contrast to crocidolite, which evokes formation of free radicals and oxidative stress (220).

In yet another study, rats received a single intrascrotal injection of 1 mg/kg bw MWCNTs (diameter 70-110 nm, length 1-4 µm, n=7), 2 mg/kg bw crocidolite (diameter 30-400 nm (81.3%), length 0.1-5 µm (91.5%), n=10), or vehicle alone (n=5), with follow-up for 52 weeks. During week 37-40, 6 of the animals injected with MWCNTs died from mesothelioma, whereas with crocidolite and vehicle alone, all of the animals survived for 52 weeks without pathological findings (288).

Following intrascrotal injection of 1 mg/kg bw MWCNTs (diameter 70-110 nm, length 1-4 µm) identical to those employed by Sakamoto *et al* and Takagi *et al* (288, 319, 320) into male Fisher 344 rats (n=3, age 12 weeks) the serum levels of a biomarker of human mesothelioma referred to as "expressed in renal carcinoma (ERC)/mesothelin" were monitored for 52 weeks. The goal was to see whether ERC/mesothelin could be used as a biomarker for mesothelioma in rats as well. When serum was collected following sacrifice of the animals and the levels of the N- and C-terminal fragments of ERC/mesothelin determined by enzyme-linked immunosorbent assay (ELISA), the animals that had received MWCNTs and developed mesothelial hyperplasia were found to exhibit elevated levels of the N-terminal region. The rats that became moribund after 40 weeks demonstrated even higher levels of ERC/mesothelin. Thus, the authors suggest that ERC/mesothelin can be used as a biomarker of mesothelial proliferative lesions in animals as well (287). Moreover, it could be speculated that this could be a useful biomarker for MWCNT-induced pathologies in humans as well.

Varga and Szend implanted hard gelatine capsules filled with 10 mg of either SWCNTs (diameter <2 nm, length 4-15 µm) or MWCNTs (diameter 10-30 nm, length 1-2 µm) in the peritoneal envelope of rats (n=6/experiment, 400 g, so that this dose was equivalent to 25 mg/kg bw). Twelve months after implantation, none of the animals had died and histopathological examination revealed dispersed bulks of either nanotube in the abdominal cavity, as well as some expansion of the gastric wall. Granulomatous reactions of the foreign-body type, including multinucleated giant cells were seen with both types of nanotubes. It was concluded that mesotheliomas did not arise under these condition and that other investigations claiming the opposite have been too preliminary to allow a firm conclusion to be drawn (352).

Conclusions concerning effects of long-term exposure and carcinogenicity

Long-term exposure and carcinogenicity studies in animals are summarised in Tables 9 and 15, respectively. In two assessments of the effects of subchronic exposure to MWCNTs, granulomatous inflammation in the lungs and lymphatic tissue, including CNT-laden macrophages, was observed. Furthermore, the pulmonary toxicity of longer (Nanocyl NC 7000 0.1-10 µm) MWCNTs was manifested

as intra-alveolar lipoproteinosis and granulomatous nodules of particle-laden macrophages present in mediastinal lymph nodes (198); while shorter (Baytubes 0.2-0.3 μm) MWCNTs resulted in sustained inflammation, diffuse interstitial fibrosis and, at high doses, thickening of the pleural wall (255).

Neither of these 90-day inhalation studies reported lesions in organs other than the lungs (except for slightly more blood neutrophils following exposure to longer CNTs). This is in contrast to some studies reporting on effects of the immune system after short-term inhalation exposure to CNTs (212, 213). It is noteworthy that the dustiness of the MWCNTs used in both the 90-day inhalation studies was stated to be low.

The results obtained with Baytubes by Pauluhn provide no direct support for the fibre/HARN hypothesis of CNT toxicity, since no free MWCNTs were observed in the lung and the effects were considered to be due to overload (255). In the aerosol employed, the MWCNTs were present primarily as agglomerates and similar agglomerates were detected in exposed lungs. In addition, free MWCNTs were difficult to generate from agglomerates during aerosolisation.

Mesothelioma has been observed in the peritoneal cavity of mice (319, 320) and scrotum of rats (287) following injection of MWCNTs at these sites. On the other hand, i.p. injection of shorter MWCNTs caused no mesotheliomas in rats (220). No cases of mesothelioma have been observed in inhalation studies, however it should be noted that cancer is unlikely to develop within the short time frame of these studies. Due to the limited number of such studies, no firm conclusion can be drawn at present concerning carcinogenicity of CNTs and further experiments in this area are clearly warranted. It has been shown that MWCNTs can reach the subpleural tissues following inhalation exposure (284) and the intrapleural space and visceral pleura following pharyngeal aspiration (207, 265).

The limited studies at hand suggest a carcinogenic potency of CNTs.

11.6 Reproductive and developmental effects

The concentrations of CNTs indicated in experiments with fish embryos below refer to the concentration in the surrounding medium in which the embryos were incubated.

SWCNTs

Pristine (diameter 2.8 nm, length 0.85 μm), oxidised (diameter 1.6 nm, length 0.76 μm) or ultraoxidised SWCNTs (diameter 1.8 nm, length 0.37 μm) were administered to female mice (n=16-23/group) on day 5.5 of gestation by injection in the retrobulbar plexus at doses of 0.01, 0.1, 0.3, 3 and 30 μg/animal, and the effects evaluated 10 days later. At the highest dose all types of SWCNTs caused malformation of foetuses and swollen uteruses. These latter were classified as early miscarriages, with the pristine SWCNTs being least potent and the ultraoxidised most. With 3 μg the number of animals that miscarried was reduced, while the proportion bearing malformed foetuses was higher. At 0.3 μg none of the SWCNTs resulted in miscarriages and at 0.01 μg no foetuses were malformed.

Placentas associated with the malformed foetuses all appeared abnormal and immunohistochemical analysis revealed reduced vessel density, reflecting the presence of thrombotic vessels. No effects in other organs were observed by histological and immunohistochemical analysis. The level of ROS was elevated in tissue homogenates of the placentas from mice exposed to ultraoxidised SWCNTs that carried malformed foetuses, as well as in the malformed foetuses themselves (258).

In addition, the effects of SWCNTs (diameter 11 nm, length 0.5-100 μm) and DWCNTs on zebrafish embryos have been assessed, employing carbon black as a control. These embryos were exposed to 20-360 mg/ml for 4-96 hours post-fertilisation, using fifteen groups of 20 animals each at each concentration. The parameters monitored included the head-trunk angle, body length, cell death, staining of blood vessels, expression of developmental genes and immunostaining of various proteins. Although no change in embryonic development was detected with as much as 360 mg/ml SWCNTs, a significant delay in hatching (from 52-72 hours post-fertilisation) was caused by exposure to 120-360 mg/ml. Examination of the chorion, surrounding the developing embryo revealed pores and aggregates of SWCNTs that were unable to cross this structure. The delay in hatching was proposed to be linked to metal impurities in the CNT preparation and/or to be a stress response elicited by interaction between the chorion and the CNTs that could not get through and attached instead to its surface (42).

MWCNTs

When female rats (n=12/group) were repeatedly exposed to MWCNTs (diameter 10-15 nm, length ~20 μm, 95% pure, 5% Fe) via oral administration at daily doses of 8-1 000 mg/kg bw on gestation days 6-19, no adverse effects on embryonic development were observed (186).

Bai and co-workers injected 5 mg/kg bw MWCNTs either functionalised with carboxyl-groups (diameter 20-30 nm, length 0.5-2 μm, 0.3% Fe, zeta-potential -57 mV in water, -48 mV in plasma) or with amino-groups (diameter 20-30 nm, length 0.5-2 μm, 0.21% Fe, zeta-potential 26 mV in water, -35 mV in plasma) i.v. into male mice (n=8) repeatedly (every 3 days 5 times) and monitored effects on fertility on days 15, 60 and 90. MWCNTs accumulated in the testes, where they caused oxidative stress as indicated by elevated level of malondialdehyde on day 15 (significant for the carboxyl-functionalised CNTs only). The malondialdehyde level had returned to normal in mice examined on days 60 and 90. Histological examination of testes revealed abnormal seminiferous tubules and reduced germinative layer thickness on day 15. These alterations were observed only occasionally in mice examined on days 60 and 90, indicating that they may have been repaired. Sperm quality was not influenced under any condition and the rates of pregnancy and delivery in female mice mated with the exposed animals were normal (13).

Asharani and colleagues examined the effects of MWCNTs (diameter 30-40 nm, length not specified) on isolated zebrafish embryos *in vitro* for as long as 72 hours post-fertilisation in accordance with OECD guidelines and found a no ob-

served effect concentration of 40 µg/ml. The lowest concentration at which the CNTs caused embryonal defects was 60 µg/ml and at higher concentrations, a slimy mucous formed around the embryos. There was a concentration-dependent drop in embryonal heart rate after 48 and 72 hours (n=3), but development of the heart remained normal. At high concentrations (≥100 µg/ml), apoptosis, enhanced mortality, delayed hatching, and abnormalities in the spinal cord occurred (n=60 per concentration), with the incidence of defects being dose-dependent. These investigators thought that the apoptotic effect was due to oxidative stress (12).

When zebrafish embryos (n=50) were exposed to 2 ng MWCNTs purified with HNO_3 and then functionalised with FITC-labelled bovine serum albumin (diameter: average 19.9 nm, median 17.5 nm, length: average 0.8 µm, median 0.7 µm, 98% purity) either by injection at the 1-cell stage or by introduction into the cardiovascular system 72 hours post-fertilisation, no adverse effects on embryonal development were detected. The labelled nanotubes were seen in the nuclei of cells whereas FITC-bovine serum albumin alone (i.e., the control) was not. Injection of the labelled MWCNTs into the cardiovascular circulation was followed by rapid distribution to all tissues, with an especially strong signal in the swim bladder, an organ of detoxification in these animals, indicating that the embryos could clear the nanotubes. After 96 hours, no fluorescent signal could be seen anywhere in the embryos. Following delivery of either FITC-bovine serum albumin-MWCNT or FITC-bovine serum albumin, but not of vehicle alone at the 1-cell stage lysosomal vesicles were present in blastoderm cells. The innate immune system also appeared to be activated, since MMP9 (an innate immune response marker) was expressed in white blood cells. However, the reproductive system developed normally. The survival rate of the zebrafish injected at the 1-cell stage was unaltered at 14, 28 and 56 days later; the larvae developed normally and spawning was successful after maturity was reached. In contrast, the survival rate of the second generation offspring 14 days after birth was reduced by injection of MWCNTs through some unknown mechanism (41).

Conclusions concerning reproduction and development

Information concerning the effects of CNTs on reproduction is scarce. However, low doses of SWCNTs administered by retrobulbar injection to pregnant mice affected the development of embryos (Table 10) (258), whereas high doses of MWCNTs administered orally to pregnant rats led to no such effect (Table 13) (186). MWCNTs i.v. injected in male mice had no effect on sperm quality or fertility, but accumulated in testes, generated oxidative stress and decreased the thickness of the seminiferous epithelium in the testis temporarily (Table 13) (13). Published results obtained on zebrafish are not consistent.

Due to limited data no conclusion concerning reproduction and development toxicity of CNTs can be drawn from these studies.

12. Observations in man

The one study on the effects of CNTs on humans that could be located in the literature focused on irritation (122).

12.1 Irritation and sensitisation

When the skin of 40 volunteers was exposed to a filter paper saturated with a mixture of CNT and fullerene soot suspended in water, no effects were detected 96 hours later (122). However, this investigation has certain weaknesses, i.e., no presentation of data, no images of the skin, no positive controls, and no indication of the concentration of CNTs present in the patches. Thus no firm conclusion concerning irritation can be drawn from the study.

There are no data on sensitisation.

12.2 Effects of single and short-term exposure

No studies found.

12.3 Effects of long-term exposure

No studies found.

12.4 Genotoxic effects

No studies found.

12.5 Carcinogenic effects

No studies found.

12.6 Reproductive and developmental effects

No studies found.

13. Dose-effect and dose-response relationships

No human toxicity data are presently available.

Dose-effect relationships observed in animal studies (mostly mouse and rat) are compiled in Tables 9-15. In some cases dose conversions were performed by the authors of this NEG criteria document in order to facilitate comparisons between studies and in those cases assumptions in the calculations are noted in the tables.

Single exposure to SWCNTs

No *inhalation* studies have been located. Single exposure studies by other routes are summarised in Table 10. When the low dose of 0.04 mg/kg bw SWCNTs was administered to rats by *i.t. instillation*, only very mild histopathological signs of inflammation were observed and no increases in the levels of inflammatory mediators or numbers of cells in BAL fluid occurred. At and above 0.2 mg/kg bw pulmonary inflammation with an early increase in the number of inflammatory cells in the BAL fluid (with number of neutrophils still being elevated 6 months post-exposure) as well as accumulation of macrophages in the alveoli became evident. At and above 1 mg/kg bw formation of granuloma followed by epithelial hypertrophy and foamy macrophages 3-6 months later were observed (164). Signs of pulmonary fibrosis was seen at and above 1.6 mg/kg bw in mice (232) and at and above 2.0 mg/kg bw in rats (3). Furthermore, at and above 2.0 mg/kg bw several signs of alterations in the epithelium, including hypertrophic cells in the alveolar and bronchial epithelium, alveolar proteinosis and foreign-body giant cells, were present in rats (164). High doses (above 16 mg/kg bw) induced severe inflammation with epithelioid granulomas in mice (175).

Administration of SWCNTs to mice by *pharyngeal aspiration* led to signs of acute transient inflammation at 0.25 mg/kg bw (305). Dispersed SWCNTs caused increased collagen production and thickness of connective tissue in mice at 0.3 mg/kg bw and lung fibrosis at 0.36 mg/kg bw (208, 346). Damage to mitochondrial DNA in aorta was detected in mice at a dose of 0.4 mg/kg bw (184). Formation of granulomas along with oxidative stress began at 0.5 mg/kg bw in mice (306). At 1.5 mg/kg bw alterations in systemic inflammatory parameters were seen in mice (79).

Effects on embryonic development in mice were reported to occur at and above 0.1 µg administered via *retrobulbar injection* (258).

Twenty µg of chitosan-functionalised SWCNTs administered to mice by *i.v. injection* were rapidly taken up and accumulated in the liver, which exhibited pathological changes, including macrophage injury. Alterations in blood coagulation parameters also occurred (150). Administration of a similar absolute dose to rats accelerated the rate of vascular thrombosis (270).

Repeated exposure to SWCNTs

Only a few studies have involved repeated exposure to SWCNTs (Tables 9 and 11). *Inhalation* exposure to 0.03 and 0.13 mg/m^3 (approximately 0.006 and 0.03

mg/kg bw) SWCNTs for 4 weeks evoked no adverse effects in the lung of rats, (215). Based on this study 0.13 mg/m^3 may be set as a NOAEL of SWCNTs for rats. Exposure to 5 mg/m^3 (~0.25 mg/kg bw) for 4 days led to granulomatous inflammation and progressive fibrosis in mice (305).

Effects on the arterial baroreflex function (involved in regulation of the cardiovascular system) occurred following repeated *i.t. instillation* of 1 mg/kg bw SWCNTs to rats (178). In addition, administration of 50 µg (~1.6 mg/kg bw once a week for 6 weeks) was shown to aggravate allergic inflammatory processes in mice (135).

Following *pharyngeal aspiration* of 40 µg SWCNTs 6 times during a period of 3 weeks to mice, pulmonary inflammation and granulomas with associated fibrosis were present (329).

Dermal exposure to approximately 2.4 mg/kg bw (40 µg once daily for 5 days) SWCNTs to mice generated no response, but increasing the dosage to 4.7 mg/kg bw caused thickening of the skin and at 9 mg/kg bw thickening of the skin due to accumulation of PMNs and mast cell was accompanied by oxidative stress and enhanced production of cytokines (231).

When 5 mg/kg bw SWCNTs was administered to mice daily for 10 days via *gastrogavage*, the CNTs were detected in the ileum and in neurons of the brain, but there were no effects on blood parameters (373).

Repeated *i.p. injection* of 0.25 mg/kg bw SWCNTs resulted in hepatocyte disruption and elevated the production of ROS in the liver of mice (250).

Single exposure of MWCNTs

The effects of a single exposure of MWCNTs via various routes have also been examined (Tables 9 and 12). Seven days after a 6-hour nose-only *inhalation* of MWCNTs at an air concentration of 11 mg/m^3 (approximately 0.2 mg/kg bw), rats exhibited an inflammatory response, as indicated by elevated number of PMNs and levels of markers of cytotoxicity in BAL fluid (76). Mice exposed to a similar estimated dose (air level of 1 mg/m^3 for 6 hours) via the same route showed no significant pleural inflammation of mononuclear cell aggregates or quantifiable levels of fibrosis up until the end of the observation period at 14 weeks post-exposure (284). However, at an air concentration of 30 mg/m^3 and an estimated deposited dose of 4 mg/kg bw, mice exhibited fibrosis of the subpleura 2 and 6 weeks post-exposure. Rats exposed to a similar dose (air level of 241 mg/m^3 for 6 hours) demonstrated a rapid inflammatory response that persisted after 3 months, along with elevated level of septal collagen, increases in the weights of the hilus lymph nodes and more foamy macrophages (76).

Responses to a single exposure to MWCNTs administered via *i.t. instillation* to rats were evident at 0.16 mg/kg bw and included acute transient inflammation of the lungs that after 3 months was still present and accompanied at this later time-point by fibrosis of the alveolar walls (1). Rats showed signs of oxidative stress at 0.2 mg/kg bw (276), evidence of microgranulomas at 0.6 mg/kg bw (1) and with 1 mg/kg bw granulomas formed (276). At this same dose hyperplasia of epithelial

cells was initiated in mice (35). At and above 3 mg/kg bw rats exhibited severe pulmonary inflammation (190) and at 5 mg/kg bw a systemic increase in cytokine levels was observed in mice (249).

Single exposure to MWCNTs via *pharyngeal aspiration* evoked responses similar to those observed following i.t. instillation. At approximately 0.5 mg/kg bw (10 µg) acute pulmonary inflammation was seen, progressive pulmonary fibrosis was detectable and one mouse also exhibited pleural inflammation. Doses of approximately 0.9 mg/kg bw led to granulomatous inflammation in the alveolar space and the interstitium, with detection of MWCNTs in the subpleura and pleural spaces (265). At 1.5 mg/kg bw markers of systemic inflammation appeared in mice (79) and in this same species hypertrophy and hyperplasia of the bronchoalveolar epithelium occurred above 3 mg/kg bw (265).

Intrapleural injection of 5 µg long, but not short MWCNTs into mice gave rise to an acute inflammation of the pleura and progressive fibrosis of the parietal pleura (223).

No effects were detected when rabbits were exposed *dermally* to 500 µg MWCNTs (158). On the other hand, *subcutaneous implantation* of 0.6 mg/kg bw (100 µg) MWCNTs produced local inflammation in rats (292), as did *submuscular implantation* of 17 mg/kg bw (corresponding to 5 mg) in rats (45).

I.p. injection of 50 µg long MWCNTs into mice gave rise to granulomatous inflammation (259).

I.v. injection of approximately 5 mg/kg bw (100 µg) led to pulmonary inflammation in mice and macrophages that had engulfed MWCNTs were detected (269).

Repeated exposure of MWCNTs

Repeated exposure to MWCNTs (Tables 9 and 13) has been accomplished primarily via *inhalation*. Exposure of rats to 0.1 mg/m^3 MWCNTs for 13 weeks was without effect, and thus identifying a NOAEL of 0.1 mg/m^3 for this species (255). However, in another 13-week inhalation study, 0.1 mg/m^3 led to minimal granulomatous inflammation with minimal diffuse histiocytosis (198). Exposure of rats to 0.37 mg/m^3 for 4 weeks transiently elevated the levels of chemokines in the lungs and activity of myeloperoxidase in the BAL fluid, whereas no histopathological alterations in the lungs were observed (216). Exposure of rats for 13 weeks to 0.4 mg/m^3 caused sustained broncho-alveolar inflammation, thicker alveolus septum indicative of interstitial fibrosis and goblet cell hyperplasia in the upper respiratory tract (255). At 0.5 mg/m^3 additional effects appeared, including intra-alveolar lipoproteinosis and goblet cell hyperplasia in the nasal cavity (198). On the basis of the study by Ma-Hock and co-workers (198), the LOAEL of MWCNTs for rat is 0.1 mg/m^3. Mice exposed to 0.3 mg/m^3 MWCNTs for 14 days demonstrated no signs of pulmonary inflammation, but were immune-suppressed (212). Thus, 0.3 mg/m^3 may be considered to be an LOAEL of MWCNTs for mice.

I.t. instillation of 50 µg (~1.6 mg/kg bw once a week for 6 weeks) MWCNTs aggravated allergic inflammatory processes in mice (133).

I.v. injection of 5 mg/kg bw MWCNTs (every 3 days 5 times) did not alter sperm quality or fertility in mice monitored up to 90 days. However, the MWCNTs accumulated in the testes, generated oxidative stress and decreased the thickness of the seminiferous epithelium in the testis temporarily (13). High doses of MWCNTs administered *orally* (up to 1 000 mg/kg bw) to rats once daily on gestation days 6-19 had no effect on embryonic development 1 day post-exposure (186).

In conclusion, single- and repeated administrations of SWCNTs or MWCNTs to the lungs via inhalation, i.t. instillation or pharyngeal aspiration resulted generally in rapid pulmonary inflammatory response, characterised primarily by more PMNs, but also mononuclear cells, as well as granulomas (containing CNTs) with or without associated fibrosis. The variation in pulmonary effects observed may reflect varying characteristics of the CNTs employed, as well as differences in the dispersion procedure and route of administration. There are no apparent differences in the pulmonary responses of the species most commonly utilised in studies on CNTs, namely, the rat and mouse although the rat shows a tendency to be more susceptible to the pulmonary toxicity of nanotubes.

In each table (see below), the animal studies are ordered by route of administration and in order of increasing dose given as mg/kg bw. Inhalation studies, studies on genotoxicity and mutagenicity as well as on carcinogenicity are in separate tables.

Table 9. Effects after single and repeated inhalation exposures to SWCNTs or MWCNTs.
Table 10. Effects after a single dose of SWCNTs.
Table 11. Effects after repeated doses of SWCNTs.
Table 12. Effects after a single dose of MWCNTs.
Table 13. Effects after repeated doses of MWCNTs.
Table 14. Genotoxic and mutagenic effects of SWCNTs and MWCNTs.
Table 15. Carcinogenic effects after a single dose of SWCNTs and MWCNTs.

Table 9. Effects after single and repeated inhalation exposures to SWCNTs or MWCNTs.

Air level (mg/m^3)	Estimated deposited dose (µg)	Dose (mg/kg bw)	Exposure duration	Species/ strain	No. and sex of animals	Diameter (nm)	Length (µm)	Surface area (m^2/g)	Attributes	Observation period	Effects	Reference
Single exposure												
11	41 [a]	0.18 [a]	6 h	Rat Wistar	6 males	10-16	-	253	MWCNTs, Baytubes, 0.53% Co	7, 28 and 90 days post-exposure	Dose-dependent increase in the levels of inflammatory cells and cytotoxic markers in BALF after 7 days, declined thereafter. Elevated level of collagen in BALF after 7 days, with further elevation until day 28, but normal after 90 days. Enhanced weights of the lungs and hilus lymph nodes after 7 and 90 days and 7 days, respectively. Minimal occurrence of foamy macrophages. No septal thickening, alveolar hyperplasia or particle-laden macrophages in BALT.	(76)
11	41 [a]	0.18 [a]	6 h	Rat Wistar	6 males	10-16	-	-	MWCNTs, Baytubes, acid-treated, 0.12% Co	7, 28 and 90 days post-exposure	Less pronounced responses than those to CNTs containing 0.53% Co (see above). Minimal focal septal thickening. Dark alveolar macrophages present in BALT.	(76)
1	4.8 [b]	0.2	6 h	Mouse C57BL/6	10 males	10-30 [c] 30-50 [d]	0.5-40 [c] 0.3-50 [d]	-	MWCNTs, 0.1-5% Ni	1 day, 2, 6 and 14 weeks post-exposure	No increase in aggregates of pleural mononuclear cells at any time-point. No increase in subpleural fibrosis.	(284)

Table 9. Effects after single and repeated inhalation exposures to SWCNTs or MWCNTs.

Air level (mg/m^3)	Estimated deposited dose (µg)	Dose (mg/kg bw)	Exposure duration	Species/ strain	No. and sex of animals	Diameter (nm)	Length (µm)	Surface area (m^2/g)	Attributes	Observation period	Effects	Reference
30	96 [b]	4	6 h	Mouse C57BL/6	10 males	10-30 [c] 30-50 [d]	0.5-40 [c] 0.3-50 [d]	-	MWCNTs, 0.1-5% Ni	1 day, 2, 6 and 14 weeks post-exposure	Elevated numbers of aggregates of pleural mononuclear cells containing CNTs after 1 day and 2 weeks. Subpleural fibrosis, as assessed by image analysis, was increased 2 and 6 weeks, but not 14 weeks after exposure. Most of the sub-pleura appeared normal, the fibrotic lesions being focal and regional.	(284)
241	890 [a]	4 [a]	6 h	Rat Wistar	6 males	10-16	-	253	MWCNTs, Baytubes, 0.53% Co	7, 28 and 90 days post-exposure	Dose-dependent increases in the levels of inflammatory cells and cytotoxic markers, elevated levels of collagen in BALF after 7 days, diminished, but still increased after 28 and 90 days (except for LDH on day 90). Focal increase in bronchoalveolar septal collagen. Enhanced weights of the lungs and hilus lymph nodes after 7 and 90 days and 7 days, respectively. Slightly more foamy macrophages. No hyperplasia or particle-laden macrophages in BALT. No change in the expression of genes en-coding collagen, suggesting extra collagen originated from exudates rather than local fibroblast production. Higher levels of mRNA encoding anti- and inflammatory regulators, responders to oxidative stress and proteins regulating endothelial and epithelial permeability in pulmonary tissue.	(76)

Table 9. Effects after single and repeated inhalation exposures to SWCNTs or MWCNTs.

Air level (mg/m^3)	Estimated deposited dose (µg)	Dose (mg/kg bw)	Exposure duration	Species/ strain	No. and sex of animals	Diameter (nm)	Length (µm)	Surface area (m^2/g)	Attributes	Observation period	Effects	Reference
100	288 [b]	12	6 h	Mouse C57BL/6	4-5 males	10-30 [c] 30-50 [d]	0.5-40 [c] 0.3-50 [d]	-	MWCNTs, 5% Ni, with and without co-exposure to OVA	1 and 14 days post-exposure	Airway fibrosis after 14 days in mice co-exposed to OVA indicated by thicker collagen in bronchiolar walls. No change in total pulmonary content of collagen. More neutrophils, PDGF-AA and TGFβ1 in BALF after 1 day. No fibrosis in mice exposed to CNTs alone, but the levels of neutrophils and PDGF-AA in BALF elevated after 1 day.	(285)
Repeated exposure												
0.03	1.9	0.006 [b]	6 h/day, 5 days/wk for 4 wks	Rat Wistar	10 males	200 (GM in air, bundles), 3 (bulk)	0.7 (GM in air, bundles)	1 064	SWCNTs, 0.05% metals	3 days, 1 and 3 months	No increases of total cell or neutrophil counts in BALF. No consistent changes in levels of ALP or HO-1 in BALF or levels of CINC-1 and -2 in lung tissue were observed. Alveolar macrophages with internalised CNTs detected up to 3 months post-exposure.	(215)
0.13	8.8	0.03 [b]	6 h/day, 5 days/wk for 4 wks	Rat Wistar	10 males	200 (GM in air, bundles), 3 (bulk)	0.7 (GM in air, bundles)	1 064	SWCNTs, 0.05% metals	3 days, 1 and 3 months	Same as above.	(215)
0.1	24 [e]	0.10 [e]	6 h/day, 5 days/wk for 13 wks	Rat Wistar	50 males, 10 females	10	0.2-0.3 (median range)	259	MWCNTs, Baytubes, 99.1% pure, 0.5% Co	13 weeks + 6 months post-exposure	No inflammation or other effects observed in the airways.	(255)

Table 9. Effects after single and repeated inhalation exposures to SWCNTs or MWCNTs.

Air level (mg/m^3)	Estimated deposited dose (µg)	Dose (mg/kg bw)	Exposure duration	Species/ strain	No. and sex of animals	Diameter (nm)	Length (µm)	Surface area (m^2/g)	Attributes	Observation period	Effects	Reference
0.3	3.75	0.15	6 h/day, for 14 days	Mouse C57BL/6	7 males	10-20	5-15	100	MWCNTs, 97% pure, 0.5% Fe, 0.5% Ni	14 days	No systemic effects detected (no suppressed immune function).	(213)
0.37	50	0.17 [b]	6 h/day, 5 days/wk for 4 wks	Rat Wistar	10 males	63 (GM in air) 44 (bulk)	1.1 (GM in air)	69	MWCNTs	3 days, 1 and 3 months	Non-significant tendency towards more neutrophils after 3 days in BALF. Transient elevated levels of chemokines (CINCs) in lung tissue and MPO in BALF 3 days post-exposure. No histopathological alteration (no granuloma, neutrophil increase or fibrosis) of the lungs observed. Occasional observation of CNTs inside alveolar macrophages.	(216)
0.3	5 [f]	0.2	6 h/day, for 14 days	Mouse C57BL/6	6 males	10-20	5-15	100	MWCNTs, purity >95%, amorphous carbon <3%	14 days	No inflammation or tissue damages as indicated by histopathology or by markers in BALF (no increase or changed distribution of lymphocytes). No alteration in gene expression in lungs. Systemic immunosuppression in spleen cells after 14, but not after 7 days.	(212)

Table 9. Effects after single and repeated inhalation exposures to SWCNTs or MWCNTs.

Air level (mg/m^3)	Estimated deposited dose (µg)	Dose (mg/kg bw)	Exposure duration	Species/ strain	No. and sex of animals	Diameter (nm)	Length (µm)	Surface area (m^2/g)	Attributes	Observation period	Effects	Reference
0.1	46.8	0.21 [g]	6 h/day on 65 of 90 days	Rat Wistar	10 males, 10 females	5-15	0.1-10	250-300	MWCNTs, Nanocyl, purity 90% carbon, 10% metal oxide (Al)	90 days	Minimal granulomatous inflammation (only single) in the lungs and lymph nodes draining this organ. Minimal diffuse histiocytosis in the lungs. No systemic effects. No pathological lesions in organs other than the lungs.	(198)
5	5	0.25 [b]	5 h/day for 4 days	Mouse C57BL/6	5 females	0.8-1.2	0.1-1	508	SWCNTs, 17.7% Fe	1, 7 and 28 days post-exposure	Granulomatous inflammation in alveolar region and progressive fibrosis (accumulation of collagen and thicker alveolar walls) after 28 days. Increased levels of pro-inflammatory cytokines in BALF after 1 day that declined thereafter, but remained significant. The level of TGFβ increased until day 7, and remained elevated throughout the observation time. Elevated frequency of mutations in K-*ras* gene in the lungs after 28 days.	(305)
10	7	0.33 [h]	5 h/day for 2 days	Mouse C57BL/6J	7-9 males	-	-	-	MWCNTs, 1.06% Fe	1 day post-exposure	Dose-dependent increase of PMNs, chemokine KC, LDH and albumin in WLL fluid. Bronchiolar epithelial cell hypertrophy and hyperplasia.	(264)

Table 9. Effects after single and repeated inhalation exposures to SWCNTs or MWCNTs.

Air level (mg/m^3)	Estimated deposited dose (µg)	Dose (mg/kg bw)	Exposure duration	Species/ strain	No. and sex of animals	Diameter (nm)	Length (µm)	Surface area (m^2/g)	Attributes	Observation period	Effects	Reference
0.4	97 [e]	0.42 [e]	6 h/day, 5 days/wk for 13 wks	Rat Wistar	50 males, 10 females	10	0.2-0.3	259	MWCNTs, Baytubes, 99.1% pure, 0.5% Co	13 weeks + 6 months post-exposure	More cytotoxicity and inflammatory markers (including granulocytes, soluble collagen, LDH activity and total protein) in BALF after 13 weeks that declined thereafter until week 39. Translocation of CNTs to lymph nodes. Minimally thicker alveolus septum indicative of interstitial fibrosis. A large number of particle-laden macrophages in BALT after 13 weeks that declined thereafter until week 39. Minimal focal increases in staining for collagen in terminal bronchioles. Goblet cell hyper/ metaplasia of the upper respiratory tract seen in some animals.	(255)
1	12.5 [f]	0.5	6 h/day for 14 days	Mouse C57BL/6	6 males	10-20	5-15	100	MWCNTs, purity >95%, amorphous carbon <3%	14 days	No change in numbers or subpopulations of lymphocytes in BALF. Systemic immunosuppression in spleen cells after 14, but not after 7 days. No alterations in gene expression in the lungs.	(212)
1	12.5	0.5	6 h/day for 14 days	Mouse C57BL/6	7 males	10-20	5-15	100	MWCNTs, 97% pure, 0.5% Fe, 0.5% Ni	14 days	Immune suppression i.e. decreased anti-body formation in the spleen, mediated by COXs. Elevated level of TGFβ in BALF.	(213)

Table 9. Effects after single and repeated inhalation exposures to SWCNTs or MWCNTs.

Air level (mg/m^3)	Estimated deposited dose (µg)	Dose (mg/kg bw)	Exposure duration	Species/ strain	No. and sex of animals	Diameter (nm)	Length (µm)	Surface area (m^2/g)	Attributes	Observation period	Effects	Reference
10	13	0.6 [h]	5 h/day for 4 days	Mouse C57BL/6J	7-9 males	-	-	-	MWCNTs, 1.06% Fe	1 day post-exposure	Dose-dependent increase of PMNs, chemokine KC, LDH and albumin in WLL fluid. Bronchioloalveolar inflammation, vascular changes, and bronchiolar epithelial cell hypertrophy and hyperplasia detected by histopathology.	(264)
0.5	243	1.1 [g]	6 h/day on 65 of 90 days	Rat Wistar	10 males, 10 females	5-15	0.1-10	250-300	MWCNTs, Nanocyl, purity 90% carbon, 10% metal oxide (Al)	90 days	Multifocal granulomatous inflammation (intraseptal granuloma, alveolar macrophages, giant cells, fibroblasts, connective tissue) slight in the lungs and lymph nodes draining this organ. Minimal lympho-reticulocellular hyperplasia. Slight diffuse histiocytosis. No signs of diffuse fibrosis. Slight, dose-dependent alveolar lipoproteinosis. Mild multifocal hyperplasia of goblet cells in the nasal cavity. No pathological lesions in organs other than the lungs.	(198)
10	23	1.1 [h]	5 h/day for 8 days	Mouse C57BL/6J	7-9 males	-	-	-	MWCNTs, 1.06% Fe	1 day post-exposure	Dose-dependent increase of PMNs, chemokine KC, LDH and albumin in WLL fluid. Bronchioloalveolar inflammation, vascular changes, mucous metaplasia, fibrosis, and bronchiolar epithelial cell hypertrophy and hyperplasia detected by histopathology.	(264)

Table 9. Effects after single and repeated inhalation exposures to SWCNTs or MWCNTs.

Air level (mg/m^3)	Estimated deposited dose (µg)	Dose (mg/kg bw)	Exposure duration	Species/ strain	No. and sex of animals	Diameter (nm)	Length (µm)	Surface area (m^2/g)	Attributes	Observation period	Effects	Reference
10	31	1.4 [h]	5 h/day for 12 days	Mouse C57BL/6J	7-9 males	-	-	-	MWCNTs, 1.06% Fe	1 day post-exposure	Same as above and pleural penetration in 2 mice.	(264)
1.5	365 [e]	1.6 [e]	6 h/day, 5 days/wk for 13 wks	Rat Wistar	50 males, 10 females	10	0.2-0.3	259	MWCNTs, Baytubes, 99.1% pure, 0.5% Co	13 weeks + 6 months post-exposure	Epithelial damage. Enhanced cytotoxicity and inflammatory markers (including granulocytes, soluble collagen, LDH and total protein) in BALF after 13 weeks that sustained until week 39. Dose-dependent alveolitis, slight sustained interstitial fibrosis. More particle-laden macrophages in BALT after 13 weeks, that remained week 39. Progressive increase in lung-associated lymph node burden and in lung weight. Goblet cell hyper/metaplasia of the upper respiratory tract.	(255)
32.6	70	2.3 [b]	6 h/day for 5 days	Mouse Kunming	6 females	50	10	280	MWCNTs, purity >95%, amorphous carbon <3%	8 days	Proliferation and increased thickness of alveolar walls. No biochemical examination was performed.	(181)
5	67.5 [f]	2.7	6 h/day for 14 days	Mouse C57BL/6	6 males	10-20	5-15	100	MWCNTs, purity >95%, amorphous carbon <3%	14 days	No inflammation, tissue damage, fibrosis or granulomas observed in the lungs. No change in numbers or subpopulations of lymphocytes in BALF. No alteration in gene expression in the lungs. CNTs engulfed by lung macrophages. Systemic immunosuppression in spleen cells after 14, but not after 7 days.	(212)

Table 9. Effects after single and repeated inhalation exposures to SWCNTs or MWCNTs.

Air level (mg/m^3)	Estimated deposited dose (µg)	Dose (mg/kg bw)	Exposure duration	Species/ strain	No. and sex of animals	Diameter (nm)	Length (µm)	Surface area (m^2/g)	Attributes	Observation period	Effects	Reference
32.6	140	4.7 [b]	6 h/day for 10 days	Mouse Kunming	6 females	50	10	280	MWCNTs, purity >95%, amorphous carbon <3%	16 days	Proliferation and increased thickness of alveolar walls. No biochemical examination was performed.	(181)
6	1 460 [e]	6.4 [e]	6 h/day, 5 days/wk for 13 wks	Rat Wistar	50 males, 10 females	10	0.2-0.3	259	MWCNTs, Baytubes, 99.1% pure, 0.5% Co	13 weeks + 6 month post-exposure	More inflammatory cells, granulomas, increased bronchoalveolar hyperplasia. Transport of CNTs to lymph nodes. Dose-dependent alveolitis, with slight interstitial fibrosis and thicker pleura week 13, with no change thereafter. More particle-laden macrophages in BALT after 13 weeks, that remained week 39. Progressive increases in lung-associated lymph node burden and in lung weight. Goblet cell hyper/metaplasia of the upper respiratory tract.	(255)
2.5	1 170	5.2 [g]	6 h/day on 65 of 90 days	Rat Wistar	10 males, 10 females	5-15	0.1-10	250-300	MWCNTs, Nanocyl, purity 90% carbon, 10% metal oxide (Al)	90 days	Multifocal granulomatous inflammation, moderate in the lungs and slight in lymph nodes draining this organ. Slight lymphoreticulocellular hyperplasia. Moderate diffuse histiocytosis. No signs of diffuse fibrosis. Moderate-to-marked alveolar lipoproteinosis. More neutrophils in blood. Slight multifocal hyperplasia of goblet cells in the nasal cavity. No pathological lesions in organs other than the lungs.	(198)

Table 9. Effects after single and repeated inhalation exposures to SWCNTs or MWCNTs.

Air level (mg/m^3)	Estimated deposited dose (μg)	Dose (mg/kg bw)	Exposure duration	Species/ strain	No. and sex of animals	Diameter (nm)	Length (μm)	Surface area (m^2/g)	Attributes	Observation period	Effects	Reference
32.6	210	7 [b]	6 h/day for 15 days	Mouse Kunming	6 females	50	10	280	MWCNTs, >95% pure, amorphous carbon<3%	24 days	Proliferation and thicker alveolar walls. No biochemical examination was performed.	(181)
32.6 [i] (13-80)	210	7 [b]	6 h/day on 15 of 30 days	Mouse Kunming	9 females	50	10	280	MWCNTs, >95% pure, amorphous carbon <3%	30 days	Slight increases in total protein, ALP, ACP and LDH in BALF. MWCNTs aggregated to the bronchial wall and had entered the alveolar wall. Occasional thickening of alveolar wall.	(180)
32.6 [i] (13-80)	420	14 [b]	6 h/day on 30 of 60 days	Mouse Kunming	9 females	50	10	280	MWCNTs, >95% pure, amorphous carbon <3%	60 days	Pulmonary toxicity. Significant increases in total protein, ALP, ACP and LDH in the BALF. MWCNTs aggregated to the bronchial wall. Larger aggregates in the bronchi, smaller aggregates in the alveoli causing significant wall thickening.	(180)
200 [j]	700	35	20 min daily for 7 days	Mouse BALB/c	6 males	1-2	0.5-2	-	SWCNTs, >90% pure	-	Pulmonary inflammation (more total cells and PMNs and elevated levels of total protein in the BALF). Fibrosis indicated by elevated levels of soluble collagen. Both SWCNTs and MWCNTs (see below), induced oxidative stress, as shown by enhanced MPO activity and higher levels of ROS and lipid peroxidation, with the responses to the SWCNTs being consistently more pronounced.	(272)

Table 9. Effects after single and repeated inhalation exposures to SWCNTs or MWCNTs.

Air level (mg/m^3)	Estimated deposited dose (µg)	Dose (mg/kg bw)	Exposure duration	Species/ strain	No. and sex of animals	Diameter (nm)	Length (µm)	Surface area (m^2/g)	Attributes	Observation period	Effects	Reference
200[j]	700	35	20 min daily for 7 days	Mouse BALB/c	6 males	20-50	0.006-0.013	-	MWCNTs, >99% pure	-	Same as above.	(272)

[a] Estimated by the authors of this NEG document assuming a mean weight of 225 g, fraction deposited of 5.7% and respiratory minute volume 0.8 l/min/kg and calculated according to: estimated dose = respiratory minute volume × deposition fraction × time of exposure × air concentration of CNTs.
[b] Calculated by the authors of this NEG document using data and formulas provided in the reference.
[c] Data provided by the manufacturer.
[d] Determined independently by the investigators.
[e] Calculated by the authors of this NEG document using data and formulas provided in the reference. Average weight of a male rat = 228 g. Estimated dose = respiratory minute volume × deposition fraction × time of exposure × air concentration of CNTs.
[f] Calculated by the authors of this NEG document, based on an average weight of a mouse = 25 g (according to Mitchell *et al* (213)).
[g] Calculated by the authors of this NEG document, assuming the average weight of a male rat to be 225 g.
[h] Calculated by the authors of this NEG document, assuming the average weight of a mouse to be 21.5 g.
[i] Weighted mean.
[j] Calculated by the authors of this NEG document using data provided in the reference and assuming a ventilation of 25 ml/min.
Al: aluminium, ACP: acid phosphatase, ALP: alkaline phosphatase, BALF: bronchoalveolar lavage fluid, BALT: bronchus-associated lymphatic tissue, CINC: cytokine-induced neutrophil chemoattractant, Co: cobalt, COX: cyclooxygenase, Fe: iron, GM: geometric mean, HO: haeme oxygenase, KC: keratinocyte-derived chemoattractant, LDH: lactate dehydrogenase, MPO: myeloperoxidase, NEG: Nordic Expert Group, Ni: nickel, OVA: ovalbumin, PDGF: platelet-derived growth factor, PMN: polymorpho-nuclear leukocyte, ROS: reactive oxygen species, TGFβ: transforming growth factor beta, WLL: whole lung lavage.

Table 10. Effects after a single dose of SWCNTs.

Absolute dose (µg)	Dose (mg/kg bw)	Species/ strain	No. and sex of animals	Diameter (nm)	Length (µm)	Attributes	Observation period	Effects	Reference
Intratracheal instillation									
11-13 [a]	0.04	Rat Crl:CD	6 males	12 (bundles)	0.32 (bundles)	0.05% metal content	Up to 6 months	No change in levels of inflammatory cells (neutrophils, macrophages, lymphocytes or eosinophils) in BALF. Minimal macrophage accumulation in alveoli up to 6 months observed by histopathology. Minimal inflammatory cell infiltration in alveoli after 3 days only.	(164)
55-65 [a]	0.2	Rat Crl:CD	6 males	12 (bundles)	0.32 (bundles)	0.05% metal content	Up to 6 months	Increased levels of neutrophils throughout the observation period, of macrophages and lymphocytes after 1 week and of eosinophils after 3 days and 1 week in BALF. Macrophage accumulation in the alveoli and interstitium up to 6 months. Inflammatory cell infiltration in alveoli up to 3 months.	(164)
100	0.4	Rat Sprague Dawley	9-13 males	-	-	10% Fe	Up to 90 days	Inflammatory responses in the lungs observed by histology (dose-dependent).	(3)
277-327 [a]	1	Rat Crl:CD	6 males	12 (bundles)	0.32 (bundles)	0.05% metal content	Up to 6 months	Increased levels of neutrophils and lymphocytes up to 3 months and macrophages after 3 days and 1 month in BALF. Mild accumulation of alveolar macrophages. Foamy macrophages after 3 and 6 months and mild granuloma after 3 days. At 3 months the granuloma formation was minimal, but after 6 months these changes were no longer present. Hypertrophy of bronchial epithelium between 3 and 6 months.	(164)

Table 10. Effects after a single dose of SWCNTs.

Absolute dose (µg)	Dose (mg/kg bw)	Species/ strain	No. and sex of animals	Diameter (nm)	Length (µm)	Attributes	Observation period	Effects	Reference
40	1.6	Mouse C57BL/6	4-8	1-2	0.1-2	Unmodified; aggregated in PBS	90 days	Inflammation and granuloma-like structures with mild fibrosis in the large airways after 30 days.	(232)
40	1.6	Mouse C57BL/6	4-8	1-2	0.1-2	Unmodified; nanoscale dispersed in Pluronic	90 days	No effects of these well dispersed CNTs. Excretion via macrophages.	(232)
500	2	Rat Sprague Dawley	9-13 males	-	-	10% Fe	Up to 90 days	Increased thickness of alveolar septa, progressive granuloma formation and inflammatory reaction. Collagen deposition and pulmonary fibrosis.	(3)
554-654 [a]	2	Rat Crl:CD	6 males	12 (bundles)	0.32 (bundles)	0.05% metal content	Up to 6 months	Macrophage accumulation up to 3 month. Foamy macrophages present at all time-points. Slight granuloma formation and foreign body giant cells. Hypertrophy of alveolar and bronchial epithelium with alveolar proteinosis throughout the observation period.	(164)
54	2.28	Mouse ApoE-/-	7 females	0.9-1.7	≤1	2% Fe	24 h	Elevated levels of total protein and percentage of neutrophils and macrophages in BALF after 24 h. Increased mRNA expression of inflammatory genes in lung tissue. Damage to the DNA of BAL cells.	(137)
100	3.3	Mouse B6C3F1	4-5 males	-	-	26% Ni, 5% Y, 0.53% Fe	7 or 90 days	No mortality. Mild inflammation.	(175)
100	3.3	Mouse B6C3F1	4-5 males	-	-	Raw; 26.9% Fe, 0.78% Ni	7 or 90 days	No mortality. Inflammation (3/5) and granulomas (5/5) present 90 days post-exposure.	(175)
100	3.3	Mouse B6C3F1	4-5 males	-	-	Purified; 2.14% Fe	7 or 90 days	No mortality. Inflammation (2/5) and granulomas (2/5) present 90 days post-exposure.	(175)

Table 10. Effects after a single dose of SWCNTs.

Absolute dose (µg)	Dose (mg/kg bw)	Species/ strain	No. and sex of animals	Diameter (nm)	Length (µm)	Attributes	Observation period	Effects	Reference
112-132 [b]	4	Mouse ICR	8 males	1.2-1.4	2-5	Unmodified; 75% pure. With and without co-exposure to 33 µg/kg LPS	24 h	Co-exposure to LPS led to aggravated lung inflammation and enhanced systemic inflammation and coagulatory disturbances accompanying lung inflammation, and higher pulmonary permeability and hyperfibrinogenemia and a reduced level of activated protein C.	(134)
1 000	4	Rat Sprague Dawley	9-13 males	-	-	10% Fe	Up to 90 days	Increased thickness of alveolar septa, progressive granuloma formation and inflammatory reaction. More pronounced collagen deposition and pulmonary fibrosis.	(3)
500	16.5	Mouse B6C3F1	4-5 males	-	-	26% Ni, 5% Y, 0.53% Fe	7 or 90 days	5 out of 9 died within 7 days. Severe inflammation and dose-dependent epithelioid granuloma. Pulmonary lesions more pronounced 90 days post-exposure than after 7 days.	(175)
500	16.5	Mouse B6C3F1	4-5 males	-	-	Raw; 26.9% Fe, 0.78% Ni	7 or 90 days	No mortality. Inflammation (3/5) and dose-dependent granulomas (5/5) present 90 days post-exposure.	(175)
500	16.5	Mouse B6C3F1	4-5 males	-	-	Purified; 2.14% Fe	7 or 90 days	No mortality. Inflammation (5/5) and dose-dependent granulomas (5/5) present 90 days post-exposure.	(175)
500	20	Mouse ICR	Males	-	-	Dispersed in Pluronic F68	3 or 14 days	Activation of alveolar macrophages, various chronic inflammatory responses and severe pulmonary granuloma formation.	(48)
Pharyngeal aspiration									
5	0.25 [c]	Mouse C57BL/6	12 females	0.8-1.2	0.1-1	Unmodified; 17.7% Fe	1, 7 and 28 days	Increased levels of inflammatory markers (PMNs, total protein, TNFα) in BALF after 24 h. Also seen at 10 and 20 µg (dose-dependent).	(305)

Table 10. Effects after a single dose of SWCNTs.

Absolute dose (µg)	Dose (mg/kg bw)	Species/ strain	No. and sex of animals	Diameter (nm)	Length (µm)	Attributes	Observation period	Effects	Reference
10	0.3 [c]	Mouse C57BL/6	4-6 males	0.69 (mean)	-	Dispersed and well separated, or non-dispersed and highly agglomerated	1 h, 1 and 7 days and 1 month	Transient neutrophilic and inflammatory responses. No granulomatous lesions or epithelioid macrophages. Greater connective tissue thickness. Dispersed SWCNTs rapidly incorporated into the alveolar interstitium, where they enhanced collagen production.	(208)
10	0.36	Mouse C57BL/6J	3 males	0.8-1.2	0.1-1	Dispersed in Sur-vanta, agglomerates 0.38×1.42 µm	2 weeks	Increased level of collagen in the lungs. Lung fibrosis. The dispersant, Survanta, itself had no effects.	(346)
10	0.4	Mouse C57BL/6	4-10 males	0.7-1.5	1	-	7, 28 and 60 days	Damage to aortic mitochondrial DNA (reduction of amplification), along with alterations in the aortic mito-chondrial GSH and protein carbonyl levels at 7, 28 and 60 days. Also seen at 40 µg.	(184)
10	0.5 [c]	Mouse C57BL/6	12/6 groups females	1-4	-	0.23% Fe	1, 3, 7, 28 or 60 days	Increases in the levels of protein, LDH and GGT in BALF. Accumulation of 4-hydroxynonenal (oxidative biomarker) and depletion of GSH in the lungs. A com-bined robust, but acute inflammation, with early pro-gressive fibrosis and granulomatous inflammation in the lungs. Deterioration in pulmonary function. Also seen at 20 and 40 µg (dose-dependent).	(306)
10	0.5 [c]	Mouse C57BL/6	12 females	0.8-1.2	0.1-1	Unmodified; 17.7% Fe	1, 7 and 28 days	Increased levels of inflammatory markers (PMNs, total protein, TNFα, IL-6) in BALF after 24 h. Also seen at 20 µg (dose-dependent).	(305)
10	0.5 [c]	Mouse C57BL/6	6 females	1-4	1-3	Unmodified; with and without co-exposure to *Listeria* 3 days later	3-10 days	Increased number of inflammatory cells in BALF. Higher responses when co-exposed to *Listeria*.	(304)

Table 10. Effects after a single dose of SWCNTs.

Absolute dose (µg)	Dose (mg/kg bw)	Species/ strain	No. and sex of animals	Diameter (nm)	Length (µm)	Attributes	Observation period	Effects	Reference
20	0.99 [c]	Mouse C57BL/6	12/6 groups females	1-4	-	0.23% Fe	1, 3, 7, 28 or 60 days	Same as at 10 µg (dose-dependent).	(306)
20	1 [c]	Mouse C57BL/6	12 females	0.8-1.2	0.1-1	Unmodified; 17.7% Fe	1, 7 and 28 days	Same as at 10 µg (dose-dependent).	(305)
40	1.4	Mouse FVB/N-TgN (Hol-luc) Xen or C57BL/6	4-10 males	0.7-1.5	1	-	7, 28 and 60 days	Activation of HO-1 in the heart at day 7 (Hol-luc). Damaged mitochondrial DNA in cells of aorta at 7, 28 and 60 days (C57BL/6).	(184)
40	1.5	Mouse C57BL/6	5 males	0.8-1.2	0.1-1	8.8 wt% Fe	4 h	Alterations in pulmonary and systemic inflammatory parameters (more PMNs in BALF and blood).	(79)
40	1.9 [c]	Mouse C57BL/6	6-12 females	1-4	-	99.7% pure, with and without vitamin E-deficient diet	28 days	Body weight loss and general oxidative stress in vitamin E-deficient mice. Increased cleavage of SOD independent of diet. Acute inflammation (increase in total number of inflammatory cells, number of PMNs, released LDH, total protein content and levels of pro-inflammatory cytokines (TNFα and IL-6) and enhanced profibrotic responses (elevation of TGFβ and collagen deposition) in BALF, which was more pronounced in vitamin E-deficient animals. Granulomatous bronchointerstitial pneumonia. Fibrosis also worse in the vitamin E-deficient mice.	(307)

Table 10. Effects after a single dose of SWCNTs.

Absolute dose (µg)	Dose (mg/kg bw)	Species/ strain	No. and sex of animals	Diameter (nm)	Length (µm)	Attributes	Observation period	Effects	Reference
40	2 [d]	Mouse NADPH-oxidase-deficient or C57BL/6	Males	1-4	-	>99% pure, 0.23% Fe	28 days	NADPH-oxidase-deficient mice responded with a marked accumulation of PMNs and neutrophils, elevated levels of apoptotic cells, production of pro-inflammatory cytokines, decreased production of the anti-inflammatory and pro-fibrotic cytokine, TGFβ, and significantly lower levels of collagen deposition in the lungs as compared to C57BL/6 mice.	(308)
40	2.0 [c]	Mouse C57BL/6	12/6 groups females	1-4	-	0.23% Fe	1, 3, 7, 28 or 60 days	Same as at 10 and 20 µg (dose-dependent).	(306)
40	2.0 [c]	Mouse C57BL/6	6 females	1-4	1-3	Unmodified; with and without exposure to *Listeria* 3 days later	3-10 days	Increased number of inflammatory cells in BALF and collagen deposition. Sequential exposure to CNT/*Listeria* amplified lung inflammation and collagen formation. CNT-dependent suppression of bacterial clearance due to decreased phagocytosis of bacteria and subsequent increases in inflammatory cytokines in BALF.	(304)
Oropharyngeal aspiration									
10	0.3	Mouse CD1	5-10 females	-	-	Unfunctionalised	24 h	No effects on creatine kinase levels in the plasma. No cardiac myofibre degeneration.	(336)
10	0.3	Mouse CD1	5-10 females	22-138 (in suspension)	-	Acid functionalised	24 h	Same as above.	(336)
40	1.25	Mouse CD1	4 females	-	-	Pristine; highly agglomerated	72 h	Modest increases in total cell numbers and total protein level in BALF 18 h after exposure.	(295)

Table 10. Effects after a single dose of SWCNTs.

Absolute dose (µg)	Dose (mg/kg bw)	Species/ strain	No. and sex of animals	Diameter (nm)	Length (µm)	Attributes	Observation period	Effects	Reference
40	1.25	Mouse CD1	4 females	-	-	Acid functionalised; highly soluble, particle size <150 nm, zeta potential -40 to -60 mV	72 h	More pronounced elevations in total cell numbers, total protein level, PMNs, LDH activity, TNFα, IL-6 and MIP-2 levels in BALF 18 and 72 h after exposure.	(295)
40	1.3	Mouse CD1	5-10 females	-	-	Unfunctionalised	24 h	Increase in plasma levels of creatine kinase. No cardiac myofibre degeneration.	(336)
40	1.3	Mouse CD1	5-10 females	22-138 (in suspension)	-	Acid functionalised	24 h	Increase in plasma levels of creatine kinase. Cardiac myofibre degeneration and greater infarct size. Less recovery of cardiac function and higher coronary flow rate.	(336)
Intranasal instillation									
150	6.98	Mouse BALB/c	8 males	1.3	3.5	0.3% Ni, 0.3% Y, co-stimulation with methacholine	24 h	Enhanced methacholine-induced airway hyper-responsiveness. Elevated number of airway macro-phages.	(102)
Oral gavage									
	1 000	Mouse Swiss	10 males/ group	1.0	>1-2; 1-2; 0.02-0.08	25% Fe; <4% Fe; <1.5% Fe		No death and no pathological abnormalities detected. Lowest lethal dose > 1 000 mg/kg bw.	(165)

Table 10. Effects after a single dose of SWCNTs.

Absolute dose (µg)	Dose (mg/kg bw)	Species/ strain	No. and sex of animals	Diameter (nm)	Length (µm)	Attributes	Observation period	Effects	Reference
Retrobulbar injection (on gestation day 5.5)									
0.01		Mouse CD1	18 females	2.8	0.85	Pristine	10 days	No abortive or teratogenic effects.	(258)
0.01		Mouse CD1	18 females	1.6	0.76	Oxidised	10 days	Same as above.	(258)
0.01		Mouse CD1	20 females	1.8	0.37	Ultraoxidised	10 days	Same as above.	(258)
0.1		Mouse CD1	20 females	2.8	0.85	Pristine	10 days	No abortive effects. Malformed foetus found in 1 dam	(258)
0.1		Mouse CD1	18 females	1.6	0.76	Oxidised	10 days	No abortive effects. Malformed foetus found in 1 dam.	(258)
0.1		Mouse CD1	23 females	1.8	0.37	Ultraoxidised	10 days	No abortive effects. Malformed foetus found in 2 dams.	(258)
0.3		Mouse CD1	19 females	2.8	0.85	Pristine	10 days	No abortive effects. Malformed foetus found in 1 dam.	(258)
0.3		Mouse CD1	20 females	1.6	0.76	Oxidised	10 days	No abortive effects. Malformed foetus found in 1 dam.	(258)
0.3		Mouse CD1	16 females	1.8	0.37	Ultraoxidised	10 days	No abortive effects. Malformed foetus found in 3 dams.	(258)
3		Mouse CD1	22 females	2.8	0.85	Pristine	10 days	Miscarriage by 1 female. Malformed foetus found in 6 dams.	(258)
3		Mouse CD1	21 females	1.6	0.76	Oxidised	10 days	Miscarriage by 1 female. Malformed foetus found in 2 dams.	(258)

Table 10. Effects after a single dose of SWCNTs.

Absolute dose (µg)	Dose (mg/kg bw)	Species/ strain	No. and sex of animals	Diameter (nm)	Length (µm)	Attributes	Observation period	Effects	Reference
3		Mouse CD1	20 females	1.8	0.37	Ultraoxidised	10 days	No abortive effects. Malformed foetus found in 9 dams.	(258)
30		Mouse CD1	21 females	2.8	0.85	Pristine	10 days	Miscarriage by 4 females. Malformed foetus found in 1 dam.	(258)
30		Mouse CD1	20 females	1.6	0.76	Oxidised	10 days	Miscarriage by 4 females. Malformed foetus found in 4 dams.	(258)
30		Mouse CD1	16 females	1.8	0.37	Ultraoxidised	10 days	Miscarriage by 5 females. Malformed foetus found in 4 dams.	(258)
Subcutaneous implantation									
2 000	129	Mouse BALB/c	30 females	0.8-2.2	-	1-1.5 wt% Fe	12 weeks	No differences in body weight and no mortality. Increased number of CD4+ cells 2 weeks to 2 months post-implantation. Reduced number of CD8+ cells 1 week post-implantation. Granulomatous tissue after 3 weeks.	(168)
Intravenous injection									
20		Mouse nude	-	1-3	0.05-0.2	Chitosan functionalised	24 h	Rapid clearance from blood (half-time of 3-4 h). Rapid uptake and high levels of CNTs in the liver. Accumulation led to pathological changes in the liver, including damage to macrophages, cellular swelling, non-specific inflammation and blood coagulation. Similar uptake and behaviour of CNTs was found in the spleen and kidney, but with no obvious pathological changes in these organs.	(150)
25	-	Rat Wistar Kyoto	5	-	-	-	15 h	Accelerated rate of vascular thrombosis.	(270)

Table 10. Effects after a single dose of SWCNTs.

Absolute dose (µg)	Dose (mg/kg bw)	Species/ strain	No. and sex of animals	Diameter (nm)	Length (µm)	Attributes	Observation period	Effects	Reference
47 000	1 880	Mouse nude	3-4 both sexes	1-5	0.05-0.2	Oxidised, covalently functionalised	12 weeks	Brownish pigment believed to be nanotubes persisted in macrophages in the liver and spleen for 4 months, but no histological abnormalities were observed in these organs.	(298)
151 000	6 040	Mouse nude	3-4 both sexes	1-5	0.1-0.3	Non-covalently modified with PEG	12 weeks	Same as above.	(298)

[a] Calculated by the authors of this NEG document using data provided in the reference (weight of the rats 277-327 g).
[b] Calculated by the authors of this NEG document using data provided in the reference (weight of the mice 28-33 g).
[c] Calculated by the authors of this NEG document using data provided in the reference.
[d] Calculated by the authors of this NEG document, assuming the average weight of a mouse to be 20 g.

BAL(F): bronchoalveolar lavage (fluid), Fe: iron, GGT: γ-glutamyl transferase, GSH: glutathione, HO: haeme oxygenase, IL: interleukin, LDH: lactate dehydrogenase, LPS: lipopolysaccharide, MIP: macrophage inflammatory protein, NADPH: nicotinamide adenine dinucleotide phosphate, NEG: Nordic Expert Group, Ni: nickel, PBS: phosphate buffered saline, PEG: polyethylene glycol, PMN: polymorphonuclear leukocyte, SOD: superoxide dismutase, TGFβ: transforming growth factor beta, TNFα: tumour necrosis factor alpha, Y: yttrium.

Table 11. Effects after repeated doses of SWCNTs.

Absolute dose per occasion/ total (μg)	Total dose (mg/kg bw)	Exposure duration	Species/ Strain	No. and sex of animals	Diameter (nm)	Length (μm)	Attributes	Observation period	Effects	Reference
Intratracheal instillation										
	2	2 times 2 weeks apart	Rat Wistar Kyoto	8 both sexes	1.2-1.6	2-5	-	Up to 4 weeks post-exposure	Reduced number of baroreflex sequences 2 and 4 weeks post-exposure; effect on the autonomic cardiovascular control regulation.	(178)
50/300	9.7 [a]	Once a week for 6 weeks	Mouse ICR	8 males	0.8-1.2; 1.2-2	0.1-1; 1-15	<35% Fe; or 75% CNT, and amorphous carbon. With and without co-stimulation by OVA	24 h post-exposure	SWCNTs aggravated allergen-induced pulmonary inflammation with mucus hyperplasia. SWCNTs together with allergen amplified lung protein levels of Th cytokines and chemokines related to allergy and exhibited adjuvant activity for allergen-specific IgG1 (and IgE). SWCNTs accentuated the level/activity of biomarkers of oxidative stress in the airways in the presence of allergen.	(135)
Pharyngeal aspiration										
20/80		4 times over 8 weeks	Mouse ApoE-/-	4-10 males	0.7-1.5	1	-		Enhanced atherosclerosis. Plaque formation in the aorta, damages to aortic mitochondrial DNA. Alterations in the levels of aortic mitochondrial GSH and protein carbonyl groups.	(184)
40/240		Twice a week for 3 weeks	Mouse C57BL/6	6/group females	0.4-1.2	0.5-2	HiPCO, 0.23% wt Fe	24 h post-exposure	Higher numbers of PMNs and alveolar macrophages in BALF. Multifocal granulomas (containing CNT agglomerates and fibrotic tissue) in the vicinity of bronchioles and adjacent alveoli. Proteomic analysis of pulmonary tissue revealed the presence of markers of inflammation.	(329)

Table 11. Effects after repeated doses of SWCNTs.

Absolute dose per occasion/ total (µg)	Total dose (mg/kg bw)	Exposure duration	Species/ Strain	No. and sex of animals	Diameter (nm)	Length (µm)	Attributes	Observation period	Effects	Reference
Dermal application										
40/200	12 [a]	Once daily for 5 days	Mouse SKH-1 hairless	3	-	-	30% Fe	24 h post-exposure	No effects on the level of oxidative stress or on the epidermis.	(231)
80/400	24 [a]	Once daily for 5 days	Mouse SKH-1 hairless	3	-	-	30% Fe	24 h post-exposure	Oxidative stress, with a 34% increase in protein carbonyls in the skin. 25% more cells in the epi-dermis.	(231)
160/800	47 [a]	Once daily for 5 days	Mouse SKH-1 hairless	3	-	-	30% Fe	24 h post-exposure	Oxidative stress, with a 41% increase in protein carbonyls, an 11% reduction in the level of GSH and a 21% elevation in MPO activity in the skin. 58% more cells in epidermis, and skin thickening due to accumulation of PMNs and mast cells. 12% more collagen and enhanced cytokine production in the skin. Release of IL-10 and IL-6 in the skin.	(231)
Intranasal instillation										
133/400		Once daily for 3 days	Mouse BALB/ cAnNCrl	10 females	1.4-10.9	0.5-100	Aggregated particle; 50% graphitic mtrl, 25% SWCNT, 25% MWCNT. With/without co-stimulation with OVA	26 days	With co-stimulation: Larger amounts of OVA-IgE in blood; higher numbers of inflammatory cells including eosinophils, and cytokine levels in BALF. Secretion of Th2-associated cytokines in the mediastinal lymph node.	(241)

Table 11. Effects after repeated doses of SWCNTs.

Absolute dose per occasion/ total (µg)	Total dose (mg/kg bw)	Exposure duration	Species/ Strain	No. and sex of animals	Diameter (nm)	Length (µm)	Attributes	Observation period	Effects	Reference
Oral administration										
105/1 050 -10 500/ 105 000 [a]	50-5 000	Once daily for 10 days	Mouse Kunming	20 males	0.8-1.2	0.05-0.3	Ultrashort	1 day post-exposure	Dose-dependent uptake in lysosomes in neurons of the brain and enterocytes of the ileum. No effect on blood parameters.	(373)
Intraperitoneal injection										
7.5/38 [a]	1.25	Once daily for 5 days	Mouse Swiss Webster	5 males	15-30	15-20	-COOH functionalised	24 h post-exposure	ROS production in liver. Hepatocyte disruption and vacuolation.	(250)
15/75 [a]	2.5	Once daily for 5 days	Mouse Swiss Webster	5 males	15-30	15-20	-COOH functionalised	24 h post-exposure	ROS production in liver. Hepatocyte disruption and vacuolation. Elevated levels of lipid hydro-peroxides, condensed nuclei, partial disruption of the central vein in the liver.	(250)
23/113 [a]	3.75	Once daily for 5 days	Mouse Swiss Webster	5 males	15-30	15-20	-COOH functionalised	24 h post-exposure	ROS production in liver. Significant histopatho-logical alterations including hepatocyte disruption and vacuolation. Elevated levels of lipid hydro-peroxides, condensed nuclei, partial disruption of the central vein in the liver. Increased blood levels of ALT and ALP.	(250)

[a] Calculated by the authors of this NEG document using data provided in the reference.

ALP: alkaline phosphatase, ALT: alanine aminotransferase, BALF: bronchoalveolar lavage fluid, Fe: iron, GSH: glutathione, HiPCO: high-pressure carbon monoxide, Ig: immunoglobulin, IL: interleukin, MPO: myeloperoxidase, NEG: Nordic Expert Group, OVA: ovalbumin, PMN: polymorphonuclear leukocyte, ROS: reactive oxygen species, Th: T helper.

Table 12. Effects after a single dose of MWCNTs.

Absolute dose (µg)	Dose (mg/kg bw)	Species/ strain	No. and sex of animals	Diameter (nm)	Length (µm)	Attributes	Observation period	Effects	Reference
Intratracheal instillation									
1	0.005 [a]	Rat Sprague Dawley	6 males	20-50	0.5-2	Dispersed in BSA, 80% of agglo-merates < 10 µm	1, 7, 30 and 90 and 180 days	No change in inflammatory cells and markers in BALF and no histopathological changes at any time-points.	(74)
11-13 [b]	0.04	Rat Crl:CD	5 males/ group	60	1.5 (median)	Mitsui MWNT-7	3 days, 1 week, 1, 3 and 6 months	No change in inflammatory cells and markers in BALF and no histopathological changes at any time-points.	(163)
10	0.05 [a]	Rat Sprague Dawley	6 males	20-50	0.5-2	Dispersed in BSA, 80% of agglo-merates <10 µm	1, 7, 30 and 90 and 180 days	No change in inflammatory cells and markers in BALF at any time-points. Evidence of apoptosis of alveolar macrophages after 30 and 90 days and induction of caspase activity after 90 days.	(74)
40	0.16	Rat Fisher 344	8 males	88	5	Mitsui, MWNT-7	1, 7, 28 and 91 days post-exposure	Slight fibrosis of the alveolar walls observed after 91 days, without associated microgranuloma. Little CNT deposition in the lungs compared to the higher dose of 0.64 mg/kg bw. Dose-dependent increases in the levels of total protein, albumin, LDH and ALP activities in BALF after 1 day that had declined, but remained elevated after 91 days. Multi-nucleated macrophages.	(1)
40-45 [c]	0.2	Rat Wistar albino	6 males	90-150	-	Arc discharge	Up to 3 months	Elevated level of LDH in BALF after 24 h that re-turned to normal after 3 months. Increased level of ALP in BALF after 1 week. More extensive lipid peroxidation.	(276)
40-45 [c]	0.2	Rat Wistar albino	6 males	60-80	-	CVD	Up to 3 months	Same as above.	(276)

Table 12. Effects after a single dose of MWCNTs.

Absolute dose (µg)	Dose (mg/kg bw)	Species/ strain	No. and sex of animals	Diameter (nm)	Length (µm)	Attributes	Observation period	Effects	Reference
40-45 [c]	0.2	Rat Wistar albino	6 males	60-80	-	Well dispersed. Hexa-gonal crystallinity	3 months	No significant effects on the histopathology of the liver, heart or kidney or on serum parameters.	(275)
40-45 [c]	0.2	Rat Wistar albino	6 males	90-150	-	Well dispersed. Cubic crystallinity	3 months	Same as above.	(275)
58-67 [b]	0.2	Rat Crl:CD	5 males/ group	60	1.5 (median)	Mitsui MWNT-7	3 days, 1 week, 1, 3 and 6 months	More neutrophils in BALF only at 3 days post-exposure. Slight accumulation of macrophages in the alveoli.	(163)
100	0.55 [a]	Rat Sprague Dawley	6 males	20-50	0.5-2	Dispersed in BSA, 80% of agglo-merates < 10 µm	1, 7, 30 and 90 and 180 days	No change in inflammatory cells and markers in BALF at any-time-points. Evidence of apoptosis of alveolar macrophages and induction of caspase activity after 30, 90 and 180 days.	(74)
160	0.64	Rat Fisher 344	8 males	88	5	Mitsui, MWNT-7	91 days	CNTs present in the bronchiolar and alveolar spaces. CNT deposition increased by day 28 and only slightly lower after 91 days. Multifocal microgranulomas, which increased over time. Certain microgranulomas associated with fibrosis indicated by thickening of alveolar walls. More inflammatory cells in BALF at day 1. Dose-dependent increases in the levels of total protein, albumin, LDH and ALP activities in BALF after 1 day that had declined, but remained elevated after 91 days. Multi-nucleated macrophages.	(1)

Table 12. Effects after a single dose of MWCNTs.

Absolute dose (µg)	Dose (mg/kg bw)	Species/ strain	No. and sex of animals	Diameter (nm)	Length (µm)	Attributes	Observation period	Effects	Reference
200	0.66	Rat Wistar	10 males	48	0.94	-	3 days up to 6 months	Dose-dependent transient increase in total cell count including neutrophils in BALF after 3 days. ALP also elevated after 3 days and 3 months, levels of CINC-1 increased after 3 days and higher MPO activity after 3 days, 1 and 3 months in BALF. Histopathology revealed only slight transient inflammation with no granuloma formation.	(216)
200-225 [c]	1	Rat Wistar albino	6 males	90-150	-	Arc discharge	Up to 3 months	Increased level of protein, LDH and ALP in BALF after 24 h, still elevated after 3 months. More products of lipid peroxidation. Dose-dependent multifocal granulomas appeared after 1 month. Dose-dependent formation of lymphoid aggregates surrounding bronchioles and of alveolar damage.	(276)
200-225 [c]	1	Rat Wistar albino	6 males	60-80	-	CVD	Up to 3 months	Same as above.	(276)
	1	Mouse CD1	10 males	20-40	100-300	Nitrogen-doped, 2-2.5% Fe, acid-treated	Up to 30 days	No mortality. No deposition of CNTs in the lungs or lymph nodes.	(35)
	1	Mouse CD1	10 males	50	Up to 450	Undoped, 2-2.5% Fe, acid-treated	Up to 30 days	30% of the mice died immediately from dyspnoea. After 2 weeks multiple granulomas in interstitium, hyperplasia of goblet cells.	(35)
200-225 [c]	1	Rat Wistar albino	6 males	60-80	-	Well dispersed. Hexagonal crystallinity	3 months	Increased serum level of ALT and creatinine. No MWCNTs observed in the liver despite effects. No cardiac effects.	(275)

Table 12. Effects after a single dose of MWCNTs.

Absolute dose (µg)	Dose (mg/kg bw)	Species/ strain	No. and sex of animals	Diameter (nm)	Length (µm)	Attributes	Observation period	Effects	Reference
200-225 [c]	1	Rat Wistar albino	6 males	90-150	-	Well dispersed. Cubic crystallinity	3 months	Same as above.	(275)
	1	Rat Vister	Males	40-60	0.5-500	Unmodified	Up to 3 months	Mild lung inflammation.	(190)
288-336 [b]	1	Rat Crl:CD	5 males/ group	60	1.5 (median)	Mitsui MWNT-7	3 days, 1 week, 1, 3 and 6 months	Elevated number of total cells, eosinophils and neutrophils only at 3 days post-exposure in BALF. Elevated levels of LDH and total protein in BALF, which returned to normal after 1 week. Partially granulomatous accumulation of macrophages in the alveoli and interstitium. Hypertrophy of the bronchial epithelium and infiltration by inflammatory cells.	(163)
50	1.7 [d]	Mouse Kunming	5 females/ group	50	10	95% pure, not well-dispersed	8, 16 and 24 days	Agglomerates of CNTs present in the bronchi 8 and 16 days later, but visible inflammation appeared only after 24 days. Injury and destruction to alveoli became more severe between 8 and 24 days post-instillation.	(181)
500	2-2.5 [e]	Rat Sprague Dawley	4-6 females	9.7	5.9	Pristine (non-ground)	Up to 60 days	Slower clearance from the lungs than ground CNTs at same dose. No significant increase of LDH in BALF. No increase of TNFα in BALF after 3 or 60 days. No fibrotic response in lungs after 60 days.	(222)
500	2-2.5 [e]	Rat Sprague Dawley	4-6 females	11.3	0.7	Ground CNTs	Up to 60 days	Dose-dependent increase of LDH in BALF. Significant increase of TNFα in BALF after 3 days that was even higher after 60 days. Fibrotic response in lungs after 60 days, as indicated by elevated levels of collagen.	(222)

Table 12. Effects after a single dose of MWCNTs.

Absolute dose (µg)	Dose (mg/kg bw)	Species/ strain	No. and sex of animals	Diameter (nm)	Length (µm)	Attributes	Observation period	Effects	Reference
	2.5	Mouse CD1	10 males	20-40	100-300	Nitrogen-doped, 2-2.5% Fe, acid-treated	Up to 30 days	No mortality. Deposition of CNTs in the lungs, but not in lymph nodes. Aggregates of CNTs adhering to bronchiolar epithelium without apparent damage or inflammation. After 1 month minor mononuclear cell granuloma.	(35)
	2.5	Mouse CD1	10 males	50	Up to 450	Undoped, 2-2.5% Fe, acid-treated	Up to 30 days	60% of the mice died immediately from dyspnoea. After 24 h aggregates of CNTs damaging the bronchiolar epithelium. At 48 h partial loss of lining epithelium, hyperplasia and hyperchromatism. Mononuclear inflammation of the lumen and interstitium of bronchioles. Multiple granulomas in the interstitium.	(35)
	3	Rat Vister	Males	40-60	0.5-500	Unmodified	Up to 3 months	Severe lung inflammation, CNTs remaining after 3 months. Also seen at 5 and 7 mg/kg bw (dose-dependent).	(190)
1 000	3.3	Rat Wistar	10 males	48	0.94	-	3 days up to 6 months	Dose-dependent transient increase in total cell count including neutrophils in BALF after 3 days. Neutrophil count remained elevated after 1 month. ALP activity in BALF increased after 1 week and 3 months, level of CINC-1 increased after 3 days up to 3 months and MPO activity elevated after 3 days, 1 week and 1 month in BALF. Histopathology showed infiltration of inflammatory cells into the alveolar space throughout the entire period of observation. Small granulomas and transient deposition of collagen.	(216)

Table 12. Effects after a single dose of MWCNTs.

Absolute dose (µg)	Dose (mg/kg bw)	Species/ strain	No. and sex of animals	Diameter (nm)	Length (µm)	Attributes	Observation period	Effects	Reference
	4	Mouse ICR	8 males	2-20	0.1-several µm	Unmodified, 75% pure. With and without co-exposure to 33 µg/kg LPS	24 h	Co-exposure to LPS led to aggravated lung inflammation (more neutrophils in BALF and higher levels of proinflammatory cytokines).	(134)
-	5	Rat Vister	Males	40-60	0.5-500	Unmodified	Up to 3 months	Severe lung inflammation, CNTs remaining after 3 months (dose-dependent).	(190)
1 000-1 125 [c]	5	Rat Wistar albino	6 males	90-150	-	Arc discharge	Up to 3 months	Increased levels of protein, LDH and ALP in BALF after 24 h, gradually decreasing, but still elevated after 3 months. Increase in lipid peroxidation products. Multifocal granulomas.	(276)
1 000-1 125 [c]	5	Rat Wistar albino	6 males	60-80	-	CVD	Up to 3 months	Same as above.	(276)
1 000-1 125 [c]	5	Rat Wistar albino	6 males	60-80	-	Well dispersed. Hexagonal crystallinity	3 months	Increased serum level of ALT and creatinine. Degeneration of hepatocytes. No MWCNTs detected in the liver despite effects. Tubular necrosis in the kidney. No cardiac effects.	(275)
1 000-1 125 [c]	5	Rat Wistar albino	6 males	90-150	-	Well dispersed. Cubic crystallinity	3 months	Same as above.	(275)
	5	Mouse ICR	10-12 males	110-170	5-9	Dispersed by sonication	14 days	Increased levels of cytokines including TNFα, IL-6 and IL-12 in BALF after 1 day with subsequent decrease with time. Elevated total number of cells in BALF. Rise in blood levels of IL-10 and IL-12. Lung lesions seen after 1 day, but not at later time-points.	(249)

Table 12. Effects after a single dose of MWCNTs.

Absolute dose (µg)	Dose (mg/kg bw)	Species/ strain	No. and sex of animals	Diameter (nm)	Length (µm)	Attributes	Observation period	Effects	Reference
	5	Mouse CD1	10 males	20-40	100-300	Nitrogen-doped, 2-2.5% Fe, acid-treated	Up to 30 days	After 48-72 h severe damage to bronchiolar walls. Granulomatous reaction involving macrophages, lymphocytes, fibroblasts and collagen deposition. Hyperplasic lymph nodes without CNT deposition. Between days 7 and 30 fibrosis in the peribronchiolar interstitium.	(35)
	5	Mouse CD1	10 males	50	Up to 450	Undoped, 2-2.5% Fe, acid-treated	Up to 30 days	90% of the mice died immediately from dyspnoea. Aggregated CNTs lined the epithelium of bronchioles, causing walls to rupture.	(35)
	6.67	Mouse Kunming	6 males	40-60	5-15	Bended and agglo-merated. 95% pure, 1.25% Ni. With and without 2.67 mg/kg benzene	7 days	MWCNTs caused more injury on their own than benzene alone. Total protein and LDH in BALF in-creased by MWCNTs or MWCNTs+benzene. ALP and ACP in BALF increased after co-exposure. More severe lesions of the lungs induced by co-exposure, aggregates observed on inner wall of bronchi.	(182)
-	7	Rat Vister	Males	40-60	0.5-500	Unmodified	Up to 3 months	Severe inflammation, CNTs remaining after 3 months (dose-dependent).	(190)
2 000	8-10 [e]	Rat Sprague Dawley	4-6 females	9.7	5.9	Pristine (non-ground)	Up to 60 days	After 3 days, significant increase of LDH in BALF. No significant increase of total protein in BALF. Transient elevation of TNFα in BALF after 3 days. Dose-dependent fibrotic response (hydroxyproline and collagen) after 60 days. Collagen-rich granulomas partially blocking the bronchial lumen.	(222)

Table 12. Effects after a single dose of MWCNTs.

Absolute dose (µg)	Dose (mg/kg bw)	Species/ strain	No. and sex of animals	Diameter (nm)	Length (µm)	Attributes	Observation period	Effects	Reference
2 000	8-10 [e]	Rat Sprague Dawley	4-6 females	11.3	0.7	Ground	Up to 60 days	After 3 days, significant increase of LDH in BALF. Higher protein levels in BALF than non-ground CNTs at same dose. Transient elevation of TNFα in BALF after 3 days, but lower than for non-ground CNTs. Dose-dependent fibrotic response (collagen) after 60 days. Collagen-rich granulomas in the interstitium.	(222)
2 000	8-10 [e]	Rat Wistar	5 females			Ground	3 and 60 days	Increased levels of LDH, neutrophils, macrophages, IL-1β, TNFα and total protein in BALF after 3 days. Elevated level of hydroxyproline in the lungs after 60 days, indicative of fibrosis.	(221)
2 000	8-10 [e]	Rat Wistar	5 females			Ground then heated to 600 °C	3 and 60 days	Increased levels of LDH and total protein in BALF after 3 days. Elevated level of hydroxyproline in the lungs after 60 days, indicative of fibrosis.	(221)
2 000	8-10 [e]	Rat Wistar	5 females			Ground then heated to 2 400 °C	3 and 60 days	Elevated levels of hydroxyproline in the lungs after 60 days, indicative of fibrosis.	(221)
2 000	8-10 [e]	Rat Wistar	5 females			Heated to 2 400 °C and then ground	3 and 60 days	Highest levels of LDH, neutrophils, macrophages and total protein in BALF after 3 days. Elevated level of hydroxyproline in the lungs after 60 days, indicative of fibrosis.	(221)
	20	Mouse ICR	10-12 males	110-170	5-9	Dispersed by sonication	14 days	Enhanced levels of cytokines including IL-1, IL-6, IL-12 and TNFα in BALF, which declined with time. Increase in total number of cells in BALF. Elevated blood levels of IL-10 and IL-12. Pulmonary lesions after 1 day, but not later.	(249)

Table 12. Effects after a single dose of MWCNTs.

Absolute dose (µg)	Dose (mg/kg bw)	Species/ strain	No. and sex of animals	Diameter (nm)	Length (µm)	Attributes	Observation period	Effects	Reference
5 000	20-25 [e]	Rat Sprague Dawley	4-6 females	9.7	5.9	Pristine (non-ground)	Up to 60 days	No mediators in BALF measured. Dose-dependent fibrotic response (hydroxyproline and collagen) after 60 days.	(222)
5 000	20-25 [e]	Rat Sprague Dawley	4-6 females	11.3	0.7	Ground CNTs	Up to 60 days	No mediators in BALF measured. Dose-dependent fibrotic response (hydroxyproline and collagen) after 60 days, but less than with pristine CNTs.	(222)
5 000	27	Rat Crl:CD	Females	100	27%> 5 µm	Non-ground	91 days	Elevated levels of LDH and total protein in BALF after 8, 29 and 91 days. CNTs observed in the bronchial area. Macrophages in the interstitium and in bronchiolar lymph nodes.	(339)
5 000	27	Rat Crl:CD	Females	-	Shorter less agglo-merated	Mechanically ground	91 days	Higher number of total cells and neutrophils in BALF after 8 days, elevated levels of LDH and total proteins in BALF after 8, 29 and 91 days. CNTs observed in alveolar region. Macrophages in the alveolus and bronchiolar lymph nodes.	(339)
	50	Mouse ICR	10-12 males	110-170	5-9	Dispersed by sonication	14 days	Increased levels of cytokines including IL-1, IL-6, IL-12 and TNFα in BALF, which declined with time. Increase in total number of cells in BALF. Elevated blood levels of IL-1, IL-6, IL-10 and IL-12. Lung lesions at 1, 3, 7 and 14 days.	(249)
12 500	55.6	Guinea pig	4-5 males	-	-	ShowaDenko, dispersed in 1% Tween-80	3 months	Increased level of IL-8 in the BALF. More severe pulmonary lesions than the other CNTs used in this same study. Lesions located in the central posterior and anterior lobes.	(95)

Table 12. Effects after a single dose of MWCNTs.

Absolute dose (µg)	Dose (mg/kg bw)	Species/ strain	No. and sex of animals	Diameter (nm)	Length (µm)	Attributes	Observation period	Effects	Reference
12 500	55.6	Guinea pig	4-5 males	-	-	NanoLabs, 95% pure, dispersed in 1% Tween-80	3 months	Increased levels of macrophages, lymphocytes and neutrophils in the BALF. Lesions in the posterior lung lobe.	(95)
12 500	55.6	Guinea pig	4-5 males	-	-	NanoLabs, 80% pure, dispersed in 1% Tween-80	3 months	Similar to the 95% pure NanoLab preparation. Increased levels of macrophages and eosinophils, but not of lymphocytes or neutrophils in BALF. Lesions in the posterior lung lobe.	(95)
12 500	55.6	Guinea pig	4-5 males	-	-	Pyrograf, dispersed in 1% Tween-80	3 months	Carbon structures observed in cells recovered from the BALF. Peripheral lesions in the posterior lung lobe.	(95)
25 000	100	Guinea pig	Males	-	-	CNT-containing soot	4 weeks	No effects on tidal volume, frequency of breathing or pulmonary resistance. No change in cellular or protein content of BALF.	(124)
15 000	-	Guinea pig	5-10	-	-	CVD-MWCNT, dispersed in SDS	90 days	Pneumonitis. Infiltration of inflammatory cells into the lungs, emphysema and alveolar exudation.	(123)
15 000	-	Guinea pig	5-10	-	-	Carbon arc MWCNT, dispersed in SDS	90 days	Pneumonitis. Elevated lung resistance. Infiltration of inflammatory cells into the lungs, emphysema and alveolar exudation.	(123)
15 000	-	Guinea pig	5-10	-	-	Nanolab, 80% purity, dispersed in SDS	90 days	Pneumonitis. Infiltration of inflammatory cells into the lungs, emphysema and alveolar exudation.	(123)
15 000	-	Guinea pig	5-10	-	-	Nanolab, 95% purity, dispersed in SDS	90 days	Pneumonitis. Infiltration of inflammatory cells into the lungs, emphysema and alveolar exudation.	(123)
15 000	-	Guinea pig	5-10	-	-	Pyrograf (PR-1), dispersed in SDS	90 days	Pneumonitis.	(123)
15 000	-	Guinea pig	5-10	-	-	Showa Denko, dispersed in SDS	90 days	Pneumonitis. Infiltration inflammatory cells into lungs, emphysema and alveolar exudation.	(123)

Table 12. Effects after a single dose of MWCNTs.

Absolute dose (µg)	Dose (mg/kg bw)	Species/ strain	No. and sex of animals	Diameter (nm)	Length (µm)	Attributes	Observation period	Effects	Reference
Pharyngeal aspiration									
10	0.47 [f]	Mouse C57BL/6	4 males	49	3.9 (median)	Mitsui MWNT-7, 0.41% Na, 0.32% Fe	1, 7, 28 and 56 days	Increased levels of PMNs in BALF after 1 day that declined by day 7. Inflammation of pleura in one mouse. Pulmonary fibrosis after 7 days that had progressed slightly after 28 days. Histopathology not performed after day 56.	(265)
10	0.47 [f]	Mouse C57BL/6J	6-8 males	49	3.9 (median)	Mitsui MWNT-7, 0.41% Na, 0.32% Fe	1, 7, 28 and 56 days	No detectable sub- or intrapleural penetration by CNTs after 56 days.	(207)
10	0.47 [f]	Mouse C57BL/6J	8 males	49	3.9 (median)	Mitsui MWNT-7, 0.41% Na, 0.32% Fe	1, 7, 28 and 56 days	Enhanced thickness (0.14 µm) of connective tissue in alveolar septa after 56 days (dose-dependent).	(206)
20	0.77	Mouse C57BL	6 females	20-30	50	Acid purified. With and without co-exposure to 0.5 ppm ozone for 3 h.	24 h	Little effect of ozone alone, while CNTs led to more cells and protein in BALF. In co-exposed animals, elevated levels of TNFα and IL-1β in BALF. Elevated levels of mucin in BALF.	(104)
20	0.9 [f]	Mouse C57BL/6	4 males	49	3.9 (median)	Mitsui MWNT-7, 0.41% Na, 0.32% Fe	1, 7, 28 and 56 days	More PMNs in BALF after 1 day, even more after 7 days, lower but still elevated after 56 days. Granulomatous inflammation in interstitium and alveolar space. Mucous metaplasia. Pulmonary fibrosis already after 7 days that progressed slightly thereafter.	(265)
20	0.9 [f]	Mouse C57BL/6J	6-8 males	49	3.9 (median)	Mitsui MWNT-7, 0.41% Na, 0.32% Fe	1, 7, 28 and 56 days	Dose-dependent sub- or intrapleural penetrations by CNTs. Granulomatous lesions after 56 days.	(207)
20	0.9 [f]	Mouse C57BL/6J	8 males	49	3.9 (median)	Mitsui MWNT-7, 0.41% Na, 0.32% Fe	1, 7, 28 and 56 days	Enhanced thickness (0.14 µm) of connective tissue in alveolar septa after 56 days (dose-dependent).	(206)

Table 12. Effects after a single dose of MWCNTs.

Absolute dose (µg)	Dose (mg/kg bw)	Species/ strain	No. and sex of animals	Diameter (nm)	Length (µm)	Attributes	Observation period	Effects	Reference
25	1-1.25 [g]	Mouse C57BL/6	-	26	1-2	Short, nanostructured and amorphous materials	1 and 6 weeks	No changed levels of granulocytes, LDH or total protein in BALF after 1 or 6 weeks. No lesions on the parietal pleura.	(224)
25	1-1.25 [g]	Mouse C57BL/6	-	15	1-5	NanoLab, tangled	1 and 6 weeks	Same as above and small, localised granuloma.	(224)
25	1-1.25 [g]	Mouse C57BL/6	-	165	36 (mean)	University of Manchester	1 and 6 weeks	Increased levels of granulocytes and LDH in BALF 1, but not 6 weeks after exposure. Extensive interstitial thickening. Collagen deposition and lymphocyte infiltrates in the interstitium. Increased levels of total protein after 1 week and of granulocytes after 1 and 6 weeks in lavage from the pleura. Lesions of cellular aggregates comprised of leukocytes and collagen deposition at the parietal pleura after 6 weeks.	(224)
40	1.5	Mouse C57BL/6	5 males	80	10-20	0.2% wt Fe	4 h	More PMNs and increased level of LDH in BALF. Higher levels of mRNA encoding proteins involved in inflammation, coagulation and oxidative stress in BALF. Systemic effects, i.e., elevated levels of inflammatory biomarkers and gene expression in blood and enhanced gene expression in heart, liver and kidney.	(79)
40	1.9 [f]	Mouse C57BL/6	4 males	49	3.9 (median)	Mitsui MWNT-7, 0.41% Na, 0.32% Fe	1, 7, 28 and 56 days	More PMNs in BALF after 1 day, even more after 7 days, less but still elevated after 56 days. Pulmonary fibrosis already after 7 days, that progressed slightly until day 28. Histopathology not performed on day 56.	(265)

Table 12. Effects after a single dose of MWCNTs.

Absolute dose (µg)	Dose (mg/kg bw)	Species/ strain	No. and sex of animals	Diameter (nm)	Length (µm)	Attributes	Observation period	Effects	Reference
40	1.9 [f]	Mouse C57BL/6J	6-8 males	49	3.9 (median)	Mitsui MWNT-7, 0.41% Na, 0.32% Fe	1, 7, 28 and 56 days	Dose-dependent sub- or intrapleural penetrations by CNTs. No data concerning possible granulomatous lesions after 56 days.	(207)
40	1.9 [f]	Mouse C57BL/6J	8 males	49	3.9 (median)	Mitsui MWNT-7, 0.41% Na, 0.32% Fe	1, 7, 28 and 56 days	Enhanced thickness (0.16 µm) of connective tissue in alveolar septa after 56 days (dose-dependent).	(206)
80	3.7 [f]	Mouse C57BL/6	4 males	49	3.9 (median)	Mitsui MWNT-7, 0.41% Na, 0.32% Fe	1, 7, 28 and 56 days	Pulmonary inflammation. Diffuse fibrosis of alveolar septa, granulomatous pneumonia. Pulmonary fibrosis already after 7 days with progression until day 28 and stable thereafter. Hypertrophy and hyperplasia of bronchoalveolar epithelium. Inflammation in the interstitium and alveolar space. Dilated subpleural lymphatic vessels. CNTs in pleura.	(265)
80	3.7 [f]	Mouse C57BL/6J	6-8 males	49	3.9 (median)	Mitsui MWNT-7, 0.41% Na, 0.32% Fe	1, 7, 28 and 56 days	Dose-dependent sub- or intrapleural penetrations by CNTs. No data concerning possible granulomatous lesions after 56 days.	(207)
80	3.7 [f]	Mouse C57BL/6J	8 males	49	3.9 (median)	Mitsui MWNT-7, 0.41% Na, 0.32% Fe	1, 7, 28 and 56 days	Progressive increase in thickness of connective tissue in alveolar septa (0.12, 0.12, 0.14 and 0.19 µm after 1, 7, 28 and 56 days, respectively). Of the total lung burden of MWCNTs 56 days post-exposure, 68% within macrophages, 20% within granulomas in the alveolar space, 8% in the alveolar interstitium and 1.6% in subpleural tissue.	(206)

Table 12. Effects after a single dose of MWCNTs.

Absolute dose (µg)	Dose (mg/kg bw)	Species/ strain	No. and sex of animals	Diameter (nm)	Length (µm)	Attributes	Observation period	Effects	Reference
Oropharyngeal aspiration									
	1	Mouse C57BL/6	6-8 males	12.5, 25	Several µm	5% wt Fe	30 days	More neutrophils and epithelial cells in BALF. No change in level of collagen in pulmonary tissue. Elevated level of Mmp13 mRNA and activity. More IL-33 mRNA and protein (more than the higher doses).	(348)
	2	Mouse C57BL/6	6-8 males	12.5, 25	Several µm	5% wt Fe	30 days	More neutrophils and epithelial cells in BALF. No change in level of collagen in pulmonary tissue. Elevated level of Mmp13 mRNA and activity. More IL-33 mRNA and protein (higher than the highest dose).	(348)
	4	Mouse C57BL/6	6-8 males	12.5, 25	Several µm	5% wt Fe	30 days	More cells, including neutrophils, epithelial cells and macrophages, in BALF. Increased level of collagen in lung tissue. Elevated level of Mmp13 mRNA and activity. Higher levels of IL-33 mRNA and protein (although less than with the lower doses). Histopathology revealed collagen rich granulomas containing agglomerates of MWCNTs.	(348)
Intrapleural injection									
5		Mouse C57BL/6	4-5/time-point, females	20-100	Maximum 56, 84%>15, 77%>20	-	24 h, 7 days, 4, 12 and 24 weeks	Acute inflammation. More granulocytes in pleural lavage after 1 and 7 days, reduced after 4 weeks, but still much higher than controls after 24 weeks. Progressive fibrosis of the parietal pleura.	(223)
5		Mouse C57BL/6	4-5/time-point, females	40-50	Average 13, 24%>15, 11.5%>20	Mitsui	24 h, 7 days, 4, 12 and 24 weeks	Acute inflammation. More granulocytes in pleural lavage. Progressive fibrosis of the parietal pleura.	(223)

Table 12. Effects after a single dose of MWCNTs.

Absolute dose (µg)	Dose (mg/kg bw)	Species/ strain	No. and sex of animals	Diameter (nm)	Length (µm)	Attributes	Observation period	Effects	Reference
5		Mouse C57BL/6	4-5/time-point, females	20-30	0.5-2		24 h, 7 days, 4, 12 and 24 weeks	No acute inflammation. No fibrosis of the parietal pleura.	(223)
Intranasal instillation									
	1.5	Mouse Swiss	8 males	1.2-3.2	1-10	DWCNTs, forming bundles 100 µm in length	48 h	Fewer free radicals after 24-48 h due to scavenging properties of CNTs. More inflammatory cytokines in blood. Increased number of pulmonary macrophages and thickened alveolar wall.	(52)
150	6.52	Mouse BALB/c	8 males	11	1.05	With and without co-stimulation by methacholine	24 h	No effect of MWCNTs on methacholine-induced airway hyper-responsiveness. No change in the number of airway macrophages.	(102)
Oral gavage									
-	5 000	Rat	-	10-15	0.2-1.0	Baytubes, 0.53% Co	-	Oral LD_{50} > 5 000 mg/kg bw.	(254)
Dermal application									
500	-	Rabbit New Zeeland white	3 females	110-170	5-9	901 nm sized in solution	1 and 24 h after 4-h exposure	No skin irritation.	(158)
500	-	Rabbit New Zeeland white	3 females	10-15	0.1-10	554 nm sized in solution	1 and 24 h after 4-h exposure	No skin irritation.	(158)
-	-	Rabbit	-	10-15	0.2-1.0	Baytubes, 0.53% Co	-	No skin irritation.	(254)
-	2 000	Rat	-	10-15	0.2-1.0	Baytubes, 0.53% Co	-	Dermal LD_{50} > 2 000 mg/kg bw.	(254)
-	-	Guinea pig	-	10-15	0.2-1.0	Baytubes, 0.53% Co	-	No skin sensitisation.	(254)

Table 12. Effects after a single dose of MWCNTs.

Absolute dose (µg)	Dose (mg/kg bw)	Species/ strain	No. and sex of animals	Diameter (nm)	Length (µm)	Attributes	Observation period	Effects	Reference
Subcutaneous injection									
200	-	Mouse BALB/ cAnNCrl	10 females	15 [h] (20-30) [i]	0.5-200	90% MWCNTs, many defects. Co-stimulation with OVA	28 days	Elevated levels of OVA-specific IgE, IgG1 and IgG2a.	(241)
Subcutaneous implantation									
100	0.6	Rat Wistar	6 males	20-50	0.22	Unmodified	1-4 weeks	Slight local inflammation, no neutrophil invasion, no necrosis. After 1 week CNTs had been engulfed by macrophages, after 4 weeks most were internalised.	(292)
100	0.6	Rat Wistar	6 males	20-50	0.825	Unmodified	1-4 weeks	Local inflammation, no neutrophil invasion, no necrosis. After 1 week, some CNTs in intercellular space and some internalised by macrophages.	(292)
1 000	45.5	Mouse BALB/c	5 females	100-150	10-20	1.2% Fe	4 weeks	Percentage of CD8+ cells lower than after heating. Higher ratio of CD4+/CD8+ cells than by 2 800 °C heated CNTs. Increased levels of IL-4, IL-6, IL-10 and IFNγ.	(167)
1 000	45.5	Mouse BALB/c	5 females	100-150	10-20	0.008% Fe, 1 800 °C heated	4 weeks	Higher ratio of CD4+/CD8+ cells than by 2 800 °C heated CNTs.	(167)
1 000	45.5	Mouse BALB/c	5 females	100-150	10-20	<0.002% Fe, 2 800 °C heated	4 weeks	No effect on levels of CD4+ or CD8+ cells or cytokines.	(167)
2 000	90.9	Mouse BALB/c	30 females	10-50	10-20	3-5 wt% Fe	12 weeks	No change in body weight and no mortality. Fewer CD4+ cells after 1 week, but elevated number after 2 weeks. Fewer CD8+ cells 1-2 weeks post-implantation. Granulomatous tissue after 3 weeks.	(168)

Table 12. Effects after a single dose of MWCNTs.

Absolute dose (µg)	Dose (mg/kg bw)	Species/ strain	No. and sex of animals	Diameter (nm)	Length (µm)	Attributes	Observation period	Effects	Reference
2 000	90.9	Mouse BALB/c	30 females	100-150	10-20	<0.03% Fe	12 weeks	No change in body weight and no mortality. Fewer CD4+ cells after 1 week, elevated number after 2 weeks, but reduced again after 3 weeks. Fewer CD8+ cells l and 3 weeks post-implantation. Granulomatous tissue after 3 weeks.	(168)
Submuscular implantation									
5 000	16.7	Rat Sprague Dawley	1 male	-	-	-	7 days	Inflammation and fibrosis at the site of implantation.	(45)
20 000	66.7	Rat Sprague Dawley	1 male	-	-	-	-	Acute pulmonary oedema, pleural reaction in-cluding pleural inflammatory liquid. The animal died 180 min after implantation.	(45)
Ocular application									
	-	Rabbit	4	-	-	Fullerene soot with high CNT content	24, 48 and 72 h (modi-fied Draize)	No eye irritation.	(122)
18 000	-	Rabbit New Zeeland white	3 females	110-170	5-9	901 nm sized in solution	1, 24, 48, 72 and 96 h (Draize)	Conjunctival redness from 1 h, totally disappeared after 96 h.	(158)
18 000	-	Rabbit New Zeeland white	3 females	10-15	0.1-10	554 nm sized in solution	1, 24, 48, 72 and 96 h (Draize)	Same as above.	(158)
≤100 000	-	Rabbit	-	10-15	0.2-1.0	Baytubes, 0.53% Co	-	Very mild eye irritation.	(254)

Table 12. Effects after a single dose of MWCNTs.

Absolute dose (µg)	Dose (mg/kg bw)	Species/ strain	No. and sex of animals	Diameter (nm)	Length (µm)	Attributes	Observation period	Effects	Reference
Intracerebral injection									
0.035	-	Mouse	3	10-30	2	2.94% metals, Pluronic F127 dispersed	18 days	No significant increase in the volume of injury after 3 days. Some glial scar formation after 18 days, but not significant different from the control.	(14)
Intraperitoneal injection									
50	2.5 [j]	Mouse C57BL/6	3-4 females	15	1-5	Tangled, packed spherical agglomerates	7 days	Slight increase in the thickness of the diaphragm.	(259)
50	2.5 [j]	Mouse C57BL/6	3-4 females	10-15	5-20	Tangled, bundles of intermediate length	7 days	Same as above.	(259)
50	2.5 [j]	Mouse C57BL/6	3-4 females	40-50/ 85 [h]	13	Long, dispersed bundles and singlets	7 days	Thicker diaphragm, granulomatous inflammation after 7 days. More PMNs and total protein in the lavageate of the peritoneal cavity after 24 h.	(259)
50	2.5 [j]	Mouse C57BL/6	3-4 females	20-10/ 165 [h]	56 (max)	Long, regular bundles and ropes	7 days	Same as above.	(259)
	10	Mouse CD1 Swiss	3-5 males	-	-	-	7 days	Slight irritation of the peritoneum, no detectable aggregated CNTs and no deaths. No antigenic reaction.	(45)
	20	Mouse CD1 Swiss	3-5 males	-	-	-	7 days	1 animal died within 7 days. Adhesive peritonitis, no other adverse signs. Aggregated CNTs observed in the abdominal cavity. Similar result at 40 mg/kg bw.	(45)

Table 12. Effects after a single dose of MWCNTs.

Absolute dose (µg)	Dose (mg/kg bw)	Species/ strain	No. and sex of animals	Diameter (nm)	Length (µm)	Attributes	Observation period	Effects	Reference
Intravenous injection									
100	4.8	Mouse BALB/c	10, both sexes	40	0.5-5	-COOH functionalised, suspended in PBS	1, 7 and 28 days	Agglomerated MWCNTs, taken up from the circulation into the lungs, where they were ingested by macrophages. Inflammation of the lungs, still present after 28 days. MWCNTs taken up by liver in increasing numbers with time, not eliminated after 28 days. More megakaryocytes and multinucleated cells in the spleen, disappeared after 28 days.	(269)
100	4.8	Mouse BALB/c	10, both sexes	40	0.5-5	-COOH functionalised, suspended in PBS/ Tween-80	1, 7 and 28 days	MWCNTs less agglomerated and well-dispersed. Not taken up into the lungs from the circulation and no inflammatory effect. MWCNTs taken up by liver, but cleared after 28 days. More megakaryocytes and multinucleated cells in the spleen, disappeared after 28 days.	(269)
	10	Mouse Kunming	20 males	10-20	0.1-1	Acid-oxidised, Tween-80 dispersed, 98% pure, 0.86% Ni	60 days	Elevation of ASAT level in blood after 15 days. Liver discoloration after 15 and 60 days.	(140)
	10	Mouse Kunming	20 males	10-20	0.1-1	Acid-oxidised, 98% pure, 0.86% Ni	60 days	Elevation of ASAT level in blood after 15 and 60 days.	(140)
	10	Mouse Kunming	10 males	10-20	<1	Acid-treated, non-PEGylated	60 days	Liver discoloration, no change in liver weight and no histological change. Plasma levels of GSH and SOD unaffected.	(380)
	10	Mouse Kunming	10 males	10-20	<1	Acid-treated, PEGylated	60 days	Same as above.	(380)

Table 12. Effects after a single dose of MWCNTs.

Absolute dose (µg)	Dose (mg/kg bw)	Species/ strain	No. and sex of animals	Diameter (nm)	Length (µm)	Attributes	Observation period	Effects	Reference
	60	Mouse Kunming	6 females	12.6	0.269	Taurine functionalised	60 days	Higher relative spleen weight initially, but returned to normal during the observation period. No change in phagocytic index. Levels of reduced GSH, SOD and MDA in spleen unaffected. MWCNT accumulation in the spleen, but no observable damage to this tissue. Similar results observed with 100 mg/kg bw.	(64)
	60	Mouse Kunming	20 males	10-20	0.1-1	Acid-oxidised, Tween-80 dispersed, 98% pure, 0.86% Ni	60 days	Inflammatory cells in the portal region of the liver, cellular and focal necrosis after 15 and 60 days. Swelling of hepatocyte mitochondria. Level of reduced GSH and activity of SOD were decreased in the liver after 15 days. Higher levels of total bilirubin and ASAT in blood. Alteration in expression of CYP450. Liver discoloration indicating presence of CNTs after 60 days.	(140)
	60	Mouse Kunming	20 males	10-20	0.1-1	Acid-oxidised, 98% pure, 0.86% Ni	60 days	Slight infiltration of inflammatory cells into the portal region of the liver after 15 and 60 days. Higher levels of ASAT after 15 and 60 days and total bilirubin after 60 days in blood. Alteration in expression of CYP450. Liver discoloration indicating presence of CNTs after 60 days.	(140)
	60	Mouse Kunming	10 males	10-20	<1	Acid-treated, non-PEGylated	60 days	Liver discoloration, no change in liver weight. Infiltration of inflammatory cells into liver, with cellular and focal necrosis in the portal region. Mitochondrial swelling and destruction after 60 days. Plasma levels of GSH and SOD unaltered. ASAT levels elevated after 60 days.	(380)

Table 12. Effects after a single dose of MWCNTs.

Absolute dose (µg)	Dose (mg/kg bw)	Species/ strain	No. and sex of animals	Diameter (nm)	Length (µm)	Attributes	Observation period	Effects	Reference
	60	Mouse Kunming	10 males	10-20	<1	Acid-treated, PEGylated	60 days	Liver discoloration, no change in liver weight. Slight infiltration of inflammatory cell into the portal region. Mild swelling of mitochondria. Plasma levels of GSH and SOD unaltered.	(380)
25	-	Rat Wistar Kyoto	5	-	-	-	15 h	Accelerated rate of vascular thrombosis.	(270)

[a] Calculated by the authors of this NEG document, on the basis of the rats weighing 180-220 g, as stated in the reference.
[b] Calculated by the authors of this NEG document, on the basis of the rats weighing 288-336 g, as stated in the reference.
[c] Calculated by the authors of this NEG document, on the basis of the rats weighing 200-225 g, as stated in the reference.
[d] Calculated by the authors of this NEG document, on the basis of the mice weighing 30 g, as stated in the reference.
[e] Calculated by the authors of this NEG document, on the basis of the rats weighing 200-250 g, as stated in the reference.
[f] Calculated by the authors of this NEG document, assuming that the mice weighed 21.5 g.
[g] Calculated by the authors of this NEG document, on the basis of the mice weighing 20-25 g, as stated in the reference.
[h] Determined by the investigators.
[i] Data provided by manufacturer.
[j] Calculated by the authors of this NEG document, assuming that the mice weighted 20 g.
ACP: acid phosphatase, ALP: alkaline phosphatase, ALT: alanine aminotransferase, ASAT: aspartate aminotransferase, BALF: bronchoalveolar lavage fluid, BSA: bovine serum albumin, CINC: cytokine-induced neutrophil chemoattractant, Co: cobalt, CVD: chemical vapour deposition, CYP450: cytochrome P450, DWCNT: double-walled carbon nanotube, GSH: glutathione, IFNγ: interferon gamma, Ig: immunoglobulin, IL: interleukin, LD_{50}: lethal dose for 50% of the exposed animals at single administration, LDH: lactate dehydrogenase, LPS: lipopolysaccharide, MDA: malondialdehyde, Mmp: matrix metallopeptidase, Na: natrium, NEG: Nordic Expert Group, Ni: nickel, OVA: ovalbumin, PBS: phosphate buffered saline, PEG: polyethylene glycol, SDS: sodium dodecyl sulphate, SOD: superoxide dismutase, TNFα: tumour necrosis factor alpha.

Table 13. Effects after repeated doses of MWCNTs.

Absolute dose per occasion/ total (μg)	Total dose (mg/kg bw)	Exposure duration	Species/ Strain	No. and sex of animals	Diameter (nm)	Length (μm)	Attributes	Observation period	Effects	Reference
Intratracheal instillation										
50/300	9.6 [a]	Once a week for 6 weeks	Mouse ICR	12-13 males	67	-	99.79% pure, dispersed in Tween-80. With/without co-exposure to OVA	1 day post-exposure	Co-exposure aggravated the MWCNT-induced effects: Infiltration of immune cells into the lungs; more goblet cells in the bronchial epithelium; elevated serum levels of IgG and IgE. T-cell proliferation detected *in vitro*. Levels of cytokines in BALF (IL-6, IL-1β) and lung tissue (MCP-1, eotaxin) enhanced after MWCNTs exposure, much more pronounced after co-exposure.	(133)
Intranasal instillation										
133/400	-	Once daily for 3 days	Mouse BALB/ cAnNCrl	10 females	15 [b] (20-30) [c]	0.5-200	90% MWCNTs, many defects. With/without co-exposure to OVA	26 days	Co-stimulation heightened the levels of OVA-IgE and IgG2a in blood, as well as the levels of eosinophils, neutrophils, inflammatory cytokines and Th2-associated cytokines in BALF.	(241)
Oral gavage										
	196	Once daily on GDs 6-19	Rat Sprague Dawley	12 females	10-15	~20	-	1 day post-exposure	No abnormal findings. No change in foetal deaths or foetal body or placental weights.	(186)
	560	Once daily on GDs 6-19	Rat Sprague Dawley	12 females	10-15	~20	-	1 day post-exposure	Decreased locomotor activity and depression in 1 dam. No change in foetal deaths or foetal body or placental weights.	(186)
	2 800	Once daily on GDs 6-19	Rat Sprague Dawley	12 females	10-15	~20	-	1 day post-exposure	No abnormal findings. No change in foetal deaths or foetal body or placental weights.	(186)

Table 13. Effects after repeated doses of MWCNTs.

Absolute dose per occasion/ total (µg)	Total dose (mg/kg bw)	Exposure duration	Species/ Strain	No. and sex of animals	Diameter (nm)	Length (µm)	Attributes	Observation period	Effects	Reference
	14 000	Once daily on GDs 6-19	Rat Sprague Dawley	12 females	10-15	~20	-	1 day post-exposure	Decreased locomotor activity and depression in 3 dams. Reduced thymus weight in dams. No change in foetal deaths or foetal body or placental weights.	(186)
Intraperitoneal injection										
148/ 1 033 [a]	35	Once daily for 7 days	Mouse CD1 Swiss	4 males	-	-	-	1 day post-exposure	Deposition of MWCNTs in the intraperitoneal cavity, connections between the surface of the liver and adjacent organs. Heterogeneous hepatic structure. No change in body weight.	(45)
165/ 4 600 [a]	280	Once daily for 28 days	Mouse ICR	8 males, 8 females	10-40	0.2-2	Phosphoryl-choline functionalised	28 days	Increased ratio of liver-to-body weight for males. Elevated ASAT levels in serum. No other patho-logical signs.	(185)
825/ 23 000 [a]	1 400	Once daily for 28 days	Mouse ICR	8 males, 8 females	10-40	0.2-2	Phosphoryl-choline functionalised	28 days	Increased ratio of spleen-to-body weight. Lower level of urea nitrogen in blood. Some CNTs present in liver, lung and spleen. Mild inflammation of the liver, spleen and lung.	(185)
4 125/ 115 000 [a]	7 000	Once daily for 28 days	Mouse ICR	8 males, 8 females	10-40	0.2-2	Phosphoryl-choline functionalised	28 days	Mice became sluggish and lethargic after 28 days. Black coloration of intraabdominal mucosa, spleen and liver. Higher tissue-to-body weight ratio for the liver, kidney and lung. Less urea nitrogen in blood. Inflammation and infiltration of cells into liver. CNTs present in liver (mainly in sinusoidal walls), lung (interstitial space) and spleen. Thickening of alveolar walls. No histopathological alterations of heart, kidneys, brain, ovaries or testes.	(185)

Table 13. Effects after repeated doses of MWCNTs.

Absolute dose per occasion/ total (µg)	Total dose (mg/kg bw)	Exposure duration	Species/ Strain	No. and sex of animals	Diameter (nm)	Length (µm)	Attributes	Observation period	Effects	Reference
Intravenous injection										
113/ 563	25	5 times over 13 days	Mouse BALB/c	8 males	20-30	0.5-2	-COOH functionalised, highly pure	Days 15, 60 and 90	No effect on sperm quality or fertility. MWCNTs detected in testes within 24 h. Abnormal seminiferous tubules and reduced germinative layer thickness after 15 days; effects observed only occasionally on days 60 and 90, indicating that they may have been re-paired. Increased MDA levels in testes after 15 days, normalised after 60 and 90 days.	(13)
113/ 563	25	5 times over 13 days	Mouse BALB/c	8 males	20-30	0.5-2	-NH_2 functionalised, highly pure	Days 15, 60 and 90	No effect on sperm quality or fertility. MWCNTs de-tected in testes. Abnormal seminiferous tubules and reduced germinative layer thickness after 15 days; effects observed only occasionally on days 60 and 90, indicating that they may have been repaired.	(13)

[a] Calculated by the authors of this NEG document on the basis of data provided in the reference.
[b] Determined by the investigators.
[c] Data provided by the manufacturer.
ASAT: aspartate aminotransferase, BALF: bronchoalveolar lavage fluid, GD: gestational day, Ig: immunoglobulin, IL: interleukin, MCP: macrophage chemoattractant protein, MDA: malondialdehyde, OVA: ovalbumin, Th: T helper.

Table 14. Genotoxic and mutagenic effects of SWCNTs and MWCNTs.

Absolute dose (µg)	Dose (mg/kg bw)	Exposure duration	Species/ Strain	No. and sex of animals	Diameter (nm)	Length (µm)	Attributes	Observation period	Effects	Reference
Inhalation										
5, estimated deposited dose	0.25 [a] (5 mg/m^3)	5 h/day for 4 days	Mouse C57BL/6	5 females	0.8-1.2	0.1-1	SWCNTs, 17.7% Fe	1, 7 and 28 days	High frequency of mutations in K-*ras* gene (4/5) in the lungs after 28 days.	(305)
Intratracheal instillation										
50	-	Single dose	Mouse ICR	5 males	90, 80% in 70-110 nm range	2, 70% in 1-4 µm range	MWCNTs, high-purity Mitsui MWNT-7	Up to 1 week	Dose-dependent increase in DNA damage of the lungs (tail moment in comet assay).	(153)
200	-	Single dose	Mouse ICR	5 males	90, 80% in 70-110 nm range	2, 70% in 1-4 µm range	MWCNTs, high-purity Mitsui MWNT-7	Up to 1 week	Same as above and elevated levels of 8-oxodG in the lungs up to 72 h after exposure.	(153)
200	-	Single dose	Mouse C57BL/6J gpt delta	6-7 males	90, 80% in 70-110 nm range	2, 70% in 1-4 µm range	MWCNTs, high-purity Mitsui MWNT-7	12 weeks	No change in the frequency of mutations in *gpt* gene in the lungs.	(153)
800	-	Once a week for 4 weeks	Mouse C57BL/6J gpt delta	6-7 males	90, 80% in 70-110 nm range	2, 70% in 1-4 µm range	MWCNTs, high-purity Mitsui MWNT-7	12 weeks	2-fold increase in frequency of mutations in *gpt* gene in the lungs 8 and 12 weeks post-exposure.	(153)
54	2.28	Single dose	Mouse ApoE-/-	7 females	0.9-1.7	≤1	SWCNTs, 2% Fe	Up to 24 h	DNA damage in BAL cells (% DNA in the tail in comet assay) after 3 h.	(137)

Table 14. Genotoxic and mutagenic effects of SWCNTs and MWCNTs.

Absolute dose (μg)	Dose (mg/kg bw)	Exposure duration	Species/ Strain	No. and sex of animals	Diameter (nm)	Length (μm)	Attributes	Observation period	Effects	Reference
500	2-2.5 [b]	Single dose	Rat Wistar	5 females	11.3	0.7	MWCNTs, 98% pure, traces of Co and Fe, aggregated, HD 1 μm	3 days	No alteration in number of micronucleated type II pneumocytes.	(219)
2 000	8-10 [b]	Single dose	Rat Wistar	5 females	11.3	0.7	Same as above	3 days	2-fold increase in number of micronucleated type II pneumocytes after 3 days.	(219)
Pharyngeal aspiration										
10	0.4	Single dose	Mouse C57BL/6J or ApoE-/-	4-10 males	0.7-1.5	1	SWCNTs	Up to 60 days	Damaged mitochondrial DNA in cells of the aorta at 7, 28 and 60 days.	(184)
20	1 [a]	Single dose	Mouse C57BL/6	5 females	0.8-1.2	0.1-1	SWCNTs, 17.7% Fe	Up to 28 days	Frequency of mutations K-*ras* gene in the lungs not different from control animals.	(305)
Oral gavage										
	0.064	Single dose	Rat Fisher 344	8 females	0.9-1.7	<1	SWCNTs, dissolved in saline or corn oil	24 h	Elevated levels of 8-oxodG in liver and lungs, with no dose-response relationship. No differences in effects with the two dispersion media. No alteration in mRNA expression of DNA repair-related genes.	(85)
	0.64	Single dose	Rat Fisher 344	8 females	0.9-1.7	<1	Same as above	24 h	Same as above.	(85)

Table 14. Genotoxic and mutagenic effects of SWCNTs and MWCNTs.

Absolute dose (µg)	Dose (mg/kg bw)	Exposure duration	Species/ Strain	No. and sex of animals	Diameter (nm)	Length (µm)	Attributes	Observation period	Effects	Reference
Intraperitoneal injection										
7.5	0.25	Once daily for 5 days	Mouse Swiss Webster	5 males	15-30	15-20	MWCNTs, >95% pure	5 days	Dose-dependent increases in number of chromosomal aberrations, frequency of micro-nuclei, level of DNA damage (% tail DNA in comet assay) and dose-dependent decrease in mitotic index. Also seen at 0.5 and 0.75 mg/kg bw.	(252)
7.5	0.25	Once daily for 5 days	Mouse Swiss Webster	5 males	11.5	15-20	MWCNTs, >95% pure, 2-7% COOH groups	5 days	Same as above although these COOH func-tionalised CNTs had higher clastogenic/geno-toxic potential than the non-functionalised CNTs. Also seen at 0.5 and 0.75 mg/kg bw (dose-dependent).	(252)
	12.5	Single dose	Mouse ICR	6 males	10-15	10	High-aspect-ratio MWCNTs	24 h	Negative micronuclei test with erythrocytes from bone marrow. Same result at 25 and 50 mg/kg bw.	(156)
	12.5	Single dose	Mouse ICR	6 males	10-15	0.15	Low-aspect-ratio MWCNTs	24 h	Same as above.	(156)

[a] Calculated by the authors of this NEG document based on data provided in the reference (average weight of a mouse 20 g).
[b] Calculated by the authors of this NEG document based on data provided in the reference (weight of a rat 200-250 g).
BAL: bronchoalveolar lavage, Co: cobalt, Fe: iron, gpt: guanine phosphoribosyltransferase, HD: hydrodynamic diameter, 8-oxodG: 8-oxo-7,8-dihydro-2'-deoxyguanosine.

Table 15. Carcinogenic effects after a single dose of SWCNTs and MWCNTs.

Absolute dose (μg)	Dose (mg/kg bw)	Species/ strain	No. and sex of animals	Diameter (nm)	Length (μm)	Attributes	Exposure route	Observation period	Effects	Reference
3	0.12 [a]	Mouse p53(+/-) C57BL/6	20 males	70-170 (range), 90 (median)	1-20 (range), 2 (median)	Mitsui MWNT-7, 0.35% Fe	I.p. injection	1 year	4/20 animals had lethal mesothelioma and 1/20 non-lethal mesothelioma. The 15 surviving mice had focal mesothelial atypical hyperplasia.	(319)
240	1	Rat Fisher 344	7 males	70-110	1-4	Mitsui MWNT-7, 0.05% Fe, 0.047% S	Intrascrotal injection	1 year	6/7 rats died within 37-40 weeks after exposure, due to mesothelioma. Mesotheliomas were observed to invade adjacent organs and tissue and metastasize to the pleura. The rat that survived for 1 year did not develop mesothelioma, but exhibited hypertrophic mesothelium and lesions.	(288)
240	1	Rat Fisher 344	3 males	70-110	1-4	Mitsui MWNT-7, 0.35% Fe, 0.047% S	Intrascrotal injection	1 year	Increased serum levels of ECR/mesothelin in animals with mesothelial hyperplasia and further elevated levels in animals that developed mesothelioma.	(287)
30	1.2 [a]	Mouse p53(+/-) C57BL/6	20 males	70-170 (range), 90 (median)	1-20 (range), 2 (median)	Mitsui MWNT-7, 0.35% Fe	I.p. injection	1 year	17/20 animals had lethal mesothelioma.	(319)
2 000	6.1	Rat Wistar	50 males	11.3	0.7	MWNTs, short, many structural defects	I.p. injection	2 years	No acute peritoneal inflammation. Two cases of mesothelioma, but no significant alteration in incidence of mesotheliomas. One case of lipoma.	(220)
300	12 [a]	Mouse p53(+/-) C57BL/6	20 males	70-170 (range), 90 (median)	1-20 (range), 2 (median)	Mitsui MWNT-7, 0.35% Fe	I.p. injection	1 year	14/20 animals had single or multiple lethal mesothelioma and 5/20 non-lethal mesothelioma.	(319)

Table 15. Carcinogenic effects after a single dose of SWCNTs and MWCNTs.

Absolute dose (µg)	Dose (mg/kg bw)	Species/ strain	No. and sex of animals	Diameter (nm)	Length (µm)	Attributes	Exposure route	Observation period	Effects	Reference
10 000	25	Rat Fisher 344	6	<2	4-15	SWCNTs	Intraabdominal implantation	1 year	Expansion of the gastric wall, granulomatous reaction to foreign bodies in the peritoneal mesothelium. No peritoneal mesothelioma.	(352)
10 000	25	Rat Fisher 344	6	10-30	1-2	MWCNTs	Intraabdominal implantation	1 year	Expansion of the gastric wall, foreign body granulomatous reaction. No mesothelioma.	(352)
20 000	61.4	Rat Wistar	50 males	11.3	0.7	MWCNTs, short, many structural defects	I.p. injection	2 years	Slight acute peritoneal inflammation. No cases of mesotheliomas, but one case each of lipoma, liposarcoma and angiosarcoma.	(220)
20 000	61.4	Rat Wistar	50 males	11.3	0.7	MWCNTs, without defects	I.p. injection	2 years	No acute peritoneal inflammation. Three cases of mesotheliomas, but no significant alteration in incidence of mesotheliomas. Three cases of lipomas at time of sacrifice.	(220)
3 000	120 [a]	Mouse p53(+/-) C57BL/6	19 males	100 (average)	>5 (27.5%)	Mitsui MWNT-7, aggregates, dispersed by sonication in Tween-80	I.p. injection	180 days	Fibrous peritoneal thickening. Foreign body granulomas and fibrous scars observed. Peritoneal mesothelial lesions, nodular mesotheliomatous pile-ups of atypical mesothelial cells. Formation of malignant mesothelial tumours with occasional central necrosis. Cumulative mortality higher than for controls exposed to crocidolite.	(320)

[a] Calculated by the authors of this NEG document, assuming the average weight of a mouse to be 25 g.

ERC/mesothelin: expressed in renal carcinoma/mesothelin (biomarker for human mesothelioma), Fe: iron, I.p.: intraperitoneal, S: sulphur.

14. Previous evaluations

No regulatory or legal binding OELs for CNTs exist to our knowledge to date.

US NIOSH systematically reviewed 54 animal studies, many of which indicated that CNTs/carbon nanofibres could cause adverse pulmonary effects including inflammation (44 of 54 studies), granulomas (27 studies), and pulmonary fibrosis (25 studies). According to NIOSH the pulmonary responses were qualitatively similar across the various types of CNTs and carbon nanofibres, purified or unpurified with various metal content, and different dimensions. Previously, in the 2010 draft of this document for public comment NIOSH indicated that risks could occur below 1 $\mu g/m^3$, but proposed a recommended exposure limit (REL) for CNTs of 7 $\mu g/m^3$ elemental carbon (EC) equivalent with the analytical limit of quantitation at time. However, based on improvement of sampling and analytical methods, NIOSH has now lowered the REL to 1 $\mu g/m^3$ EC. Furthermore it was stated that until results from research can fully explain the physical-chemical properties of CNTs and carbon nanofibres that define their inhalation toxicity, all types of CNTs and carbon nanofibres should be considered a respiratory hazard and exposure should be controlled below the REL. The REL is based on a quantitative risk assessment (benchmark modelling) using the two subchronic studies by Ma-Hock and co-workers and by Pauluhn (198, 255) as well as short-term studies (175, 206, 222, 305, 306) with sufficient dose-response data of early-stage fibrotic and inflammatory responses. NIOSH estimated that the risk of developing early-stage lung effects over a working life if exposed to CNTs at the analytical limit quantitation (NMAM No. 5040 (238)) of 1 $\mu g/m^3$ (8-hour TWA as respirable EC) is approximately 0.5% to 16% (240).

An interim OEL of 30 $\mu g/m^3$ for both SWCNTs and MWCNTs has been proposed by the Japanese New Energy and Industrial Technology Department Organization (NEDO). This organisation derived an OEL using data from the 4-week rat inhalation studies by Morimoto and colleagues on SWCNTs (215) and MWCNTs (216). The identified NOAELs for pulmonary effects of 0.13 mg/m^3 for SWCNTs and 0.37 mg/m^3 for MWCNTs were calculated to be equivalent to 0.03 and 0.08 mg/m^3 in humans (uncertainty factor of 6). A relationship between specific surface area and toxicity was observed and after taken this into consideration a period-limit (15-years) OEL of 0.03 mg/m^3 was recommended for both SWCNTs and MWCNTs (233).

There are also some suggestions from non-national and non-international bodies. To date, two manufacturers have proposed in-house limits of exposure to their MWCNTs products (198, 254, 301). One of these limits, 50 $\mu g/m^3$, is based on the NOAEL obtained in the 13-week subchronic inhalation study on rats by Pauluhn (18, 254, 255). The other in-house limit, estimated from the LOAEL of 100 $\mu g/m^3$ obtained in the 90-day repeated inhalation study on rats by Ma-Hock (198) and by application of an overall assessment factor of 40 to this value is 2.5 $\mu g/m^3$ (234).

Aschberger and collaborators calculated human indicative no-effect levels (INELs) for acute and chronic exposures (11). The INEL for acute exposure of 150 μg/m^3 is based on the LOAEL of 11 mg/m^3 for inflammatory effects of MWCNTs in the study by Ellinger-Ziegelbauer and Pauluhn (76). The INEL of 1-2 μg/m^3 for chronic exposure is based on the NOAEL of 100 μg/m^3 for MWCNTs obtained in the 13-week inhalation study by Pauluhn (255).

The British Standards Institute (BSI) has proposed a benchmark exposure limit (BEL) for fibrous nanomaterials e.g., CNT of 0.01 fibre/cm^3 or one-tenth of their asbestos exposure limit (34). Based on this recommendation, the Institute for Occupational Safety and Health of the German Social Accident Insurance (IFA) also recommends a BEL for CNTs of 0.01 fibre/cm^3 (128).

Safe Work Australia commissioned National Industrial Chemicals Notification and Assessment Scheme (NICNAS) to conduct a health hazard classification of CNTs. Based on the two subchronic studies (by Ma-Hock *et al* and Pauluhn (198, 255)) MWCNTs were classified as Harmful: Danger of serious damage to health by prolonged exposure through inhalation. Moreover, based on data available on mesothelioma formation in animals and "difficulty in conclusively determining whether a specific MWCNT can present as a fibre of pathogenic dimension", all MWCNTs were classified as Harmful: Limited evidence of carcinogenic effect. It was also stated that "SWCNTs are not expected to behave differently and that it is therefore prudent to consider the above classification for SWCNTs" (235).

15. Evaluation of human health risks

15.1 Assessment of health risks

There are no human toxicological data, but studies on experimental animals indicate that pulmonary exposure to CNTs does pose a health risk. CNTs are, however, not a homogenous group. They can vary considerably in dimensions and morphology, chemical composition including metal impurities, non-CNT carbonaceous material and functionalisation and therefore also in degree of agglomeration and biopersistence. All these variations may modify the biological response to CNTs.

Occupational exposure to CNTs may occur during the manufacturing, but also when CNTs are incorporated in other products as well as in down-stream applications. It is not clear which metric for air sampling that best correlates with the health effects caused by CNTs. The most common metric used to assess occupational exposure to CNTs is mass concentrations in different fractions of dust. These concentrations are typically 100 μg/m^3 or lower. Estimation of exposure in this manner is uncertain, since airborne particles other than CNTs are also included. Respirable EC levels have also been measured and were generally 5 μg/m^3 or less. Another approach used is to count the number of CNT structures (concentrations typically 0.01 structures/cm^3).

The exposure route of highest concern is inhalation, and pulmonary toxicity has been evaluated in numerous animal studies with exposure to CNTs via inhalation, pharyngeal aspiration or i.t. instillation.

Pulmonary effects were observed in two 13-weeks inhalation studies of rats exposed to MWCNTs via inhalation. In the first one (using Nanocyl NC 7000 MWCNTs) there were signs of minimal granulomatous inflammation and minimal diffuse histiocytosis at 0.1 mg/m^3. At the higher concentration of 0.5 mg/m^3 the effects also included intra-alveolar lipoproteinosis and goblet cell hyperplasia in the nasal cavity (198). In the second study using shorter MWCNTs (Baytubes) no pulmonary effects were observed at 0.1 mg/m^3, whereas 0.4 mg/m^3 caused sustained broncho-alveolar inflammation, thickening of the alveolus septum indicative of interstitial fibrosis, and goblet cell hyperplasia in the upper respiratory tract (255). Exposure of rats for 4 weeks to a similar level (0.37 mg/m^3 MWCNTs) evoked transiently increased levels of chemokines in the lungs and of myeloperoxidase in BAL fluid. Meanwhile, no histopathological alterations were seen in the lungs (216). Exposure of rats to 0.13 mg/m^3 SWCNTs for 4 weeks evoked no adverse effects in the lungs (215). At higher concentrations (5 mg/m^3 SWCNTs for 4 days) granulomatous inflammation in the lungs along with progressive fibrosis were observed in mice (305). Taken together inhalation studies and studies using pharyngeal aspiration and i.t. instillation consistently demonstrate that single and repeated exposures of rats and mice to various types of CNTs induce pulmonary inflammation with subsequent formation of granuloma and lung fibrosis.

Mesothelioma has been described following i.p. injection of MWCNTs to p53 heterozygous mice (319, 320) and intrascrotal injection of MWCNTs to rats (288). On the other hand, i.p. injections of shorter MWCNTs to rats caused no mesotheliomas (220). Genotoxicity is generally considered to be an important mechanism in the pathogenesis of cancer. Genotoxic effects including chromosomal aberrations (252), formation of micronuclei (219, 252) and DNA strand-breaks (137, 153, 252), and modification of bases in DNA (153, 305) have been observed. Thus, available data suggest a genotoxic and carcinogenic potency of CNTs.

Present data suggest that CNTs have low acute oral and dermal toxicity (165, 254), are slightly irritating to the eyes, but not irritating to the skin (158, 254) and do not produce skin sensitisation (254).

Limited data suggest that CNTs may affect the cardiovascular system (79, 178, 184, 270, 336), suppress systemic immune function (212, 213) and aggravate allergic airway inflammation (133, 135, 241, 285).

Furthermore, at present it is not possible to conclude on the reproductive and developmental toxicity of CNTs due to the scare data base.

15.2 Groups at extra risk

There are no human data available to identify groups at extra risk. Data from animal studies suggest that individuals with pre-existing allergic airway inflammation including asthma may be at increased risk (133, 135, 241, 285).

15.3 Scientific basis for an occupational exposure limit

No human data are presently available. There are a limited number of animal studies using the inhalation route, which is considered to be the most important route of exposure for humans. Based on these studies, the critical effect is inflammatory responses in the lungs.

Inhalation exposure to 0.1 mg/m^3 MWCNTs for 13 weeks was without effect in rats (255). However, in another 13-week inhalation study exposure of rats to 0.1 mg/m^3 MWCNTs led to minimal granulomatous inflammation with minimal diffuse histiocytosis (198). Thus, 0.1 mg/m^3 may be identified as a LOAEL for MWCNTs in rats. Mice exposed to 0.3 mg/m^3 MWCNTs for 2 weeks demonstrated no signs of pulmonary inflammation, but were immunosuppressed (212).

Inhalation exposure to 0.13 mg/m^3 SWCNTs for 4 weeks evoked no adverse effects in the lungs of rats (215). Therefore, a NOAEL for SWCNTs in rats of 0.13 mg/m^3 may be identified. Mice exposed to 5 mg/m^3 SWCNTs for 4 days demonstrated granulomatous inflammation in the lungs along with progressive fibrosis (305).

Based on the above studies, an overall LOAEL for CNTs of 0.1 mg/m^3 can be estimated. However, this LOAEL should be cautiously interpreted, as the toxicity of CNTs is likely to vary widely depending on their physical and chemical characteristics and choice of dose metrics as discussed in previous sections.

16. Research needs

To be able to evaluate the occupational exposure, safety and the health concerns of workers handling CNTs and CNT-containing material, more information concerning exposure is required. Moreover, the toxicological effects of CNTs, especially after long-term exposure, are far from being fully understood and require further investigations. Below, some specific needs in this context are discussed.

Exposure measurements

More standardised and systematic measurements of occupational exposure during primary and secondary manufacturing of CNTs, as well as during down-stream applications are needed. Given the increasing production and use of CNTs new exposure situations may arise that also need to be evaluated. The exposure should be measured using filter-based sampling (in the breathing zone or work area during e.g., an 8-hour work-shift or a specific work task) followed by gravimetric,

chemical and microscopic analysis. Observation of profound alterations of airborne aerosol's characteristics including size, morphology and aggregation state from one work task to another emphasise the need for characterisation with real-time aerosol instruments as well. Also more standardised criteria for electron microscopy-based methods for counting CNT structures should be developed.

Toxicological studies

Further research is needed to determine which dose metric for air sampling that correlates best with the toxicological effects caused by CNTs, but also other dose metrics or properties of CNT that describe the toxicological responses needs to be further investigated.

There is a need to perform long-term animal inhalation studies to further evaluate the risk of developing cancer and non-cancer pulmonary effects. In addition, more data are needed on the possible cardiovascular and immunological effects of CNTs.

The agglomeration state of the CNTs needs to be better characterised in animal inhalation studies. The agglomeration state is critical for the site of deposition in the airways and may thus influence the toxicological response.

It is also desirable to conduct studies on the correlations between the aspect ratio and agglomeration state and the lung deposition, absorption and toxic effects of different CNTs. More information is needed about the agglomeration state in the lungs after deposition i.e., if the agglomeration state in air is preserved or if it changes upon contact with surfactants and proteins in the lung lining fluid.

It is important to study the influence of the various dispersants used *in vitro* and for instillation/aspiration and to develop test protocols that reduce the effects of such dispersants.

Health effect following inhalation exposure to or dermal contact with composite materials containing CNTs is another area that needs to be investigated.

17. Summary

Hedmer M, Kåredal M, Gustavsson P, Rissler J. *The Nordic Expert Group for Criteria Documentation of Health Risks from Chemicals. 148. Carbon nanotubes.* Arbete och Hälsa 2013;47(5):1-238.

Carbon nanotubes (CNTs) can be seen as graphene sheets rolled to form cylinders. CNTs may be categorised as single- (SWCNT) or multi-walled (MWCNT). Due to the small size, the number of particles as well as the surface area per mass unit is extremely high.

CNTs are highly diverse, differing with respect to e.g., diameter, length, chiral angles, chemical functionalisation, purity, stiffness and bulk density. Today, CNTs are utilised primarily for the reinforcement of composite polymers, but there is considerable potential for other applications. The rapidly growing production and use of CNTs increases the risk for occupational exposure. Since CNTs in bulk form are of very low density and much dust is produced during their handling, exposure by inhalation appears to represent the greatest potential risk in the work place. However, most work place measurements involved sampling periods that are too short, varying sampling techniques and non-specific analytical methods.

CNTs may be absorbed via inhalation and ingestion. Systemic uptake via the skin has not been demonstrated.

Human toxicity data on CNTs are lacking and interpretation of animal studies is often problematic since the physical properties and chemical composition are diverse, impurities may be present and data are sometimes omitted. Because of the physical similarities between asbestos and CNTs, it can be suspected that the latter may also cause lung fibrosis, mesothelioma and lung cancer following inhalation. Intraperitoneal and intrascrotal administration of CNTs causes mesothelioma in animals, but no inhalation carcinogenicity studies have been conducted. Thus, it is too early conclude whether CNTs cause mesothelioma and lung cancer in humans.

Both SWCNTs and MWCNTs cause inflammation and fibrosis in the lungs of relevant animal types and for MWCNTs these effects are also seen in the pleura. For instance, minimal histiocytosis and mild granulomatous inflammation in the lungs and lung-draining lymph nodes have been observed in rats exposed for 13 weeks to 0.1 mg/m^3 MWCNTs (lowest observed adverse effect level, LOAEL), with more pronounced inflammation in both mice and rats at higher doses. Thus, inflammatory responses in the lungs may be considered as the critical effect. However, the LOAEL of CNTs should be interpreted cautiously, since their toxicity is likely to vary widely, depending on the structure and physicochemical properties, as well as the contribution from non-carbon components. It is also uncertain which dose metric (e.g., mass, number or surface area per air volume unit) is most appropriate. Some studies indicate that longer straight CNTs evoke more pronounced biological effects than shorter or tangled fibres.

Keywords: carbon nanotubes, CNTs, fibrosis, inflammation, lung effects, occupational exposure limit, review, risk assessment, toxicity.

18. Summary in Swedish

Hedmer M, Kåredal M, Gustavsson P, Rissler J. *The Nordic Expert Group for Criteria Documentation of Health Risks from Chemicals. 148. Carbon nanotubes.* Arbete och Hälsa 2013;47(5):1-238.

Kolnanorör (CNTs) kan ses som grafenark som rullats ihop till cylindrar. De kan kategoriseras som enkel- (SWCNTs) eller flerväggiga (MWCNTs). De små dimensionerna medför att antalet partiklar såväl som ytarean är extremt hög per massenhet.

CNTs skiljer sig med avseende på t.ex. diameter, längd, kirala vinklar, kemisk funktionalisering, renhet, styvhet och bulkdensitet. Idag används CNTs främst för armering av kompositpolymerer, men det finns betydande potential för andra tillämpningar. Den snabbt ökande produktionen och användningen av CNTs ökar risken för yrkesmässig exponering. Eftersom CNTs i bulkform har mycket låg densitet och dammar vid hanteringen förefaller exponering via inhalation vara förenat med störst potentiell risk på arbetsplatser. Resultat från mätningar på arbetsplatser är dock ofta svårtolkade på grund av för korta mättider, varierande provtagningsteknik och ospecifika analysmetoder.

CNTs kan absorberas via luftvägarna och mag-tarmkanalen. Systemiskt upptag via hud har inte påvisats.

Humandata för CNTs toxicitet saknas och djurstudier är ofta svårtolkade eftersom CNTs fysikaliska egenskaper och kemiska sammansättning varierar liksom förekomsten av föroreningar, men också för att data ibland utelämnats. På grund av likheterna mellan asbest och CNTs kan det misstänkas att även de sistnämnda kan orsaka lungfibros, mesoteliom och lungcancer efter inhalation. Intraperitoneal och intrascrotal administrering av CNTs orsakar mesoteliom hos djur, men inga karcinogenicitetsstudier med inhalation har utförts. Det är därför för tidigt att avgöra om CNTs orsakar mesoteliom och lungcancer hos människor.

Både SWCNTs och MWCNTs orsakar inflammation och fibros i lungorna hos relevanta djurslag och MWCNTs även i lungsäcken. Minimal histiocytos och mild granulomatös inflammation i lungorna och dränerande lymfnoder har observerats hos råttor som exponerats 13 veckor för 0,1 mg/m^3 MWCNTs (lägsta observerade effektnivå, LOAEL), med mer uttalad inflammation hos både möss och råttor vid högre doser. Inflammatorisk respons i lungorna bedöms vara den kritiska effekten. Dock bör detta LOAEL tolkas med försiktighet eftersom toxiciteten sannolikt varierar kraftigt beroende på kolnanorörens struktur och fysikalisk-kemiska egenskaper samt bidrag från icke-kolföreningar. Det är också osäkert vilken dosmått (t.ex. massa, antal eller ytarea per volymsenhet luft) som bör användas. Vissa studier tyder på att långa, raka CNTs orsakar mer uttalade biologiska effekter än korta eller tilltrasslade fibrer.

Nyckelord: CNTs, fibros, hygieniskt gränsvärde, inflammation, kolnanorör, lungeffekter, riskbedömning, toxicitet, översikt.

19. References

1. Aiso S, Yamazaki K, Umeda Y, Asakura M, Kasai T, Takaya M, Toya T, Koda S, Nagano K, Arito H, Fukushima S. Pulmonary toxicity of intratracheally instilled multiwall carbon nanotubes in male Fischer 344 rats. *Ind Health* 2010;48:783-795.
2. Aitken RJ, Chaudhry MQ, Boxall AB, Hull M. Manufacture and use of nanomaterials: current status in the UK and global trends. *Occup Med (Lond)* 2006;56:300-306.
3. Al Faraj A, Bessaad A, Cieslar K, Lacroix G, Canet-Soulas E, Cremillieux Y. Long-term follow-up of lung biodistribution and effect of instilled SWCNTs using multiscale imaging techniques. *Nanotechnology* 2010;21:175103.
4. Al Faraj A, Cieslar K, Lacroix G, Gaillard S, Canet-Soulas E, Cremillieux Y. In vivo imaging of carbon nanotube biodistribution using magnetic resonance imaging. *Nano Lett* 2009;9: 1023-1027.
5. Albini A, Mussi V, Parodi A, Ventura A, Principi E, Tegami S, Rocchia M, Francheschi E, Sogno I, Cammarota R, Finzi G, Sessa F, Noonan DM, Valbusa U. Interactions of single-wall carbon nanotubes with endothelial cells. *Nanomedicine* 2010;6:277-288.
6. Alpatova AL, Shan W, Babica P, Upham BL, Rogensues AR, Masten SJ, Drown E, Mohanty AK, Alocilja EC, Tarabara VV. Single-walled carbon nanotubes dispersed in aqueous media via non-covalent functionalization: effect of dispersant on the stability, cytotoxicity, and epi-genetic toxicity of nanotube suspensions. *Water Res* 2010;44:505-520.
7. Anantram MP, Léonard P. Physics of carbon nanotube electronic devices. *Rep Prog Phys* 2006;69:507-561.
8. Andrawes B, Chan LY. Compression and tension stress-sensing of carbon nanotube-reinforced cement. *Magazine of Concrete Research* 2012;64:253-258.
9. Arnold MS, Green AA, Hulvat JF, Stupp SI, Hersam MC. Sorting carbon nanotubes by electronic structure using density differentiation. *Nat Nanotechnol* 2006;1:60-65.
10. Asakura M, Sasaki T, Sugiyama T, Takaya M, Koda S, Nagano K, Arito H, Fukushima S. Genotoxicity and cytotoxicity of multi-wall carbon nanotubes in cultured Chinese hamster lung cells in comparison with chrysotile A fibers. *J Occup Health* 2010;52:155-166.
11. Aschberger K, Johnston HJ, Stone V, Aitken RJ, Hankin SM, Peters SA, Tran CL, Christensen FM. Review of carbon nanotubes toxicity and exposure--appraisal of human health risk assessment based on open literature. *Crit Rev Toxicol* 2010;40:759-790.
12. Asharani PV, Serina NG, Nurmawati MH, Wu YL, Gong Z, Valiyaveettil S. Impact of multi-walled carbon nanotubes on aquatic species. *J Nanosci Nanotechnol* 2008;8:3603-3609.
13. Bai Y, Zhang Y, Zhang J, Mu Q, Zhang W, Butch ER, Snyder SE, Yan B. Repeated administrations of carbon nanotubes in male mice cause reversible testis damage without affecting fertility. *Nat Nanotechnol* 2010;5:683-689.
14. Bardi G, Tognini P, Ciofani G, Raffa V, Costa M, Pizzorusso T. Pluronic-coated carbon nanotubes do not induce degeneration of cortical neurons in vivo and in vitro. *Nanomedicine* 2009;5:96-104.
15. Barillet S, Simon-Deckers A, Herlin-Boime N, Mayne-L'Hermite M, Reynaud C, Cassio D, Gouget B, Carrière M. Toxicological consequences of TiO_2, SiC nanoparticles and multi-walled carbon nanotubes exposure in several mammalian cell types: an in vitro study. *J Nanopart Res* 2010;12:61-73.
16. Barkauskas J, Stankevicien I, Selskis A. A novel purification method of carbon nanotubes by high-temperature treatment with tetrachloromethane. *Sep Purif Technol* 2010; 71:331-336.
17. Baron AA, Maynard AD, Foley M. *Evaluation of aerosol release during the handling of unrefined single walled carbon nanotube material*. Technical report, 22 pp. Cincinnati, OH: US National Institute for Occupational Safety and Health, 2003.
18. Bayer Material Science. *Toxicity of carbon nanotubes*. http://ihcp.jrc.ec.europa.eu/docs/nbs_enpra/toxicity_ragot.pdf (assessed Aug 20, 2013).

Presented at joint CASG-Nano and ENPRA workshop on "Early harvest on research results in nanosafety", 14-15 April 2010, Ispra, Italy.

19. Bello D, Hart AJ, Ahn K, Hallock M, Yamamoto N, Garcia EJ, Ellenbecker MJ, Wardle BL. Particle exposure levels during CVD growth and subsequent handling of vertically-aligned carbon nanotube films. *Carbon* 2008;46:974-977.
20. Bello D, Hsieh SF, Schmidt DF, Rogers EJ. Nanomaterials properties vs. biological oxidative damage: Implications for toxicity screening and exposure assessment. *Nanotoxicology* 2009;3:249-261.
21. Bello D, Wardle BL, Yamamoto N, de Villoria RG, Garcia EJ, Hart AJ, Ahn K, Ellenbecker MJ, Hallock M. Exposure to nanoscale particles and fibers during machining of hybrid advanced composites containing carbon nanotubes. *J Nanopart Res* 2008;11:231-250.
22. Bello D, Wardle BL, Zhang J, Yamamoto N, Santeufemio C, Hallock M, Virji MA. Characterization of exposures to nanoscale particles and fibers during solid core drilling of hybrid carbon nanotube advanced composites. *Int J Occup Environ Health* 2010;16:434-450.
23. Belyanskaya L, Manser P, Spohn P, Bruinink A, Wick P. The reliability and limits of the MTT reduction assay for carbon nanotubes–cell interaction. *Carbon* 2007;45:2643-2648.
24. Belyanskaya L, Weigel S, Hirsch C, Tobler U, Krug HF, Wick P. Effects of carbon nanotubes on primary neurons and glial cells. *Neurotoxicology* 2009;30:702-711.
25. Bernholc J, Roland C, Yakobson BI. Nanotubes. *Curr Opin Solid State Mater Sci* 1997;2:-706-715.
26. Beyer G. Short communication: carbon nanotubes as flame retardants for polymers. *Fire Mater* 2002;26:291-293.
27. Bhushan B. *Springer handbook of nanotechnology*. Berlin, Heidelberg, Germany: Springer, 2004.
28. Bitterle E, Karg E, Schroeppel A, Kreyling WG, Tippe A, Ferron GA, Schmid O, Heyder J, Maier KL, Hofer T. Dose-controlled exposure of A549 epithelial cells at the air-liquid interface to airborne ultrafine carbonaceous particles. *Chemosphere* 2006;65:1784-1790.
29. Bottini M, Bruckner S, Nika K, Bottini N, Bellucci S, Magrini A, Bergamaschi A, Mustelin T. Multi-walled carbon nanotubes induce T lymphocyte apoptosis. *Toxicol Lett* 2006;160: 121-126.
30. Brown DM, Kinloch IA, Bangert U, Windle AH, Walter DM, Walker GS, Scotchford CA, Donaldson K, Stone V. An in vitro study of the potential of carbon nanotubes and nanofibres to induce inflammatory mediators and frustrated phagocytosis. *Carbon* 2007;45:1743-1756.
31. Brown JS, Wilson WE, Grant LD. Dosimetric comparisons of particle deposition and retention in rats and humans. *Inhal Toxicol* 2005;17:355-385.
32. Bruinink A, Pius Manser P, Hasler S. In vitro effects of SWCNT: Role of treatment duration. *Phys Status Solidi B* 2009;246:2423-2427.
33. Brunauer S, Emmett PH, Teller E. Adsorption of gases in multimolecular layers. *J Am Chem Soc* 1938;60:309-319.
34. BSI 2007. *Nanotechnologies – Part 2: Guide to safe handling and disposal of manufactured nanomaterials.* PD 6699-2:2007. London: British Standards, 2007.
35. Carrero-Sanchez JC, Elias AL, Mancilla R, Arrellin G, Terrones H, Laclette JP, Terrones M. Biocompatibility and toxicological studies of carbon nanotubes doped with nitrogen. *Nano Lett* 2006;6:1609-1616.
36. Casey A, Herzog E, Davoren M, Lyng FM, Byrne HJ, Chambers G. Spectroscopic analysis confirms the interactions between single walled carbon nanotubes and various dyes commonly used to assess cytotoxicity. *Carbon* 2007;45:1425-1432.
37. Casey A, Herzog E, Lyng FM, Byrne HJ, Chambers G, Davoren M. Single walled carbon nanotubes induce indirect cytotoxicity by medium depletion in A549 lung cells. *Toxicol Lett* 2008;179:78-84.

38. Chakravarty P, Marches R, Zimmerman NS, Swafford AD, Bajaj P, Musselman IH, Pantano P, Draper RK, Vitetta ES. Thermal ablation of tumor cells with antibody-functionalized single-walled carbon nanotubes. *Proc Natl Acad Sci U S A* 2008;105:8697-8702.
39. Chen BT, Schwegler-Berry D, McKinney W, Stone S, Cumpston JL, Friend S, Porter DW, Castranova V, Frazer DG. Multi-walled carbon nanotubes: sampling criteria and aerosol characterization. *Inhal Toxicol* 2012;24:798-820.
40. Cheng C, Muller KH, Koziol KK, Skepper JN, Midgley PA, Welland ME, Porter AE. Toxicity and imaging of multi-walled carbon nanotubes in human macrophage cells. *Biomaterials* 2009;30:4152-4160.
41. Cheng J, Chan CM, Veca LM, Poon WL, Chan PK, Qu L, Sun YP, Cheng SH. Acute and long-term effects after single loading of functionalized multi-walled carbon nanotubes into zebrafish (Danio rerio). *Toxicol Appl Pharmacol* 2009;235:216-225.
42. Cheng J, Flahaut E, Cheng SH. Effect of carbon nanotubes on developing zebrafish (Danio rerio) embryos. *Environ Toxicol Chem* 2007;26:708-716.
43. Cherukuri P, Gannon CJ, Leeuw TK, Schmidt HK, Smalley RE, Curley SA, Weisman RB. Mammalian pharmacokinetics of carbon nanotubes using intrinsic near-infrared fluorescence. *Proc Natl Acad Sci U S A* 2006;103:18882-18886.
44. Cheung W, Pontoriero F, Taratula O, Chen AM, He H. DNA and carbon nanotubes as medicine. *Adv Drug Deliv Rev* 2010;62:633-649.
45. Chiaretti M, Mazzanti G, Bosco S, Bellucci S, Cucina A, Le Foche F, Carru GA, Mastrangelo S, Di Sotto A, Masciangelo R, Chiaretti AM, Balasubramanian C, De Bellis G, Micciulla F, Porta N, Deriu G, Tiberia A. Carbon nanotubes toxicology and effects on metabolism and immunological modification *in vitro* and *in vivo*. *J Phys Condens Matter* 2008;20:474203.
46. Chico L, Crespi VH, Benedict LX, Louie SG, Cohen ML. Pure carbon nanoscale devices: Nanotube heterojunctions. *Phys Rev Lett* 1996;76:971-974.
47. Choi SJ, Oh JM, Choy JH. Toxicological effects of inorganic nanoparticles on human lung cancer A549 cells. *J Inorg Biochem* 2009;103:463-471.
48. Chou CC, Hsiao HY, Hong QS, Chen CH, Peng YW, Chen HW, Yang PC. Single-walled carbon nanotubes can induce pulmonary injury in mouse model. *Nano Lett* 2008;8:437-445.
49. Chung KT, Sabo A, Pica AP. Electrical permittivity and conductivity of carbon black-polyvinyl chloride composites. *J Appl Phys* 1982;53:6867-6879.
50. Coccini T, Roda E, Sarigiannis DA, Mustarelli P, Quartarone E, Profumo A, Manzo L. Effects of water-soluble functionalized multi-walled carbon nanotubes examined by different cytotoxicity methods in human astrocyte D384 and lung A549 cells. *Toxicology* 2010;269:41-53.
51. Cornelis R, Crews H, Caruso J, Heumann K (eds). *Handbook of elemental speciation: Techniques and methodology.* West Sussex, England: John Wiley & Sons, 2003.
52. Crouzier D, Follot S, Gentilhomme E, Flahaut E, Arnaud R, Dabouis V, Castellarin C, Debouzy JC. Carbon nanotubes induce inflammation but decrease the production of reactive oxygen species in lung. *Toxicology* 2010;272:39-45.
53. Crouzier T, Nimmagadda A, Nollert MU, McFetridge PS. Modification of single walled carbon nanotube surface chemistry to improve aqueous solubility and enhance cellular interactions. *Langmuir* 2008;24:13173-13181.
54. Cui D, Tian F, Ozkan CS, Wang M, Gao H. Effect of single wall carbon nanotubes on human HEK293 cells. *Toxicol Lett* 2005;155:73-85.
55. Cveticanin J, Joksic G, Leskovac A, Petrovic S, Sobot AV, Neskovic O. Using carbon nanotubes to induce micronuclei and double strand breaks of the DNA in human cells. *Nanotechnology* 2010;21:015102.
56. Dahm MM, Evans DE, Schubauer-Berigan MK, Birch ME, Deddens JA. Occupational exposure assessment in carbon nanotube and nanofiber primary and secondary manufacturers: mobile direct-reading sampling. *Ann Occup Hyg* 2013;57:328-344.

57. Dahm MM, Evans DE, Schubauer-Berigan MK, Birch ME, Fernback JE. Occupational exposure assessment in carbon nanotube and nanofiber primary and secondary manufacturers. *Ann Occup Hyg* 2012;56:542-556.
58. Dai H. Carbon nanotubes: synthesis, integration, and properties. *Acc Chem Res* 2002;35: 1035-1044.
59. Davoren M, Herzog E, Casey A, Cottineau B, Chambers G, Byrne HJ, Lyng FM. In vitro toxicity evaluation of single walled carbon nanotubes on human A549 lung cells. *Toxicol In Vitro* 2007;21:438-448.
60. De La Zerda A, Zavaleta C, Keren S, Vaithilingam S, Bodapati S, Liu Z, Levi J, Smith BR, Ma TJ, Oralkan O, Cheng Z, Chen XY, Dai HJ, Khuri-Yakub BT, Gambhir SS. Carbon nanotubes as photoacoustic molecular imaging agents in living mice. *Nature Nanotechnology* 2008;3:557-562.
61. De Nicola M, Nuccitelli S, Gattia DM, Traversa E, Magrini A, Bergamaschi A, Ghibelli L. Effects of carbon nanotubes on human monocytes. *Ann N Y Acad Sci* 2009;1171:600-605.
62. Delaney P, Choi HJ, Ihm J, Louie SG, Cohen ML. Broken symmetry and pseudogaps in ropes of carbon nanotubes. *Nature* 1998;391:466-468.
63. Deng X, Jia G, Wang H, Sun H, Wang X, Yang S, Wang T, Liu Y. Translocation and fate of multi-walled carbon nanotubes in vivo. *Carbon* 2007;45:1419-1424.
64. Deng X, Wu F, Liu Z, Luo M, Li L, Ni Q, Jiao Z, Wu M, Liu Y. The splenic toxicity of water soluble multi-walled carbon nanotubes in mice. *Carbon* 2009;47:1421-1428.
65. Di Sotto A, Chiaretti M, Carru GA, Bellucci S, Mazzanti G. Multi-walled carbon nanotubes: Lack of mutagenic activity in the bacterial reverse mutation assay. *Toxicol Lett* 2009;184: 192-197.
66. Donaldson K, Aitken R, Tran L, Stone V, Duffin R, Forrest G, Alexander A. Carbon nanotubes: a review of their properties in relation to pulmonary toxicology and workplace safety. *Toxicol Sci* 2006;92:5-22.
67. Donaldson K, Murphy F, Schinwald A, Duffin R, Poland CA. Identifying the pulmonary hazard of high aspect ratio nanoparticles to enable their safety-by-design. *Nanomedicine (Lond)* 2011;6:143-156.
68. Donaldson K, Murphy FA, Duffin R, Poland CA. Asbestos, carbon nanotubes and the pleural mesothelium: a review of the hypothesis regarding the role of long fibre retention in the parietal pleura, inflammation and mesothelioma. *Particle Fibre Toxicol* 2010;7:5.
69. Dong L, Joseph KL, Witkowski CM, Craig MM. Cytotoxicity of single-walled carbon nanotubes suspended in various surfactants. *Nanotechnology* 2008;19:255702.
70. Dumortier H, Lacotte S, Pastorin G, Marega R, Wu W, Bonifazi D, Briand JP, Prato M, Muller S, Bianco A. Functionalized carbon nanotubes are non-cytotoxic and preserve the functionality of primary immune cells. *Nano Lett* 2006;6:1522-1528.
71. Dutta D, Sundaram SK, Teeguarden JG, Riley BJ, Fifield LS, Jacobs JM, Addleman SR, Kaysen GA, Moudgil BM, Weber TJ. Adsorbed proteins influence the biological activity and molecular targeting of nanomaterials. *Toxicol Sci* 2007;100:303-315.
72. Elder A, Gelein R, Silva V, Feikert T, Opanashuk L, Carter J, Potter R, Maynard A, Ito Y, Finkelstein J, Oberdorster G. Translocation of inhaled ultrafine manganese oxide particles to the central nervous system. *Environ Health Perspect* 2006;114:1172-1178.
73. Elgrabli D, Abella-Gallart S, Aguerre-Chariol O, Robidel F, Rogerieux F, Boczkowski J, Lacroix G. Effect of BSA on carbon nanotube dispersion for in vivo and in vitro studies. *Nanotoxicology* 2007;1:266-278.
74. Elgrabli D, Abella-Gallart S, Robidel F, Rogerieux F, Boczkowski J, Lacroix G. Induction of apoptosis and absence of inflammation in rat lung after intratracheal instillation of multi-walled carbon nanotubes. *Toxicology* 2008;253:131-136.

75. Elgrabli D, Floriani M, Abella-Gallart S, Meunier L, Gamez C, Delalain P, Rogerieux F, Boczkowski J, Lacroix G. Biodistribution and clearance of instilled carbon nanotubes in rat lung. *Part Fibre Toxicol* 2008;5:20.

76. Ellinger-Ziegelbauer H, Pauluhn J. Pulmonary toxicity of multi-walled carbon nanotubes (Baytubes) relative to alpha-quartz following a single 6h inhalation exposure of rats and a 3 months post-exposure period. *Toxicology* 2009;266:16-29.

77. Endo M, Strano MS, Ajayan PM. Potential applications of carbon nanotubes. In: Jorio A, Dresselhaus G, Dresselhaus MS, eds. *Carbon nanotubes. Advanced topics in the synthesis, structure, properties and applications.* Topics in Applied Physics. Vol 111. Pp 13-62. Berlin Heidelberg: Springer Verlag, 2008.

78. ENRHES. *Engineered nanoparticles - Review of health and environmental safety (ENRHES).* http://ihcp.jrc.ec.europa.eu/whats-new/enhres-final-report (assessed May 30, 2013). ENRHES project, 2009.

79. Erdely A, Hulderman T, Salmen R, Liston A, Zeidler-Erdely PC, Schwegler-Berry D, Castranova V, Koyama S, Kim YA, Endo M, Simeonova PP. Cross-talk between lung and systemic circulation during carbon nanotube respiratory exposure. Potential biomarkers. *Nano Lett* 2009;9:36-43.

80. European Commission. Commission recommendation of 18 October 2011 on the definition of nanomaterial. Text with EEA relevance. 2011/696/EU. http://eur-lex.europa.eu/LexUriServ/LexUriServ.do?uri=OJ:L:2011:275:0038:0040:EN:PDF. *Official Journal of the European Union* 20.10.2011:L 275/38-40.

81. Fenoglio I, Greco G, Tomatis M, Muller J, Raymundo-Pinero E, Beguin F, Fonseca A, Nagy JB, Lison D, Fubini B. Structural defects play a major role in the acute lung toxicity of multi-wall carbon nanotubes: physicochemical aspects. *Chem Res Toxicol* 2008;21:1690-1697.

82. Fenoglio I, Tomatis M, Lison D, Muller J, Fonseca A, Nagy JB, Fubini B. Reactivity of carbon nanotubes: free radical generation or scavenging activity? *Free Radic Biol Med* 2006;40:1227-1233.

83. Fiorito S, Monthioux M, Psaila R, Pierimarchi P, Zonfrillo M, D'Emilia E, Grimaldi S, Lisi A, Béguin F, Almairac R, Noé L, Serafino A. Evidence for electro-chemical interactions between multi-walled carbon nanotubes and human macrophages. *Carbon* 2009;47:2789-2804.

84. Fiorito S, Serafino A, Andreola F, Bernier P. Effects of fullerenes and single-wall carbon nanotubes on murine and human macrophages. *Carbon* 2006;44:1100-1105.

85. Folkmann JK, Risom L, Jacobsen NR, Wallin H, Loft S, Moller P. Oxidatively damaged DNA in rats exposed by oral gavage to C60 fullerenes and single-walled carbon nanotubes. *Environ Health Perspect* 2009;117:703-708.

86. Gaillard C, Cellot G, Li S, Toma FM, Dumortier H, Spalluto G, Cacciari B, Prato M, Ballerini L, Bianco A. Carbon nanotubes carrying cell-adhesion peptides do not interfere with neuronal functionality. *Adv Mater* 2009;21:2903-2908.

87. Garibaldi S, Brunelli C, Bavastrello V, Ghigliotti G, Nicolini C. Carbon nanotube biocompatibility with cardiac muscle cells. *Nanotechnology* 2006;17:391-397.

88. Garza KM, Soto KF, Murr LE. Cytotoxicity and reactive oxygen species generation from aggregated carbon and carbonaceous nanoparticulate materials. *Int J Nanomedicine* 2008; 3:83-94.

89. Gaschen A, Lang D, Kalberer M, Savi M, Geiser T, Gazdhar A, Lehr CM, Bur M, Dommen J, Baltensperger U, Geiser M. Cellular responses after exposure of lung cell cultures to secondary organic aerosol particles. *Environ Sci Technol* 2010;44:1424-1430.

90. Ge C, Du J, Zhao L, Wang L, Liu Y, Li D, Yang Y, Zhou R, Zhao Y, Chai Z, Chen C. Binding of blood proteins to carbon nanotubes reduces cytotoxicity. *Proc Natl Acad Sci U S A* 2011;108:16968-16973.

91. Georgin D, Czarny B, Botquin M, Mayne-L'hermite M, Pinault M, Bouchet-Fabre B, Carriere M, Poncy JL, Chau Q, Maximilien R, Dive V, Taran F. Preparation of (14)C-labeled multi-

walled carbon nanotubes for biodistribution investigations. *J Am Chem Soc* 2009;131:14658-14659.

92. Geys J, Nemery B, Hoet PH. Assay conditions can influence the outcome of cytotoxicity tests of nanomaterials: better assay characterization is needed to compare studies. *Toxicol In Vitro* 2010;24:620-629.
93. Giechaskiel B, Alfoldy B, Drossinos Y. A metric for health effects studies of diesel exhaust particles. *Journal of Aerosol Science* 2009;40:639-651.
94. Grabinski C, Hussain S, Lafdi K, Braydich-Stolle L, Schlager J. Effect of particle dimension on biocompatibility of carbon nanomaterials. *Carbon* 2007;45:2828-2835.
95. Grubek-Jaworska H, Nejman P, Czuminska K, Przybylowski T, Huczko A, Lange H, Bystrzejewski M, Baranowski P, R. C. Preliminary results on the pathogenic effects of intratracheal exposure to one-dimensional nanocarbons. *Carbon* 2006;44:1057-1063.
96. Guo F, Ma N, Horibe Y, Kawanishi S, Murata M, Hiraku Y. Nitrative DNA damage induced by multi-walled carbon nanotube via endocytosis in human lung epithelial cells. *Toxicol Appl Pharmacol* 2012;260:183-192.
97. Guo J, Zhang X, Li Q, Li W. Biodistribution of functionalized multiwall carbon nanotubes in mice. *Nucl Med Biol* 2007;34:579-583.
98. Guo L, Von Dem Bussche A, Buechner M, Yan A, Kane AB, Hurt RH. Adsorption of essential micronutrients by carbon nanotubes and the implications for nanotoxicity testing. *Small* 2008;4:721-727.
99. Guo T, Nikolaev P, Rinzler AG, Tomanek D, Colbert DT, Smalley RE. Self-assembly of tubular fullerenes. *J Phys Chem B* 1995;99:10694-10697.
100. Guo T, Nikolaev P, Thess A, Colbert DT, Smalley RE. Catalytic growth of single-walled nanotubes by laser vaporization. *Chem Phys Lett* 1995;243:49-54.
101. Gupta A, Gaspar DJ, Yost MG, Gross GM, Rempes PE, Clark ML. Evaluating the potential for release of carbon nanotubes and subsequent occupational exposure during processing of a nanocomposite. *Nanotechnology occupational and environmental health and safety*, Cincinnati, OH, 2006.
102. Hamilton RF, Buford MC, Wood MB, Arnone B, Morandi M, Holian A. Engineered carbon nanoparticles alter macrophage immune function and initiate airway hyper-responsiveness in the BALB/c mouse model. *Nanotoxicology* 2007;1:104-117.
103. Han JH, Lee EJ, Lee JH, So KP, Lee YH, Bae GN, Lee SB, Ji JH, Cho MH, Yu IJ. Monitoring multiwalled carbon nanotube exposure in carbon nanotube research facility. *Inhal Toxicol* 2008;20:741-749.
104. Han SG, Andrews R, Gairola CG, Bhalla DK. Acute pulmonary effects of combined exposure to carbon nanotubes and ozone in mice. *Inhal Toxicol* 2008;20:391-398.
105. Harris PJF. Carbon nanotube composites. *Int Mat Rev* 2004;49:31-43.
106. Harvey J, Dong L, Kim K, Hayden J, Wang J. Uptake of single-walled carbon nanotubes conjugated with DNA by microvascular endothelial cells. *J Nanotechnology* 2012:196189.
107. He X, Young SH, Schwegler-Berry D, Chisholm WP, Fernback JE, Ma Q. Multiwalled carbon nanotubes induce a fibrogenic response by stimulating reactive oxygen species production, activating NF-kappaB signaling, and promoting fibroblast-to-myofibroblast transformation. *Chem Res Toxicol* 2011;24:2237-2248.
108. Heister E, Lamprecht C, Neves V, Tilmaciu C, Datas L, Flahaut E, Soula B, Hinterdorfer P, Coley HM, Silva SR, McFadden J. Higher dispersion efficacy of functionalized carbon nanotubes in chemical and biological environments. *ACS Nano* 2010;4:2615-2626.
109. Helfenstein M, Miragoli M, Rohr S, Muller L, Wick P, Mohr M, Gehr P, Rothen-Rutishauser B. Effects of combustion-derived ultrafine particles and manufactured nanoparticles on heart cells in vitro. *Toxicology* 2008;253:70-78.
110. Helland A, Wick P, Koehler A, Schmid K, Som C. Reviewing the environmental and human health knowledge base of carbon nanotubes. *Environ Health Perspect* 2007;115:1125-1131.

111. Hersam MC. Progress towards mono disperse single-walled carbon nanotubes. *Nat Nanotechnol* 2008;3:387-394.

112. Herzog E, Byrne HJ, Davoren M, Casey A, Duschl A, Oostingh GJ. Dispersion medium modulates oxidative stress response of human lung epithelial cells upon exposure to carbon nanomaterial samples. *Toxicol Appl Pharmacol* 2009;236:276-281.

113. Herzog E, Casey A, Lyng FM, Chambers G, Byrne HJ, Davoren M. A new approach to the toxicity testing of carbon-based nanomaterials--the clonogenic assay. *Toxicol Lett* 2007; 174:49-60.

114. Hinds WC. *Aerosol technology: Properties, behavior, and measurement of airborne particles.* 2nd ed. New York: John Wiley & Sons, Inc., 1999.

115. Hirano S, Fujitani Y, Furuyama A, Kanno S. Uptake and cytotoxic effects of multi-walled carbon nanotubes in human bronchial epithelial cells. *Toxicol Appl Pharmacol* 2010;249:8-15.

116. Hirano S, Kanno S, Furuyama A. Multi-walled carbon nanotubes injure the plasma membrane of macrophages. *Toxicol Appl Pharmacol* 2008;232:244-251.

117. Hirsch A, Vostrowsky O. Functionalization of carbon nanotubes. In: Schluter AD, ed. *Functional molecular nanostructures. Topics in Current Chemistry*. Vol 245. Pp 193-237. Berlin, Heidelberg: Springer-Verlag, 2005.

118. Holt BD, Short PA, Rape AD, Wang YL, Islam MF, Dahl KN. Carbon nanotubes reorganize actin structures in cells and ex vivo. *ACS Nano* 2010;4:4872-4878.

119. Hou PX, Xu ST, Ying Z, Yang QH, Liu C, Cheng HM. Hydrogen adsorption/desorption behavior of multi-walled carbon nanotubes with different diameters. *Carbon* 2003;41:2471-2476.

120. Hu X, Cook S, Wang P, Hwang HM, Liu X, Williams QL. In vitro evaluation of cytotoxicity of engineered carbon nanotubes in selected human cell lines. *Sci Total Environ* 2010;408: 1812-1817.

121. Huang X, McLean RS, Zheng M. High-resolution length sorting and purification of DNA-wrapped carbon nanotubes by size-exclusion chromatography. *Anal Chem* 2005;77:6225-6228.

122. Huczko A, Lange H. Carbon nanotubes: Experimental evidence for a null risk of skin irritation and allergy. *Fullerenes Science and Technology* 2001;9:247-250.

123. Huczko A, Lange H, Bystrzejewski M, Baranowski P, Grubek-Jaworska H, Nejman P, Przybyłowski T, Czuminska K, Glapinski J, Walton DRM, Kroto HW. Pulmonary toxicity of 1-D nanocarbon materials. *Fullerenes, Nanotubes, and Carbon Nanostructures* 2005;13: 141-145.

124. Huczko A, Lange H, Calko E, Grubek-Jaworska H, Droszcz P. Physiological testing of carbon nanotubes: Are they asbestos-like? *Fullerenes Science and Technology* 2001;9:251-254.

125. Hussain F, Hojjati M, Okamoto M, Gorga RE. Review article: Polymer-matrix nanocomposites, processing, manufacturing, and application: An overview. *J Comp Mat* 2006;40:1511-1575.

126. Högberg SM, Åkerstedt HO, Lundström S, Freund JB. Respiratory deposition of fibers in the non-inertial regime - development and application of a semi-analytical model. *Aerosol Sci Technol* 2010;44:847-860.

127. ICRP. *Human respiratory tract model for radiological protection. ICRP Publication 66.* Ann. ICRP 24 (1-3). Ottawa, Ontario, Canada: The International Commission on Radiological Protection, 1994.

128. IFA. *Criteria for assessment of the effectiveness of protective measures*. http://www.dguv.de/ifa/en/fac/nanopartikel/beurteilungsmassstaebe/index.jsp (assessed Sep 3, 2010). Sankt Augustin, Germany: Institut fuer Arbeitsschutz der Deutschen Gesetzlichen

Unfallversicherung (the Institute for Occupational Safety and Health of the German Social Accident Insurance), 2009.

129. Iijima S. Helical microtubules of graphitic carbon. *Nature* 1991;354:56-58.
130. Iijima S, Brabec C, Maiti A, Bernholc J. Structural flexibility of carbon nanotubes. *J Chem Phys* 1996;104:2089-2092.
131. ILSI. The relevance of the rat lung response to particle overload for human risk assessment: a workshop consensus report. ILSI Risk Science Institute Workshop Participants. *Inhal Toxicol* 2000;12:1-17.
132. Ingle T, Dervishi E, Biris AR, Mustafa T, Buchanan RA, Biris AS. Raman spectroscopy analysis and mapping the biodistribution of inhaled carbon nanotubes in the lungs and blood of mice. *J Appl Toxicol* 2013;33:1044-1052.
133. Inoue K, Koike E, Yanagisawa R, Hirano S, Nishikawa M, Takano H. Effects of multi-walled carbon nanotubes on a murine allergic airway inflammation model. *Toxicol Appl Pharmacol* 2009;237:306-316.
134. Inoue K, Takano H, Koike E, Yanagisawa R, Sakurai M, Tasaka S, Ishizaka A, Shimada A. Effects of pulmonary exposure to carbon nanotubes on lung and systemic inflammation with coagulatory disturbance induced by lipopolysaccharide in mice. *Exp Biol Med (Maywood)* 2008;233:1583-1590.
135. Inoue K, Yanagisawa R, Koike E, Nishikawa M, Takano H. Repeated pulmonary exposure to single-walled carbon nanotubes exacerbates allergic inflammation of the airway: Possible role of oxidative stress. *Free Radic Biol Med* 2010;48:924-934.
136. Ishigami M, Choi HJ, Aloni S, Louie SG, Cohen ML, Zettl A. Identifying defects in nanoscale materials. *Phys Rev Lett* 2004;93:196803.
137. Jacobsen NR, Møller P, Jensen KA, Vogel U, Ladefoged O, Loft S, Wallin H. Lung inflammation and genotoxicity following pulmonary exposure to nanoparticles in ApoE-/- mice. *Part Fibre Toxicol* 2009;6:2.
138. Jacobsen NR, Pojana G, White P, Moller P, Cohn CA, Korsholm KS, Vogel U, Marcomini A, Loft S, Wallin H. Genotoxicity, cytotoxicity, and reactive oxygen species induced by single-walled carbon nanotubes and C(60) fullerenes in the FE1-Mutatrade markMouse lung epithelial cells. *Environ Mol Mutagen* 2008;49:476-487.
139. Jasti R, Bhattacharjee J, Neaton JB, Bertozzi CR. Synthesis, characterization, and theory of [9]-, [12]-, and [18]cycloparaphenylene: carbon nanohoop structures. *J Am Chem Soc* 2008;130:17646-17647.
140. Ji Z, Zhang D, Li L, Shen X, Deng X, Dong L, Wu M, Liu Y. The hepatotoxicity of multi-walled carbon nanotubes in mice. *Nanotechnology* 2009;20:445101.
141. Jia FM, Wu L, Meng J, Yang M, Kong H, Liu TJ, Xu HY. Preparation, characterization and fluorescent imaging of multi-walled carbon nanotube-porphyrin conjugate. *J Mater Chem* 2009;19:8950-8957.
142. Jia G, Wang H, Yan L, Wang X, Pei R, Yan T, Zhao Y, Guo X. Cytotoxicity of carbon nanomaterials: single-wall nanotube, multi-wall nanotube, and fullerene. *Environ Sci Technol* 2005;39:1378-1383.
143. Johnson DR, Methner MM, Kennedy AJ, Steevens JA. Potential for occupational exposure to engineered carbon-based nanomaterials in environmental laboratory studies. *Environ Health Perspect* 2010;118:49-54.
144. Jorio A, Saito R, Hafner JH, Lieber CM, Hunter M, McClure T, Dresselhaus G, Dresselhaus MS. Structural (n, m) determination of isolated single-wall carbon nanotubes by resonant Raman scattering. *Phys Rev Lett* 2001;86:1118-1121.
145. Jos A, Pichardo S, Puerto M, Sanchez E, Grilo A, Cameán M. Cytotoxicity of carboxylic acid functionalized single wall carbon nanotubes on the human intestinal cell line Caco-2. *Toxicol In Vitro* 2009;23:1491-1496.

146. Journet C, Maser WK, Bernier P, Loiseau A, de la Chapelle ML, Lefrant S, Deniard P, Lee R, Fischer JE. Large-scale production of single-walled carbon nanotubes by the electric-arc technique. *Nature* 1997;388:756-758.

147. Kagan VE, Konduru NV, Feng W, Allen BL, Conroy J, Volkov Y, Vlasova II, Belikova NA, Yanamala N, Kapralov A, Tyurina YY, Shi J, Kisin ER, Murray AR, Franks J, Stolz D, Gou P, Klein-Seetharaman J, Fadeel B, Star A, Shvedova AA. Carbon nanotubes degraded by neutrophil myeloperoxidase induce less pulmonary inflammation. *Nat Nanotechnol* 2010;5: 354-359.

148. Kagan VE, Tyurina YY, Tyurin VA, Konduru NV, Potapovich AI, Osipov AN, Kisin ER, Schwegler-Berry D, Mercer R, Castranova V, Shvedova AA. Direct and indirect effects of single walled carbon nanotubes on RAW 264.7 macrophages: role of iron. *Toxicol Lett* 2006;165:88-100.

149. Kam NW, O'Connell M, Wisdom JA, Dai H. Carbon nanotubes as multifunctional biological transporters and near-infrared agents for selective cancer cell destruction. *Proc Natl Acad Sci U S A* 2005;102:11600-11605.

150. Kang B, Yu D, Dai Y, Chang S, Chen D, Ding Y. Biodistribution and accumulation of intravenously administered carbon nanotubes in mice probed by Raman spectroscopy and fluorescent labeling. *Carbon* 2009;47:1189-1192.

151. Karlsson HL, Cronholm P, Gustafsson J, Möller L. Copper oxide nanoparticles are highly toxic: a comparison between metal oxide nanoparticles and carbon nanotubes. *Chem Res Toxicol* 2008;21:1726-1732.

152. Karthikeyan S, Mahalingam P, Karthik M. Large scale synthesis of carbon nanotubes. *E-Journal of Chemistry* 2009;6:1-12.

153. Kato T, Totsuka Y, Ishino K, Matsumoto Y, Tada Y, Nakae D, Goto S, Masuda S, Ogo S, Kawanishi M, Yagi T, Matsuda T, Watanabe M, Wakabayashi K. Genotoxicity of multi-walled carbon nanotubes in both in vitro and in vivo assay systems. *Nanotoxicology* 2013; 7:452-461.

154. KEMI. *Användningen av nanomaterial i Sverige 2008 – analys och prognos*. PM 1/9. Sundbyberg, Stockholm: Kemikalieinspektionen (Swedish Chemicals Agency), 2008 (in Swedish).

155. Keren S, Zavaleta C, Cheng Z, de la Zerda A, Gheysens O, Gambhir SS. Noninvasive molecular imaging of small living subjects using Raman spectroscopy. *Proc Natl Acad Sci U S A* 2008;105:5844-5849.

156. Kim JS, Lee K, Lee YH, Cho HS, Kim KH, Choi KH, Lee SH, Song KS, Kang CS, Yu IJ. Aspect ratio has no effect on genotoxicity of multi-wall carbon nanotubes. *Arch Toxicol* 2011;85:775-786.

157. Kim JS, Song KS, Joo HJ, Lee JH, Yu IJ. Determination of cytotoxicity attributed to multi-wall carbon nanotubes (MWCNT) in normal human embryonic lung cell (WI-38) line. *J Toxicol Environ Health A* 2010;73:1521-1529.

158. Kishore AS, Surekha P, Murthy PB. Assessment of the dermal and ocular irritation potential of multi-walled carbon nanotubes by using in vitro and in vivo methods. *Toxicol Lett* 2009; 191:268-274.

159. Kisin ER, Murray AR, Keane MJ, Shi XC, Schwegler-Berry D, Gorelik O, Arepalli S, Castranova V, Wallace WE, Kagan VE, Shvedova AA. Single-walled carbon nanotubes: geno- and cytotoxic effects in lung fibroblast V79 cells. *J Toxicol Environ Health A* 2007; 70:2071-2079.

160. Kitiyanan B, Alvarez WE, Harwell JH, Resasco DE. Controlled production of single-wall carbon nanotubes by catalytic decomposition of CO on bimetallic Co-Mo catalysts. *Chem Phys Lett* 2000;317:497-503.

161. Kiura K, Sato Y, Yasuda M, Fugetsu B, Watari F, Tohji K, Shibata K. Activation of human monocytes and mouse splenocytesby single-walled carbon nanotubes. *J Biomed Nanotechnol* 2005;1:359-364.

162. Klobes P, Munro RG. *Porosity and specific surface area measurements for solid materials*. Special publication 960-17. 89 pp. NIST recommended practice guide. National Institute of Standards and Technology, US Department of Commerce, 2006.

163. Kobayashi N, Naya M, Ema M, Endoh S, Maru J, Mizuno K, Nakanishi J. Biological response and morphological assessment of individually dispersed multi-wall carbon nanotubes in the lung after intratracheal instillation in rats. *Toxicology* 2010;276:143-153.

164. Kobayashi N, Naya M, Mizuno K, Yamamoto K, Ema M, Nakanishi J. Pulmonary and systemic responses of highly pure and well-dispersed single-wall carbon nanotubes after intratracheal instillation in rats. *Inhal Toxicol* 2011;23:814-828.

165. Kolosnjaj-Tabi J, Hartman KB, Boudjemaa S, Ananta JS, Morgant G, Szwarc H, Wilson LJ, Moussa F. In vivo behavior of large doses of ultrashort and full-length single-walled carbon nanotubes after oral and intraperitoneal administration to Swiss mice. *ACS Nano* 2010;4: 1481-1492.

166. Kostarelos K, Bianco A, Prato M. Promises, facts and challenges for carbon nanotubes in imaging and therapeutics. *Nat Nanotechnol* 2009;4:627-633.

167. Koyama S, Ahm Kim YA, Hayashi T, Takeuchi K, Fujii C, Kuroiwa N, Koyama H, Tsukahara T, Endo M. In vivo immunological toxicity in mice of carbon nanotubes with impurities. *Carbon* 2009;47:1365-1372.

168. Koyama S, Endo M, Kim YA, Hayashi T, Yanagisawa T, Osaka K, Koyama H, Haniu H, Kuroiwa N. Role of systemic T-cells and histopathological aspects after subcutaneous implantation of various carbon nanotubes in mice. *Carbon* 2006;44:1079-1092.

169. Kumar M, Ando Y. Chemical vapor deposition of carbon nanotubes: a review on growth mechanism and mass production. *J Nanosci Nanotechnol* 2010;10:3739-3758.

170. Kymakis E, Alexandou I, Amaratunga GAJ. Single-walled carbon nanotube-polymer composites: electrical, optical and structural investigation. *Synthetic Metals* 2002;127:59-62.

171. Köhler AR, Som C, Helland A, Gottschalk F. Studying the potential release of carbon nanotubes throughout the application life cycle. *J Cleaner Production* 2008;16:927-937.

172. Lacerda L, Herrero MA, Venner K, Bianco A, Prato M, Kostarelos K. Carbon-nanotube shape and individualization critical for renal excretion. *Small* 2008;4:1130-1132.

173. Lacerda L, Soundararajan A, Singh R, Pastorin G, Al-Jamal KT, Turton J, Frederik P, Herrero MA, Li S, Bao A, Emfietzoglou D, Mather S, Phillips WT, Prato M, Bianco A, Goins B, Kostarelos K. Dynamic imaging of functionalized multi-walled carbon nanotube systemic circulation and urinary excretion. *Advanced Material* 2008;20:225-230.

174. Lam CW, James JT, McCluskey R, Arepalli S, Hunter RL. A review of carbon nanotube toxicity and assessment of potential occupational and environmental health risks. *Crit Rev Toxicol* 2006;36:189-217.

175. Lam CW, James JT, McCluskey R, Hunter RL. Pulmonary toxicity of single-wall carbon nanotubes in mice 7 and 90 days after intratracheal instillation. *Toxicol Sci* 2004;77:126-134.

176. Lee BG, Lee JH, Bae GN. Size response of an SMPS–APS system to commercial multi-walled carbon nanotubes. *J Nanopart Res* 2010;12:501-512.

177. Lee JH, Lee SB, Bae GN, Jeon KS, Yoon JU, Ji JH, Sung JH, Lee BG, Yang JS, Kim HY, Kang CS, Yu IJ. Exposure assessment of carbon nanotube manufacturing workplaces. *Inhal Toxicol* 2010;22:369-381.

178. Legramante JM, Valentini F, Magrini A, Palleschi G, Sacco S, Iavicoli I, Pallante M, Moscone D, Galante A, Bergamaschi E, Bergamaschi A, Pietroiusti A. Cardiac autonomic regulation after lung exposure to carbon nanotubes. *Hum Exp Toxicol* 2009;28:369-375.

179. Li J, Xue Y, Han B, Li Q, Liu L, Xiao T, Li W. Application of X-ray phase contrast imaging technique in detection of pulmonary lesions induced by multi-walled carbon nanotubes in rats. *J Nanosci Nanotechnol* 2008;8:3357-3362.

180. Li JG, Li QN, Xu JY, Cai XQ, Liu RL, Li YJ, Ma JF, Li WX. The pulmonary toxicity of multi-wall carbon nanotubes in mice 30 and 60 days after inhalation exposure. *J Nanosci Nanotechnol* 2009;9:1384-1387.

181. Li JG, Li WX, Xu JY, Cai XQ, Liu RL, Li YJ, Zhao QF, Li QN. Comparative study of pathological lesions induced by multiwalled carbon nanotubes in lungs of mice by intratracheal instillation and inhalation. *Environ Toxicol* 2007;22:415-421.

182. Li YS, Li YF, Li QN, Li JG, Li J, Huang Q, Li WX. The acute pulmonary toxicity in mice induced by multiwall carbon nanotubes, benzene, and their combination. *Environ Toxicol* 2010;25:409-417.

183. Li YY, Hsieh CC. Synthesis of carbon nanotubes by combustion of a paraffin wax candle. *Micro & Nano Letters* 2007;2:63-66.

184. Li Z, Hulderman T, Salmen R, Chapman R, Leonard SS, Young SH, Shvedova A, Luster MI, Simeonova PP. Cardiovascular effects of pulmonary exposure to single-wall carbon nanotubes. *Environ Health Perspect* 2007;115:377-382.

185. Liang G, Yin L, Zhang J, Liu R, Zhang T, Ye B, Pu Y. Effects of subchronic exposure to multi-walled carbon nanotubes on mice. *J Toxicol Environ Health A* 2010;73:463-470.

186. Lim JH, Kim SH, Lee IC, Moon C, Shin DH, Kim HC, Kim JC. Evaluation of maternal toxicity in rats exposed to multi-wall carbon nanotubes during pregnancy. *Environ Health Toxicol* 2011;26:e2011006.

187. Lin T, Bajpai V, Ji T, Dai LM. Chemistry of carbon nanotubes. *Aust J Chem* 2003;56:635-651.

188. Lindberg HK, Falck GC, Suhonen S, Vippola M, Vanhala E, Catalan J, Savolainen K, Norppa H. Genotoxicity of nanomaterials: DNA damage and micronuclei induced by carbon nanotubes and graphite nanofibres in human bronchial epithelial cells in vitro. *Toxicol Lett* 2009;186:166-173.

189. Lippmann M. Effects of fiber characteristics on lung deposition, retention, and disease. *Environ Health Perspect* 1990;88:311-317.

190. Liu A, Sun K, Yang J, Zhao D. Toxicological effects of multi-wall carbon nanotubes in rats. *J Nanopart Res* 2008;10:1303-1307.

191. Liu D, Yi C, Zhang D, Zhang J, Yang M. Inhibition of proliferation and differentiation of mesenchymal stem cells by carboxylated carbon nanotubes. *ACS Nano* 2010;4:2185-2195.

192. Liu J, Rinzler AG, Dai H, Hafner JH, Bradley RK, Boul PJ, Lu A, Iverson T, Shelimov K, Huffman CB, Rodriguez-Macias F, Shon YS, Lee TR, Colbert DT, Smalley RE. Fullerene pipes. *Science* 1998;280:1253-1256.

193. Liu Z, Cai W, He L, Nakayama N, Chen K, Sun X, Chen X, Dai H. In vivo biodistribution and highly efficient tumour targeting of carbon nanotubes in mice. *Nat Nanotechnol* 2007; 2:47-52.

194. Liu Z, Davis C, Cai W, He L, Chen X, Dai H. Circulation and long-term fate of functionalized, biocompatible single-walled carbon nanotubes in mice probed by Raman spectroscopy. *Proc Natl Acad Sci U S A* 2008;105:1410-1415.

195. Lu X, Chen Z. Curved pi-conjugation, aromaticity, and the related chemistry of small fullerenes (< C60) and single-walled carbon nanotubes. *Chem Rev* 2005;105:3643-3696.

196. Ludvigsson, L. *Emission and exposure assessment of arc discharge produced multiwalled carbon nanotubes in an industrial environment.* Ergonomics and Aerosol Technology, Lund University, 2012 (master's degree).

197. Lynch I, Dawson KA. Protein-nanoparticle interactions. *Nano Today* 2008;3:40-47.

198. Ma-Hock L, Treumann S, Strauss V, Brill S, Luizi F, Mertler M, Wiench K, Gamer AO, van Ravenzwaay B, Landsiedel R. Inhalation toxicity of multiwall carbon nanotubes in rats exposed for 3 months. *Toxicol Sci* 2009;112:468-481.

199. Magrez A, Kasas S, Salicio V, Pasquier N, Seo JW, Celio M, Catsicas S, Schwaller B, Forró L. Cellular toxicity of carbon-based nanomaterials. *Nano Lett* 2006;6:1121-1125.

200. Mahar B, Laslau C, Yip R, Sun Y. Development of carbon nanotube-based sensors - A review. *Ieee Sensors Journal* 2007;7:266-284.

201. Malarkey EB, Reyes RC, Zhao B, Haddon RC, Parpura V. Water soluble single-walled carbon nanotubes inhibit stimulated endocytosis in neurons. *Nano Lett* 2008;8:3538-3542.

202. Manna SK, Sarkar S, Barr J, Wise K, Barrera EV, Jejelowo O, Rice-Ficht AC, Ramesh GT. Single-walled carbon nanotube induces oxidative stress and activates nuclear transcription factor-kappaB in human keratinocytes. *Nano Lett* 2005;5:1676-1684.

203. Maynard AD, Baron PA, Foley M, Shvedova AA, Kisin ER, Castranova V. Exposure to carbon nanotube material: aerosol release during the handling of unrefined single-walled carbon nanotube material. *J Toxicol Environ Health A* 2004;67:87-107.

204. Maynard AD, Ku BK, Emery M, Stolzenburg M, McMurry PH. Measuring particle size-dependent physicochemical structure in airborne single walled carbon nanotube agglomerates. *J Nanopart Res* 2007;9:85-92.

205. McDevitt MR, Chattopadhyay D, Jaggi JS, Finn RD, Zanzonico PB, Villa C, Rey D, Mendenhall J, Batt CA, Njardarson JT, Scheinberg DA. PET imaging of soluble yttrium-86-labeled carbon nanotubes in mice. *PLoS One* 2007;2:e907.

206. Mercer RR, Hubbs AF, Scabilloni JF, Wang L, Battelli LA, Friend S, Castranova V, Porter DW. Pulmonary fibrotic response to aspiration of multi-walled carbon nanotubes. *Part Fibre Toxicol* 2011;8:21.

207. Mercer RR, Hubbs AF, Scabilloni JF, Wang L, Battelli LA, Schwegler-Berry D, Castranova V, Porter DW. Distribution and persistence of pleural penetrations by multi-walled carbon nanotubes. *Part Fibre Toxicol* 2010;7:28.

208. Mercer RR, Scabilloni J, Wang L, Kisin E, Murray AR, Schwegler-Berry D, Shvedova AA, Castranova V. Alteration of deposition pattern and pulmonary response as a result of improved dispersion of aspirated single-walled carbon nanotubes in a mouse model. *Am J Physiol Lung Cell Mol Physiol* 2008;294:L87-97.

209. Methner M, Hodson L, Dames A, Geraci C. Nanoparticle emission assessment technique (NEAT) for the identification and measurement of potential inhalation exposure to engineered nanomaterials--Part B: Results from 12 field studies. *J Occup Environ Hyg* 2010; 7:163-176.

210. Methner M, Hodson L, Geraci C. Nanoparticle emission assessment technique (NEAT) for the identification and measurement of potential inhalation exposure to engineered nanomaterials--part A. *J Occup Environ Hyg* 2010;7:127-132.

211. Migliore L, Saracino D, Bonelli A, Colognato R, D'Errico MR, Magrini A, Bergamaschi A, Bergamaschi E. Carbon nanotubes induce oxidative DNA damage in RAW 264.7 cells. *Environ Mol Mutagen* 2010;51:294-303.

212. Mitchell LA, Gao J, Wal RV, Gigliotti A, Burchiel SW, McDonald JD. Pulmonary and systemic immune response to inhaled multiwalled carbon nanotubes. *Toxicol Sci* 2007; 100:203-214.

213. Mitchell LA, Lauer FT, Burchiel SW, McDonald JD. Mechanisms for how inhaled multiwalled carbon nanotubes suppress systemic immune function in mice. *Nat Nanotechnol* 2009;4:451-456.

214. Morgan A. Deposition of inhaled asbestos and man-made mineral fibres in the respiratory tract. *Ann Occup Hyg* 1995;39:747-758.

215. Morimoto Y, Hirohashi M, Kobayashi N, Ogami A, Horie M, Oyabu T, Myojo T, Hashiba M, Mizuguchi Y, Kambara T, Lee BW, Kuroda E, Shimada M, Wang WN, Mizuno K, Yamamoto K, Fujita K, Nakanishi J, Tanaka I. Pulmonary toxicity of well-dispersed single-wall carbon nanotubes after inhalation. *Nanotoxicology* 2012;6:766-775.

216. Morimoto Y, Hirohashi M, Ogami A, Oyabu T, Myojo T, Todoroki M, Yamamoto M, Hashiba M, Mizuguchi Y, Lee BW, Kuroda E, Shimada M, Wang WN, Yamamoto K, Fujita K, Endoh S, Uchida K, Kobayashi N, Mizuno K, Inada M, Tao H, Nakazato T, Nakanishi J,

Tanaka I. Pulmonary toxicity of well-dispersed multi-wall carbon nanotubes following inhalation and intratracheal instillation. *Nanotoxicology* 2012;6:587-599.

217. Morrow PE. Possible mechanisms to explain dust overloading of the lungs. *Fundam Appl Toxicol* 1988;10:369-384.
218. Mu Q, Broughton DL, Yan B. Endosomal leakage and nuclear translocation of multiwalled carbon nanotubes: developing a model for cell uptake. *Nano Lett* 2009;9:4370-4375.
219. Muller J, Decordier I, Hoet PH, Lombaert N, Thomassen L, Huaux F, Lison D, Kirsch-Volders M. Clastogenic and aneugenic effects of multi-wall carbon nanotubes in epithelial cells. *Carcinogenesis* 2008;29:427-433.
220. Muller J, Delos M, Panin N, Rabolli V, Huaux F, Lison D. Absence of carcinogenic response to multiwall carbon nanotubes in a 2-year bioassay in the peritoneal cavity of the rat. *Toxicol Sci* 2009;110:442-448.
221. Muller J, Huaux F, Fonseca A, Nagy JB, Moreau N, Delos M, Raymundo-Pinero E, Beguin F, Kirsch-Volders M, Fenoglio I, Fubini B, Lison D. Structural defects play a major role in the acute lung toxicity of multiwall carbon nanotubes: toxicological aspects. *Chem Res Toxicol* 2008;21:1698-1705.
222. Muller J, Huaux F, Moreau N, Misson P, Heilier JF, Delos M, Arras M, Fonseca A, Nagy JB, Lison D. Respiratory toxicity of multi-wall carbon nanotubes. *Toxicol Appl Pharmacol* 2005; 207:221-231.
223. Murphy FA, Poland CA, Duffin R, Al-Jamal KT, Ali-Boucetta H, Nunes A, Byrne F, Prina-Mello A, Volkov Y, Li S, Mather SJ, Bianco A, Prato M, Macnee W, Wallace WA, Kostarelos K, Donaldson K. Length-dependent retention of carbon nanotubes in the pleural space of mice initiates sustained inflammation and progressive fibrosis on the parietal pleura. *Am J Pathol* 2011;178:2587-2600.
224. Murphy FA, Poland CA, Duffin R, Donaldson K. Length-dependent pleural inflammation and parietal pleural responses after deposition of carbon nanotubes in the pulmonary air-spaces of mice. *Nanotoxicology* 2013;7:1157-1167.
225. Murphy FA, Schinwald A, Poland CA, Donaldson K. The mechanism of pleural inflammation by long carbon nanotubes: interaction of long fibres with macrophages stimulates them to amplify pro-inflammatory responses in mesothelial cells. *Part Fibre Toxicol* 2012;9:8.
226. Murr LE, Bang JJ, Esquivel EV, Guerrero PA, Lopez A. Carbon nanotubes, nanocrystal forms, and complex nanoparticle aggregates in common fuel-gas combustion sources and the ambient air. *J Nanopart Res* 2004;6:241-251.
227. Murr LE, Esquivel EV, Bang JJ, de la Rosa G, Gardea-Torresdey JL. Chemistry and nano-particulate compositions of a 10,000 year-old ice core melt water. *Water Res* 2004;38:4282-4296.
228. Murr LE, Garza KM. Natural and anthropogenic environmental nanoparticulates: Their microstructural characterization and respiratory health implications. *Atmospheric Environment* 2009;43:2683-2692.
229. Murr LE, Guerrero PA. Carbon nanotubes in wood soot. *Atmos Sci Lett* 2006;7:93-95.
230. Murr LE, Soto KF. A TEM study of soot, carbon nanotubes, and related fullerene nano-polyhedra in common fuel-gas combustion sources. *Materials Characterization* 2005;55: 50-65.
231. Murray AR, Kisin E, Leonard SS, Young SH, Kommineni C, Kagan VE, Castranova V, Shvedova AA. Oxidative stress and inflammatory response in dermal toxicity of single-walled carbon nanotubes. *Toxicology* 2009;257:161-171.
232. Mutlu GM, Budinger GR, Green AA, Urich D, Soberanes S, Chiarella SE, Alheid GF, McCrimmon DR, Szleifer I, Hersam MC. Biocompatible nanoscale dispersion of single-walled carbon nanotubes minimizes in vivo pulmonary toxicity. *Nano Lett* 2010;10:1664-1670.

233. Nakanishi J (ed). *Risk assessment of manufactured nanomaterials: carbon nanotubes (CNT)*. Final report issued on Aug 17, 2011. Executive summary. NEDO project (P06041) – Research and development of nanoparticle characterization methods, 2011.

234. Nanocyl. *Responsible care and nanomaterials case study Nanocyl*. http://www.cefic.org/Documents/ResponsibleCare/04_Nanocyl.pdf (assessed May 28, 2013). Presentation at European Responsible Care Conference, Prague, October 21-23, 2009.

235. NICNAS. *Human health hazard assessment and classification of carbon nanotubes.* Canberra, Australia: National Industrial Chemicals Notification and Assessment Scheme, Safe Work Australia, 2012.

236. NIOSH. Asbestos and other fibers by PCM. Method 7400: Issue 2. In: *NIOSH Manual of* Analytical Methods (NMAM), Fourth edition. http://www.cdc.gov/niosh/docs/2003-154/pdfs/7400.pdf. Atlanta, Georgia: Centers for Disease Control and Prevention, National Institute for Occupational Safety and Health, 1994.

237. NIOSH. Asbestos by TEM. Method 7402: Issue 2. In: *NIOSH Manual of Analytical Methods* (NMAM), Fourth edition. http://www.cdc.gov/niosh/docs/2003-154/pdfs/7402.pdf. Atlanta, Georgia: Centers for Disease Control and Prevention, National Institute for Occupational Safety and Health, 1994.

238. NIOSH. Diesel particulate matter (as elemental carbon). Method 5040: Issue 3. In: *NIOSH Manual of Analytical Methods (NMAM), Fourth edition*. http://www.cdc.gov/niosh/docs/2003-154/pdfs/5040.pdf. Atlanta, Georgia: Centers for Disease Control and Prevention, National Institute for Occupational Safety and Health, 2003.

239. NIOSH. *Approaches to safe nanotechnology. Managing the health and safety concerns associated with engineered nanomaterials.* Cincinnati, OH: US Department of Health and Human Services, Centers for Disease Control and Prevention, National Institute for Occupational Safety and Health, 2009.

240. NIOSH. *Occupational exposure to carbon nanotubes and nanofibers. Current intelligence bulletin 65.* Cincinnati, OH: US Department of Health and Human Services, Centers for Disease Control and Prevention, National Institute for Occupational Safety and Health, 2013.

241. Nygaard UC, Hansen JS, Samuelsen M, Alberg T, Marioara CD, Lovik M. Single-walled and multi-walled carbon nanotubes promote allergic immune responses in mice. *Toxicol Sci* 2009; 109:113-123.

242. Oberdorster G, Oberdorster E, Oberdorster J. Nanotoxicology: an emerging discipline evolving from studies of ultrafine particles. *Environ Health Perspect* 2005;113:823-839.

243. Ochoa-Olmos OE, Montero-Montoya R, Serrano-Garcia L, Basiuk EV. Genotoxic properties of nylon-6/MWNTs nanohybrid. *J Nanosci Nanotechnol* 2009;9:4727-4734.

244. Ogura I, Sakurai H, Mizuno K, Gamo M. Release potential of single-wall carbon nanotubes produced by super-growth method during manufacturing and handling. *J Nanopart Res* 2011; 13:1265-1280.

245. Pacurari M, Yin XJ, Ding M, Leonard SS, Schwegler-Berry D, Ducatman BS, Chirila M, Endo M, Castranova V, Vallyathan V. Oxidative and molecular interactions of multi-wall carbon nanotubes (MWCNT) in normal and malignant human mesothelial cells. *Nanotoxicology* 2008;2:155-170.

246. Pacurari M, Yin XJ, Zhao J, Ding M, Leonard SS, Schwegler-Berry D, Ducatman BS, Sbarra D, Hoover MD, Castranova V, Vallyathan V. Raw single-wall carbon nanotubes induce oxidative stress and activate MAPKs, AP-1, NF-kappaB, and Akt in normal and malignant human mesothelial cells. *Environ Health Perspect* 2008;116:1211-1217.

247. Palomäki J, Karisola P, Pylkkänen L, Savolainen K, Alenius H. Engineered nanomaterials cause cytotoxicity and activation on mouse antigen presenting cells. *Toxicology* 2010;267: 125-131.

248. Palomäki J, Välimäki E, Sund J, Vippola M, Clausen PA, Jensen KA, Savolainen K, Matikainen S, Alenius H. Long, needle-like carbon nanotubes and asbestos activate the NLRP3 inflammasome through a similar mechanism. *ACS Nano* 2011;5:6861-6870.

249. Park EJ, Cho WS, Jeong J, Yi J, Choi K, Park K. Pro-inflammatory and potential allergic responses resulting from B cell activation in mice treated with multi-walled carbon nanotubes by intratracheal instillation. *Toxicology* 2009;259:113-121.

250. Patlolla A, McGinnis B, Tchounwou P. Biochemical and histopathological evaluation of functionalized single-walled carbon nanotubes in Swiss-Webster mice. *J Appl Toxicol* 2011; 31:75-83.

251. Patlolla A, Patlolla B, Tchounwou P. Evaluation of cell viability, DNA damage, and cell death in normal human dermal fibroblast cells induced by functionalized multiwalled carbon nanotube. *Mol Cell Biochem* 2010;338:225-232.

252. Patlolla AK, Hussain SM, Schlager JJ, Patlolla S, Tchounwou PB. Comparative study of the clastogenicity of functionalized and nonfunctionalized multiwalled carbon nanotubes in bone marrow cells of Swiss-Webster mice. *Environ Toxicol* 2010;25:608-621.

253. Pauluhn J. Comparative pulmonary response to inhaled nanostructures: considerations on test design and endpoints. *Inhal Toxicol* 2009;21 Suppl 1:40-54.

254. Pauluhn J. Multi-walled carbon nanotubes (Baytubes): approach for derivation of occupational exposure limit. *Regul Toxicol Pharmacol* 2010;57:78-89.

255. Pauluhn J. Subchronic 13-week inhalation exposure of rats to multiwalled carbon nanotubes: toxic effects are determined by density of agglomerate structures, not fibrillar structures. *Toxicol Sci* 2010;113:226-242.

256. Paur HR, Cassee FR, Teeguarden J, Fissan H, Diabate S, Aufderheide M, Kreyling W, Hänninen O, Kasper G, Riediker M, Rothen-Rutishauser B, Schmid O. In-vitro cell exposure studies for the assessment of nanoparticle toxicity in the lung—A dialog between aerosol science and biology. *J Aerosol Sci* 2011;42:668-692.

257. Peigney A, Laurent C, Flahaut E, Bacsa RR, Rousset A. Specific surface area of carbon nanotubes and bundles of carbon nanotubes. *Carbon* 2001;39:507-514.

258. Pietroiusti A, Massimiani M, Fenoglio I, Colonna M, Valentini F, Palleschi G, Camaioni A, Magrini A, Siracusa G, Bergamaschi A, Sgambato A, Campagnolo L. Low doses of pristine and oxidized single-wall carbon nanotubes affect mammalian embryonic development. *ACS Nano* 2011;5:4624-4633.

259. Poland CA, Duffin R, Kinloch I, Maynard A, Wallace WA, Seaton A, Stone V, Brown S, Macnee W, Donaldson K. Carbon nanotubes introduced into the abdominal cavity of mice show asbestos-like pathogenicity in a pilot study. *Nat Nanotechnol* 2008;3:423-428.

260. Pop E, Mann D, Wang Q, Goodson K, Dai H. Thermal conductance of an individual single-wall carbon nanotube above room temperature. *Nano Lett* 2006;6:96-100.

261. Popov VN. Carbon nanotubes: properties and application. *Materials Science & Engineering R-Reports* 2004;43:61-102.

262. Porter AE, Gass M, Bendall JS, Muller K, Goode A, Skepper JN, Midgley PA, Welland M. Uptake of noncytotoxic acid-treated single-walled carbon nanotubes into the cytoplasm of human macrophage cells. *ACS Nano* 2009;3:1485-1492.

263. Porter AE, Gass M, Muller K, Skepper JN, Midgley PA, Welland M. Direct imaging of single-walled carbon nanotubes in cells. *Nat Nanotechnol* 2007;2:713-717.

264. Porter DW, Hubbs AF, Chen BT, McKinney W, Mercer RR, Wolfarth MG, Battelli L, Wu N, Sriram K, Leonard S, Andrew M, Willard P, Tsuruoka S, Endo M, Tsukada T, Munekane F, Frazer DG, Castranova V. Acute pulmonary dose-responses to inhaled multi-walled carbon nanotubes. *Nanotoxicology* 2013;7:1179-1194.

265. Porter DW, Hubbs AF, Mercer RR, Wu N, Wolfarth MG, Sriram K, Leonard S, Battelli L, Schwegler-Berry D, Friend S, Andrew M, Chen BT, Tsuruoka S, Endo M, Castranova V. Mouse pulmonary dose- and time course-responses induced by exposure to multi-walled carbon nanotubes. *Toxicology* 2010;269:136-147.

266. Prylutska SV, Grynyuk II, Grebinyk SM, Matyshevska OP, Prylutskyy YI, Ritter U, Siegmund C, Scharff P. Comparative study of biological action of fullerenes C-60 and carbon nanotubes in thymus cells. *Materialwissenschaft Und Werkstofftechnik* 2009;40:238-241.

267. Pulskamp K, Diabate S, Krug HF. Carbon nanotubes show no sign of acute toxicity but induce intracellular reactive oxygen species in dependence on contaminants. *Toxicol Lett* 2007;168:58-74.

268. Pulskamp K, Worle-Knirsch JM, Hennrich F, Kern K, Krug HF. Human lung epithelial cells show biphasic oxidative burst after single-walled carbon nanotube contact. *Carbon* 2007;45: 2241-2249.

269. Qu G, Bai Y, Zhang Y, Jia Q, Zhang W, Yan B. The effect of multiwalled carbon nanotube agglomeration on their accumulation in and damage to organs in mice. *Carbon* 2009;47: 2060-2069.

270. Radomski A, Jurasz P, Alonso-Escolano D, Drews M, Morandi M, Malinski T, Radomski MW. Nanoparticle-induced platelet aggregation and vascular thrombosis. *Br J Pharmacol* 2005;146:882-893.

271. Raja PM, Connolley J, Ganesan GP, Ci L, Ajayan PM, Nalamasu O, Thompson DM. Impact of carbon nanotube exposure, dosage and aggregation on smooth muscle cells. *Toxicol Lett* 2007;169:51-63.

272. Ravichandran P, Baluchamy S, Gopikrishnan R, Biradar S, Ramesh V, Goornavar V, Thomas R, Wilson BL, Jeffers R, Hall JC, Ramesh GT. Pulmonary biocompatibility assessment of inhaled single-wall and multiwall carbon nanotubes in BALB/c mice. *J Biol Chem* 2011;286: 29725-29733.

273. Ravichandran P, Periyakaruppan A, Sadanandan B, Ramesh V, Hall JC, Jejelowo O, Ramesh GT. Induction of apoptosis in rat lung epithelial cells by multiwalled carbon nanotubes. *J Biochem Mol Toxicol* 2009;23:333-344.

274. RCEP. *Novel materials in the environment: The case of nanotechnology*. 27th report. http://www.official-documents.gov.uk/document/cm74/7468/7468.pdf. London, UK: Royal Commission on Environmental Pollution, 2008.

275. Reddy AR, Krishna DR, Reddy YN, Himabindu V. Translocation and extra pulmonary toxicities of multi wall carbon nanotubes in rats. *Toxicol Mech Methods* 2010;20:267-272.

276. Reddy AR, Reddy YN, Krishna DR, Himabindu V. Pulmonary toxicity assessment of multiwalled carbon nanotubes in rats following intratracheal instillation. *Environ Toxicol* 2012;27: 211-219.

277. Reisch MS. Carbon nanotubes coat ship hull. *Chemical & Engineering News* 2009;87:18.

278. Rinzler AG, Liu J, Dai H, Nikolaev P, Huffman CB, Rodriguez-Macias FJ, Boul PJ, Lu AH, Heymann D, Colbert DT, Lee RS, Fischer JE, Rao AM, Eklund PC, Smalley RE. Large-scale purification of single-wall carbon nanotubes: process, product, and characterization. *Applied Physics a-Materials Science & Processing* 1998;67:29-37.

279. Rissler J, Swietlicki E, Bengtsson A, Boman C, Pagels J, Sandström T, Blomberg A, Löndahl J. Experimental determination of deposition of diesel exhaust particles in the human respiratory tract. *J Aerosol Sci* 2012;46:18-33.

280. Rotoli BM, Bussolati O, Barilli A, Zanello PP, Bianchi MG, Magrini A, Pietroiusti A, Bergamaschi A, Bergamaschi E. Airway barrier dysfunction induced by exposure to carbon nanotubes in vitro: which role for fiber length? *Hum Exp Toxicol* 2009;28:361-368.

281. Rotoli BM, Bussolati O, Bianchi MG, Barilli A, Balasubramanian C, Bellucci S, Bergamaschi E. Non-functionalized multi-walled carbon nanotubes alter the paracellular permeability of human airway epithelial cells. *Toxicol Lett* 2008;178:95-102.

282. Ruggiero A, Villa CH, Bander E, Rey DA, Bergkvist M, Batt CA, Manova-Todorova K, Deen WM, Scheinberg DA, McDevitt MR. Paradoxical glomerular filtration of carbon nanotubes. *Proc Natl Acad Sci U S A* 2010;107:12369-12374.

283. Ruoff RS, Tersoff J, Lorents DC, Subramoney S, Chan B. Radial deformation of carbon nanotubes by van-der-Waals forces. *Nature* 1993;364:514-516.

284. Ryman-Rasmussen JP, Cesta MF, Brody AR, Shipley-Phillips JK, Everitt JI, Tewksbury EW, Moss OR, Wong BA, Dodd DE, Andersen ME, Bonner JC. Inhaled carbon nanotubes reach the subpleural tissue in mice. *Nat Nanotechnol* 2009;4:747-751.

285. Ryman-Rasmussen JP, Tewksbury EW, Moss OR, Cesta MF, Wong BA, Bonner JC. Inhaled multiwalled carbon nanotubes potentiate airway fibrosis in murine allergic asthma. *Am J Respir Cell Mol Biol* 2009;40:349-358.

286. Saito S, Zettl A. Carbon nanotubes: Quantum cylinders of graphene. Vol 3. Pp 1-215. In: Burstein E, Cohen ML, Mills DL, Stiles PJ, eds. Series: *Contemporary concepts of condensed matter science*. Oxford, UK: Elsevier, 2008.

287. Sakamoto Y, Dai N, Hagiwara Y, Satoh K, Ohashi N, Fukamachi K, Tsuda H, Hirose A, Nishimura T, Hino O, Ogata A. Serum level of expressed in renal carcinoma (ERC)/ mesothelin in rats with mesothelial proliferative lesions induced by multi-wall carbon nanotube (MWCNT). *J Toxicol Sci* 2010;35:265-270.

288. Sakamoto Y, Nakae D, Fukumori N, Tayama K, Maekawa A, Imai K, Hirose A, Nishimura T, Ohashi N, Ogata A. Induction of mesothelioma by a single intrascrotal administration of multi-wall carbon nanotube in intact male Fischer 344 rats. *J Toxicol Sci* 2009;34:65-76.

289. Salvador-Morales C, Flahaut E, Sim E, Sloan J, Green ML, Sim RB. Complement activation and protein adsorption by carbon nanotubes. *Mol Immunol* 2006;43:193-201.

290. Sargent LM, Shvedova AA, Hubbs AF, Salisbury JL, Benkovic SA, Kashon ML, Lowry DT, Murray AR, Kisin ER, Friend S, McKinstry KT, Battelli L, Reynolds SH. Induction of aneuploidy by single-walled carbon nanotubes. *Environ Mol Mutagen* 2009;50:708-717.

291. Sass J, Musu T, Burns K, Illuminato I. Nanomaterials: brief review of policy frameworks in the US and Europe and recommendations from an occupational and environmental perspective. *European Journal of Oncology* 2008;13:211-218.

292. Sato Y, Yokoyama A, Shibata K, Akimoto Y, Ogino S, Nodasaka Y, Kohgo T, Tamura K, Akasaka T, Uo M, Motomiya K, Jeyadevan B, Ishiguro M, Hatakeyama R, Watari F, Tohji K. Influence of length on cytotoxicity of multi-walled carbon nanotubes against human acute monocytic leukemia cell line THP-1 in vitro and subcutaneous tissue of rats in vivo. *Mol Biosyst* 2005;1:176-182.

293. Savi M, Kalberer M, Lang D, Ryser M, Fierz M, Gaschen A, Ricka J, Geiser M. A novel exposure system for the efficient and controlled deposition of aerosol particles onto cell cultures. *Environ Sci Technol* 2008;42:5667-5674.

294. Savolainen K, Pylkkanen L, Norppa H, Falck G, Lindberg H, Tuomi T, Vippola M, Alenius H, Hameri K, Koivisto J, Brouwer D, Mark D, Bard D, Berges M, Jankowska E, Posniak M, Farmer P, Singh R, Krombach F, Bihari P, Kasper G, Seipenbusch M. Nanotechnologies, engineered nanomaterials and occupational health and safety - A review. *Safety Science* 2010;48:957-963.

295. Saxena RK, Williams W, McGee JK, Daniels MJ, Boykin E, Gilmour MI. Enhanced in vitro and in vivo toxicity of poly-dispersed acid-functionalized single-wall carbon nanotubes. *Nanotoxicology* 2007;1:291-300.

296. Sayes CM, Liang F, Hudson JL, Mendez J, Guo W, Beach JM, Moore VC, Doyle CD, West JL, Billups WE, Ausman KD, Colvin VL. Functionalization density dependence of single-walled carbon nanotubes cytotoxicity in vitro. *Toxicol Lett* 2006;161:135-142.

297. Schins RPF, Knaapen AM. Genotoxicity of poorly soluble particles. *Inhal Toxicol* 2007;19: 189-198.

298. Schipper ML, Nakayama-Ratchford N, Davis CR, Kam NW, Chu P, Liu Z, Sun X, Dai H, Gambhir SS. A pilot toxicology study of single-walled carbon nanotubes in a small sample of mice. *Nat Nanotechnol* 2008;3:216-221.

299. Schneider T, Jansson A, Alstrup JK, Kristjansson V, Luotamo M, Nygren O, Savolainen K, Skaug V, Thomassen Y, Tossavainen A, Tuomi T, Wallin H. *Evaluation and control of*

occupational health risks from nanoparticles. TemaNord 2007:581. Copenhagen, Denmark: Nordic Council of Ministers, 2007.

300. Schulte PA, Kuempel ED, Zumwalde RD, Geraci CL, Schubauer-Berigan MK, Castranova V, Hodson L, Murashov V, Dahm MM, Ellenbecker M. Focused actions to protect carbon nanotube workers. *Am J Ind Med* 2012;55:395-411.
301. Schulte PA, Murashov V, Zumwalde R, Kuempel ED, Geraci CL. Occupational exposure limits for nanomaterials: state of the art. *J Nanopart Res* 2010;12:1971-1987.
302. Shi Z, Lian Y, Liao FH, Zhou X, Gu Z, Zhang Y, Iijima S, Li H, Yue KT, Zhang SL. Large scale synthesis of single-wall carbon nanotubes by arc-discharge method. *J Phys Chem Solids* 2000;61:1031-1036.
303. Shvedova AA, Castranova V, Kisin ER, Schwegler-Berry D, Murray AR, Gandelsman VZ, Maynard A, Baron P. Exposure to carbon nanotube material: assessment of nanotube cytotoxicity using human keratinocyte cells. *J Toxicol Environ Health A* 2003;66:1909-1926.
304. Shvedova AA, Fabisiak JP, Kisin ER, Murray AR, Roberts JR, Tyurina YY, Antonini JM, Feng WH, Kommineni C, Reynolds J, Barchowsky A, Castranova V, Kagan VE. Sequential exposure to carbon nanotubes and bacteria enhances pulmonary inflammation and infectivity. *Am J Respir Cell Mol Biol* 2008;38:579-590.
305. Shvedova AA, Kisin E, Murray AR, Johnson VJ, Gorelik O, Arepalli S, Hubbs AF, Mercer RR, Keohavong P, Sussman N, Jin J, Yin J, Stone S, Chen BT, Deye G, Maynard A, Castranova V, Baron PA, Kagan VE. Inhalation vs. aspiration of single-walled carbon nanotubes in C57BL/6 mice: inflammation, fibrosis, oxidative stress, and mutagenesis. *Am J Physiol Lung Cell Mol Physiol* 2008;295:L552-565.
306. Shvedova AA, Kisin ER, Mercer R, Murray AR, Johnson VJ, Potapovich AI, Tyurina YY, Gorelik O, Arepalli S, Schwegler-Berry D, Hubbs AF, Antonini J, Evans DE, Ku BK, Ramsey D, Maynard A, Kagan VE, Castranova V, Baron P. Unusual inflammatory and fibrogenic pulmonary responses to single-walled carbon nanotubes in mice. *Am J Physiol Lung Cell Mol Physiol* 2005;289:L698-708.
307. Shvedova AA, Kisin ER, Murray AR, Gorelik O, Arepalli S, Castranova V, Young SH, Gao F, Tyurina YY, Oury TD, Kagan VE. Vitamin E deficiency enhances pulmonary inflammatory response and oxidative stress induced by single-walled carbon nanotubes in C57BL/6 mice. *Toxicol Appl Pharmacol* 2007;221:339-348.
308. Shvedova AA, Kisin ER, Murray AR, Kommineni C, Castranova V, Fadeel B, Kagan VE. Increased accumulation of neutrophils and decreased fibrosis in the lung of NADPH oxidase-deficient C57BL/6 mice exposed to carbon nanotubes. *Toxicol Appl Pharmacol* 2008;231: 235-240.
309. Simon-Deckers A, Gouget B, Mayne-L'hermite M, Herlin-Boime N, Reynaud C, Carriere M. In vitro investigation of oxide nanoparticle and carbon nanotube toxicity and intracellular accumulation in A549 human pneumocytes. *Toxicology* 2008;253:137-146.
310. Singh N, Manshian B, Jenkins GJ, Griffiths SM, Williams PM, Maffeis TG, Wright CJ, Doak SH. NanoGenotoxicology: the DNA damaging potential of engineered nanomaterials. *Biomaterials* 2009;30:3891-3914.
311. Singh R, Pantarotto D, Lacerda L, Pastorin G, Klumpp C, Prato M, Bianco A, Kostarelos K. Tissue biodistribution and blood clearance rates of intravenously administered carbon nanotube radiotracers. *Proc Natl Acad Sci U S A* 2006;103:3357-3362.
312. Sinha S, Barjami S, Iannacchione G, Schwab A, Muench G. Off-axis thermal properties of carbon nanotube films. *J Nanopart Res* 2005;7:651-657.
313. Sinnott SB. Chemical functionalization of carbon nanotubes. *J Nanosci Nanotechnol* 2002;2: 113-123.
314. Sinnott SB, Andrews R, Qian D, Rao AM, Mao Z, Dickey EC, Derbyshire F. Model of carbon nanotube growth through chemical vapor deposition. *Chem Phys Lett* 1999;315:25-30.

315. Stankovich S, Dikin DA, Piner RD, Kohlhaas KA, Kleinhammes A, Jia Y, Wu Y, Nguyen ST, Ruoff RS. Synthesis of graphene-based nanosheets via chemical reduction of exfoliated graphite oxide. *Carbon* 2007;45:1558-1565.

316. Stanton MF, Layard M, Tegeris A, Miller E, May M, Morgan E, Smith A. Relation of particle dimension to carcinogenicity in amphibole asbestoses and other fibrous minerals. *J Natl Cancer Inst* 1981;67:965-975.

317. Sund J, Alenius H, Vippola M, Savolainen K, Puustinen A. Proteomic characterization of engineered nanomaterial-protein interactions in relation to surface reactivity. *ACS Nano* 2011;5:4300-4309.

318. Tabet L, Bussy C, Amara N, Setyan A, Grodet A, Rossi MJ, Pairon JC, Boczkowski J, Lanone S. Adverse effects of industrial multiwalled carbon nanotubes on human pulmonary cells. *J Toxicol Environ Health A* 2009;72:60-73.

319. Takagi A, Hirose A, Futakuchi M, Tsuda H, Kanno J. Dose-dependent mesothelioma induction by intraperitoneal administration of multi-wall carbon nanotubes in p53 heterozygous mice. *Cancer Sci* 2012;103:1440-1444.

320. Takagi A, Hirose A, Nishimura T, Fukumori N, Ogata A, Ohashi N, Kitajima S, Kanno J. Induction of mesothelioma in p53+/- mouse by intraperitoneal application of multi-wall carbon nanotube. *J Toxicol Sci* 2008;33:105-116.

321. Takaya M, Ono-Ogasawara M, Shinohara Y, Kubota H, Tsuruoka S, Koda S. Evaluation of exposure risk in the weaving process of MWCNT-coated yarn with real-time particle concentration measurements and characterization of dust particles. *Ind Health* 2012;50:147-155.

322. Takaya M, Serita F, Ono-Ogasawara M, Shinohara Y, Saito H, Koda S. [Airborne particles in a multi-wall carbon nanotube production plant: observation of particle emission and personal exposure 1: Measurement in the packing process]. *Sangyo Eiseigaku Zasshi* 2010;52:182-188 (Japanese, English abstract).

323. Takaya M, Serita F, Yamazaki K, Aiso S, Kubota H, Asakura M, Ikawa N, Nagano K, Arito H, Fukushima S. Characteristics of multiwall carbon nanotubes for an intratracheal instillation study with rats. *Ind Health* 2010;48:452-459.

324. Tanaka I, Yamato H, Oyabu T, Ogami A. Biopersistence of man-made fibers by animal inhalation experiments in recent reports. *Ind Health* 2001;39:114-118.

325. Tanaka T, Jin H, Miyata Y, Fujii S, Suga H, Naitoh Y, Minari T, Miyadera T, Tsukagoshi K, Kataura H. Simple and scalable gel-based separation of metallic and semiconducting carbon nanotubes. *Nano Lett* 2009;9:1497-1500.

326. Tanaka T, Urabe Y, Nishide D, Kataura H. Continuous separation of metallic and semiconducting carbon nanotubes using agarose gel. *Applied Physics Express* 2009;2:125002.

327. Tang WZ, Advani SG. Dynamic simulation of carbon nanotubes in simple shear flow. *Cmes-Computer Modeling in Engineering & Sciences* 2008;25:149-164.

328. Teeguarden JG, Hinderliter PM, Orr G, Thrall BD, Pounds JG. Particokinetics in vitro: dosimetry considerations for in vitro nanoparticle toxicity assessments. *Toxicol Sci* 2007;95:300-312.

329. Teeguarden JG, Webb-Robertson BJ, Waters KM, Murray AR, Kisin ER, Varnum SM, Jacobs JM, Pounds JG, Zanger RC, Shvedova AA. Comparative proteomics and pulmonary toxicity of instilled single-walled carbon nanotubes, crocidolite asbestos, and ultrafine carbon black in mice. *Toxicol Sci* 2011;120:123-135.

330. Thess A, Lee R, Nikolaev P, Dai H, Petit P, Robert J, Xu C, Lee YH, Kim SG, Rinzler AG, Colbert DT, Scuseria GE, Tomanek D, Fischer JE, Smalley RE. Crystalline ropes of metallic carbon nanotubes. *Science* 1996;273:483-487.

331. Thomas T, Bahadori T, Savage N, Thomas K. Moving toward exposure and risk evaluation of nanomaterials: challenges and future directions. *Wiley Interdiscip Rev Nanomed Nanobiotechnol* 2009;1:426-433.

332. Thostenson ET, Li CY, Chou TW. Nanocomposites in context. *Compos Sci Technol* 2005; 65:491-516.

333. Thostenson ET, Ren ZF, Chou TW. Advances in the science and technology of carbon nanotubes and their composites: a review. *Compos Sci Technol* 2001;61:1899-1912.

334. Tian F, Cui D, Schwarz H, Estrada GG, Kobayashi H. Cytotoxicity of single-wall carbon nanotubes on human fibroblasts. *Toxicol In Vitro* 2006;20:1202-1212.

335. Tippe A, Heinzmann U, Roth C. Deposition of fine and ultrafine aerosol particles during exposure at the air/cell interface. *J Aerosol Sci* 2002;33:207-218.

336. Tong H, McGee JK, Saxena RK, Kodavanti UP, Devlin RB, Gilmour MI. Influence of acid functionalization on the cardiopulmonary toxicity of carbon nanotubes and carbon black particles in mice. *Toxicol Appl Pharmacol* 2009;239:224-232.

337. Tsai SJ, Hofmann M, Hallock M, Ada E, Kong J, Ellenbecker M. Characterization and evaluation of nanoparticle release during the synthesis of single-walled and multiwalled carbon nanotubes by chemical vapor deposition. *Environ Sci Technol* 2009;43:6017-6023.

338. Tu X, Manohar S, Jagota A, Zheng M. DNA sequence motifs for structure-specific recognition and separation of carbon nanotubes. *Nature* 2009;460:250-253.

339. Wako K, Kotani Y, Hirose A, Doi T, Hamada S. Effects of preparation methods for multi-wall carbon nanotube (MWCNT) suspensions on MWCNT induced rat pulmonary toxicity. *J Toxicol Sci* 2010;35:437-446.

340. Walker VG, Li Z, Hulderman T, Schwegler-Berry D, Kashon ML, Simeonova PP. Potential in vitro effects of carbon nanotubes on human aortic endothelial cells. *Toxicol Appl Pharmacol* 2009;236:319-328.

341. Walters DA, Ericson LM, Casavant MJ, Liu J, Colbert DT, Smith KA, Smalley RE. Elastic strain of freely suspended single-wall carbon nanotube ropes. *Appl Phys Lett* 1999;74:3803-3805.

342. Wang H, Wang J, Deng X, Sun H, Shi Z, Gu Z, Liu Y, Zhao Y. Biodistribution of carbon single-wall carbon nanotubes in mice. *J Nanosci Nanotechnol* 2004;4:1019-1024.

343. Wang J, Deng XY, Yang ST, Wang HF, Zhao YL, Liu YF. Rapid translocation and pharmaco-kinetics of hydroxylated single-walled carbon nanotubes in mice. *Nanotoxicology* 2008;2:28-32.

344. Wang J, Liu Y, Jiao F, Lao F, Li W, Gu Y, Li Y, Ge C, Zhou G, Li B, Zhao Y, Chai Z, Chen C. Time-dependent translocation and potential impairment on central nervous system by intranasally instilled TiO(2) nanoparticles. *Toxicology* 2008;254:82-90.

345. Wang J, Sun RH, Zhang N, Nie H, Liu JH, Wang JN, Wang H, Liu Y. Multi-walled carbon nanotubes do not impair immune functions of dendritic cells. *Carbon* 2009;47:1752-1760.

346. Wang L, Castranova V, Mishra A, Chen B, Mercer RR, Schwegler-Berry D, Rojanasakul Y. Dispersion of single-walled carbon nanotubes by a natural lung surfactant for pulmonary in vitro and in vivo toxicity studies. *Part Fibre Toxicol* 2010;7:31.

347. Wang X, Jia G, Wang H, Nie H, Yan L, Deng XY, Wang S. Diameter effects on cytotoxicity of multi-walled carbon nanotubes. *J Nanosci Nanotechnol* 2009;9:3025-3033.

348. Wang X, Katwa P, Podila R, Chen P, Ke PC, Rao AM, Walters DM, Wingard CJ, Brown JM. Multi-walled carbon nanotube instillation impairs pulmonary function in C57BL/6 mice. *Part Fibre Toxicol* 2011;8:24.

349. Wang X, Li Q, Xie J, Jin Z, Wang J, Li Y, Jiang K, Fan S. Fabrication of ultralong and electrically uniform single-walled carbon nanotubes on clean substrates. *Nano Lett* 2009;9:3137-3141.

350. Wang Z, Zhang K, Zhao J, Liu X, Xing B. Adsorption and inhibition of butyrylcholinesterase by different engineered nanoparticles. *Chemosphere* 2010;79:86-92.

351. Wang Z, Zhao J, Li F, Gao D, Xing B. Adsorption and inhibition of acetylcholinesterase by different nanoparticles. *Chemosphere* 2009;77:67-73.

352. Varga C, Szendi K. Carbon nanotubes induce granulomas but not mesotheliomas. *In Vivo* 2010;24:153-156.

353. Velasco-Santos C, Martinez-Hernandez AL, Consultchi A, Rodriguez R, Castano VM. Naturally produced carbon nanotubes. *Chem Phys Lett* 2003;373:272-276.

354. WHO. *Determination of airborne fibre number concentrations*. A recommended method, by phase-contrast optical microscopy (membrane filter method). http://www.who.int/occupational_health/publications/en/oehairbornefibre.pdf. Geneva: World Health Organization, 1997.

355. Wick P, Manser P, Limbach LK, Dettlaff-Weglikowska U, Krumeich F, Roth S, Stark WJ, Bruinink A. The degree and kind of agglomeration affect carbon nanotube cytotoxicity. *Toxicol Lett* 2007;168:121-131.

356. Wildoer JWG, Venema LC, Rinzler AG, Smalley RE, Dekker C. Electronic structure of atomically resolved carbon nanotubes. *Nature* 1998;391:59-62.

357. Vippola M, Falck GC, Lindberg HK, Suhonen S, Vanhala E, Norppa H, Savolainen K, Tossavainen A, Tuomi T. Preparation of nanoparticle dispersions for in-vitro toxicity testing. *Hum Exp Toxicol* 2009;28:377-385.

358. Wirnitzer U, Herbold B, Voetz M, Ragot J. Studies on the in vitro genotoxicity of baytubes, agglomerates of engineered multi-walled carbon-nanotubes (MWCNT). *Toxicol Lett* 2009; 186:160-165.

359. Witasp E, Shvedova AA, Kagan VE, Fadeel B. Single-walled carbon nanotubes impair human macrophage engulfment of apoptotic cell corpses. *Inhal Toxicol* 2009;21 Suppl 1:131-136.

360. Vittorio O, Raffa V, Cuschieri A. Influence of purity and surface oxidation on cytotoxicity of multiwalled carbon nanotubes with human neuroblastoma cells. *Nanomedicine* 2009;5:424-431.

361. Wohlleben W, Brill S, Meier MW, Mertler M, Cox G, Hirth S, von Vacano B, Strauss V, Treumann S, Wiench K, Ma-Hock L, Landsiedel R. On the lifecycle of nanocomposites: Comparing released fragments and their in-vivo hazards from three release mechanisms and four nanocomposites. *Small* 2011;7:2384-2395.

362. Worle-Knirsch JM, Pulskamp K, Krug HF. Oops they did it again! Carbon nanotubes hoax scientists in viability assays. *Nano Lett* 2006;6:1261-1268.

363. *WTEC Panel report on international assessment of carbon nanotube manufacturing and applications.* Baltimore, Maryland: World Technology Evaluation Center, Inc., 2007.

364. Wu M, Gordon RE, Herbert R, Padilla M, Moline J, Mendelson D, Litle V, Travis WD, Gil J. Case report: Lung disease in World Trade Center responders exposed to dust and smoke: carbon nanotubes found in the lungs of World Trade Center patients and dust samples. *Environ Health Perspect* 2010;118:499-504.

365. Xiao Y, Gao X, Taratula O, Treado S, Urbas A, Holbrook RD, Cavicchi RE, Avedisian CT, Mitra S, Savla R, Wagner PD, Srivastava S, He H. Anti-HER2 IgY antibody-functionalized single-walled carbon nanotubes for detection and selective destruction of breast cancer cells. *BMC Cancer* 2009;9:351.

366. Xu H, Bai J, Meng J, Hao W, Cao JM. Multi-walled carbon nanotubes suppress potassium channel activities in PC12 cells. *Nanotechnology* 2009;20:285102.

367. Yacobi NR, Phuleria HC, Demaio L, Liang CH, Peng CA, Sioutas C, Borok Z, Kim KJ, Crandall ED. Nanoparticle effects on rat alveolar epithelial cell monolayer barrier properties. *Toxicol In Vitro* 2007;21:1373-1381.

368. Yamashita K, Yoshioka Y, Higashisaka K, Morishita Y, Yoshida T, Fujimura M, Kayamuro H, Nabeshi H, Yamashita T, Nagano K, Abe Y, Kamada H, Kawai Y, Mayumi T, Yoshikawa T, Itoh N, Tsunoda S, Tsutsumi Y. Carbon nanotubes elicit DNA damage and inflammatory response relative to their size and shape. *Inflammation* 2010;33:276-280.

369. Yang ST, Fernando KA, Liu JH, Wang J, Sun HF, Liu Y, Chen M, Huang Y, Wang X, Wang H, Sun YP. Covalently PEGylated carbon nanotubes with stealth character in vivo. *Small* 2008;4:940-944.

370. Yang ST, Guo W, Lin Y, Deng XY, Wang HF, Sun HF, Liu YF, Wang X, Wang W, Chen M, Huang YP, Sun YP. Biodistribution of pristine single-walled carbon nanotubes in vivo. *J Phys Chem C* 2007;111:17761-17764.

371. Yang ST, Wang H, Meziani MJ, Liu Y, Wang X, Sun YP. Biodefunctionalization of functionalized single-walled carbon nanotubes in mice. *Biomacromolecules* 2009;10:2009-2012.

372. Yang ST, Wang X, Jia G, Gu Y, Wang T, Nie H, Ge C, Wang H, Liu Y. Long-term accumulation and low toxicity of single-walled carbon nanotubes in intravenously exposed mice. *Toxicol Lett* 2008;181:182-189.

373. Yang Z, Zhang Y, Yang Y, Sun L, Han D, Li H, Wang C. Pharmacological and toxicological target organelles and safe use of single-walled carbon nanotubes as drug carriers in treating Alzheimer disease. *Nanomedicine* 2010;6:427-441.

374. Ye SF, Wu YH, Hou ZQ, Zhang QQ. ROS and NF-kappaB are involved in upregulation of IL-8 in A549 cells exposed to multi-walled carbon nanotubes. *Biochem Biophys Res Commun* 2009;379:643-648.

375. Ye Y, Ahn CC, Witham C, Fultz B, Liu J, Rinzler AG, Colbert D, Smith KA, Smalley RE. Hydrogen adsorption and cohesive energy of single-walled carbon nanotubes. *Appl Phys Lett* 1999;74:2307-2309.

376. Yeganeh B, Kull CM, Hull MS, Marr LC. Characterization of airborne particles during production of carbonaceous nanomaterials. *Environ Sci Technol* 2008;42:4600-4606.

377. Yi CQ, Fong CC, Chen WW, Qi SJ, Tzang CH, Lee ST, Yang MS. Interactions between carbon nanotubes and DNA polymerase and restriction endonucleases. *Nanotechnology* 2007;18:025102.

378. Yu MF, Files BS, Arepalli S, Ruoff RS. Tensile loading of ropes of single wall carbon nanotubes and their mechanical properties. *Phys Rev Lett* 2000;84:5552-5555.

379. Zeni O, Palumbo R, Bernini R, Zeni L, Sarti M, Scarfi MR. Cytotoxicity investigation on cultured human blood cells treated with single-wall carbon nanotubes. *Sensors* 2008;8:488-499.

380. Zhang D, Deng X, Ji Z, Shen X, Dong L, Wu M, Gu T, Liu Y. Long-term hepatotoxicity of polyethylene-glycol functionalized multi-walled carbon nanotubes in mice. *Nanotechnology* 2010;21:175101.

381. Zhang H, Cao GP, Wang ZY, Yang YS, Shi ZJ, Gu ZA. Carbon nanotube array anodes for high-rate Li-ion batteries. *Electrochimica Acta* 2010;55:2873-2877.

382. Zhang LW, Zeng L, Barron AR, Monteiro-Riviere NA. Biological interactions of functionalized single-wall carbon nanotubes in human epidermal keratinocytes. *Int J Toxicol* 2007;26:103-113.

383. Zhang MF, Yudasaka M, Koshio A, Iijima S. Thermogravimetric analysis of single-wall carbon nanotubes ultrasonicated in monochlorobenzene. *Chem Phys Lett* 2002;364:420-426.

384. Zhang Q, Yu Z, Du P, Su C. Carbon nanomaterials used as conductive additives in lithium ion batteries. *Recent Pat Nanotechnol* 2010;4:100-110.

385. Zhang T, Xu M, He L, Xi K, Gu M, Jiang Z. Synthesis, characterization and cytotoxicity of phosphoryl choline-grafted water-soluble carbon nanotubes. *Carbon* 2008;46:1782-1791.

386. Zhu L, Chang DW, Dai L, Hong Y. DNA damage induced by multiwalled carbon nanotubes in mouse embryonic stem cells. *Nano Lett* 2007;7:3592-3597.

387. Zhu Y, Li W, Li Q, Li Y, Li Y, Zhang X, Huang Q. Effects of serum proteins on intracellular uptake and cytotoxicity of carbon nanoparticles. *Carbon* 2009;47:1351-1358.

388. Zuin S, Pojana G, Marcomini A. Effect-oriented physicochemical characterization of nanomaterials. Chapter 3. Pp 456. In: *Nanotoxicology: Characterization, dosing, and health effects*. 1st ed. New York, NY: Informa Healthcare, 2007.

20. Data bases used in search of literature

In the search for literature the following data bases were used: NIOSHTIC-2, Medline and Web of Science.

For studies included in Chapters 7-11, conference proceedings before 2009 were omitted as well as abstract-only reports.

The following terms were used in the literature search: carbon nanotube(s), toxicity, toxicology, animals, cells, genotoxicity, toxicokinetics and bio-distribution.

Last search was performed in December 2012.

Submitted for publication October 21, 2013.

Appendix 1. Previous NEG criteria documents

NEG documents published in the scientific serial Arbete och Hälsa (Work and Health).

Substance/Agent	Arbete och Hälsa issue
Acetonitrile	1989:22, 1989:37*
Acid aerosols, inorganic	1992:33, 1993:1*
Acrylonitrile	1985:4
Allyl alcohol	1986:8
Aluminium and aluminium compounds	1992:45, 1993:1*, 2011;45(7)*D
Ammonia	1986:31, 2005:13*
Antimony	1998:11*
Arsenic, inorganic	1981:22, 1991:9, 1991:50*
Arsine	1986:41
Asbestos	1982:29
Benomyl	1984:28
Benzene	1981:11
1,2,3-Benzotriazole	2000:24*D
Boric acid, Borax	1980:13
1,3-Butadiene	1994:36*, 1994:42
1-Butanol	1980:20
γ-Butyrolactone	2004:7*D
Cadmium	1981:29, 1992:26, 1993:1*
7/8 Carbon chain aliphatic monoketones	1990:2*D
Carbon monoxide	1980:8, 2012;46(7)*
Ceramic Fibres, Refractory	1996:30*, 1998:20
Chlorine, Chlorine dioxide	1980:6
Chloromequat chloride	1984:36
4-Chloro-2-methylphenoxy acetic acid	1981:14
Chlorophenols	1984:46
Chlorotrimethylsilane	2002:2
Chromium	1979:33
Cobalt	1982:16, 1994:39*, 1994:42
Copper	1980:21
Creosote	1988:13, 1988:33*
Cyanoacrylates	1995:25*, 1995:27
Cyclic acid anhydrides	2004:15*D
Cyclohexanone, Cyclopentanone	1985:42
n-Decane	1987:25, 1987:40*
Deodorized kerosene	1985:24
Diacetone alcohol	1989:4, 1989:37*
Dichlorobenzenes	1998:4*, 1998:20
Diesel exhaust	1993:34, 1993:35*
Diethylamine	1994:23*, 1994:42
2-Diethylaminoethanol	1994:25*N
Diethylenetriamine	1994:23*, 1994:42
Diisocyanates	1979:34, 1985:19
Dimethylamine	1994:23*, 1994:42
Dimethyldithiocarbamates	1990:26, 1991:2*
Dimethylethylamine	1991:26, 1991:50*
Dimethylformamide	1983:28
Dimethylsulfoxide	1991:37, 1991:50*
Dioxane	1982:6
Endotoxins	2011;45(4)*D
Enzymes, industrial	1994:28*, 1994:42

NEG documents published in the scientific serial Arbete och Hälsa (Work and Health).

Substance/Agent	Arbete och Hälsa issue
Epichlorohydrin	1981:10
Ethyl acetate	1990:35*
Ethylbenzene	1986:19
Ethylenediamine	1994:23*, 1994:42
Ethylenebisdithiocarbamates and Ethylenethiourea	1993:24, 1993:35*
Ethylene glycol	1980:14
Ethylene glycol monoalkyl ethers	1985:34
Ethylene oxide	1982:7
Ethyl ether	1992:30* N
2-Ethylhexanoic acid	1994:31*, 1994:42
Flour dust	1996:27*, 1998:20
Formaldehyde	1978:21, 1982:27, 2003:11*D
Fungal spores	2006:21*
Furfuryl alcohol	1984:24
Gasoline	1984:7
Glutaraldehyde	1997:20*D, 1998:20
Glyoxal	1995:2*, 1995:27
Halothane	1984:17
n-Hexane	1980:19, 1986:20
Hydrazine, Hydrazine salts	1985:6
Hydrogen fluoride	1983:7
Hydrogen sulphide	1982:31, 2001:14*D
Hydroquinone	1989:15, 1989:37*
Industrial enzymes	1994:28*
Isoflurane, sevoflurane and desflurane	2009;43(9)*
Isophorone	1991:14, 1991:50*
Isopropanol	1980:18
Lead, inorganic	1979:24, 1992:43, 1993:1*
Limonene	1993:14, 1993:35*
Lithium and lithium compounds	2002:16*
Manganese	1982:10
Mercury, inorganic	1985:20
Methacrylates	1983:21
Methanol	1984:41
Methyl bromide	1987:18, 1987:40*
Methyl chloride	1992:27*D
Methyl chloroform	1981:12
Methylcyclopentadienyl manganese tricarbonyl	1982:10
Methylene chloride	1979:15, 1987:29, 1987:40*
Methyl ethyl ketone	1983:25
Methyl formate	1989:29, 1989:37*
Methyl isobutyl ketone	1988:20, 1988:33*
Methyl methacrylate	1991:36*D
N-Methyl-2-pyrrolidone	1994:40*, 1994:42
Methyl-tert-butyl ether	1994:22*D
Microbial volatile organic compounds (MVOCs)	2006:13*
Microorganisms	1991:44, 1991:50*
Mineral fibers	1981:26
Nickel	1981:28, 1995:26*, 1995:27
Nitrilotriacetic acid	1989:16, 1989:37*
Nitroalkanes	1988:29, 1988:33*
Nitrogen oxides	1983:28
N-Nitroso compounds	1990:33, 1991:2*

NEG documents published in the scientific serial Arbete och Hälsa (Work and Health).

Substance/Agent	Arbete och Hälsa issue
Nitrous oxide	1982:20
Occupational exposure to chemicals and hearing impairment	2010;44(4)*
Oil mist	1985:13
Organic acid anhydrides	1990:48, 1991:2*
Ozone	1986:28
Paper dust	1989:30, 1989:37*
Penicillins	2004:6*
Permethrin	1982:22
Petrol	1984:7
Phenol	1984:33
Phosphate triesters with flame retardant properties	2010;44(6)*
Phthalate esters	1982:12
Platinum	1997:14*D, 1998:20
Polychlorinated biphenyls (PCBs)	2012;46(1)*
Polyethylene,	1998:12*
Polypropylene, Thermal degradation products in the processing of plastics	1998:12*
Polystyrene, Thermal degradation products in the processing of plastics	1998:12*
Polyvinylchloride, Thermal degradation products in the processing of plastics	1998:12*
Polytetrafluoroethylene, Thermal degradation products in the processing of plastics	1998:12*
Propene	1995:7*, 1995:27
Propylene glycol	1983:27
Propylene glycol ethers and their acetates	1990:32*N
Propylene oxide	1985:23
Refined petroleum solvents	1982:21
Refractory Ceramic Fibres	1996:30*
Selenium	1992:35, 1993:1*
Silica, crystalline	1993:2, 1993:35*
Styrene	1979:14, 1990:49*, 1991:2
Sulphur dioxide	1984:18
Sulphuric, hydrochloric, nitric and phosphoric acids	2009;43(7)*
Synthetic pyretroids	1982:22
Tetrachloroethane	1996:28*D
Tetrachloroethylene	1979:25, 2003:14*D
Thermal degradation products of plastics	1998:12*
Thiurams	1990:26, 1991:2*
Tin and inorganic tin compounds	2002:10*D
Toluene	1979:5, 1989:3, 1989:37*, 2000:19*
1,1,1-Trichloroethane	1981:12
Trichloroethylene	1979:13, 1991:43, 1991:50*
Triglycidyl isocyanurate	2001:18*
n-Undecane	1987:25, 1987:40*
Vanadium	1982:18
Vinyl acetate	1988:26, 1988:33*
Vinyl chloride	1986:17
Welding gases and fumes	1990:28, 1991:2*
White spirit	1986:1
Wood dust	1987:36
Xylene	1979:35
Zinc	1981:13

* in English, remaining documents are in a Scandinavian language.
D = collaboration with the Dutch Expert Committee on Occupational Safety (DECOS).
N = collaboration with the US National Institute for Occupational Safety and Health (NIOSH).
To order further copies in this series, please contact:
Arbets- och miljömedicin, Göteborgs universitet
Att: Cina Holmer, Box 414, SE-405 30 Göteborg, Sweden
E-mail: arbeteochhalsa@amm.gu.se
The NEG documents are also available on the web at:
www.nordicexpertgroup.org or *www.amm.se/aoh*

Latest issues in the scientific serial WORK AND HEALTH

2010:44(3). L Holm, M Torgén, A Hansson, R Runeson, M Josephson, M Helgesson och E Vingård. Återgång i arbete efter sjukskrivning för rörelseorganens sjukdomar och lättare psykisk ohälsa.

2010;44(4). A Johnson and T C Morata. The Nordic Expert Group for Criteria Documentation of Health Risks from Chemicals. 142. Occupational exposure to chemicals and hearing impairment.

2010:44(5). J Montelius (Ed.) Scientific Basis for Swedish Occupational Standards XXX. Swedish Criteria Group for Occupational Standards.

2010:44(6). B Sjögren, A Iregren and J Järnberg. The Nordic Expert Group for Criteria Documentation of Health Risks from Chemicals. 143. Phosphate triesters with flame retardant properties.

2010;44(7). G Aronsson, W Astvik och K Gustafsson. Arbetsvillkor, återhämtning och hälsa – en studie av förskola, hemtjänst och socialtjänst.

2010;44(8). K Torén, M Albin och B Järvholm. Systematiska kunskapsöversikter; 1. Betydelsen av fukt och mögel i inomhusmiljö för astma hos vuxna.

2010;44(9). C Wulff, P Lindfors och M Sverke. Hur förhåller sig begåvning i skolåldern och psykosocial arbetsbelastning i vuxenlivet till olika aspekter av självrapporterad hälsa bland yrkesarbetande kvinnor och män?

2010;44(10). H Kantelius Inhyrningens logik Långtidsinhyrda arbetare och tjänstemäns utvecklingsmöjligheter och upplevda anställningsbarhet.

2011;45(1). E Tengelin, A Kihlman, M Eklöf och L Dellve. Chefskap i sjukvårdsmiljö: Avgränsning och kommunikation av egen stress.

2011;45(2) A Grimby-Ekman. Epidemiological aspects of musculoskeletal pain in the upper body.

2011;45(3). J Montelius (Ed.) Vetenskapligt Underlag för Hygieniska Gränsvärden 31. Kriteriegruppen för hygieniska gränsvärden.
2011;45(4). The Nordic Expert Group for Criteria Documentation of Health Risks from Chemicals and the Dutch Expert Committee on Occupational Safety. 144. Endotoxins.

2011;45(5). Ed. Editors: Maria Albin, Johanna Alkan-Olsson, Mats Bohgard, Kristina Jakobsson, Björn Karlson, Peter Lundqvist, Mikael Ottosson, Fredrik Rassner, Måns Svensson, and Håkan Tinnerberg.
55th Nordic Work Environment Meeting.
The Work Environment – Impact of Technological, Social and Climate Change.

2011;45(6). J Montelius (Ed.) Scientific Basis for Swedish Occupational Standards XXXI. Swedish Criteria Group for Occupational Standards.

2011;45(7). The Nordic Expert Group for Criteria Documentation of Health Risks from Chemicals and the Dutch Expert Committee on Occupational Safety. 145. Aluminium and aluminium compounds.

2012;46(1). Birgitta Lindell. The Nordic Expert Group for Criteria Documentation of Health Risks from Chemicals. 146. Polychlorinated biphenyls. (PCBs)

2012:46(2). K Torén, M Albin och B Järvholm.
Systematiska kunskapsöversikter;
2. Exponering för helkroppsvibrationer och uppkomst av ländryggssjuklighet.

2012:46(3). G Sjögren Lindquist och E Wadensjö. Kunskapsöversikt kring samhällsekonomiska kostnader för arbetsskador.

2012;46(4). C Mellner, G Aronsson och G Kecklund. Segmentering och integrering– om mäns och kvinnors gränssättningsstrategier i högkvalificerat arbete.

2012;46(5) T. Muhonen. Stress, coping och hälsa under kvinnliga chefers och specialisters karriärer.

2012;46(6). J Montelius (Ed.) Vetenskapligt Underlag för Hygieniska Gränsvärden 32. Kriteriegruppen för hygieniska gränsvärden.

2012;46(7) Helene Stockmann-Juvala. The Nordic Expert Group for Criteria Documentation of Health Risks from Chemicals. 147. Carbon monoxide.

2013;47(1) I Lundberg, P Allebeck, Y Forsell och P Westerholm.
Systematiska kunskapsöversikter;
3. Kan arbetsvillkor orsaka depressionstillstånd? En systematisk översikt över longitudinella studier i den vetenskapliga litteraturen 1998-2012.

2013;47(2). K Elgstrand and E Vingård (Ed.) Occupational Safety and Health in Mining. Anthology on the situation in 16 mining countries.

2013;47(3). A Knutsson och A Kempe.
Systematiska kunskapsöversikter; 4. Diabetes och arbete.

2013;47(4). K Jakobsson och P Gustavsson.
Systematiska kunskapsöversikter;
5. Arbetsmiljöexponeringar och stroke – en kritisk granskning av evidens för samband mellan exponeringar i arbetsmiljön och stroke.

2013;47(5) Maria Hedmer, Monica Kåredal, Per Gustavsson and Jenny Rissler. The Nordic Expert Group for Criteria Documentation of Health Risks from Chemicals. 148. Carbon nanotubes.